

EXTREME MEDICINE

SCIENTIFIC AND PRACTICAL REVIEWED JOURNAL OF FMBA OF RUSSIA

EDITOR-IN-CHIEF Veronika Skvortsova, DSc, professor, RAS corresponding member

DEPUTY EDITOR-IN-CHIEF Igor Berzin, DSc, professor; Daria Kryuchko, DSc

EDITORS Vsevolod Belousov, DSc, professor; Anton Keskinov, PhD

TRANSLATORS Ekaterina Tretiyakova, Vyacheslav Vityuk

DESIGN AND LAYOUT Marina Doronina

EDITORIAL BOARD

Agapov VK, DSc, professor (Moscow, Russia)
Baranov VM, member of RAS, DSc, professor (Moscow, Russia)
Bogomolov AV, DSc, professor (Moscow, Russia)
Bushmanov AY, DSc, professor (Moscow, Russia)
Daikhes NA, member of RAS, DSc, professor (Moscow, Russia)
Dubina MV, member of RAS, DSc, professor (Saint-Petersburg, Russia)
Dudarenko SV, DSc (Saint-Petersburg, Russia)
Ilyin LA, member of RAS, DSc, professor (Moscow, Russia)
Lobzin YV, member of RAS, DSc, professor (Saint-Petersburg, Russia)
Nikiforov VV, DSc, professor (Moscow, Russia)
Olesova VN, DSc, professor (Moscow, Russia)

Petrov RV, member of RAS, DSc, professor (Moscow, Russia)
Sadilov AS, DSc, professor (Saint-Petersburg, Russia)
Rembovsky VR, DSc, professor (Saint-Petersburg, Russia)
Samoilov AS, member of RAS, DSc, professor (Moscow, Russia)
Sergienko VI, member of RAS, DSc, professor (Moscow, Russia)
Troitsky AV, DSc, professor (Moscow, Russia)
Ushakov IB, member of RAS, DSc, professor (Moscow, Russia)
Khaitov MR, member of RAS, DSc, professor (Moscow, Russia)
Khaitov RM, member of RAS, DSc, professor (Moscow, Russia)
Chechetkin AV, DSc, professor (Saint-Petersburg, Russia)
Yudin SM, DSc, professor (Moscow, Russia)

ADVISORY BOARD

Akleev AV, DSc, professor (Chelyabinsk, Russia)
Arakelov SA, DSc, professor (Saint-Petersburg, Russia)
Baklaushev VP, DSc, professor (Moscow, Russia)
Degteva MO, PhD (Chelyabinsk, Russia)
Efimenko NV, DSc, professor (Pyatigorsk, Russia)
Kazakevich EV, DSc, professor (Arkhangelsk, Russia)
Katuntsev VP, DSc, professor (Moscow, Russia)
Klimanov VA, DSc, professor (Moscow, Russia)
Klinov DV, PhD (Moscow, Russia)
Koshurnikova NA, DSc, professor (Ozersk, Russia)
Minnullin IP, DSc, professor (Saint-Petersburg, Russia)

Mosyagin IG, DSc, professor (Saint-Petersburg, Russia)
Panasenko OM, DSc, professor (Moscow, Russia)
Rogozhnikov VA, DSc, (Moscow, Russia)
Romanov SA, PhD (Ozersk, Russia)
Sotnichenko SA, DSc (Vladivostok, Russia)
Suranova TG, PhD, docent (Moscow, Russia)
Takhauov RM, DSc, professor (Seversk, Russia)
Shandala NK, DSc, professor (Moscow, Russia)
Shinkarev SM, DSc (Moscow, Russia)
Shipulin GA, PhD (Moscow, Russia)
Yakovleva TV, DSc (Moscow, Russia)

SUBMISSION editor@fmbs.press

CORRESPONDENCE editor@fmbs.press

COLLABORATION manager@fmbs.press

ADDRESS Volokolamskoe shosse, 30, str. 1, Moscow, Russia, 123182

Indexed in RSCI. IF 2018: 0,570

Listed in HAC 31.01.2020 (№ 1292)

Open access to archive



Issue DOI: 10.47183/mes.2021-03

The mass media registration certificate № 25124 issued on July 27, 2006

Founder and publisher: Federal medical-biological agency fmbs.gov.ru

The journal is distributed under the terms of Creative Commons Attribution 4.0 International License www.creativecommons.org



Approved for print 30.09.2021
Circulation: 500 copies. Printed by Print.Formula
www.print-formula.ru

МЕДИЦИНА ЭКСТРЕМАЛЬНЫХ СИТУАЦИЙ

НАУЧНО-ПРАКТИЧЕСКИЙ РЕЦЕНЗИРУЕМЫЙ ЖУРНАЛ ФМБА РОССИИ

ГЛАВНЫЙ РЕДАКТОР Вероника Скворцова, д. м. н., профессор, член-корреспондент РАН

ЗАМЕСТИТЕЛЬ ГЛАВНОГО РЕДАКТОРА Игорь Берзин, д. м. н., профессор; Дарья Крючко, д. м. н.

НАУЧНЫЕ РЕДАКТОРЫ Всеволод Белоусов, д. м. н., профессор; Антон Кескинов, к. м. н.

ПЕРЕВОДЧИКИ Екатерина Третьякова, Вячеслав Витюк

ДИЗАЙН И ВЕРСТКА Марины Дорониной

РЕДАКЦИОННАЯ КОЛЛЕГИЯ

В. К. Агапов, д. м. н., профессор (Москва, Россия)

В. М. Баранов, д. м. н., профессор, академик РАН (Москва, Россия)

А. В. Богомолов, д. т. н., профессор (Москва, Россия)

А. Ю. Бушманов, д. м. н., профессор (Москва, Россия)

Н. А. Дайхес, д. м. н., профессор, член-корр. РАН (Москва, Россия)

М. В. Дубина, д. м. н., профессор, академик РАН (Санкт-Петербург, Россия)

С. В. Дударенко, д. м. н., доцент (Санкт-Петербург, Россия)

Л. А. Ильин, д. м. н., профессор, академик РАН (Москва, Россия)

Ю. В. Лобзин, д. м. н., профессор, академик РАН (Санкт-Петербург, Россия)

В. В. Никифоров, д. м. н., профессор (Москва, Россия)

В. Н. Олесова, д. м. н., профессор (Москва, Россия)

Р. В. Петров, д. м. н., профессор, академик РАН (Москва, Россия)

А. С. Радилев, д. м. н., профессор (Санкт-Петербург, Россия)

В. Р. Рембовский, д. м. н., профессор (Санкт-Петербург, Россия)

А. С. Самойлов, д. м. н., профессор, член-корр. РАН (Москва, Россия)

В. А. Сергиенко, д. м. н., профессор, член-корр. РАН

А. В. Троицкий, д. м. н., профессор (Москва, Россия)

И. Б. Ушаков, д. м. н., профессор, академик РАН (Москва, Россия)

М. Р. Хаитов, д. м. н., профессор, член-корр. РАН (Москва, Россия)

Р. М. Хаитов, д. м. н., профессор, академик РАН (Москва, Россия)

А. В. Чечеткин, д. м. н., профессор (Санкт-Петербург, Россия)

С. М. Юдин, д. м. н., профессор (Москва, Россия)

РЕДАКЦИОННЫЙ СОВЕТ

А. В. Аклеев, д. м. н., профессор (Челябинск, Россия)

С. А. Аракепов, д. б. н., профессор (Санкт-Петербург, Россия)

В. П. Баклаушев, д. м. н., профессор (Москва, Россия)

М. О. Дегтева, к. т. н. (Челябинск, Россия)

Н. В. Ефименко, д. м. н., профессор (Гятыгорск, Россия)

Е. В. Казакевич, д. м. н., профессор (Архангельск, Россия)

В. П. Катунцев, д. м. н., профессор (Москва, Россия)

В. А. Климанов, д. ф.-м. н., профессор (Москва, Россия)

Д. В. Клинов, к. ф. м. н., (Москва, Россия)

Н. А. Кошурникова, д. м. н., профессор (Озерск, Россия)

И. П. Миннуллин, д. м. н., профессор (Санкт-Петербург, Россия)

И. Г. Мосягин, д. м. н., профессор (Санкт-Петербург, Россия)

О. М. Панасенко, д. б. н., профессор (Москва, Россия)

В. А. Рогожников, д. м. н. (Москва, Россия)

С. А. Романов, к. б. н. (Озерск, Россия)

С. А. Сотниченко, д. м. н. (Владивосток, Россия)

Т. Г. Суранова, к. м. н., доцент (Москва, Россия)

Р. М. Тахауов, д. м. н., профессор (Северск, Россия)

Н. К. Шандала, д. м. н., профессор (Москва, Россия)

С. М. Шинкарев, д. т. н. (Москва, Россия)

Г. А. Шипулин, к. м. н. (Москва, Россия)

Т. В. Яковлева, д. м. н. (Москва, Россия)

ПОДАЧА РУКОПИСЕЙ editor@fmba.press

ПЕРЕПИСКА С РЕДАКЦИЕЙ editor@fmba.press

СОТРУДНИЧЕСТВО manager@fmba.press

АДРЕС РЕДАКЦИИ Волоколамское шоссе, д. 30, стр. 1, г. Москва, 123182

Журнал включен в РИНЦ. IF 2018: 0,570

Журнал включен в Перечень 31.01.2020 (№ 1292)

Здесь находится открытый архив журнала



ВЫСШАЯ
АТТЕСТАЦИОННАЯ
КОМИССИЯ (ВАК)

CYBERLENINKA

DOI выпуска: 10.47183/mes.2021-03

Свидетельство о регистрации средства массовой информации № ФС77-25124 от 27 июля 2006 года

Учредитель и издатель: Федеральное медико-биологическое агентство fmba.gov.ru

Журнал распространяется по лицензии Creative Commons Attribution 4.0 International www.creativecommons.org



Подписано в печать 30.09.2021

Тираж 500 экз. Отпечатано в типографии Print.Formula
www.print-formula.ru

Contents

Содержание

ORIGINAL RESEARCH	5
<hr/>	
Peripheral blood hematopoietic stem cell pool in individuals chronically exposed to radiation over a long-term period Kotikova AI, Blinova EA, Akleyev AV Пул гемопоэтических стволовых клеток в периферической крови хронически облученных лиц в отдаленном периоде А. И. Котикова, Е. А. Блинова, А. В. Аклеев	
ORIGINAL RESEARCH	10
<hr/>	
BCL-2, CDKN1A and ATM gene methylation in chronically exposed individuals Blinova EA, Nikiforov VS, Yanishevskaya MA, Akleyev AV Метилирование генов BCL-2, CDKN1A и ATM у лиц, подвергшихся хроническому облучению Е. А. Блинова, В. С. Никифоров, М. А. Янишевская, А. В. Аклеев	
ORIGINAL RESEARCH	15
<hr/>	
Isolation and characterization of <i>Pseudomonas aeruginosa</i> bacteriophages — potential agents for phage therapy Kornienko MA, Kuptsov NS, Danilov DI, Gorodnichen RB, Malakhova MV, Bespiatykh DA, Veselovsky VA, Shitikov EA, Iliina EN Выделение и характеристика бактериофагов <i>Pseudomonas aeruginosa</i> — потенциальных агентов для фаговой терапии М. А. Корниенко, Н. С. Купцов, Д. И. Данилов, Р. Б. Городничев, М. В. Малахова, Д. А. Беспятых, В. А. Веселовский, Е. А. Шитиков, Е. Н. Ильина	
ORIGINAL RESEARCH	22
<hr/>	
Experimental and clinical evaluation of mefloquine effectiveness against the infection caused by SARS-CoV-2 Filin KN, Gladkikh VD, Bykov VN Оценка эффективности мефлохина в отношении инфекции, вызванной SARS-CoV-2 в клинических и экспериментальных условиях К. Н. Филин, В. Д. Гладких, В. Н. Быков	
ORIGINAL RESEARCH	28
<hr/>	
Comparison of methods for purification of bacteriophage lysates of gram-negative bacteria for personalized therapy Gorodnichen RB, Kornienko MA, Kuptsov NS, Efimov AD, Bogdan VI, Letarov AV, Shitikov EA, Iliina EN Сравнение методов очистки фаговых лизатов грамотрицательных бактерий для персонализированной терапии Р. Б. Городничев, М. А. Корниенко, Н. С. Купцов, А. Д. Ефимов, В. И. Богдан, А. В. Летаров, Е. А. Шитиков, Е. Н. Ильина	
ORIGINAL RESEARCH	36
<hr/>	
Interaction of cationic antiseptics with cardiolipin-containing model bacterial membranes Kholina EG, Bozdaganyan ME, Strakhovskaya MG, Kovalenko IB Взаимодействие катионных антисептиков с кардиолипинсодержащей модельной бактериальной мембраной Е. Г. Холина, М. Е. Боздаганян, М. Г. Страховская, И. Б. Коваленко	
ORIGINAL RESEARCH	43
<hr/>	
Assessing hepatoprotective effects of antioxidants on amiodarone-induced cytotoxicity in human hepatoma HepaRG cell line Filimonova KS, Rogovskaya NYu, Belyukov PP, Babakov VN Оценка гепатопротекторного эффекта антиоксидантов на амиодарон-индуцированную цитотоксичность в клетках гепатомы человека линии HepaRG К. С. Филимонова, Н. Ю. Роговская, П. П. Бельтюков, В. Н. Бабаков	
ORIGINAL RESEARCH	52
<hr/>	
Respiratory muscle strength in patients after COVID-19 Savushkina OI, Malashenko MM, Cherniak AV, Kryukov EV, Sinityn EA, Zykov KA Исследование силы дыхательных мышц у больных, перенесших COVID-19 О. И. Савушкина, М. М. Малашенко, А. В. Черняк, Е. В. Крюков, Е. А. Синицын, К. А. Зыков	
ORIGINAL RESEARCH	57
<hr/>	
Environmental impact assessment of the territories in the vicinity of commissioning regional radioactive waste management facility Zozul YuN, Kiselev SM, Laschenova TN, Shlygin VV, Akhromeev SV, Gimadova TI, Malakhova AN, Shashkova OB, Oskina KYu Комплексная гигиеническая оценка территорий в районе размещения строящегося регионального центра по обращению с радиоактивными отходами Ю. Н. Зозуль, С. М. Киселев, Т. Н. Лашенцова, В. В. Шлыгин, С. В. Ахромеев, Т. И. Гимадова, А. Н. Малахова, О. Б. Шашкова, К. Ю. Оськина	

ORIGINAL RESEARCH

64

Current trends in anticancer drug prototype *in vitro* pharmacology: bibliometric analysis 2019–2021

Ershov PV, Makarova AS

Современные тенденции *in vitro* фармакологии прототипов противоопухолевых лекарств: библиометрический анализ за 2020–2021 гг.

П. В. Ершов, А. С. Макарова

ORIGINAL RESEARCH

78

Evaluation of avian adenovirus inactivation methods used in the production of influenza vaccines

Savina NN, Ekimov AA, Trukhin VP, Evtushenko AE, Zhirenkina EN, Sinegubova EO, Slita AV

Оценка методов инактивирования аденовируса птиц при производстве гриппозных вакцин

Н. Н. Савина, А. А. Екимов, В. П. Трухин, А. Э. Евушенко, Е. Н. Жиренкина, Е. О. Синегубова, А. В. Слита

ORIGINAL RESEARCH

84

Molecular genetic characterization of three new *Klebsiella pneumoniae* bacteriophages suitable for phage therapy

Gorodnichenov RB, Kornienko MA, Kuptsov NS, Malakhova MV, Bespiatykh DA, Veselovsky VA, Shitikov EA, Ilina EN

Молекулярно-генетическая характеристика трех новых бактериофагов *Klebsiella pneumoniae*, перспективных для применения в фаговой терапии

П. Б. Городничев, М. А. Корниенко, Н. С. Купцов, М. В. Малахова, Д. А. Беспятых, В. А. Веселовский, Е. А. Шитиков, Е. Н. Ильина

REVIEW

91

Antenatal and early postnatal etiological verification of relevant congenital viral infectious diseases

Vasilyev VV, Grineva AA, Rogozina NV, Ivanova RA, Ushakova GM

Аntenальная и ранняя постнатальная этиологическая верификация актуальных врожденных вирусных инфекций

В. В. Васильев, А. А. Гринева, Н. В. Рогозина, Р. А. Иванова, Г. М. Ушакова

REVIEW

99

Mechanisms of B lymphocyte involvement in the pathogenesis of multiple sclerosis

Melnikov MV, Rogovskii VS, Lopatina AV, Sviridova AA, Volkov AI, Boyko AN

Механизмы участия В-лимфоцитов в патогенезе рассеянного склероза

М. В. Мельников, В. С. Роговский, А. В. Лопатина, А. А. Свиридова, А. И. Волков, А. Н. Бойко

REVIEW

106

Diabetes mellitus management strategies in athletes

Dergacheva LI, Derevoyedov AA, Vykhodets IT, Pavlova AA, Parastayev SA

Стратегии управления сахарным диабетом у спортсменов

Л. И. Дергачева, А. А. Деревоедов, И. Т. Выходец, А. А. Павлова, С. А. Парастаев

REVIEW

114

Brain concussion in young athletes: major pain points

Klyuchnikov SO, Feshchenko VS, Zholinsky AV, Tarasova MS, Slivin AV, Efimov PV

«Болевые точки» сотрясения головного мозга у юных спортсменов

С. О. Ключников, В. С. Фещенко, А. В. Жолинский, М. С. Тарасова, А. В. Сливин, П. В. Ефимов

CLINICAL CASE

121

Central vein sign for differential diagnosis of demyelinating diseases of CNS

Belov SE, Gubsky IL, Lelyuk VG, Boyko AN

Использование симптома центральной вены для дифференциальной диагностики демиелинизирующих заболеваний центральной нервной системы

С. Е. Белов, И. Л. Губский, В. Г. Лелюк, А. Н. Бойко

PERIPHERAL BLOOD HEMATOPOIETIC STEM CELL POOL IN INDIVIDUALS CHRONICALLY EXPOSED TO RADIATION OVER A LONG-TERM PERIOD

Kotikova AI^{1,2} ✉, Blinova EA^{1,2}, Akleyev AV^{1,2}

¹ Ural Research Center for Radiation Medicine, Chelyabinsk, Russia

² Chelyabinsk State University, Chelyabinsk, Russia

Changes in the peripheral blood cellular composition were observed in the long term period in the residents of the Techa riverside villages chronically exposed to radiation, which may be the consequence of structural and functional disorders in the pool of hematopoietic stem cells (HSC) and progenitor cells. Therefore, the study was aimed to quantify peripheral blood CD34⁺ cell pool in individuals chronically exposed to radiation over a long-term period. Sixty years after the onset of exposure, a total of 153 individuals were examined, who were divided into four groups: individuals exposed *in utero* and postnatally (the average postnatal absorbed dose was 570 mGy); individuals exposed only postnatally (the average postnatal absorbed dose was 790 mGy), and two comparison groups, in which the average postnatal absorbed dose to red bone marrow did not exceed 70 mGy. Absolute and relative peripheral blood CD34⁺ cell counts in chronically exposed individuals were assessed by flow cytometry. No changes in CD34⁺ cell counts compared to comparison group were revealed in the group of individuals exposed *in utero* and postnatally; no age-related changes were registered as well. However, a significant decline in absolute HSC and progenitor cell counts with increased absorbed dose to red bone marrow was observed. In the group of individuals exposed only postnatally, there was a significant increase in peripheral blood CD34⁺ cell counts compared to comparison group ($p = 0.004$ for absolute cell count; $p = 0.009$ for relative cell count), dose-dependent increase in peripheral blood HSC and precursor cell counts ($p = 0.02$ for absolute cell count; $p = 0.03$ for relative cell count), along with age-related decline in these cells' counts ($p = 0.02$ for absolute cell count; $p = 0.04$ for relative cell count).

Keywords: hematopoietic stem cells, chronic exposure, late effects, peripheral blood, flow cytometry

Funding: the study was carried out within the framework of the State assignment "Human Cell-Mediated Immunity During Realization of Chronic Radiation Exposure Late Effects" (code 27.002.20.800).

Author contribution: Kotikova AI — method design, laboratory tests, statistical analysis, manuscript writing; Blinova EA — method design, manuscript writing; Akleyev AV — study concept, scientific management.

Compliance with ethical standards: the study was approved by the Ethics Committee of Urals Research Center for Radiation Medicine (protocol № 3 dated July 20, 2021). All the subjects enrolled in the studies conducted by Laboratory of Molecular and Cellular Radiobiology of Urals Research Center for Radiation Medicine submitted the informed consent.

✉ **Correspondence should be addressed:** Alisa I. Kotikova
Vorovskogo, 68, corp. A, Chelyabinsk, Russia, 454141; kotikovaalisa@gmail.com

Received: 21.07.2021 **Accepted:** 10.08.2021 **Published online:** 03.09.2021

DOI: 10.47183/mes.2021.023

ПУЛ ГЕМОПОЭТИЧЕСКИХ СТЕЛОВЫХ КЛЕТОК В ПЕРИФЕРИЧЕСКОЙ КРОВИ ХРОНИЧЕСКИ ОБЛУЧЕННЫХ ЛИЦ В ОТДАЛЕННОМ ПЕРИОДЕ

А. И. Котикова^{1,2} ✉, Е. А. Блинова^{1,2}, А. В. Аклеев^{1,2}

¹ Уральский научно-практический центр радиационной медицины Федерального медико-биологического агентства, Челябинск, Россия

² Челябинский государственный университет, Челябинск, Россия

У жителей прибрежных сел реки Течи, подвергавшихся хроническому радиационному воздействию, отмечают изменения клеточного состава периферической крови в отдаленном периоде, что может быть следствием структурных и функциональных нарушений в пуле гемопоэтических стволовых клеток (ГСК) и клеток-предшественников. Целью работы было оценить количественные характеристики пула CD34⁺-клеток периферической крови у хронически облученных лиц в отдаленном периоде. Через 60 лет после начала облучения обследовано 153 человека, которых разделили на четыре группы: лиц, облученных в период внутриутробного и постнатального развития (средняя поглощенная постнатальная доза составила 570 мГр); лиц, облученных только постнатально (средняя поглощенная постнатальная доза составила 790 мГр), а также две группы сравнения, в которых поглощенные постнатальные дозы облучения красного костного мозга (ККМ) не превышали 70 мГр. Оценка абсолютного и относительного количества CD34⁺-клеток в периферической крови у хронически облученных лиц проводили методом проточной цитометрии. В группе лиц, облученных в период внутриутробного и постнатального развития, не выявлено изменение количества CD34⁺-клеток относительно группы сравнения, возрастная зависимость также не зарегистрирована. При этом отмечено значимое снижение абсолютного количества ГСК и клеток-предшественников с увеличением дозы облучения ККМ. В группе лиц, облученных только постнатально, обнаружено значимое увеличение показателей CD34⁺-клеток периферической крови относительно группы сравнения (для абсолютного количества $p = 0,004$; для относительного — $p = 0,009$), отмечено дозозависимое увеличение ГСК и клеток-предшественников в периферической крови (для абсолютного количества $p = 0,02$; для относительного — $p = 0,03$), при этом зарегистрировано снижение данного типа клеток с возрастом (для абсолютного количества $p = 0,02$, для относительного — $p = 0,04$).

Ключевые слова: гемопоэтические стволовые клетки, хроническое облучение, отдаленные эффекты, периферическая кровь, проточная цитометрия

Финансирование: исследование выполнено в рамках государственного задания «Состояние клеточного иммунитета человека в период реализации отдаленных эффектов хронического радиационного воздействия» (код 27.002.20.800).

Вклад авторов: А. И. Котикова — постановка методики, лабораторные исследования, статистическая обработка, написание текста статьи; Е. А. Блинова — постановка методики, написание текста статьи; А. В. Аклеев — концепция исследования, научное руководство.

Соблюдение этических стандартов: исследование одобрено этическим комитетом ФГБУН УНПЦ РМ ФМБА России (протокол № 3 от 20 июля 2021 г.). Добровольное информированное согласие было получено от всех участников исследований, проводимых на базе лаборатории молекулярно-клеточной радиобиологии ФГБУН УНПЦ РМ ФМБА России.

✉ **Для корреспонденции:** Алиса Игоревна Котикова
ул. Воровского, д. 68, corp. А, г. Челябинск, Россия, 454141; kotikovaalisa@gmail.com

Статья получена: 21.07.2021 **Статья принята к печати:** 10.08.2021 **Опубликована онлайн:** 03.09.2021

DOI: 10.47183/mes.2021.023

More than 60 years ago, residents of the villages located along the Techa River, were chronically exposed to radiation due to liquid radioactive waste discharged by Mayak Production Association. Uneven radiation dose distribution in the body was the feature of the exposure. The highest radiation dose was received by red bone marrow due to accumulation of osteotropic ^{90}Sr in bone tissue [1]. As a result, there had been a stable decrease in peripheral blood platelet and leukocyte counts in exposed individuals in the early days with the dose rate exceeding 0.3–0.5 Gy/year [2].

Currently, restoration of the majority of immunocompetent cell pools is observed [3]. However, pro-inflammatory shift in the cytokine system together with steady decline in the neutrophil counts are registered against a background of normal G-CSF and GM-CSF [3, 4]. Structural and functional impairments in hematopoietic stem cell (HSC) pool and progenitor cells resulting from long-term radiation exposure to both HSCs and microenvironment cells can be the cause of the observed late effects on the immune system.

The study was aimed to quantify peripheral blood CD34⁺ cell pool in individuals chronically exposed to radiation over a long-term period.

METHODS

A total of 153 patients of the Ural Research Center for Radiation Medicine clinical department were enrolled. Inclusion criteria: residence in the villages located along the Techa River in 1950–1960; availability of calculated absorbed dose to red bone marrow, thymus and peripheral lymphoid organs [5]; no diagnostic or therapeutic radiation exposure for a period of 6 months before the study; no history of cancer, autoimmune diseases, acute or chronic inflammatory disorders (exacerbation of inflammation) for a period of 6 months before the study; no treatment with hormones, antibiotics and cytostatic drugs for a period of 6 months before the study. Exclusion criteria: failure

to meet any of the listed above criteria.

All the subjects were divided into several groups: individuals born in 1950–1960, individuals exposed *in utero* and postnatally, comparison group 1; individuals born until 1949 inclusive exposed only postnatally, comparison group 2. Comparison groups included patients living in similar economic and social environment with their postnatal absorbed dose to red bone marrow not exceeding 70 mGy [6]. Characteristics of the studied population are provided in Table 1.

Individuals exposed *in utero* and postnatally were significantly older compared to individuals of the comparison group 1 ($p < 0.001$). It is worthy of note, however, that both groups were of similar age range (Table 1). No significant differences in ethnicity and gender were revealed (Table 1).

Hematopoietic stem cells (HSCs) and progenitor cells, expressing CD34 receptor on their surface, are primarily concentrated in the bone marrow. However, a small proportion of these cells (about 10% of all HSCs present in human body) are also found in peripheral blood of healthy adult humans [7, 8]. In order to quantify CD34⁺ cells and immunocompetent cells, the 9 ml samples of venous blood from the patients' cubital vein were collected in the fasting state using the vacuum tube with K3-EDTA (Greiner Bio-One; Austria). Quantification of CD34⁺ cells in peripheral blood of the subjects was performed by flow cytometry with the use of StemKit Reagents (Beckman Coulter; France) and Epics flow cytometer (Beckman Coulter; USA) in accordance with the manufacturer's instructions.

Statistical data processing was performed using SigmaPlot software (Systat Software Inc; USA). Mann–Whitney U test was used to compare CD34⁺ cell counts in peripheral blood of patients from the studied groups. The differences were considered significant when $p < 0.05$. The relationship between the peripheral blood CD34⁺ cell counts and the absorbed dose to red bone marrow, thymus, and peripheral lymphoid organs, or age, was defined using the Spearman's rank-order correlation; correlations were considered significant

Table 1. Characteristics of the studied population

Criteria		Individuals born in 1950–1960		Individuals born until 1949 inclusive	
		Comparison group 1 $n^* = 60$	Individuals exposed <i>in utero</i> and postnatally $n = 27$	Comparison group 2 $n = 19$	Individuals exposed only postnatally $n = 47$
Ethnicity, % (n)	Slavs	62 (37)	52 (14)	32 (6)	45 (21)
	Turks	38 (23)	48 (13) $p^{***} = 0,5$	68 (13)	55 (26) $p^{***} = 0,5$
Gender, % (n)	Males	40 (24)	30 (8)	37 (7)	21 (10)
	Females	60 (36)	70 (19) $p^{****} = 0,5$	63 (12)	79 (37) $p^{****} = 0,5$
Average age, years, $M \pm SE^{**}$ (min–max)		63,71 \pm 0,35 (60–69)	68,07 \pm 0,25 (66–71) $p^{*****} < 0,001$	77,05 \pm 1,06 (70–87)	74,72 \pm 0,58 (70–84) $p^{*****} = 0,06$
Postnatal absorbed dose to red bone marrow, mGy, $M \pm SE$ (min–max)		20 \pm 2 (0–68)	570 \pm 90 (80–1720)	10 \pm 4 (0,4–50)	790 \pm 90 (80–2930)
Postnatal absorbed dose to thymus and peripheral lymphoid organs, mGy, $M \pm SE$ (min–max)		0,9 \pm 0,2 (0–8)	80 \pm 20 (2–430)	8 \pm 2 (0,08–30)	110 \pm 10 (8–370)
Fetal absorbed dose to red bone marrow, mGy, $M \pm SE$ (min–max)		8 \pm 2 (0,2–3)	70 \pm 20 (0–360)	–	–
Fetal absorbed dose to thymus and peripheral lymphoid organs, mGy, $M \pm SE$ (min–max)		0,9 \pm 0,2 (0–8)	10 \pm 7 (0–170)	–	–

Note: n^* — studied population size; $M \pm SE$ — mean \pm standard error of the mean; *** — significance level for intergroup differences in ethnicity; **** — significance level for intergroup differences in gender; ***** — significance level for intergroup differences in age.

Table 2. Levels of CD34⁺ cells in peripheral blood of the subjects

Indicator		Absolute CD34 ⁺ cell counts, cells/ μ L	Relative CD34 ⁺ cell counts, %
Me (25%–75%)	Comparison group 1, $n = 60$	37,00 (24–64)	0,04 (0,03–0,07)
	Individuals exposed in utero and postnatally, $n = 27$	31,00 (22–61) $p_1 = 0,32$	0,04 (0,03–0,06) $p_2 = 0,67$
	Comparison group 2, $n = 19$	20,00 (15–28)	0,03 (0,02–0,04)
	Individuals exposed only postnatally, $n = 47$	36,00 (20–50) $p_3 = 0,004$	0,04 (0,03–0,07) $p_4 = 0,009$

Note: Me — median; p_1 — significance level for differences in absolute CD34⁺ cell counts in the groups of individuals born in 1950–1960; p_2 — significance level for differences in relative CD34⁺ cell counts in the groups of individuals born in 1950–1960; p_3 — significance level for differences in absolute CD34⁺ cell counts in the groups of individuals born until 1949 inclusive; p_4 — significance level for differences in relative CD34⁺ cell counts in the groups of individuals born until 1949 inclusive.

when $p < 0.05$. Qualitative features of the correlation were defined based on the correlation coefficients in accordance with the Chaddock scale.

RESULTS

No significant changes in absolute and relative peripheral blood CD34⁺ cell counts were detected in individuals, exposed *in utero* and postnatally, compared to the 1st comparison group ($p = 0,32$ and $p = 0,67$ respectively). However, in the group of individuals exposed only postnatally, a significant increase in peripheral blood CD34⁺ cell counts was observed compared to individuals from the 2nd comparison group (Table 2) (significance level for differences in absolute CD34⁺ cell counts: $p = 0.004$; significance level for differences in relative CD34⁺ cell counts: $p = 0.009$).

In the group of individuals born in 1950–1960, there was a slight significant decline in absolute CD34⁺ cell counts in relation to postnatal absorbed dose to red bone marrow ($r = -0.24$; $p = 0.03$). Moreover, a slight significant decline in both absolute ($r = -0.26$; $p = 0.02$) and relative ($r = -0.23$; $p = 0.03$) CD34⁺ cell counts in peripheral blood in relation to postnatal absorbed dose to thymus and peripheral lymphoid organs was observed. No significant relationships between the studied parameters and fetal doses (significance level for fetal absorbed dose to red bone marrow and absolute CD34⁺ cell counts: $p = 0.94$; significance level for relative cell counts: $p = 0.98$; significance

level for fetal absorbed dose to thymus and peripheral lymphoid organs and absolute CD34⁺ cell counts: $p = 0.48$; significance level for relative cell counts: $p = 0.74$). Regression analysis revealed no significant dose-dependent changes in peripheral blood CD34⁺ cell counts in individuals born in 1950–1960.

In the group of individuals born until 1949 inclusive, correlation analysis of dose-dependent changes in peripheral blood CD34⁺ cell counts revealed a slight significant decline in both absolute ($r = 0.29$; $p = 0.02$) and relative ($r = 0.26$; $p = 0.03$) CD34⁺ cell counts in relation to postnatal absorbed dose to red bone marrow. No significant correlations between the CD34⁺ cell counts and postnatal absorbed dose to thymus and peripheral lymphoid organs were found (significance level for absolute HSC and progenitor cell counts: $p = 0.14$; significance level for relative cell counts: $p = 0.19$). Regression analysis revealed no significant relationships between CD34⁺ cell counts and postnatal absorbed dose to red bone marrow, thymus and peripheral lymphoid organs.

On order to define the relationship between CD34⁺ cell counts and age, we decided to merge comparison group 1 (individuals born in 1950–1960) and comparison group 2 (individuals born until 1949 inclusive) for correlation analysis. In the joint comparison group, a slight significant decline in peripheral blood absolute ($r = -0.58$; $p < 0.001$) and relative ($r = -0.44$; $p < 0.001$) CD34⁺ cell counts with age was observed. Correlation of blood HSC and progenitor cell counts with age in the joint comparison group was assessed with the use of

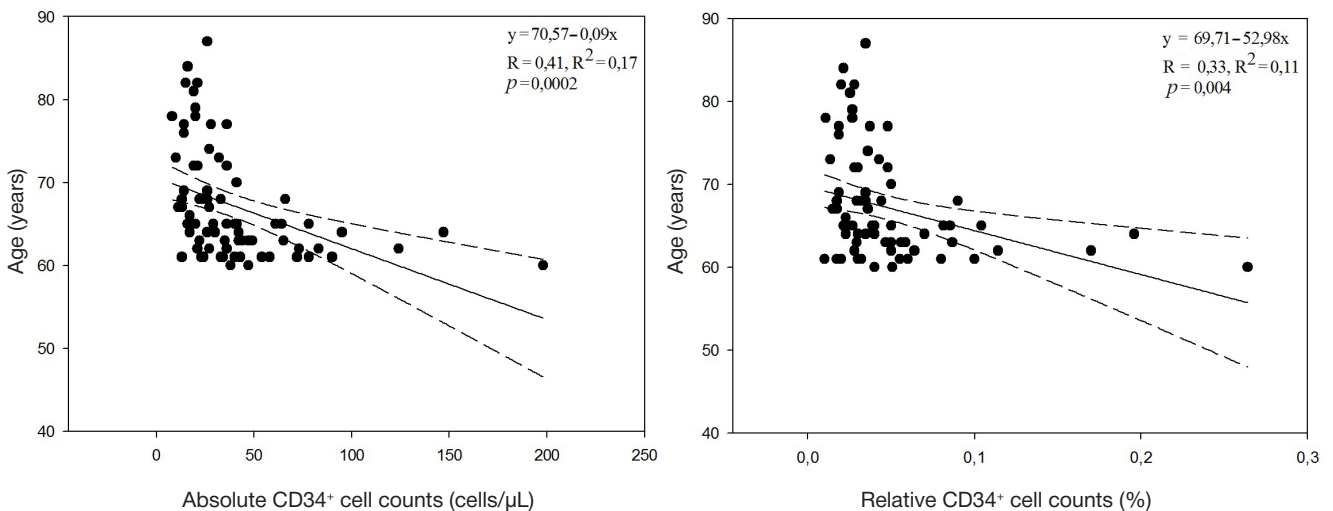


Fig. Correlation of peripheral blood CD34⁺ cell counts with age in individuals of joint comparison group

regression analysis. Results of regression analysis of age-related changes in peripheral blood absolute and relative CD34⁺ cell counts in individuals from the joint comparison group are presented in Fig.

In the group of individuals exposed *in utero* and postnatally, no significant correlation of peripheral blood absolute ($p = 0.14$) and relative ($p = 0.36$) CD34⁺ cell counts with age was observed at the time of the study.

In the group of individuals exposed only postnatally, there was a significant decline in peripheral blood CD34⁺ cell counts with age at the time of the study (significance level for absolute counts: $p = 0.02$ ($r = -0.33$); significance level for relative counts: $p = 0.04$ ($r = -0.29$)). Regression analysis revealed no significant correlation of peripheral blood HSC and progenitor cell counts with age in individuals exposed only postnatally.

DISCUSSION

Currently, there are no reliable data on the condition of HSC pool over a long time following chronic exposure to radiation. However, there is evidence obtained during experiments on mice, which demonstrates the following late effects of radiation exposure: permanent phenotypic change in the population of red bone marrow HSCs [10], increased levels of apoptosis in HSCs, as well as accumulation of DNA damage in HSCs and progenitor cells [10–12]. The observed effects are believed to result from asymmetric division of HSCs in the bone marrow: one daughter cell remains a stem cell retaining genomic alterations resulting from the parent cell radiation exposure, together with the bystander effect, observed during the experiment involving transplantation of exposed and non-exposed murine HSCs [12]. Functional failure in HSCs and progenitor cells over a long-term period could be a result of all listed above late effects of radiation exposure.

The paper reports preliminary results of the peripheral blood HSC pool and progenitor cell assessment in chronically exposed residents of the villages located along the Techa River over a long-term period after the onset of exposure. Peripheral blood CD34⁺ cell counts were defined in chronically exposed individuals 60 years after the beginning of the exposure against a background of involution changes. Earlier, high levels of unstable chromosome aberrations in peripheral blood lymphocytes, which could not be explained by the dose from current exposure, were observed in residents of the villages located along the Techa River during assessment, performed over a long-term period [13].

The detected dose-dependent decline in peripheral blood CD34⁺ cell counts in individuals, exposed *in utero* and postnatally, could be due to radiation-induced damage to the HSC pool precisely during the period of embryonic development, being the most sensitive to ionizing radiation exposure [14]. Meanwhile, lack of age-related changes in peripheral blood HSC and progenitor cell counts in this group could be explained by age range of individuals, exposed *in utero* and postnatally, inadequate (five years only) for establishing the relationship. It should be noted that in the group of individuals

exposed only postnatally, there was a negative correlation between the CD34⁺ cell counts and the subjects' age. Age-related decline in CD34⁺ cell counts in the group of individuals exposed only postnatally does not conflict with the literary evidence. Literature sources report reduced pool of HSCs and progenitor cells in peripheral blood of Japanese Hiroshima atomic bomb survivors [7, 9, 15].

Old age of exposed individuals creates a burden on the body. Thus, age-related alterations in HSC and progenitor cell metabolism have been shown [16], resulting in cellular adaptation deterioration. Such involution processes occurring against a background of chronic exposure make it possible to register effects of HSC pool and progenitor cell deficits over a long time after chronic radiation exposure.

Furthermore, in the group of individuals exposed only postnatally, there was a positive correlation between the HSC and progenitor cell counts and postnatal absorbed dose to red bone marrow; these indicator values were higher compared to the 2nd comparison group. However, alterations in peripheral blood cell composition, i.e. low neutrophil and lymphocyte counts, are registered in individuals exposed only postnatally even 60 and more years after the onset of chronic radiation exposure [3]. Thus, our findings may reflect activation of compensatory mechanisms, enabling continuous proliferation of HSCs and progenitor cells in response to the listed above alterations.

The resulting data on dose-dependent changes in peripheral blood CD34⁺ cell counts of chronically exposed individuals differ from the previously published data [16], showing no dose-dependent changes in peripheral blood HSC and progenitor cell counts of the ageing cohort of Hiroshima atomic bomb survivors. This fact could be due to the nature of radiation exposure: residents of the villages located along the Techa River were exposed mainly to chronic ⁹⁰Sr contamination, affecting precisely haematopoietic areas of red bone marrow.

CONCLUSIONS

The study shows increased hematopoietic stem cell (HSC) pool size and progenitor cells in peripheral blood of individuals exposed postnatally. The group of individuals exposed *in utero* and postnatally was comparable to comparison group 1 based on peripheral blood CD34⁺ cell counts. Slight significant correlations of CD34⁺ cell counts with the dose have been defined in the groups of individuals exposed *in utero* and postnatally, and individuals exposed only postnatally. However, the correlations were multidirectional: peripheral blood HSC and progenitor cell counts in individuals exposed *in utero* and postnatally dose dependently decrease; blood HSC and progenitor cell counts in individuals exposed only postnatally dose dependently increase. The results obtained are preliminary. Further research will make it possible to acquire more reliable data on the impact of low-intensity irradiation of red bone marrow on the number of HSCs and progenitor cells over a long time after chronic radiation exposure.

References

1. Akleyev AV, et al., editors. Consequences of radioactive contamination of the Techa River. Federal Medical and Biological Agency, Ural Research Center for Radiation Medicine. Chelyabinsk, 2016; 390 p. Russian.
2. ICRP Statement on tissue reactions. Early and late effects of radiation in normal tissues and organs — threshold doses for tissue reactions in a radiation protection context. ICRP Publication 118. Ann ICRP. 2012; 41 (1/2); 322 p.

3. Akleyev AA. Immune status of a man long after chronic radiation exposure. *medical radiology and radiation safety*. 2020; 65 (4): 29–35. DOI: 10.12737/1024-6177-2020-65-4-29-35. Russian.
4. Varfolomeyeva TA, Akleyev AA, Mandrykina AS. The characteristics of homeostasis in individuals chronically exposed to radiation in the South Urals at late time after exposure. *Medical Radiology and Radiation Safety*. 2016; 61 (2): 39–45. Russian.
5. Degteva MO, Napier BA, Tolstykh EI, Shishkina EA, Bougrov NG, Krestinina LYu, Akleyev AV. Individual dose distribution in cohort of people exposed as a result of radioactive contamination of the Techa river. *Medical Radiology and Radiation Safety*. 2019; 64 (3): 46–53. DOI: 10.12737/article_5cf2364cb49523.98590475. Russian.
6. СанПин 2.6.1.2523-09 "Standards of radiation safety (NRB - 99/2009)". М., 2009; 225p.
7. Kato K, Omori A, Kashiwakura I. Radiosensitivity of human haematopoietic stem/progenitor cells. *J Radiol Prot*. 2013; 33 (1): 71–80. DOI:10.1088/0952-4746/33/1/71.
8. Mauch P, Constine L, Greenberger J, et al. Hematopoietic stem cell compartment: acute and late effects of radiation therapy and chemotherapy. *Int J Radiat Oncol Biol Phys*. 1995; 31 (5): 1319–39. DOI: 10.1016/0360-3016(94)00430-S.
9. Kato K, Kuwabara M, Kashiwakura I. The influence of gender- and age-related differences in the radiosensitivity of hematopoietic progenitor cells detected in steady-state human peripheral blood. *J Radiat Res*. 2011; 52 (3): 293–9. DOI: 10.1269/jrr.10142.
10. Simonnet AJ, Nehmé J, Vaigot P, Barroca V, Leboulch P, Tronik-Le Roux D. Phenotypic and functional changes induced in hematopoietic stem/progenitor cells after gamma-ray radiation exposure. *Stem Cells*. 2009; 27 (6): 1400–9. DOI: 10.1002/stem.66.
11. Lorimore SA, Wright EG. Radiation-induced genomic instability and bystander effects: related inflammatory-type responses to radiation-induced stress and injury? A review. *Int J Radiat Biol*. 2003; 79 (1): 15–25.
12. Harfouche G, Martin MT. Response of normal stem cells to ionizing radiation: a balance between homeostasis and genomic stability. *Mutat Res*. 2010; 704 (1–3): 167–74. DOI: 10.1016/j.mrrev.2010.01.007.
13. Vozilova AV, Shagina NB, Degteva MO, Akleyev AV. Chronic radioisotope effects on residents of the Techa river (Russia) region: Cytogenetic analysis more than 50 years after onset of exposure. *Mutation Research/Genetic Toxicology and Environmental Mutagenesis*. 2013; 756 (1–2): 115–18. DOI: 10.1016/j.mrgentox.2013.05.016.
14. Barber RC, Hardwick RJ, Shanks ME, et al. The effects of in utero irradiation on mutation induction and transgenerational instability in mice. *Mutat Res*. 2009; 664: 6–12. DOI: 10.1016/j.mrfmmm.2009.01.011.
15. Vorotelyak EA, Vasiliev AV, Terskikh VV. The problem of stem cell definition. *Cytology*. 2019; 61 (1): 3–15. DOI: 10.1134/S0041377119010073.
16. Kyoizumi S, Kubo Y, Misumi M, et al. Circulating hematopoietic stem and progenitor cells in aging atomic bomb survivors. *Radiat Res*. 2016; 185 (1): 69–76. DOI:10.1667/RR14209.1.

Литература

1. Аклеев А. В. и др., редакторы. Последствия радиоактивного загрязнения реки Течи. Федеральное медико-биологическое агентство, Уральский научно-практический центр радиационной медицины. Челябинск, 2016; 390 с.
2. ICRP Statement on tissue reactions. Early and late effects of radiation in normal tissues and organs — threshold doses for tissue reactions in a radiation protection context. ICRP Publication 118. *Ann ICRP*. 2012; 41 (1/2); 322 p.
3. Аклеев А. А. Иммунный статус человека в отдаленном периоде хронического радиационного воздействия. *Медицинская радиология и радиационная безопасность*. 2020; 65 (4): 29–35. DOI: 10.12737/1024-6177-2020-65-4-29-35.
4. Варфоломеева Т. А., Аклеев А. А., Мандрыкина А. С. Показатели гомеостаза в отдаленном периоде у лиц, подвергшихся хроническому облучению на Южном Урале. *Медицинская радиология и радиационная безопасность*. 2016; 61 (2): 39–45.
5. Дегтева М. О., Напье Б.А., Толстых Е.И., Шишкина Е. А., Бугров Н. Г., Крестинина Л. Ю., Аклеев А. В. Распределение индивидуальных доз в когорте людей, облученных в результате радиоактивного загрязнения реки Течи. *Медицинская радиология и радиационная безопасность*. 2019; 64 (3): 46–53. DOI: 10.12737/article_5cf2364cb49523.98590475.
6. СанПин 2.6.1.2523-09 «Нормы радиационной безопасности (НРБ - 99/2009)». М., 2009; 225 с.
7. Kato K, Omori A, Kashiwakura I. Radiosensitivity of human haematopoietic stem/progenitor cells. *J Radiol Prot*. 2013; 33 (1): 71–80. DOI:10.1088/0952-4746/33/1/71.
8. Mauch P, Constine L, Greenberger J, et al. Hematopoietic stem cell compartment: acute and late effects of radiation therapy and chemotherapy. *Int J Radiat Oncol Biol Phys*. 1995; 31 (5): 1319–39. DOI: 10.1016/0360-3016(94)00430-S.
9. Kato K, Kuwabara M, Kashiwakura I. The influence of gender- and age-related differences in the radiosensitivity of hematopoietic progenitor cells detected in steady-state human peripheral blood. *J Radiat Res*. 2011; 52 (3): 293–9. DOI: 10.1269/jrr.10142.
10. Simonnet AJ, Nehmé J, Vaigot P, Barroca V, Leboulch P, Tronik-Le Roux D. Phenotypic and functional changes induced in hematopoietic stem/progenitor cells after gamma-ray radiation exposure. *Stem Cells*. 2009; 27 (6): 1400–9. DOI: 10.1002/stem.66.
11. Lorimore SA, Wright EG. Radiation-induced genomic instability and bystander effects: related inflammatory-type responses to radiation-induced stress and injury? A review. *Int J Radiat Biol*. 2003; 79 (1): 15–25.
12. Harfouche G, Martin MT. Response of normal stem cells to ionizing radiation: a balance between homeostasis and genomic stability. *Mutat Res*. 2010; 704 (1–3): 167–74. DOI: 10.1016/j.mrrev.2010.01.007.
13. Vozilova AV, Shagina NB, Degteva MO, Akleyev AV. Chronic radioisotope effects on residents of the Techa river (Russia) region: Cytogenetic analysis more than 50 years after onset of exposure. *Mutation Research/Genetic Toxicology and Environmental Mutagenesis*. 2013; 756 (1–2): 115–18. DOI: 10.1016/j.mrgentox.2013.05.016.
14. Barber RC, Hardwick RJ, Shanks ME, et al. The effects of in utero irradiation on mutation induction and transgenerational instability in mice. *Mutat Res*. 2009; 664: 6–12. DOI: 10.1016/j.mrfmmm.2009.01.011.
15. Воротеяк Е. А., Васильев А. В., Терских В. В. Проблема дефиниции стволовой клетки. *Цитология*. 2019; 61 (1): 3–15. DOI: 10.1134/S0041377119010073.
16. Kyoizumi S, Kubo Y, Misumi M, et al. Circulating hematopoietic stem and progenitor cells in aging atomic bomb survivors. *Radiat Res*. 2016; 185 (1): 69–76. DOI:10.1667/RR14209.1.

BCL-2, CDKN1A AND ATM GENE METHYLATION IN CHRONICALLY EXPOSED INDIVIDUALSBlinova EA^{1,2}✉, Nikiforov VS^{1,2}, Yanishevskaya MA¹, Akleyev AV^{1,2}¹ Urals Research Center for Radiation Medicine of the Federal Medical Biological Agency, Chelyabinsk, Russia² Chelyabinsk State University, Chelyabinsk, Russia

DNA methylation is the most common epigenetic modification, caused by ionizing radiation. There may be both hypermethylation, which suppresses transcription of gene promoter regions, and hypomethylation, resulting in gene activation. Both mechanisms may be involved in carcinogenesis. The study was aimed to assess methylation status of CpG islands in the protective system *BCL-2*, *CDKN1A* and *ATM* gene promoters in the peripheral blood cells of the chronically exposed individuals, living in the villages, located along the Techa River, over a long-term period. Methylation of *BCL-2*, *CDKN1A* and *ATM* gene promoter regions in 68 residents of the villages, located along the Techa River (Chelyabinsk region), was assessed by the real-time methylation-specific PCR. The group of exposed individuals included 54 people with accumulated dose to red bone marrow within the range of 0.09–3.51 Gy. The comparison group included 14 people, living in similar economic and social environment, with the dose to red bone marrow, accumulated during the whole life, not exceeding 70 mGy. The pilot study of exposed individuals over a long period of time after chronic low-dose radiation exposure revealed no significant changes in methylation levels of CpG islands in the *CDKN1A*, *BCL-2*, *ATM* gene promoter regions compared to the comparison group. None were revealed in the dose subgroups “87–994 mGy” and “over 1000 mGy”.

Keywords: DNA methylation, CpG islands, long-term effects of exposure, chronic exposure, methylation-specific PCR

Funding: the study was carried out within the framework of the State assignment of Russian Federal Medical Biological Agency “Human Cell-Mediated Immunity During Realization of Chronic Radiation Exposure Late Effects” (code 27.002.20.800).

Author contribution: Blinova EA — literature analysis, experimental procedure, data processing, manuscript writing; Nikiforov VS — literature analysis, experimental procedure, manuscript writing; Yanishevskaya MA — experimental procedure, manuscript editing; Akleyev AV — general management, manuscript writing.

Compliance with ethical standards: the study was approved by the Ethics Committee of Ural Research Center for Radiation Medicine of Russian Federal Medical Biological Agency (protocol № 2 dated July 20, 2021). The informed consent was submitted by all examined individuals.

✉ **Correspondence should be addressed:** Evgeniya A. Blinova
Vorovskogo, 68, korp. 1, Chelyabinsk, 454141; blinova@urcrm.ru

Received: 27.07.2021 **Accepted:** 29.08.2021 **Published online:** 21.09.2021

DOI: 10.47183/mes.2021.028

МЕТИЛИРОВАНИЕ ГЕНОВ *BCL-2*, *CDKN1A* И *ATM* У ЛИЦ, ПОДВЕРГШИХСЯ ХРОНИЧЕСКОМУ ОБЛУЧЕНИЮЕ. А. Блинова^{1,2}✉, В. С. Никифоров^{1,2}, М. А. Янишевская¹, А. В. Аклеев^{1,2}¹ Уральский научно-практический центр радиационной медицины Федерального медико-биологического агентства, Челябинск, Россия² Челябинский государственный университет, Челябинск, Россия

Метилирование ДНК является наиболее распространенной эпигенетической модификацией, вызываемой ионизирующим излучением. При этом можно наблюдать как гиперметилирование, которое подавляет транскрипцию промоторных областей генов, так и гипометилирование, приводящее к активации генов. Оба указанных механизма могут принимать участие в канцерогенезе. Целью настоящего исследования было оценить статус метилирования CpG-островков промоторов генов защитных систем *BCL-2*, *CDKN1A* и *ATM* в клетках периферической крови у хронически облученных жителей прибрежных сел р. Течи (Челябинская область) в отдаленные сроки. Оценку метилирования промоторных регионов генов *BCL-2*, *CDKN1A* и *ATM* у 68 человек, проживающих в селах, расположенных по берегам р. Течи, проводили методом метилспецифичной ПЦР в реальном времени. В группу облученных лиц вошли 54 человека, у которых кумулятивные дозы красного костного мозга находились в диапазоне от 0,09 до 3,51 Гр. Группа сравнения состояла из 14 человек, проживающих в схожих социально-экономических условиях с накопленной дозой облучения красного костного мозга менее 70 мГр за весь период своей жизни. В результате проведенного пилотного исследования у облученных лиц в отдаленном периоде после хронического низкоинтенсивного радиационного воздействия не были выявлены значимые изменения в уровне метилирования CpG-островков промоторных регионов генов *CDKN1A*, *BCL-2*, *ATM* относительно группы сравнения, также не были отмечены изменения в дозовых подгруппах «от 87 до 994 мГр» и «более 1000 мГр».

Ключевые слова: метилирование ДНК, CpG-островки, отдаленные эффекты облучения, хроническое облучение, метилспецифичная ПЦР

Финансирование: исследование в рамках государственного задания Федерального медико-биологического агентства России «Состояние клеточного иммунитета человека в период реализации отдаленных эффектов хронического радиационного воздействия» (27.002.20.800).

Вклад авторов: Е. А. Блинова — анализ литературы, экспериментальная часть, обработка данных, написание текста статьи; В. С. Никифоров — анализ литературы, экспериментальная часть, написание текста статьи; М. А. Янишевская — экспериментальная часть, редактирование текста статьи; А. В. Аклеев — общее руководство, написание текста статьи.

Соблюдение этических стандартов: исследование одобрено этическим комитетом ФГБУН УНПЦ РМ ФМБА России (протокол № 2 от 20 июля 2021 г.). Все обследованные лица подписали информированное согласие на участие в исследовании.

✉ **Для корреспонденции:** Евгения Андреевна Блинова
ул. Воровского, д. 68, корп. 1, г. Челябинск, 454141; blinova@urcrm.ru

Статья получена: 27.07.2021 **Статья принята к печати:** 29.08.2021 **Опубликована онлайн:** 21.09.2021

DOI: 10.47183/mes.2021.028

DNA methylation is the most common epigenetic modification, playing a vital part in regulation of cellular processes, especially in gene expression and genomic instability [1]. Of all epigenetic modifications, hypermethylation, which suppresses transcription of gene promoter regions, decreasing gene expression or causing the total shutdown of genes, is the most extensively studied [2]. However, recently there is also growing information on global hypomethylation as a factor of carcinogenesis [3].

DNA methylation status, being a rather labile system, depends largely on endogenous factors (aberrant methyltransferase activity, defects in cell's repair machinery) [4], and exogenous factors, including factors related to radiation. Thus, experimental studies involving mice showed a pronounced abnormal methylation of the tumor suppressor gene *p16(INKa)* promoter upon chronic low-dose radiation exposure (50 cGy). Moreover, the authors note that chronic exposure to low-dose radiation is a more powerful inducer of epigenetic effects and therefore of genomic destabilization, than the same dose acute exposure [5].

However, regardless of the actively studied human methylation status upon exposure to various adverse factors, there are currently just a few studies, showing the induction and long-term persistence of epigenetic modifications in human peripheral blood leukocytes after exposure. The existing results of a number of studies show that ionizing radiation mediates persistent DNA methylation status changes in a wide range of doses. Thus, the paper [6] reports aberrant radiation-induced methylation of genes *GSTP1*, *CDKN2A*, *ARF* and *RASSF1A* over a long period of time after exposure in the Chernobyl liquidators. Radiographers, who experienced radiation exposure in a low dose range, had genome methylation levels significantly lower compared to non-exposed individuals [7]. Hypomethylation was identified during the following study [8]: the decline in methylation of apoptosis genes (*BAD*, *BID*, *HRK*) with increasing absorbed dose was observed in blood lymphocytes of employees, who experienced occupational exposure to external radiation. Such an effect may be indicative of the differential epigenome response to low-dose and high-dose radiation exposure.

In order to present reliable findings on the DNA methylation influence on the phenotype, the changes in methylation status of gene promoter regions should be presented in the context of altered gene expression patterns. As demonstrated earlier, in the peripheral blood cells of exposed individuals after a long period of time since after exposure, the changes in homeostatic system and cellular immune response gene mRNA expression were observed. In particular, low proportion of the *BCL-2* and *NFKB1* gene mRNAs together with high levels of the *BAX* and *PADI4* gene mRNAs were revealed in chronically exposed individuals over a long-term period. The decreased expression of the *CDKN1A* and *ATM* gene mRNAs was revealed in individuals, having doses to red bone marrow exceeding 1000 mGy [9].

The study was aimed to assess methylation status of CpG islands in *BCL-2*, *CDKN1A* and *ATM* gene promoters in peripheral blood cells of chronically exposed residents of the villages, located along the Techa River, over a long-term period.

METHODS

Methylation of gene promoter regions was assessed in individuals, living in the villages, located along the Techa River (Chelyabinsk region). The subjects were selected using the medical-dosimetric database developed by the department

“Database “Man” of the Urals Research Center for Radiation Medicine of the Federal Medical Biological Agency. Inclusion criteria: individuals born until 1960 inclusive; permanent residence in the territories along the Techa River in 1950–1960; availability of reconstructed absorbed dose to red bone marrow, calculated using the TRDS-2016 (Techa River Dosimetry System, version 2016) by specialists of the biophysics laboratory of the Urals Research Center for Radiation Medicine [10]. Exclusion criteria: chronic inflammatory diseases, cancer or autoimmune disorders; treatment with antibiotics, hormones or cytostatic drugs; diagnostic or therapeutic radiation exposure during a period of 6 months prior to blood sample collection; occupational exposure to chemical (genotoxic) agents.

The group of exposed individuals included 54 people with accumulated dose to red bone marrow within the range of 87–3510 mGy (the average value was 960 ± 100 mGy). Accumulated dose to red bone marrow in the majority of exposed people (36 individuals, 66.7%) was within the range of 100–994 mGy. In 18 individuals, the dose exceeded 1000 mGy (33.3%). The comparison group included 14 individuals, living in similar economic, social and household environment (rural population). However, their annual dose to red bone marrow did not exceed 1 mGy/year, and the dose accumulated during the whole life was less than 70 mGy. The studied group included males and females of the following ethnic groups: Turks (mostly Tatars, Bashkirs) and Slavs, represented mostly by Russians. Characteristics of the studied groups are presented in Table 1.

DNA methylation was assessed in peripheral blood leukocytes. Samples were collected in the morning from the individuals in the fasting state using vacuum tubes with K3-EDTA. DNA was extracted from the whole blood using the GeneJET Genomic DNA Purification Kit (Thermo Scientific; USA) in accordance with the manufacturer's protocol.

The method of DNA methylation analysis was based on the specific detection of 5-methylcytosine or the products of 5-methylcytosine bisulfite conversion. Complete denaturation of genomic DNA and bisulfite treatment were performed in conditions, in which cytosine was converted stoichiometrically to uracil, but 5-methylcytosine remained nonreactive. Bisulfite conversion was performed using the EpiJET Bisulfite Conversion Kit (Thermo Scientific; USA) in accordance with the manufacturer's protocol.

Bisulfite-converted DNA was amplified with primers, specific for methylated and unmethylated DNA regions. The search for primers, required for amplification of the cell homeostatic system gene (*ATM*, *BCL-2*, *CDKN1A*) promoter region fragments using PCR, was carried out based on the available literature data. Oligonucleotides were synthesized by the DNA-Synthesis company (Russia). Characteristics of primers are presented in Table 2.

Methylation status of the gene sequences of interest was performed by the real-time methylation-specific PCR (RT-MS-PCR) using the StepOnePlus Real-Time PCR System (Applied Biosystems; USA). RT-MS-PCR was carried out with the use of the qPCRmix-HS SYBR ready-to-use reaction mix (Evrogen; Russia), containing high-fidelity Taq DNA polymerase with specific monoclonal antibodies, SYBR Green I dye, and the mixture of dNTP, Mg^{2+} , and PCR buffer. The PCR mixture component volume and amplification conditions complied with the manufacturer's protocol and instructions.

After amplification, the target product was assessed in the PCR mixture by 2% agarose gel electrophoresis. Qualitative assessment of the presence or absence of aberrant methylation in the studied samples was performed based on the results of the described above analysis.

Table 1. Characteristics of studied groups

Parameters of the groups		Exposed group <i>n</i> = 54	Comparison group <i>n</i> = 14
Age, years, mean ± SD (min-max)		73.5 ± 0.57 (65-83)	74.0 ± 0.97 (68-79)
Gender, <i>N</i> , (%)	Males	15 (27.8)	4 (28.6)
	Females	39 (72.2)	10 (79.0)
Ethnicity, <i>N</i> , (%)	Slavs	29 (46.3)	7 (50.0)
	Turks	31 (53.7)	7 (50.0)
Average dose to red bone marrow, mGy mean ± SD (min-max)		960 ± 100 (87-3510)	22 ± 4 (3-49)

CpG Methylated Human Genomic DNA (Thermo Scientific; USA) with known methylation levels ($\geq 98\%$) was used as a methylation-positive control for all genes.

PCR with primers for methylated and unmethylated gene sequences was performed for each sample. The results of gel electrophoresis were visualized using the Gel Doc XR+ gel documentation system (BioRad; USA). The presence of the amplified products after the RT-MS-PCR with primers for methylated gene regions, detected by gel electrophoresis, indicated the presence of aberrant methylation, and the presence of the amplified products with primers for unmethylated gene regions indicated no methylation.

Statistical processing of the results was performed with the Statistica software package (StatSoft; USA). The data were compared using Fisher's exact test. The differences were considered significant when $p < 0.05$.

RESULTS

The number of cases of the CpG islands' methylation in the *BCL-2*, *CDKN1A* and *ATM* gene promoters in peripheral blood cells of chronically exposed individuals is presented in Table 3.

There are no significant differences in the rate of CpG islands' methylation in the *BCL-2*, *CDKN1A* and *ATM* gene promoters between the exposed individuals and the comparison group. Comparison of CpG islands' methylation cases in the examined individuals of the dose subgroups "87-994 mGy" and "over 1000 mGy" with the comparison group also revealed no significant differences.

DISCUSSION

Epigenetic regulation, involving DNA methylation, plays a vital part in cellular processes, maintaining proper gene expression regulation. However, aberrant methylation may result in a

number of pathological conditions, genome instability and cancer [11]. It is known that ionizing radiation, being a genotoxic agent, contributes both to DNA hyper- and hypomethylation. The majority of *in vitro* and *in vivo* studies have shown that the genome epigenetic state changes have been dynamic enough early after the exposure [12]. However, there are just a few studies focused on the human DNA methylation status over a long period of time after radiation exposure. Thus, hypermethylation of CpG islands in the *p16/INKA* and *GSTP1* gene promoters was found in blood leukocytes of the Chernobyl liquidators and the Mayak Production Association employees, dealing with reactors and radiochemical production, over a long period of time after radiation exposure [13]. The opposite results were obtained when assessing radiographers. Thus, the paper [7] reports that low-dose radiation exposure (20 mSv per year or 100 mSv per 5 years) contributes to hypomethylation of genomic DNA in blood cells.

The results of our pilot study demonstrate no changes in methylation status of the CpG islands' methylation in the *CDKN1A*, *BCL-2* and *ATM* gene promoter regions in chronically exposed individuals over a long period of time.

It should be noted that radiation-induced effects, associated with DNA methylation, can be affected by a number of factors: type of exposed cells, physiological characteristics of examined individuals, radiation type, dose, and time after exposure.

The results obtained are inconclusive. Better understanding of the effects of chronic low-dose radiation exposure on methylation levels requires studying the greater sample of examined individuals, and quantitative analysis, involving calculating the proportion of the gene promoter region methylation.

CONCLUSIONS

The study revealed no differences in the number of cases of CpG islands' methylation in the *CDKN1A*, *BCL-2* and *ATM*

Table 2. Characteristics of oligonucleotides used for analysis

Gene	Primer type	Primer sequences (5'-3')	T _m , °C	Amplicon length, bps	Reference
<i>BCL-2</i>	Meth	Forward GTTTTACGTTTCGGTATCGG Reverse AAATCTCTATCCACGAAACCGC	60	192	[8]
	Unmeth	Forward GGGTTTTAGTGTGGTATTGG Reverse AAATCTCTATCCACAAAACCACTTC	59	194	
<i>ATM</i>	Meth	Forward GGAGTTCGAGTCGAAGGGC Reverse CTACCTACTCCCGCTTCCGA	59	239	[9]
	Unmeth	Forward GTTTTGGAGTTTGGAGTTGAAGGGT Reverse AACTACCTACTCCCACTTCCAA	56	246	
<i>CDKN1A</i>	Meth	Forward GTCGAAGTTAGTTTTTGTGGAGTC Reverse CGAAATCCCCTATTATCTACGC	65	230	[10]
	Unmeth	Forward TTGAAGTTAGTTTTTGTGGAGTTG Reverse CCAAATCCCCTATTATCTACCAC	66	230	

Note: T_m — melting temperature; Meth — methylated primer; Unmeth — unmethylated primer.

Table 3. Rate of CpG islands' methylation in *BCL-2*, *CDKN1A* and *ATM* gene promoters in peripheral blood cells of chronically exposed individuals

Gene/ <i>n</i> '	Comparison group < 49 mGy		All exposed individuals with the dose of 87–3510 mGy		Exposed individuals with the dose of 87–994 mGy		Exposed individuals with dose > 1000 mGy	
	MP % (<i>n</i>)	UMP % (<i>n</i>)	MP % (<i>n</i>)	UMP % (<i>n</i>)	MP % (<i>n</i>)	UMP % (<i>n</i>)	MP % (<i>n</i>)	UMP % (<i>n</i>)
<i>CDKN1A</i>	7.1 (1)	92.9 (13)	0.0 (0)	100 (53)	0 (0)	100 (36)	0 (0)	100 (17)
			F	<i>p</i>	F	<i>p</i>	F	<i>p</i>
			0.21	>0.05	0.28	>0.05	0.45	>0.05
<i>BCL-2</i>	18.2 (2)	81.8 (9)	40.4 (21)	59.6 (31)	50 (17)	50 (17)	22.2 (4)	77.8 (14)
			F	<i>p</i>	F	<i>p</i>	F	<i>p</i>
			0.3	>0.05	0.08	>0.05	1	>0.05
<i>ATM</i>	63.6 (7)	36.4 (4)	83.7 (41)	16.3 (8)	82.4 (28)	17.6 (6)	86.7 (13)	13.3 (2)
			F	<i>p</i>	F	<i>p</i>	F	<i>p</i>
			0.2	>0.05	0.23	>0.05	>0.05	1

Note: MP — number of individuals with methylated promoter; UMP — number of individuals with unmethylated promoter; F — Fisher's exact test; *p* — significance level.

gene promoter regions between the exposed individuals and the comparison group. The results obtained are provisional. Further on it is planned to extend the panel of

studied genes, and to define the proportion of methylation for each promoter region of the gene in the group of examined individuals.

References

- Spainhour JC, Lim HS, Yi SV, Qiu P. Correlation patterns between DNA methylation and gene expression in the Cancer Genome Atlas. *Cancer Inform.* 2019; (18): 1–11. DOI: 10.1177/1176935119828776. PMID: 30792573. PMCID: PMC6376553.
- Greenberg MVC, Bourchis D. The diverse roles of DNA methylation in mammalian development and disease. *Nat Rev Mol Cell Biol.* 2019; (20): 590–607. DOI: 10.1038/s41580-019-0159-6. PMID: 31399642.
- Van Tongelen A, Lorient A, De Smet C. Oncogenic roles of DNA hypomethylation through the activation of cancer-germline genes. *Cancer Lett.* 2017; 28 (396): 130–7. DOI: 10.1016/j.canlet.2017.03.029. PMID: 28342986.
- Edwards JR, Yarychivska O, Boulard M, Bestor TH. DNA methylation and DNA methyltransferases. *Epigenetics & Chromatin.* 2017; 10 (23): 1–10. DOI: 10.1186/s13072-017-0130-8.
- Kovalchuk O, Burke P, Besplug J, Slovack M, Filkowski J, Pogridny I. Methylation changes in muscle and liver tissues of male and female mice exposed to acute and chronic low dose X-ray irradiation. *Mutat Res.* 2004; 548 (1–2): 75–84. DOI: 10.1016/j.mrfmmm.2003.12.016. PMID: 15063138.
- Kuzmina NS. Изучение aberrантного метилирования в лейкоцитах крови ликвидаторов аварии на ЧАЭС. *Радиационная биология. Радиоэкология.* 2014; 54 (2): 127–39. Russian.
- Cho YH, Jang Y, Woo HD, Kim YJ, Kim SY, Christensen S, et al. LINE-1 Hypomethylation is associated with radiation-induced genomic instability in industrial radiographers. *Environ Mol Mutagen.* 2018; 60 (2): 174–84. DOI: 10.1002/em.22237.
- Isubakova DS, Cymbal OS, Bronikovskaja EV, Litvjakov NV, Milto IV, Tahauov RM. Метилирование промоторов генов апоптоза в лимфоцитах крови работников, подвергавшихся в процессе профессиональной деятельности долговременному внешнему облучению. *Бюллетень экспериментальной биологии и медицины.* 2021; 171 (3): 339–43. Russian.
- Nikiforov VS, Blinova EA, Akleev AV. Влияние комплекса факторов радиационной и нерadiационной природы на профиль транскрипционной активности генов у лиц, подвергшихся хроническому радиационному воздействию. *Вопросы радиационной безопасности.* 2019; 2 (94): 64–70. Russian.
- Degteva MO, Napier BA, Tolstykh EI, Shiskina EA, Bougrov NG, Krestinina LYu, Akleev AV. Individual dose distribution in cohort of people exposed as a result of radioactive contamination of the Techa River. *Medical Radiology and Radiation Safety.* 2019; 64 (3): 46–53. DOI: 10.12737/article_5cf2364cb49523.98590475.
- Kulis M, Esteller M. DNA methylation and cancer. *Adv Genet.* 2010; (70): 27–56. DOI: 10.1016/B978-0-12-380866-0.60002-2. PMID: 20920744.
- Jaenisch R. Epigenetic regulation of gene expression: how the genome integrates intrinsic and environmental signals. *Nat Genet.* 2003; (33): 245–54. DOI: 10.1038/ng1089. PMID: 12610534.
- Kuzmina NS, Lapteva NS, Rubanovich AB. Hypermethylation of gene promoters in peripheral blood leukocytes in humans long term after radiation exposure. *Environ Res.* 2016; (146): 10–17. DOI: 10.1016/j.envres.2015.12.008.

Литература

- Spainhour JC, Lim HS, Yi SV, Qiu P. Correlation patterns between DNA methylation and gene expression in the Cancer Genome Atlas. *Cancer Inform.* 2019; (18): 1–11. DOI: 10.1177/1176935119828776. PMID: 30792573. PMCID: PMC6376553.
- Greenberg MVC, Bourchis D. The diverse roles of DNA methylation in mammalian development and disease. *Nat Rev Mol Cell Biol.* 2019; (20): 590–607. DOI: 10.1038/s41580-019-0159-6. PMID: 31399642.
- Van Tongelen A, Lorient A, De Smet C. Oncogenic roles of DNA hypomethylation through the activation of cancer-germline genes. *Cancer Lett.* 2017; 28 (396): 130–7. DOI: 10.1016/j.canlet.2017.03.029. PMID: 28342986.
- Edwards JR, Yarychivska O, Boulard M, Bestor TH. DNA methylation and DNA methyltransferases. *Epigenetics & Chromatin.* 2017; 10 (23): 1–10. DOI: 10.1186/s13072-017-0130-8.
- Kovalchuk O, Burke P, Besplug J, Slovack M, Filkowski J, Pogridny I. Methylation changes in muscle and liver tissues of male and female mice exposed to acute and chronic low dose X-ray irradiation. *Mutat Res.* 2004; 548 (1–2): 75–84. DOI: 10.1016/j.mrfmmm.2003.12.016. PMID: 15063138.
- Кузьмина Н. С. Изучение aberrантного метилирования в лейкоцитах крови ликвидаторов аварии на ЧАЭС. *Радиационная биология. Радиоэкология.* 2014; 54 (2): 127–39.
- Cho YH, Jang Y, Woo HD, Kim YJ, Kim SY, Christensen S, et al. LINE-1 Hypomethylation is associated with radiation-induced genomic instability in industrial radiographers. *Environ Mol Mutagen.* 2018; 60 (2): 174–84. DOI: 10.1002/em.22237.

- Mutagen. 2018; 60 (2): 174–84. DOI: 10.1002/em.22237.
8. Исубакова Д. С., Цымбал О. С., Брониковская Е. В., Литвяков Н. В., Мильто И. В., Тахауов Р. М. Метилирование промоторов генов апоптоза в лимфоцитах крови работников, подвергавшихся в процессе профессиональной деятельности долговременному внешнему облучению. Бюллетень экспериментальной биологии и медицины. 2021; 171 (3); 339–43.
 9. Никифоров В. С., Блинова Е. А., Аклеев А. В. Влияние комплекса факторов радиационной и нерадиационной природы на профиль транскрипционной активности генов у лиц, подвергшихся хроническому радиационному воздействию. Вопросы радиационной безопасности. 2019; 2 (94): 64–70.
 10. Degteva MO, Napier BA, Tolstykh EI, Shiskina EA, Bougrov NG, Krestinina LYu, Akleev AV. Individual dose distribution in cohort of people exposed as a result of radioactive contamination of the Techa River. *Medical Radiology and Radiation Safety*. 2019; 64 (3): 46–53. DOI: 10.12737/article_5cf2364cb49523.98590475.
 11. Kulis M, Esteller M. DNA methylation and cancer. *Adv Genet*. 2010; (70): 27–56. DOI: 10.1016/B978-0-12-380866-0.60002-2. PMID: 20920744.
 12. Jaenisch R. Epigenetic regulation of gene expression: how the genome integrates intrinsic and environmental signals. *Nat Genet*. 2003; (33): 245–54. DOI: 10.1038/ng1089. PMID: 12610534.
 13. Kuzmina NS, Lapteva NSh, Rubanovich AB. Hypermethylation of gene promoters in peripheral blood leukocytes in humans long term after radiation exposure. *Environ Res*. 2016; (146): 10–17. DOI: 10.1016/j.envres.2015.12.008.

ISOLATION AND CHARACTERIZATION OF *PSEUDOMONAS AERUGINOSA* BACTERIOPHAGES — POTENTIAL AGENTS FOR PHAGE THERAPYKornienko MA , Kuptsov NS, Danilov DI, Gorodnichev RB, Malakhova MV, Bespiatykh DA, Veselovsky VA, Shitikov EA, Ilina EN

Federal Research and Clinical Center of Physical-Chemical Medicine of Federal Medical Biological Agency, Moscow, Russia

Pseudomonas aeruginosa — is one of the pathogens characterized by the critical number of multidrug-resistant (MDR) strains. Phage therapy is considered an alternative to antibiotics, especially in treatment of infections caused by MDR strains. The aim of this study was to isolate and characterize *P. aeruginosa* phages that could potentially be suitable for treating infectious diseases. To isolate the *P. aeruginosa* phages, enrichment cultures were used. The lytic activity spectrum was confirmed by spot testing on 40 *P. aeruginosa* strains. Whole-genome sequencing was performed using Illumina MiSeq instrument. Phylogenetic analysis was done using VICTOR tool. Isolated phages vB_PaeA-55-1w and vB_PaeM-198 from *Autographiviridae* and *Myoviridae* families, respectively, had a broad spectrum of lytic activity (about 50% each), including lysis of MDR strains. The genomes vB_PaeA-55-1w and vB_PaeM-198 comprise double-stranded DNA of 42.5 and 66.3 kbp in length, respectively. Open reading frames were annotated for both phages (52 for vB_PaeA-55-1w, and 95 for vB_PaeM-198), no integrases and toxins were detected. On a phylogenetic tree, vB_PaeA-55-1w phage was clustered with phages from the *Phikmvirus* genus (*Autographiviridae* family), which are also used in phage therapy. vB_PaeM-198 phage was clustered with phages from the *Pbunavirus* genus (*Myoviridae* family). vB_PaeA-55-1w and vB_PaeM-198 phages could be considered as candidates for phage therapy and may be used to treat infections caused by MDR *P. aeruginosa*.

Keywords: *Pseudomonas aeruginosa*, virulent bacteriophages, phage therapy, *Autographiviridae*, *Myoviridae*, whole genome sequencing, phylogenetic analysis

Funding: The study was supported by the State Assignment on the Development of a personalized approach to the therapy of infections using virulent bacteriophages (Code: Bacteriophage) (Russia).

Acknowledgments: the authors thank the Center for Precision Genome Editing and Genetic Technologies for Biomedicine, the Federal Research and Clinical Center of Physical-Chemical Medicine of the Federal Medical Biological Agency for their help with sequencing the genomes of bacteriophages.

Author contribution: Kornienko MA — study plan, data collection and processing, article authoring; Kuptsov NS — data collection and processing, article authoring; Danilov DI, Gorodnichev RB, Malakhova MV, Veselovsky VA — data collection; Bespiatykh DA — data processing, Shitikov EA — research plan, data processing, article authoring; Ilina EN — research plan, article authoring.

Compliance with ethical standards: the experiment was carried out in compliance with the Sanitary and Epidemiological Rules SP 1.3.2322-08 "Safe work with microorganisms of III–IV pathogenicity (hazardousness) groups and pathogens of parasitic diseases"; Sanitary and Epidemiological Rules SP 1.3.2518-09 "Amendments and additions #1 to the sanitary and epidemiological rules" Safe work with microorganisms of III–IV pathogenicity (hazardousness) groups and pathogens of parasitic diseases"; Sanitary and Epidemiological Rules SanPIN 2.1.7.2790-10 "Sanitary and epidemiological requirements for medical waste management"; Federal Clinical Recommendations "Rational use of bacteriophages in medical and anti-epidemic practice."

 **Correspondence should be addressed:** Maria A. Kornienko
Malaya Pirogovskaya, 1a, Moscow, 119435; kornienkomariya@gmail.com

Received: 19.07.2021 **Accepted:** 05.08.2021 **Published online:** 18.09.2021

DOI: 10.47183/mes.2021.027

ВЫДЕЛЕНИЕ И ХАРАКТЕРИСТИКА БАКТЕРИОФАГОВ *PSEUDOMONAS AERUGINOSA* — ПОТЕНЦИАЛЬНЫХ АГЕНТОВ ДЛЯ ФАГОВОЙ ТЕРАПИИМ. А. Корниенко , Н. С. Купцов, Д. И. Данилов, Р. Б. Городничев, М. В. Малахова, Д. А. Беспятых, В. А. Веселовский, Е. А. Шитиков, Е. Н. Ильина

Федеральный научно-клинический центр физико-химической медицины Федерального медико-биологического агентства, Москва, Россия

Одним из патогенов, характеризующихся критическим показателем доли штаммов с множественной лекарственной устойчивостью (МЛУ), является *Pseudomonas aeruginosa*. В качестве альтернативы антибиотикам при терапии инфекций, вызванных штаммами с МЛУ, рассматривают фаготерапию. Целью исследования было выделить и охарактеризовать бактериофаг *P. aeruginosa*, потенциально пригодный для терапии инфекционных заболеваний. Выделение проводили методом накопительных культур. Спектр литической активности устанавливали с помощью тестирования на коллекции из 40 штаммов *P. aeruginosa*. Полногеномное секвенирование выполняли на платформе MiSeq (Illumina). Филогенетический анализ геномов проводили с помощью VICTOR. Выделенные бактериофаги vB_PaeA-55-1w и vB_PaeM-198, принадлежащие к семействам *Autographiviridae* и *Myoviridae* соответственно, обладали широким спектром литической активности (около 50% каждый), в том числе вызывали лизис штаммов с МЛУ. Геномы vB_PaeA-55-1w и vB_PaeM-198 представлены двухцепочечной ДНК длиной 42,5 и 66,3 т.п.н. соответственно. В составе геномов аннотировано 52 (vB_PaeA-55-1w) и 95 (vB_PaeM-198) открытых рамок считывания, среди них гены интеграз и токсинов не обнаружены. На филогенетическом древе vB_PaeA-55-1w располагался в кластере совместно с бактериофагами рода *Phikmvirus* семейства *Autographiviridae*, в том числе с используемыми в фаготерапии, а vB_PaeM-198 входил в кластер, включающий бактериофаги рода *Pbunavirus* семейства *Myoviridae*. Бактериофаги vB_PaeA-55-1w и vB_PaeM-198 можно рассматривать в качестве кандидатов для применения в фаготерапии, в том числе и для лечения инфекций, вызванных штаммами *P. aeruginosa* с МЛУ.

Ключевые слова: *Pseudomonas aeruginosa*, вирулентные бактериофаги, фаготерапия, *Autographiviridae*, *Myoviridae*, полногеномное секвенирование, филогенетический анализ

Финансирование: исследование выполнено за счет средств, предоставленных для выполнения государственного задания «Разработка персонализированного подхода терапии инфекционных процессов с применением вирулентных бактериофагов» (ШИФР: Бактериофаг).

Благодарности: авторы благодарят Центр высокоточного редактирования и генетических технологий для биомедицины ФГБУ ФНКЦ ФХМ ФМБА России за секвенирование геномов бактериофагов.

Вклад авторов: М. А. Корниенко — план исследований, набор и обработка данных, написание статьи; Н. С. Купцов — набор и обработка данных, написание статьи; Д. И. Данилов, Р. Б. Городничев, М. В. Малахова, В. А. Веселовский — набор данных; Д. А. Беспятых — обработка данных, Е. А. Шитиков — план исследований, обработка данных, написание статьи; Е. Н. Ильина — план исследований, написание статьи.

Соблюдение этических стандартов: экспериментальная работа выполнена с соблюдением норм Санитарно-эпидемиологических правил «Безопасность работы с микроорганизмами III–IV групп патогенности (опасности) и возбудителями паразитарных болезней» СП 1.3.2322-08; Санитарно-эпидемиологических правил СП 1.3.2518-09 — «Дополнения и изменения № 1 к санитарно-эпидемиологическим правилам «Безопасность работы с микроорганизмами III–IV групп патогенности (опасности) и возбудителями паразитарных болезней» СП 1.3.2322-08; Санитарно-эпидемиологических правил «Санитарно-эпидемиологические требования к обращению с медицинскими отходами» СанПиН 2.1.7.2790-10, а также Федеральных клинических рекомендаций «Рациональное применение бактериофагов в лечебной и противоэпидемической практике».

 **Для корреспонденции:** Мария Андреевна Корниенко
ул. Малая Пироговская, д. 1а, г. Москва, 119435; kornienkomariya@gmail.com

Статья получена: 19.07.2021 **Статья принята к печати:** 05.08.2021 **Опубликована онлайн:** 18.09.2021

DOI: 10.47183/mes.2021.027

According to the World Health Organization, antibiotic resistance is rising to dangerously high levels in all parts of the world [1]. Gram-negative bacteria, including *Pseudomonas aeruginosa*, occupy the first places in the global priority list of antibiotic-resistant bacteria posing the greatest threat to human health [1]. The bacteria of this species are ubiquitous, their genetic plasticity and environmental adaptability are high. The wide variety of pathogenicity mechanisms often makes the infection general in cases of infestation with *P. aeruginosa* strains [2]. *P. aeruginosa* causes a wide range of diseases, from intoxication to extensive pyoinflammatory processes and septic shock [2]. According to AMRmap portal, the share of *P. aeruginosa* isolates, which occupy the top lines in the list of most common nosocomial pathogens in Russia, was 16.83% among all such pathogens isolated in 2015–2020 [3]. Besides, about 30% of *P. aeruginosa* strains circulating in the population are multidrug-resistant (MDR), i.e., they are resistant to at least one antibiotic drug out of three or more antibiotic groups, and about 15% of the circulating *P. aeruginosa* strains show extreme drug resistance (XDR), i.e., they are resistant to at least one antibiotic from all groups of antibiotics, with the exception of 1–2 groups; these factors drive the related patient mortality up [4].

An urgent task currently is to develop alternative, non-antibiotic treatments for infectious diseases caused by MDR and XDR pathogens. One of the most promising alternatives are virulent bacteriophages, which are the basis of phage therapy [5]. The promise is in the capability of virulent bacteriophages to lyse both antibiotic-sensitive and antibiotic-resistant strains of bacteria. In addition, bacteriophages do not cause toxic and allergic side effects, have no contraindications [6] and can be prescribed to pregnant women in combination with other medications [7].

A number of reports and preclinical and clinical trials [8, 9] confirm the success of phage therapy against *P. aeruginosa* infections both in animals and humans. There are several commercial therapeutic drugs designed to counter infections caused by *P. aeruginosa* that are produced in Russia: *Pseudomonas aeruginosa* bacteriophage, Intesti-bacteriophage, Polyvalent purified pyobacteriophage (Microgen; Russia).

Despite the availability of bacteriophage preparations active against *P. aeruginosa* and the successful experience of their use, phage collections need to be constantly updated, as the specifics of modern phage therapy require. Since virulent bacteriophages have a rather narrow specificity and usually target only several strains, updating the collections means extending them with phages that cause lysis of current bacterial strains. Moreover, there are reported cases [10] when bacteria mutate and acquire resistance to bacteriophages [10]. Isolation of new bacteriophages and their inclusion in the composition of therapeutic drugs solves this problem.

In connection with the above, the purpose of this work is to isolate and characterize *P. aeruginosa* bacteriophages that can be used to treat infectious diseases.

Table 1. Characteristics of *P. aeruginosa* bacteriophage host strains

Strain	MLST sequence type	Antibacterial susceptibility pattern			
		ceftriaxone	gentamicin	ciprofloxacin	meropenem
PA198	ST508	R	S	S	R
PA55	ST2690	R	S	S	S

METHODS

Bacterial strains

The study used *P. aeruginosa* strains ($n = 40$) selected from the collection of bacterial strains of the laboratory of molecular genetics of microorganisms of the Federal Research and Clinical Center of Physical-chemical Medicine of Federal Medical Biological Agency of Russia. The strains of the collection were characterized by the profile of drug susceptibility (to ceftriaxone, gentamicin, ciprofloxacin, and meropenem), as well as by genotypes according to the results of multilocus sequence typing (MLST) [11]. The bacteria were cultivated for 18–24 h in the lysogeny broth (LB) nutrient medium (Oxoid; UK) at 37 °C.

Isolation of bacteriophages

The bacteriophages were isolated by enriching cultures from natural sources (sewage, water samples from various rivers) with *P. aeruginosa* strains PA55 and PA198 (Table 1). A sample of water (50 ml) was drawn through a Millipore filter with a polyvinylidene fluoride membrane, pore diameter of 0.45 μm (Merck Millipore; USA), and then two-fold LB broth was added to it. Subsequently, 300 ml of an overnight culture of the host strain was added and incubated on a shaker at 37 °C for 18 h. After cultivation, bacterial cells were centrifuged for 10 minutes at 3500 g to achieve precipitation. The supernatant was put through a Millipore filter with a polyethersulfone membrane and a pore diameter of 0.22 μm (Merck Millipore; USA). Individual bacteriophages were obtained by sequential (threefold) isolation from individual negative colonies. Further on, bacteriophages were grown in 50 ml of LB broth containing 300 μl of the bacterial strain overnight culture. The concentration of the bacteriophage in the phage lysate was estimated by the standard Grazia titration method [12].

Bacteriophage lytic capability range determination

Bacteriophage lytic capability range was determined by spot testing. Phagolysates with a titer of 3×10^6 PFU/ml (plaque-forming units per ml) were used in the tests with the aim to prevent non-specific lysis. An overnight culture (10^{10} CFU/ml) of the tested bacterial strain was sequentially diluted in LB broth to a cell concentration of 10^6 CFU/ml, then 0.1 ml thereof was mixed with 5 ml of semisolid LB agar (0.6% agar) and added to a Petri dish containing a thin layer of LB agar (1.5% agar). After solidification of the semisolid agar, a drop (5 μL) of the studied bacteriophage was applied to the dish's surface. Petri dishes were incubated at 37 °C for 18–24 h. Lytic capability was assessed visually: the bacterial strain was considered sensitive to the bacteriophage in case there appeared a transparent spot or separate negative colonies. In the absence of such a lysis spot or if it was opaque the bacterial strain was classified as resistant.

Table 2. Genetic characteristics of the collection strains and range of the hosts of vB_PaeA-55-1w and vB_PaeM-198 bacteriophages

MLST sequence typing	Total number of strains	Share of strains lysed by vB_PaeA-55-1w, %	Share of strains lysed by vB_PaeM-198, %
ST12	5	0	100
ST17	1	0	0
ST186	1	100	100
ST198	2	100	50
ST207	2	100	0
ST233	1	100	100
ST235	1	0	0
ST244	4	100	75
ST266	1	100	100
ST357	1	100	0
ST395	1	0	0
ST483	1	0	0
ST498	1	0	0
ST499	2	100	100
ST508	1	0	100
ST569	1	0	0
ST589	1	0	100
ST654	3	33,3	0
ST1094	1	100	100
ST1292	1	0	0
ST1527	1	0	0
ST2427	1	0	0
ST2690	1	100	100
Unique type 15-5-11-8-4-4-1*	2	0	50
Unique type 15-2-11- 3-3-38-3*	2	100	50
Unique type 17 -5-12-3-14-4-7*	1	0	0

Note: * — the allele numbers of genes included in the standard MLST pattern (*arcC-aroE-glpF-gmk-pta-tpi-yqi*) [21] are indicated for each unique sequence type.

Isolation of bacteriophage DNA and whole genome sequencing

Total bacteriophage DNA was isolated by phenol-chloroform extraction method [13] with preliminary enzymatic treatment of phage lysates with RNase A, DNase I, and proteinase K (Thermo Fisher Scientific; USA) in accordance with the manufacturer's instructions.

The library was prepared with 250 ng of genomic DNA. Covaris S220 System (Covaris; United States) enabled DNA fragmentation to 400–500 bps. Quality of the fragmented samples was assessed with Agilent 2100 bioanalyzer (Agilent; USA) in accordance with the manufacturer's instructions. The NEBNext Ultra II DNA Library Prep Kit (New England Biolabs; USA) was used to prepare genomic libraries, and the NEBNext Multiplex Oligos kit for Illumina (96 index primers, New England Biolabs; USA) was used to index the libraries. Quantitative analysis of the libraries was performed with the help of Quant-iT DNA Assay Kit, High Sensitivity (Thermo Scientific; USA). Sequencing was done with the MiSeq system and MiSeq Reagent Nano Kit v2 (500 cycle) (Illumina; USA) in accordance with the manufacturer's recommendations.

Bioinformatic analysis of bacteriophage genomes

Prokka v1.14.6 software [14] was used to assemble the whole genome sequences of bacteriophages. Rapid Annotation

using Subsystem Technology (RAST) enabled bacteriophage genome annotation [15]. The functions of some open reading frames (ORF) have been predicted using BLASTP (<https://blast.ncbi.nlm.nih.gov/Blast.cgi>) and HHpred (<https://toolkit.tuebingen.mpg.de/#/tools/hhpred>). Transport RNAs (tRNAs) were searched for with ARAGORN software [16]. The obtained genomes were deposited into the GenBank database under numbers MZ553931 and MZ553930 for bacteriophages vB_PaeA-55-1w and vB_PaeM-198, respectively.

The taxonomy of the studied bacteriophages was determined based on the homology of their genomic sequences with the sequences of bacteriophages registered in the GenBank database using the BLASTN service (<https://blast.ncbi.nlm.nih.gov/Blast.cgi>). Naming of the bacteriophages followed ICTV (International Committee on Taxonomy of Viruses) recommendations [17] and depended on their taxonomic position.

Phylogenetic analysis of the genomes was performed with the help of VICTOR online tool (Genome-BLAST Distance Phylogeny); the settings were as recommended for prokaryotic viruses [18]. The branches were processed with FASTME [19] according to the D0 formula, visualization done with FigTree [20]. For bacteriophage vB_PaeA-55-1w, we used the following bacteriophage genomes (GenBank database numbers) for comparison: NC_054890, NC_047953, NC_047967, NC_048201, NC_047965, NC_026602, NC_027375, NC_047956, NC_047957, NC_031014, NC_016764, NC_030923, NC_028836, NC_013638, NC_004665,

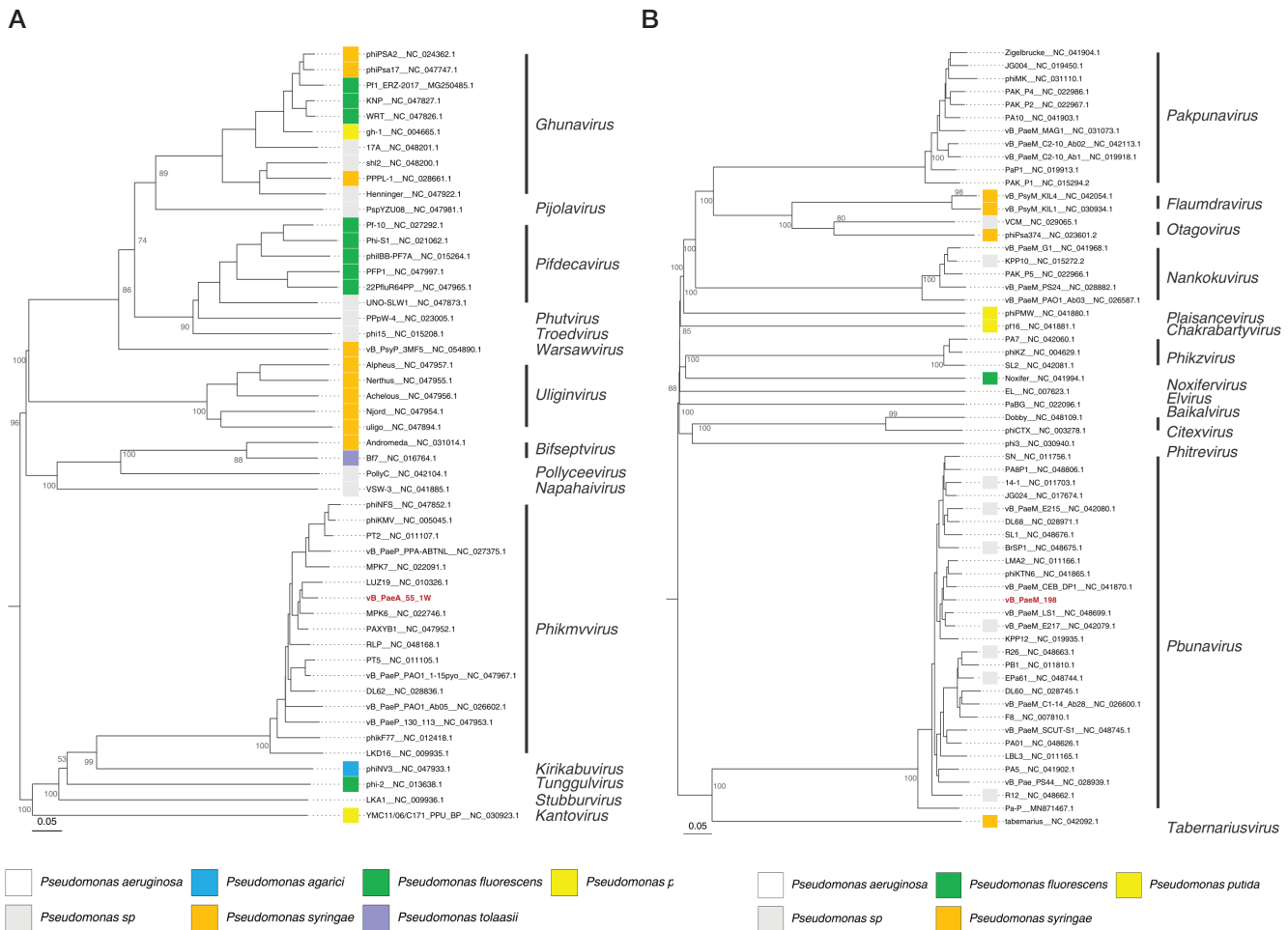


Fig. 1. Phylogenetic analysis of the whole genome sequences of *Pseudomonas* spp bacteriophages **A.** Phylogenetic tree of the Autographviridae family bacteriophages ($n = 50$). **B.** Phylogenetic tree of the Myoviridae family bacteriophages ($n = 60$). Bacteriophages vB_PaeA-55-1w and vB_PaeM-198 are marked in red

NC_047922, NC_015264, NC_012418, NC_047827,
 NC_009936, NC_009935, NC_010326, NC_022746,
 NC_022091, NC_047955, NC_047852, NC_047954,
 NC_047933, NC_047952, NC_027292, MG250485,
 NC_047997, NC_015208, NC_005045, NC_047747,
 NC_024362, NC_021062, NC_042104, NC_028661,
 NC_023005, NC_047981, NC_011107, NC_011105,
 NC_048168, NC_048200, NC_047894, NC_047873,
 NC_041885, NC_047826. For bacteriophage vB_PaeM-198,
 the genomes were as follows: NC_048675, NC_048744,
 NC_048626, NC_048662, NC_048663, NC_048676,
 NC_048745, NC_011703, NC_026587, NC_026600,
 NC_042113, NC_019918, NC_028745, NC_028971,
 NC_048109, NC_041870.1, NC_042080, NC_042079,
 NC_007623, NC_007810, NC_041968, NC_019450,
 NC_017674, NC_042054, NC_030934, NC_015272,
 NC_019935, NC_041865, NC_011165, NC_011166,
 NC_048699.1, NC_031073, NC_031073, MN871467,
 NC_041994, NC_041903, NC_041902.1, NC_042060,
 NC_048806, NC_022096, NC_015294, NC_022967.1,
 NC_022966, NC_022986, NC_019913, NC_011810,
 NC_041881, NC_030940, NC_003278, NC_004629,
 NC_031110, NC_041880, NC_028882, NC_028939,
 NC_023601, NC_042081, NC_042081, NC_042081,
 NC_011756, NC_042092, NC_029065, NC_041904.

Modular structure of the genomes was determined based on the annotation and when establishing homology of the nucleotide sequences of individual ORFs with BLASTN (<https://blast.ncbi.nlm.nih.gov/Blast.cgi>).

RESULTS

Isolation of bacteriophages and characterization of the lytic capability range

To isolate bacteriophages active against the *P. aeruginosa* species we selected strains PA55 and PA198 from the bacterial strains collection of the Federal Research and Clinical Center of Physical-Chemical Medicine (Table 1). These host strains allowed isolating two bacteriophages, which were later named vB_PaeA-55-1w and vB_PaeM-198. As for their lytic capability, vB_PaeA-55-1w phage caused lysis of 19 strains of the collection (47.5%) and vB_PaeM-198 lysed 20 strains (50%) (Table 2). It should also be noted that out of 17 MDR strains vB_PaeA-55-1w lysed 8 (47%) and vB_PaeM-198 — 6 (35%).

Whole genome sequencing of the bacteriophages

Detailed characterization of the studied bacteriophages relied on the whole genome sequencing data and annotation thereof. Genomes of the bacteriophages were double-stranded DNA 42.5 kbp (vB_PaeA-55-1w) and 66.3 kbp (vB_PaeM-198) long. Bacteriophage vB_PaeA-55-1w encoded 52 ORFs, while vB_PaeM-198 encoded 95 ORFs. None of the analyzed bacteriophages contained tRNA in the genome.

Taxonomic position of the bacteriophages and their closest relative were established by comparing the obtained genome-wide sequences with the genomes available in the Genbank database. Bacteriophage vB_PaeA-55-1w belonged to the

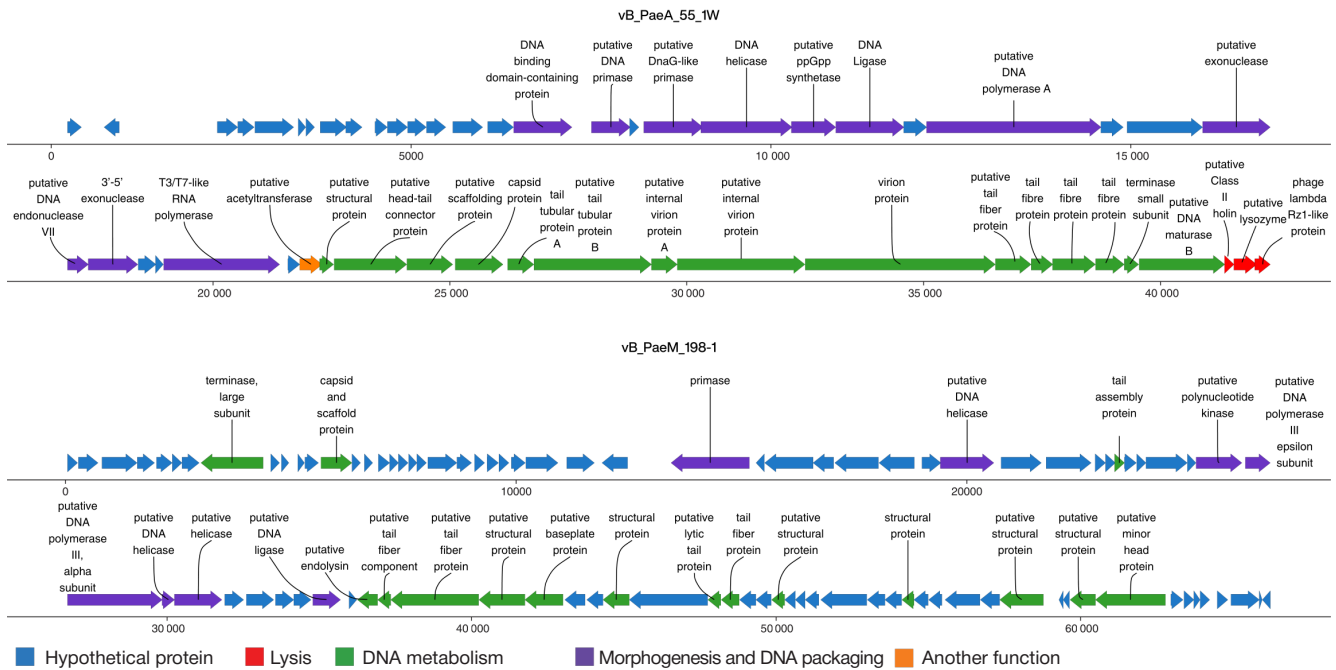


Fig. 2. Main structural modules of the genomes of vB_PaeA-55-1w and vB_PaeM-198-1 *P. aeruginosa* bacteriophage

Phikmvirus genus of the *Autographiviridae* family, and the closest genome corresponded to the *Pseudomonas* phage MYY9 (95% similarity, 97.59% alignment length, Genbank number — MW406975.1). Bacteriophage vB_PaeM-198 belonged to the *Pbunavirus* genus of the *Myoviridae* family and was highly similar to *Pseudomonas* phage phiKT28 (99% similarity, 96.34% alignment length, Genbank number — KP340287.1).

Phylogenetic analysis of *Pseudomonas* spp. bacteriophages

To position the studied bacteriophages within their respective families we relied on the reference genomes recommended by ICTV [17]. Phylogenetic analysis of the *Autographiviridae* family included 50 genomes of *Pseudomonas* spp. bacteriophages (Fig. 1A), that of the *Myoviridae* family — 60 genomes (Fig. 1B).

Two large clusters can be identified on the phylogenetic tree of *Pseudomonas* spp. bacteriophages belonging to the *Autographiviridae* family (Fig. 1A). The first cluster includes bacteriophages that have *P. aeruginosa* species as hosts, and *Pseudomonas agarici*, *Pseudomonas putida* and *Pseudomonas fluorescens* bacteriophages (one of each). It should be noted that phylogenetic analysis results match taxonomic classification of these viruses. Within the first cluster, *P. aeruginosa* bacteriophages are grouped separately and belong to the *Phikmvirus* genus, including the investigated vB_PaeA-55-1w bacteriophage. The only exception is *Pseudomonas* phage LKA1, which has its own branch on the phylogenetic tree. The taxonomy has this bacteriophage belonging to another *Stubburvirus* genus. As for *Pseudomonas agarici*, *Pseudomonas putida* and *Pseudomonas fluorescens* in the first large cluster, each of them also occupies an individual branch of the phylogenetic tree and belongs to a separate taxon, namely, genera *Kirikabuvirus*, *Tunggulvirus*, and *Kantovirus*, respectively. The second large cluster on the phylogenetic tree is comprised of the bacteriophages that have *Pseudomonas syringae*, *Pseudomonas tolaasii*, *Pseudomonas putida*, *Pseudomonas fluorescens* as hosts, as well as *Pseudomonas* genus bacteria with unestablished

species identity. Phylogenetic subgroups of the second cluster are also consistent with genera of their bacteriophages, namely *Pifdecavirus*, *Ghunavirus*, *Troedvirus*, *Pollycevirus*, *Phutvirus*, *Napahaivirus*, *Pijolavirus*, *Pifdecavirus*, *Bifseptvirus*, *Uliginivirus*. It should be noted that several genera within the family had hosts belonging to different species: *Bifseptvirus* — hosts of *P. syringae* and *P. tolaasii*; *Ghunavirus* — hosts of *P. fluorescens*, *P. putida*, *P. syringae*.

P. aeruginosa bacteriophages of the *Myoviridae* family were found in different parts of the phylogenetic tree and corresponded to seven genera: *Baikalvirus*, *Citexvirus*, *Elvirus*, *Nankokuvirus*, *Pakpunavirus*, *Pbunavirus* and *Phikzvirus* (Fig. 1B). The studied vB_PaeM-198 bacteriophage shares the position on the phylogenetic tree with 26 other *Pbunavirus* bacteriophages. *P. fluorescens*, *P. putida*, *P. syringae* bacteriophages of the *Myoviridae* families belong to 6 different genera: *Chakrabartyvirus*, *Flaumdravirus*, *Noxifervirus*, *Otagovirus*, *Plaisancevirus* and *Tabernariusvirus*.

Modular structure of the vB_PaeA-55-1w and vB_PaeM-198 bacteriophages

To describe the genomic organization of bacteriophages vB_PaeA-55-1w and vB_PaeM-198, we analyzed functional modules of the genomes. It should be noted that the number of genes the functions of which were identified was higher for the vB_PaeA-55-1w bacteriophage ($n = 30/52$, 58%) than for vB_PaeM-198 ($n = 24/95$, 25%) (Fig. 2). The analysis also yielded localization of the modules of nucleic acid metabolism and morphogenesis and packaging. The location of the lysis module was established for the vB_PaeA-55-1w bacteriophage. Targeted search revealed no known bacterial toxins and various integrases in the vB_PaeA-55-1w and vB_PaeM-198 genomes.

DISCUSSION

Due to antibiotic crisis associated with the spread of MDR and XDR bacteria, *P. aeruginosa* bacteriophages are used in therapeutic practice more and more often. Infections caused

by *P. aeruginosa* are most often treated with phages of the *Autographiviridae* and *Myoviridae* families [22, 23]. For this study, we isolated *Autographiviridae* (vB_PaeA-55-1w) and *Myoviridae* (vB_PaeM-198) bacteriophages from natural sources; these bacteriophages offer a wide range of lysing capability (47.5% and 50%, respectively), which is comparable to the *P. aeruginosa* bacteriophages of the corresponding families [24, 25]. It should be noted that the bacteriophages lysed various strains, which can make therapy more efficient with a phage cocktail that includes both of the studied bacteriophages.

It should also be emphasized that the bacteriophages caused lysis of the strains that belong to different sequence types, including ST235 ($n = 1$), ST244 ($n = 4$), and ST395 ($n = 1$). Isolates belonging to these sequence types are among the most widespread throughout the world; they are often associated with outbreaks of infectious diseases, and they have higher resistance to antibacterial drugs [26]. It seems interesting to further study the lytic capability of vB_PaeA-55-1w and vB_PaeM-198 on a collection of *S. aureus* strains of the high epidemic risk sequence types.

Current requirements for therapeutic drugs prescribe describing them in detail, and in the case of bacteriophages, it is also necessary to determine their genomic sequences [27] and thus confirm the virulent nature thereof through showing there are no integrase genes in their genomes. Temperate bacteriophages are not used for therapy because they can facilitate transfer of genes of bacterial toxins and determinants of antibiotic resistance in the bacterial population [27]. Besides, in order to assess therapeutic safety of a bacteriophage its genome is searched for genes of known toxins [27].

The studied bacteriophages (both families) were shown to have typical modular genome structure [24, 28], including

a nucleic acid metabolism module, a morphogenesis and packaging module. In addition, localization of the lysis module was established for vB_PaeA-55-1w (*Autographiviridae*). In case of the vB_PaeM-198 (family *Myoviridae*) bacteriophage, no genes highly similar to the known genes of lysines or cholines were found. Both studied bacteriophages were found to have no lysogeny module with integrase genes, which confirms their virulent nature, nor were they established to contain known genes of toxins, which makes them potentially usable in therapy.

Based on the results of phylogenetic analysis of *Pseudomonas spp.* bacteriophages belonging to the *Autographiviridae* and *Myoviridae* families, it was shown that *P. aeruginosa* bacteriophages, regardless of their family, form separate clusters on phylogenetic trees that correspond to genera *Phikmvirus* and *Stubburvirus* (family *Autographiviridae*), as well as *Elvirus*, *Nankokuvirus*, *Pakpunavirus*, *Pbunavirus*, *Phikzvirus*, *Phitrevirus* (*Myoviridae* family). This fact indicates that *P. aeruginosa* bacteriophages are species-specific. On a separate note, bacteriophages previously described and used in phage therapy (phiKMV, PPA-ABTNL, MPK6, RLP), including ФНН-4 (*Pbunaviruses*) and PAK_P1 (*Pakpunavirus*), have shown their efficacy in animal models [29, 30], and they also cluster together with the studied vB_PaeA-55-1w and vB_PaeM-198 bacteriophages.

CONCLUSIONS

Based on the analysis performed, bacteriophages vB_PaeA-55-1w and vB_PaeM-198 can be recommended for use in phage therapy, including the protocols designed to combat infections caused by MDR strains of *P. aeruginosa*.

References

- Tacconelli E, Carrara E, Savoldi A, Harbarth S, Mendelson M, Monnet DL, et al. Discovery, research, and development of new antibiotics: the WHO priority list of antibiotic-resistant bacteria and tuberculosis. *Lancet Infect Dis.* 2018; 18 (3): 318–27.
- Horcajada JP, Montero M, Oliver A, Sorlí L, Luque S, Gómez-Zorrilla S, et al. Epidemiology and treatment of multidrug-resistant and extensively drug-resistant *Pseudomonas aeruginosa* infections. *Clin Microbiol Rev.* 2019; 32 (4).
- Kuzmenkov AY, Trushin IV, Vinogradova AG, Avramenko AA, Sukhorukova MV, Malhotra-Kumar S, et al. AMRmap: an interactive web platform for analysis of antimicrobial resistance surveillance data in Russia. *Front Microbiol.* 2021; 12: 620002.
- Pena C, Cabot G, Gómez-Zorrilla S, Zamorano L, Ocampo-Sosa A, Murillas J, et al. Influence of virulence genotype and resistance profile in the mortality of *Pseudomonas aeruginosa* bloodstream infections. *Clin Infect Dis.* 2015; 60 (4): 539–48.
- 2020 Antibacterial agents in clinical and preclinical development: an overview and analysis. Geneva: World Health Organization, 2021. Available from: <https://www.who.int/publications/item/9789240021303>.
- Gordillo Altamirano FL, Barr JJ. Phage therapy in the postantibiotic era. *Clinical Microbiology Reviews.* 2019; 32 (2): e00066-18. DOI: 10.1128/CMR.00066-18.
- Akimkin VG, Darbeeva OS, Kolkov VF. Bakteriofagi: istoricheskie i sovremennye aspekty ih primeneniya: opyt i perspektivy. *Klinicheskaja praktika.* 2010; 1 (4): 48–54. Russian.
- Chen F, Cheng X, Li J, Yuan X, Huang X, Lian M, et al. Novel lytic phages protect cells and mice against *Pseudomonas aeruginosa* infection. *J Virol.* 2021; 95 (8): e01832-20. DOI: 10.1128/JVI.01832-20.
- Jault P, Cheng X, Li J, Yuan X, Huang X, Lian M, et al. Efficacy and tolerability of a cocktail of bacteriophages to treat burn wounds infected by *Pseudomonas aeruginosa* (PhagoBurn): a randomised, controlled, double-blind phase 1/2 trial. *Lancet Infect Dis.* 2019; 19 (1): 35–45.
- Oechslin F. Resistance development to bacteriophages occurring during bacteriophage therapy. *Viruses.* 2018; 10 (7): 351. DOI: 10.3390/v10070351.
- Kuptsov NS, Kornienko MA, Gorodnichev RB, Danilov DI, Malakhova MV, Parfenova TV, et al. Efficacy of commercial bacteriophage products against ESKAPE pathogens. *Bulletin of RSMU.* 2020; (3): 18–24.
- Mazzocco A, et al. Enumeration of bacteriophages using the small drop plaque assay system. *Methods Mol Biol.* 2009; 501: 81–85.
- Sambrook J, Fritsch EF, Maniatis T. *Molecular cloning: a laboratory manual.* Cold Spring Harbor Laboratory Pr. 1989, 2200 p.
- Seemann T. *Prokka: Rapid prokaryotic genome annotation.* *Bioinformatics.* Oxford University Press. 2014; 30 (14): 2068–9.
- Aziz RK, et al. The RAST Server: Rapid annotations using subsystems technology. *BMC Genomics.* BioMed Central. 2008; 9: 75.
- Laslett D. ARAGORN, a program to detect tRNA genes and tmRNA genes in nucleotide sequences. *Nucleic Acids Res.* 2004; 32 (1): 11–16.
- Lefkowitz EJ, et al. Virus taxonomy: The database of the International Committee on Taxonomy of Viruses (ICTV). *Nucleic Acids Res.* 2018; 46 (1): 708–17.
- Meier-Kolthoff JP, Göker M. VICTOR: genome-based phylogeny and classification of prokaryotic viruses. *Bioinformatics.* 2017; 33 (21): 3396–404.

19. Lefort V, Desper R, Gascuel O. FastME 2.0: A comprehensive, accurate, and fast distance-based phylogeny inference program. *Mol Biol.* 2015; 32 (10): 2798–800.
20. FigTree. Available from: <http://tree.bio.ed.ac.uk/software/figtree/>. (Data obrashhenija: 16.07.2021).
21. Enright MC, et al. Multilocus sequence typing for characterization of methicillin-resistant and methicillin-susceptible clones of *Staphylococcus aureus*. *J Clin Microbiol.* 2000; 38 (3): 1008–15.
22. Alvi IA, et al. RLP, a bacteriophage of the family Podoviridae, rescues mice from bacteremia caused by multi-drug-resistant *Pseudomonas aeruginosa*. *Arch Virol.* 2020. 165 (6): 1289–97.
23. Farlow J, et al. Complete Genome Sequences of 10 Phages Lytic against Multidrug-Resistant *Pseudomonas aeruginosa*. *Microbiol Resour.* 2020. 9: 29.
24. Alvi IA, Asif M, Rehman S. A single dose of a virulent bacteriophage vB PaeP-SaPL, rescues bacteremic mice infected with multi drug resistant *Pseudomonas aeruginosa*. *Virus Res.* 2021; 292: 198250.
25. Adnan M, et al. Isolation and characterization of bacteriophage to control multidrug-resistant *Pseudomonas aeruginosa* planktonic cells and biofilm. *Biologicals.* 2020; 63: 89–96.
26. Treepong P, et al. Global emergence of the widespread *Pseudomonas aeruginosa* ST235 clone. *Clin Microbiol Infect.* 2018; 24 (3): 258–66.
27. Principi N, Silvestri E, Esposito S. Advantages and Limitations of Bacteriophages for the Treatment of Bacterial Infections. *Front Pharmacol.* 2019; 10: 513.
28. Guo Y, Chen P, Lin Z, Wang T. Characterization of Two *Pseudomonas aeruginosa* Viruses vB_PaeM_SCUT-S1 and vB_PaeM_SCUT-S2. *Viruses.* 2019; 11 (4): 318. DOI: 10.3390/v11040318.
29. Alemayehu D, Casey PG, McAuliffe O, Guinane CM, Martin JG, Shanahan F, et al. Bacteriophages ϕ MR299-2 and ϕ NH-4 can eliminate *Pseudomonas aeruginosa* in the murine lung and on cystic fibrosis lung airway cells. *MBio.* 2012; 3 (2): e00029-12. DOI: 10.1128/mBio.00029-12.
30. Debarbieux L, Leduc D, Maura D, Morello E, Criscuolo A, Grossi O, et al. Bacteriophages can treat and prevent *Pseudomonas aeruginosa* lung infections. *J Infect Dis.* 2010; 201 (7): 1096–104.

Литература

1. Tacconelli E, Carrara E, Savoldi A, Harbarth S, Mendelson M, Monnetet DL, et al. Discovery, research, and development of new antibiotics: the WHO priority list of antibiotic-resistant bacteria and tuberculosis. *Lancet Infect Dis.* 2018; 18 (3): 318–27.
2. Horcajada JP, Montero M, Oliver A, Sorlí L, Luque S, Gómez-Zorrilla S, et al. Epidemiology and treatment of multidrug-resistant and extensively drug-resistant *Pseudomonas aeruginosa* infections. *Clin Microbiol Rev.* 2019; 32 (4).
3. Kuzmenkov AY, Trushin IV, Vinogradova AG, Avramenko AA, Sukhorukova MV, Malhotra-Kumar S, et al. AMRmap: an interactive web platform for analysis of antimicrobial resistance surveillance data in Russia. *Front Microbiol.* 2021; 12: 620002.
4. Pena C, Cabot G, Gómez-Zorrilla S, Zamorano L, Ocampo-Sosa A, Murillas J, et al. Influence of virulence genotype and resistance profile in the mortality of *Pseudomonas aeruginosa* bloodstream infections. *Clin Infect Dis.* 2015; 60 (4): 539–48.
5. 2020 Antibacterial agents in clinical and preclinical development: an overview and analysis. Geneva: World Health Organization, 2021. Available from: <https://www.who.int/publications/item/9789240021303>.
6. Gordillo Altamirano FL, Barr JJ. Phage therapy in the postantibiotic era. *Clinical Microbiology Reviews.* 2019; 32 (2): e00066-18. DOI: 10.1128/CMR.00066-18.
7. Акимкин В. Г., Дарбеева О. С., Колков В.Ф. Бактериофаги: исторические и современные аспекты их применения: опыт и перспективы. *Клиническая практика.* 2010; 1 (4): 48–54.
8. Chen F, Cheng X, Li J, Yuan X, Huang X, Lian M, et al. Novel lytic phages protect cells and mice against *Pseudomonas aeruginosa* infection. *J Virol.* 2021; 95 (8): e01832-20. DOI: 10.1128/JVI.01832-20.
9. Jault P, Cheng X, Li J, Yuan X, Huang X, Lian M, et al. Efficacy and tolerability of a cocktail of bacteriophages to treat burn wounds infected by *Pseudomonas aeruginosa* (PhagoBurn): a randomised, controlled, double-blind phase 1/2 trial. *Lancet Infect Dis.* 2019; 19 (1): 35–45.
10. Oechslin F. Resistance development to bacteriophages occurring during bacteriophage therapy. *Viruses.* 2018; 10 (7): 351. DOI: 10.3390/v10070351.
11. Кулцов Н. С. и др. Эффективность препаратов бактериофагов против патогенов группы ESKAPE. *Вестник РГМУ.* 2020; (3): 19–26.
12. Mazzocco A, et al. Enumeration of bacteriophages using the small drop plaque assay system. *Methods Mol Biol.* 2009; 501: 81–85.
13. Sambrook J, Fritsch EF, Maniatis T. *Molecular cloning: a laboratory manual.* Cold Spring Harbor Laboratory Pr. 1989, 2200 p.
14. Seemann T. Prokka: Rapid prokaryotic genome annotation. *Bioinformatics.* Oxford University Press. 2014; 30 (14): 2068–9.
15. Aziz RK, et al. The RAST Server: Rapid annotations using subsystems technology. *BMC Genomics.* BioMed Central. 2008; 9: 75.
16. Laslett D. ARAGORN, a program to detect tRNA genes and tmRNA genes in nucleotide sequences. *Nucleic Acids Res.* 2004; 32 (1): 11–16.
17. Lefkowitz EJ, et al. Virus taxonomy: The database of the International Committee on Taxonomy of Viruses (ICTV). *Nucleic Acids Res.* 2018; 46 (1): 708–17.
18. Meier-Kolthoff JP, Göker M. VICTOR: genome-based phylogeny and classification of prokaryotic viruses. *Bioinformatics.* 2017; 33 (21): 3396–404.
19. Lefort V, Desper R, Gascuel O. FastME 2.0: A comprehensive, accurate, and fast distance-based phylogeny inference program. *Mol Biol.* 2015; 32 (10): 2798–800.
20. FigTree. Available from: <http://tree.bio.ed.ac.uk/software/figtree/>. (Дата обращения: 16.07.2021).
21. Enright MC, et al. Multilocus sequence typing for characterization of methicillin-resistant and methicillin-susceptible clones of *Staphylococcus aureus*. *J Clin Microbiol.* 2000; 38 (3): 1008–15.
22. Alvi IA, et al. RLP, a bacteriophage of the family Podoviridae, rescues mice from bacteremia caused by multi-drug-resistant *Pseudomonas aeruginosa*. *Arch Virol.* 2020. 165 (6): 1289–97.
23. Farlow J, et al. Complete Genome Sequences of 10 Phages Lytic against Multidrug-Resistant *Pseudomonas aeruginosa*. *Microbiol Resour.* 2020. 9: 29.
24. Alvi IA, Asif M, Rehman S. A single dose of a virulent bacteriophage vB PaeP-SaPL, rescues bacteremic mice infected with multi drug resistant *Pseudomonas aeruginosa*. *Virus Res.* 2021; 292: 198250.
25. Adnan M, et al. Isolation and characterization of bacteriophage to control multidrug-resistant *Pseudomonas aeruginosa* planktonic cells and biofilm. *Biologicals.* 2020; 63: 89–96.
26. Treepong P, et al. Global emergence of the widespread *Pseudomonas aeruginosa* ST235 clone. *Clin Microbiol Infect.* 2018; 24 (3): 258–66.
27. Principi N, Silvestri E, Esposito S. Advantages and Limitations of Bacteriophages for the Treatment of Bacterial Infections. *Front Pharmacol.* 2019; 10: 513.
28. Guo Y, Chen P, Lin Z, Wang T. Characterization of Two *Pseudomonas aeruginosa* Viruses vB_PaeM_SCUT-S1 and vB_PaeM_SCUT-S2. *Viruses.* 2019; 11 (4): 318. DOI: 10.3390/v11040318.
29. Alemayehu D, Casey PG, McAuliffe O, Guinane CM, Martin JG, Shanahan F, et al. Bacteriophages ϕ MR299-2 and ϕ NH-4 can eliminate *Pseudomonas aeruginosa* in the murine lung and on cystic fibrosis lung airway cells. *MBio.* 2012; 3 (2): e00029-12. DOI: 10.1128/mBio.00029-12.
30. Debarbieux L, Leduc D, Maura D, Morello E, Criscuolo A, Grossi O, et al. Bacteriophages can treat and prevent *Pseudomonas aeruginosa* lung infections. *J Infect Dis.* 2010; 201 (7): 1096–104.

EXPERIMENTAL AND CLINICAL EVALUATION OF MEFLOQUINE EFFECTIVENESS AGAINST THE INFECTION CAUSED BY SARS-COV-2

Filin KN, Gladkikh VD ✉, Bykov VN

Federal State Unitary Enterprise Research & Production Center "Pharmaceutical Protection" of Federal Medical Biological Agency, Khimki, Moscow Region, Russia

The efficacy of mefloquine has not been studied in the *in vivo* experiments and clinical trials involving COVID-19 patients. The study was aimed to assess the effects of mefloquine on the SARS-CoV-2 accumulation in the lungs of infected animals and to study the efficacy and safety of mefloquine compared to hydroxychloroquine in patients with COVID-19. During the experiment, a total of 96 Syrian hamsters were infected with SARS-CoV-2. Accumulation of the virus in lungs was compared in the groups of animals treated with mefloquine and ribavirin and in the control group. During the clinical trial, the mefloquine and hydroxychloroquine safety and efficacy in patients with mild and moderate COVID-19 (172 individuals) was assessed based on the symptom changes over time and the computed tomography results. The experiment showed that the SARS-CoV-2 accumulation in the lungs of Syrian hamsters 6 days after infection and mefloquine treatment was 2.2 ± 0.18 lg PFU/g, which was lower ($p < 0.05$) than in the control group (3.5 ± 0.21 lg PFU/g) and ribavirin group (5.2 ± 0.05 lg PFU/g). During the clinical trial, it was found that 50.0% of patients in the mefloquine group and 32.4% in the hydroxychloroquine group ($p < 0.05$) developed a mild disease, and the completely resolved respiratory failure was registered in 76.5% and 44.6%, respectively ($p < 0.001$). Adverse events were observed in 86.7% and 77% of patients in the mefloquine and hydroxychloroquine groups, respectively ($p > 0.05$). Thus, during the experiment, mefloquine contributed to the faster virus titer reduction in the lungs. During the clinical trial, the mefloquine efficacy was non-inferiority or, based on a number of indicators, higher compared to hydroxychloroquine, with comparable safety.

Keywords: hydroxychloroquine, SARS-CoV-2, mefloquine, antiviral activity, COVID-19

Author contribution: Filin KN — study concept and design, manuscript writing; Gladkikh VD — manuscript writing and editing; Bykov VN — literature analysis, data acquisition and processing, manuscript writing.

Compliance with ethical standards: animal experiments were approved by the Bioethics Commission of RMC "Home of Pharmacy" (protocol № 3.71/20 dated December 23, 2020); all the procedures involving animals were performed in accordance with the Directive N 2010/63/EC of the European Parliament and of the Council of the European Union "On the Protection of Animals Used for Scientific Purposes" of September 22, 2010. The animals' housing and care complied with GOST R 53434-2009 (Principles of Good Laboratory Practice) and the Guidelines for Laboratory Animals (2010). The clinical trial was approved by the Ethics Committees of the clinical centers of Burnasyan Federal Medical Biophysical Center of FMBA, Federal Clinical Center for High Medical Technologies of FMBA, Center for Specialized Medical Assistance and Medical Technologies of FMBA, National Medical Research Center for Otorhinolaryngology of FMBA; the trial was carried out in accordance with the Russian Federation Government Decree № 441 of April 3, 2020; the informed consent was obtained from all patients.

✉ **Correspondence should be addressed:** Vadim D. Gladkikh
Vaschutinskoe shosse, 11, g. Himki, Moskovskaja oblast, 141402; gladkikh2007@rambler.ru

Received: 21.07.2021 **Accepted:** 26.08.2021 **Published online:** 30.09.2021

DOI: 10.47183/mes.2021.036

ОЦЕНКА ЭФФЕКТИВНОСТИ МЕФЛОХИНА В ОТНОШЕНИИ ИНФЕКЦИИ, ВЫЗВАННОЙ SARS-COV-2 В КЛИНИЧЕСКИХ И ЭКСПЕРИМЕНТАЛЬНЫХ УСЛОВИЯХ

К. Н. Филин, В. Д. Гладких ✉, В. Н. Быков

Научно-производственный центр «Фармзащита» Федерального медико-биологического агентства, Химки, Московская обл., Россия

Эффективность мефлохина в экспериментах *in vivo* и клинических исследованиях у пациентов с COVID-19 не установлена. Целью исследования было оценить влияние мефлохина на накопление SARS-CoV-2 в легких инфицированных животных и изучить эффективность и безопасность мефлохина в сравнении с гидроксихлорохином при лечении пациентов с COVID-19. В ходе эксперимента 96 сирийских хомячков инфицировали SARS-CoV-2. Оценивали накопление вируса в легких в группах животных, которым вводили мефлохин, препарат сравнения рибавирин и контроля. В ходе клинического исследования безопасность и эффективность мефлохина и гидроксихлорохина в лечении пациентов с COVID-19 с легким и средне-тяжелым течением заболевания (172 участника) оценивали по динамике симптомов и результатам компьютерной томографии. В результате эксперимента накопление SARS-CoV-2 в легких сирийских хомячков через 6 суток после заражения и лечения мефлохином составило $2,2 \pm 0,18$ лг БОЕ/г, что было ниже ($p < 0,05$), чем в группе контроля ($3,5 \pm 0,21$ лг БОЕ/г) и в группе рибавирина ($5,2 \pm 0,05$ лг БОЕ/г). В результате клинического исследования 50,0% пациентов в группе мефлохина и 32,4% в группе гидроксихлорохина ($p < 0,05$) достигли легкой степени тяжести заболевания, у 76,5% и 44,6% соответственно зарегистрировали полное разрешение дыхательной недостаточности ($p < 0,001$). Нежелательные явления наблюдались у 86,7 и у 77% пациентов в группах мефлохина и гидроксихлорохина соответственно ($p > 0,05$). Таким образом, мефлохин в эксперименте способствовал более быстрому снижению титра вируса в легких, а в ходе клинических исследований эффективность мефлохина была не хуже, а по некоторым показателям лучше, чем у гидроксихлорохина, при сравнимой безопасности.

Ключевые слова: гидроксихлорохин, SARS-CoV-2, мефлохин, противовирусная активность, COVID-19

Вклад авторов: К. Н. Филин — концепция и дизайн исследования, написание текста; В. Д. Гладких — написание текста, редактирование; В. Н. Быков — сбор литературных данных, сбор и обработка материала, написание текста.

Соблюдение этических стандартов: экспериментальное исследование на лабораторных животных одобрено Комиссией по биоэтике АО НПО «Дом Фармации» (протокол № 3.71/20 от 23 декабря 2020 г.); все процедуры с животными проводили в соответствии с Директивой № 2010/63/ЕС Европейского парламента и Совета Европейского Союза «О защите животных, использующихся для научных целей» от 22.09.2010. Содержание и обслуживание животных осуществляли в соответствии с ГОСТ Р 53434-2009 (Принципы надлежащей лабораторной практики) и «Руководством по лабораторным животным» (2010). Клиническое исследование одобрено этическими комитетами клинических центров ФГБУ ГНЦ ФМБЦ им. А. И. Бурназяна ФМБА России, ФГБУ ФКЦ ВМТ ФМБА России, ФГБУ ФНКЦ СВМП МТ ФМБА России, ФГБУ НМИЦО ФМБА России; проведено в соответствии с Постановлением Правительства Российской Федерации от 03.04.2020 № 441; все пациенты подписали информированное согласие.

✉ **Для корреспонденции:** Вадим Дмитриевич Гладких
Вашутинское шоссе, д. 11, г. Химки, Московская область, 141402, Россия; gladkikh2007@rambler.ru

Статья получена: 21.07.2021 **Статья принята к печати:** 26.08.2021 **Опубликована онлайн:** 30.09.2021

DOI: 10.47183/mes.2021.036

Quinoline derivatives, hydroxychloroquine and chloroquine, are the antimalarials that have proven effective in treatment of infections, caused by coronaviruses [1]. The drugs have a similar chemical structure and pharmacological activity, however, hydroxychloroquine is less toxic [2]. It has been shown that EC_{50} of hydroxychloroquine against SARS-CoV-2 *in vitro* in case of adding the drug 1 h before infection is 4.51–12.96 μM , and the cytotoxic dose is 100 times higher [2]. In case of adding hydroxychloroquine to the culture medium 2 h after infection with SARS-CoV-2, EC_{50} is 0.72–6.14 μM [3]. The above mentioned concentrations can be achieved *in vivo* after receiving the 400 mg therapeutic dose of the drug, given that the drug levels in lungs are 6 times higher than plasma levels.

Mefloquine is one more antimalarial that have proven effective against SARS-CoV-2 *in vitro* [4, 5]. The activity of mefloquine against causative agents of a number of dangerous viral infections [6, 7], including coronaviruses [8–10], has been established. It has been shown that mefloquine inhibits cytopathic effects of the coronavirus in cell culture and prevents the virus from replication at a concentration not exceeding 10 μM (4 $\mu\text{g/L}$) [9]. Clarification of the dosing ranges has established that *in vitro* suppression of SARS-CoV-2 replication is achieved by adding mefloquine to the Vero C1008 cell culture at a concentration exceeding 1.25 μM (0.5 $\mu\text{g/mL}$). Furthermore, the concentration of mefloquine sufficient for SARS-CoV-2 elimination could be achieved 2–3 days after starting taking the drug at a dose equivalent to therapeutic dose [5, 10, 11].

Based on the positive results obtained in experimental studies and clinical trials [12, 13], hydroxychloroquine was included in the treatment regimen for patients with COVID-19 in many countries of the world, including Russia [14]. Antiviral activity of mefloquine against SARS-CoV-2, revealed during the experiment, contributed to mefloquine inclusion in the guidelines for treatment of patients with COVID-19, issued by the Ministry of Health of the Russian Federation in 2020 [14].

Regardless of the fact, that mefloquine has been approved as a treatment for patients with COVID-19, to date, no *in vivo* experimental studies of mefloquine effects on the course of the disease, as well as clinical trials of mefloquine efficacy against the novel coronavirus infection, have been carried out. This has defined the relevance of the study.

The study was aimed to assess the effects of mefloquine on the SARS-CoV-2 accumulation in the lungs of infected animals and to study the efficacy and safety of mefloquine compared to hydroxychloroquine in patients with COVID-19.

METHODS

Experimental procedure

The study involved male Syrian hamsters with body weight of 50–70 g (RMC "Home of Pharmacy"; Russia). The animals were kept under standard housing conditions, with free access to water and 12 h/12 h day/night cycle. The drug was suspended in the 1% starch solution, and the animals received the oral gavage of 100 μL daily for six days according to the following scheme: days 1 and 2 — 8.8 mg/kg; days 3–6 — 3.3 mg/kg. The controls received the 1% starch solution according to the same scheme. Ribavirin (Dragon Hwa ChemPharm Co. Ltd; China), administered by the intramuscular route at a dose of 14.3 mg/kg once a day for six days, was used as a reference substance. Each group included 10 animals.

The virus used was variant B of SARS-nCoV (48th Central Research Institute, Federal State Budgetary Institution under the Ministry of Defense of the Russian Federation). The infecting preparation was prepared using the Vero C1008 cell culture; multiplicity of infection was 1 PFU (plaque-forming unit) per cell. The viral activity in the reference culture was 7.4 lg PFU/mL, and the cytopathic effect (CPE) was 6.5 CPE₅₀/mL. The animals were infected orally at a dose of 3×10^5 PFU and followed up for 7 days. Virus accumulation (lg PFU/g) in lungs was assessed in animals, receiving mefloquine, compared to the control animals and animals, receiving ribavirin, on days 1, 2, 4 and 6 after infection. In addition, inhibitory quotient and the decrease in the virus accumulation in lungs were calculated.

Clinical trial

The open-label randomized multicenter comparative study of the efficacy and safety of mefloquine and hydroxychloroquine off-label use in treatment of patients with novel coronavirus infection, caused by SARS-CoV-2, was carried out in accordance with paragraph 3 of the Decree of the Government of the Russian Federation № 441 of 03.04.2020 from April 7, 2020 to July 21, 2020.

Inclusion criteria: male and female patients over 18 years of age with mild or moderate novel coronavirus infection, confirmed by PCR test for identification of viral RNA; hospitalization of the patient; submitted informed consent to participation (a total of 172 individuals). The patients with moderate course of the disease accounted for over 95%. The recommended classification was used to define the disease severity [14].

Table 1. Results of assessing the infectious SARS-CoV-2 titre in the lungs of Syrian hamsters

Drug	Parameters	Day after infection			
		1	2	4	6
Control	Virus accumulation, lg PFU/g, $M \pm \sigma$	6.0 \pm 0.21	6.0 \pm 0.38	6.3 \pm 0.04	3.5 \pm 0.21*
Mefloquine	Virus accumulation, lg PFU/g, $M \pm \sigma$	6.8 \pm 0.07	5.8 \pm 0.07	6.2 \pm 0.04	2.2 \pm 0.18
	Decrease in virus accumulation, Δlg	no	0.28	0.03	1.34
	Inhibitory quotient, %	no	47.5	7.4	95.5
Ribavirin	Virus accumulation, lg PFU/g, $M \pm \sigma$	6.2 \pm 0.04	5.0 \pm 0.06	6.4 \pm 0.03	5.2 \pm 0.05*
	Decrease in virus accumulation, Δlg	no	0,08	no	no
	Inhibitory quotient, %	no	17.1	no	no

Note: * — the differences from the mefloquine group are considered significant when $p < 0.05$.

Table 2. Comparative evaluation of mefloquine and hydroxychloroquine efficacy based on primary efficacy endpoints

Indicator	Number of patients having reached the point, <i>n</i> (%)		Average time for achieving the endpoint (SD), days	
	Mefloquine	Hydroxychloroquine	Mefloquine	Hydroxychloroquine
Developing mild disease	49/98* (50.0%)	24/74 (32.4%)	11,3 (6.08)	10.0 (10.34)
Resolved respiratory failure	75/98# (76.5 %)	33/74 (44.6 %)	6.5 (6.40)	4.4 (5.68)

Note: * — significant differences from the comparison group, $p < 0.05$; # — significant differences from the comparison group, $p < 0.001$.

Exclusion criteria: severe and critical COVID-19; neurological and mental disorders; history of mental disorder; seizures or low seizure threshold, epilepsy; cardiomyopathy, retinopathy; pregnancy and lactation; liver failure or exacerbation of chronic liver disease; active cancer; severe uncontrolled cardiovascular disease; other disorders and conditions that prevented the patients from the study participation.

The average age of the patients was 52.5 years, the ratio of men to women was 45/55. The patients were randomized and divided into two groups: the patients of group 1 (98 individuals) were prescribed mefloquine, and the patients of group 2 (74 individuals) were prescribed hydroxychloroquine. The drug were prescribed in accordance with the schemes, recommended by the Ministry of Health of Russian Federation [14].

The average duration of the disease prior to screening ($M \pm SD$) was 8.4 ± 5.35 days in the mefloquine group, and 7.9 ± 4.66 in the hydroxychloroquine group. The main symptoms of the disease were as follows: body temperature exceeding 38.5°C , nonproductive cough, fatigue and chest congestion. According to computed tomography (CT), the lung involvement matched CT-2–CT-3 grade.

Both groups received the drugs for 7 days. The clinical status of the patient was registered 11 days after starting taking the drug. In case of clinical recovery, the patient was discharged from the hospital. In case of the need for longer hospital stay, the follow-up was continued.

The following indicators of clinical improvement were used as the primary efficacy endpoints: development of mild coronavirus infection, resolved respiratory failure.

Secondary efficacy endpoints: patient's condition improvement based on CT; achieved CT grade 1 or lower; resolved pneumonia; achieved grade 1 respiratory failure; being provided oxygen support.

The frequency of adverse events (AEs) and serious adverse events (SAEs) was analyzed, and the conditions, which served as basis for the studied drug withdrawal, were registered in order to assess the drug safety.

Statistical analysis was performed using the SAS version 9.3 software package (SAS Institute Inc.; USA). Comparative analysis of parametric data was carried out using the two-way ANOVA for parametric indicators, as well as the comparison of the results using the contingency table approach (chi-square test or Fisher's exact test). The data were tested for normality with the Shapiro–Wilk test. The groups were compared

using the Student's *t*-test (for normal distribution) or the Mann–Whitney *U* test. The differences between groups were considered significant when $p < 0.05$.

RESULTS

Experimental assessment of mefloquine effects on the virus accumulation in lung tissue of Syrian hamsters infected with SARS-CoV-2

The results of assessing the infectious SARS-CoV-2 titre in the lung tissue of Syrian hamsters are presented in Table 1. In addition, the decrease in the virus accumulation and the inhibitory quotient are provided for the mefloquine and ribavirin groups, calculated in relation to the controls.

On day 2 after the infection, the decrease in the viral load was observed in animals, which received mefloquine and ribavirin. However, there were no significant differences from the control group. On day 4 after the infection, the increased viral load was observed in all groups. On day 6, the virus titre in the mefloquine group was significantly lower ($p < 0.05$) compared to both controls and ribavirin group. The decrease in SARS-CoV-2 accumulation compared to controls was 1.34 lg, and the inhibitory quotient was 95.5%.

Comparative evaluation of mefloquine and hydroxychloroquine efficacy in patients with novel coronavirus infection

The results of the primary efficacy endpoint analysis are presented in Table 2.

The proportion of patients having developed the mild disease was significantly higher ($p = 0.021$) in the mefloquine group compared to the hydroxychloroquine group. Regardless of the fact that this endpoint was reached faster after receiving hydroxychloroquine, there were no significant differences between groups ($p > 0.05$).

The proportion of patients with completely resolved respiratory failure (RF) was higher ($p < 0.001$) in the mefloquine group compared to the hydroxychloroquine group. Regardless of the fact that RF resolved faster after receiving hydroxychloroquine, there were no significant differences between groups according to this indicator.

Table 3. Comparative evaluation of mefloquine and hydroxychloroquine efficacy based on secondary efficacy endpoints

Indicator	Number of patients having reached the point, <i>n</i> (%)		Average time for achieving the endpoint (SD), days	
	Mefloquine	Hydroxychloroquine	Mefloquine	Hydroxychloroquine
Improvement based on CT	50 (51.0%)	32 (43.2%)	9.4 (4.48)	9.0 (4.56)
Score CT-1 or lower	54 (55.1%)	36 (48.6%)	2.5 (5.62)	1.1 (4.24)
Resolved pneumonia	15 (15.3%)	9 (12.2%)	7.3 (8.37)	4.4 (5.15)
Achieved grade 1 respiratory failure	77 (78.6%)	54 (73.0%)	1.5 (3.26)	1.0 (3.02)
O ₂ support provided	30 (30.6%)	18 (24.3%)	3.8 (1.93)	4.1 (3.42)

Table 4. Adverse events registered during the study

Indicator	Number of subjects, <i>n</i> (%)		Number of events, <i>n</i>		<i>p</i> -value (Fisher's exact test)
	Mefloquine	Hydroxychloroquine	Mefloquine	Hydroxychloroquine	
Laboratory and instrumental assessment data					
Any AE	54 (55.1%)	29 (39.2%)	54	29	0.046
Elevated transaminase levels	48 (49.0%)	29 (39.2%)	48	29	0.218
Decreased O2 saturation	5 (5.1%)	0 (0.0%)	5	0	0.071
Vascular dysfunction					
Any AE	37 (37.8%)	24 (32.4%)	37	24	0.521
Blood pressure fluctuations	37 (37.8%)	24 (32.4%)	37	24	0.521
Nervous system disorders					
Any AE	30 (30.6%)	23 (31.1%)	34	28	0.99
Headache	17 (17.4%)	19 (25.7%)	17	19	0.192
Vertigo	17 (17.4%)	9 (12.2%)	17	9	0.396
Gastrointestinal disorders					
Any AE	20 (20.4%)	18 (24.3%)	25	19	0.581
Diarrhea	9 (9.2%)	14 (18.9%)	9	14	0.073
Nausea	11 (11.2%)	4 (5.4%)	11	4	0.275
Vomiting	4 (4.1%)	0 (0.0%)	4	0	0.135
Abdominal pain	1 (1%)	1 (1.4%)	1	1	0.99

The results of the primary efficacy endpoint analysis, obtained during the clinical trial, are presented in Table 3.

Analysis of secondary efficacy endpoints revealed no significant differences in any of the studied parameters between the groups of patients, who received mefloquine and hydroxychloroquine.

When assessing safety, a total of 165 adverse events (AEs) were registered in 85 patients (86.73%) of the mefloquine group and 112 AEs were registered in 57 patients (77.03%) of the hydroxychloroquine group (no significant differences between groups, $p = 0.108$). The total number of serious adverse events (SAEs) was 5 in four patients (86.7%) of the mefloquine group and 1 in one patient (1.35%) of the hydroxychloroquine group. Characteristics of the adverse events are presented in Table 4.

Other AEs, including mental disorders (associated with the main risk of mefloquine treatment), were observed in a few cases. Moreover, such AEs as delirium and acute psychosis were registered in only one patient after mefloquine administration.

Mild AEs were registered in the majority of the patients enrolled: 81 (82.7%) patients (160 events) after mefloquine administration and 56 (75.7%) patients (111 events) after hydroxychloroquine administration ($p = 0.339$). Moderate AEs were registered in one (1.02%) patient (1 event — acute psychosis) after mefloquine administration and in 0 (0.0%) patients after hydroxychloroquine administration ($p = 0.99$). Severe AEs were registered in four (4.08%) patients (5 events) after mefloquine administration and in one (1.35%) patient (1 event) after hydroxychloroquine administration ($p = 0.392$):

- mefloquine group: reduced oxygen saturation level in four patients (4.08%), and delirium in one (1.02%) patient;
- comparison group: acute coronary syndrome in one patient (1.35%).

The development of delirium required drug treatment (administration of antipsychotic medication), in other cases SAEs resolved after the drug withdrawal.

Association of AE with the studied drug was regarded as “possible” in one case and as “probable” in one case after

mefloquine administration. The associations for other AEs were questionable or have not been established both for mefloquine and hydroxychloroquine.

DISCUSSION

When performing systematic review of the studies related to the use of hydroxychloroquine in patients with novel coronavirus infection, it was concluded that the drug reduces the rate of disease progression and accelerates the regression of clinical symptoms [15], however, the drug has no effect on the SARS-CoV-2 PCR negative conversion [16], hospital stay length, mortality and the need for mechanical ventilation [17]. Meta-analysis of clinical trials has shown that the use of hydroxychloroquine is associated with excess mortality in patients with COVID-19 [18]. However, this type of effect could be due to the fact that the drug dose used for treatment of the novel coronavirus infection often exceeds the safe dose [19].

Our study has showed that the efficacy of mefloquine prescribed to patients with novel coronavirus infection, which was assessed based on the reduction of symptom severity and dynamic changes of computed tomography imaging, was non-inferiority or, based on a number of indicators, higher compared to hydroxychloroquine. Mefloquine and hydroxychloroquine used in patients with novel coronavirus infection had comparable safety.

Currently, antimalarial medications have been excluded from the guidelines for treatment of COVID-19 patients due to unproven efficacy and the risk of side effects. However, the study results indicate that the effects of mefloquine on SARS-CoV2 in the *in vivo* experiments could be achieved by administration of the drug doses, 3–10 times lower compared to the single dose recommended for humans developing COVID-19 based on the interspecific transfer results [20]. Therefore, it can be assumed that confirmation of the lower-dose mefloquine antiviral activity would make it possible to reconsider the perspectives on using mefloquine in patients with COVID-19 and other viral infections.

CONCLUSIONS

1. In case of the course mefloquine administration at a dose of 75–150 mg in Syrian hamsters infected with SARS-CoV-2 at a dose of 5×10^5 PFU, the significantly decreased accumulation of the virus in lung tissue was observed compared to the control animals, receiving no treatment, and the group, receiving ribavirin.
2. When prescribed to patients with mild or moderate COVID-19,

confirmed by PCR test for identification of viral RNA, the efficacy of mefloquine was non-inferiority or, based on a number of indicators, significantly higher compared to hydroxychloroquine.

3. Safety assessment results show the comparable safety profiles of mefloquine and hydroxychloroquine when used for treatment of patients with COVID-19 (mild and moderate course). Moreover, all registered adverse events are specified in the instruction leaflet for medical use of the medicinal product.

References

1. Chan KW, Wong VT, Tang SCW. COVID-19: An Update on the Epidemiological, Clinical, Preventive and Therapeutic Evidence and Guidelines of Integrative Chinese-Western Medicine for the Management of 2019 Novel Coronavirus Disease. *Am J Chin Med.* 2020; 48 (3): 737–762. DOI: 10.1142/S0192415X20500378.
2. Liu J, Cao R, Xu M, Wang X, Zhang H, Hu H, et al. Hydroxychloroquine, a less toxic derivative of chloroquine, is effective in inhibiting SARS-CoV-2 infection in vitro. *Cell Discov.* 2020 Mar 18; 6: 16. DOI: 10.1038/s41421-020-0156-0.
3. Yao X, Ye F, Zhang M, et al. In Vitro Antiviral Activity and Projection of Optimized Dosing Design of Hydroxychloroquine for the Treatment of Severe Acute Respiratory Syndrome Coronavirus 2 (SARS-CoV-2). *Clin Infect Dis.* 2020 Jul 28; 71 (15): 732–9. DOI: 10.1093/cid/ciaa237.
4. Sweeney TR. The present status of malaria chemotherapy: Mefloquine, a novel antimalarial. *Medicinal Research Reviews.* 1981; 1 (3): 281–301. DOI: 10.1002/med.2610010304.
5. Karbwang J, Na-Bangchang K. Clinical application of mefloquine pharmacokinetics in the treatment of *P falciparum* malaria. *Fundam Clin Pharmacol.* 1994; 8 (6): 491–502. DOI: 10.1111/j.1472-8206.1994.tb00830.x.
6. Sun W, He S, Martínez-Romero C, et al. Synergistic drug combination effectively blocks Ebola virus infection. *Antiviral Research.* 2017 Jan; 137: 165–72. DOI: 10.1016/j.antiviral.2016.11.017.
7. Balasubramanian A, Teramoto T, Kulkarni AA, Bhattacharjee AK, Padmanabhan R. Antiviral activities of selected antimalarials against dengue virus type 2 and Zika virus. *Antiviral Research.* 2017; 137: 141–50. DOI: 10.1016/j.antiviral.2016.11.015.
8. McDonagh P, Sheehy PA, Fawcett A, Norris JM. Antiviral effect of mefloquine on feline calicivirus in vitro. *Vet Microbiol.* 2015 Apr 17; 176 (3–4): 370–7. DOI: 10.1016/j.vetmic.2015.02.007.
9. Fan HH, Wang LQ, Liu WL, et al. Repurposing of clinically approved drugs for treatment of coronavirus disease 2019 in a 2019-novel coronavirus (2019-nCoV) related coronavirus model. *Chin Med J (Engl).* 2020 May 5; 133 (9): 1051–6. DOI: 10.1097/CM9.0000000000000797.
10. Filin KN, Berzin IA, Bykov VN, Gladkih VD, Loginova SYa, Savenko SV, Shhukina VN. Jeksperimental'naja ocenka aktivnosti preparata meflohin v otnoshenii koronavirusa SARS-Cov-2. *Medicina jekstremal'nyh situacij.* 2020; 3: 13–18. DOI: 10.47183/mes.2020.006. Russian.
11. Ferreira MVD, Vieira JLF, Almeida ED, et al. Pharmacokinetics of mefloquine administered with artesunate in patients with uncomplicated *falciparum* malaria from the Brazilian Amazon basin. *Malar J.* 2018 Jul 16; 17 (1): 268. DOI: 10.1186/s12936-018-2416-0.
12. Gautret P, Lagier JC, Parola P, Hoang VT, Meddeb L, Sevestre J, et al. Clinical and microbiological effect of a combination of hydroxychloroquine and azithromycin in 80 COVID 19 patients with at least a six-day follow up: A pilot observational study. *Travel Med Infect Dis.* 2020 Mar–Apr; 34: 101663. DOI: 10.1016/j.tmaid.2020.101663.
13. Cortegiani A, Ingoglia G, Ippolito M, Giarratano A, Einav S. A systematic review on the efficacy and safety of chloroquine for the treatment of COVID-19. *J Crit Care.* 2020 Jun; 57: 279–83. DOI: 10.1016/j.jcrc.2020.03.005.
14. Vremennye metodicheskie rekomendacii. Profilaktika, diagnostika i lechenie novoj koronavirusnoj infekcii (COVID-19). Versija 5 (08.04.20). Moskva: Ministerstvo zdavoohranenija Rossijskoj Federacii. Available from: https://static-1.rosminzdrav.ru/system/attachments/attaches/000/049/951/original/09042020_MR_COVID-19_v5.pdf. Russian.
15. Sama P, Kaur H, Kumar H, Mahendru D, Avti P, Bhattacharyya A, et al. Virological and clinical cure in COVID-19 patients treated with hydroxychloroquine: A systematic review and meta-analysis. *J Med Virol.* 2020 Jul; 92 (7): 776–85. DOI: 10.1002/jmv.25898.
16. Tang W, Cao Z, Han M, Wang Z, Chen J, Sun W, et al. Hydroxychloroquine in patients with mainly mild to moderate coronavirus disease 2019: open label, randomised controlled trial. *BMJ.* 2020 May 14; 369: m1849. DOI: 10.1136/bmj.m1849.
17. WHO Solidarity Trial Consortium, Pan H, Peto R, Henao-Restrepo AM, Preziosi MP, Sathiyamoorthy V, Abdool Karim Q, et al. Repurposed Antiviral Drugs for Covid-19 — Interim WHO Solidarity Trial Results. *N Engl J Med.* 2021; 384 (6): 497–511. DOI: 10.1056/NEJMoa2023184.
18. Axfors C, Schmitt AM, Janiaud P, Vant Hoof J, Abd-Elsalm S, Abdo EF, et al. Mortality outcomes with hydroxychloroquine and chloroquine in COVID-19 from an international collaborative meta-analysis of randomized trials. *Nat Commun.* 2021. 12 (1): 2349. DOI: 10.1038/s41467-021-22446-z.
19. Li R, Yin K, Zhang K, Wang YY, Wu QP, Tang SB, Cheng JD. Application Prospects of Virtual Autopsy in Forensic Pathological Investigations on COVID-19. *Fa Yi Xue Za Zhi.* 2020 Apr; 36 (2): 149–56. DOI: 10.12116/j.issn.1004-5619.2020.02.001.
20. Filin KN, Bykov VN, Gladkih VD, Lugovik IA, Grebenyuk AN. Evaluation of toxicity and effectiveness of the anti-malaria preparation mefloquine with respect to SARS-CoV-2 in experiments on animals. *Toxicological Review.* 2021; (3): 44–49. DOI: 10.36946/0869-7922-2021-29-3-44-49. Russian.

Литература

1. Chan KW, Wong VT, Tang SCW. COVID-19: An Update on the Epidemiological, Clinical, Preventive and Therapeutic Evidence and Guidelines of Integrative Chinese-Western Medicine for the Management of 2019 Novel Coronavirus Disease. *Am J Chin Med.* 2020; 48 (3): 737–762. DOI: 10.1142/S0192415X20500378.
2. Liu J, Cao R, Xu M, Wang X, Zhang H, Hu H, et al. Hydroxychloroquine, a less toxic derivative of chloroquine, is effective in inhibiting SARS-CoV-2 infection in vitro. *Cell Discov.* 2020 Mar 18; 6: 16. DOI: 10.1038/s41421-020-0156-0.
3. Yao X, Ye F, Zhang M, et al. In Vitro Antiviral Activity and Projection of Optimized Dosing Design of Hydroxychloroquine for the Treatment of Severe Acute Respiratory Syndrome Coronavirus 2 (SARS-CoV-2). *Clin Infect Dis.* 2020 Jul 28; 71 (15): 732–9. DOI: 10.1093/cid/ciaa237.
4. Sweeney TR. The present status of malaria chemotherapy: Mefloquine, a novel antimalarial. *Medicinal Research Reviews.* 1981; 1 (3): 281–301. DOI: 10.1002/med.2610010304.
5. Karbwang J, Na-Bangchang K. Clinical application of mefloquine pharmacokinetics in the treatment of *P falciparum* malaria. *Fundam Clin Pharmacol.* 1994; 8 (6): 491–502. DOI: 10.1111/

- j.1472-8206.1994.tb00830.x.
6. Sun W, He S, Martínez-Romero C, et al. Synergistic drug combination effectively blocks Ebola virus infection. *Antiviral Research*. 2017 Jan; 137: 165–72. DOI: 10.1016/j.antiviral.2016.11.017.
 7. Balasubramanian A, Teramoto T, Kulkarni AA, Bhattacharjee AK, Padmanabhan R. Antiviral activities of selected antimalarials against dengue virus type 2 and Zika virus. *Antiviral Research*. 2017; 137: 141–50. DOI: 10.1016/j.antiviral.2016.11.015.
 8. McDonagh P, Sheehy PA, Fawcett A, Norris JM. Antiviral effect of mefloquine on feline calicivirus in vitro. *Vet Microbiol*. 2015 Apr 17; 176 (3–4): 370–7. DOI: 10.1016/j.vetmic.2015.02.007.
 9. Fan HH, Wang LQ, Liu WL, et al. Repurposing of clinically approved drugs for treatment of coronavirus disease 2019 in a 2019-novel coronavirus (2019-nCoV) related coronavirus model. *Chin Med J (Engl)*. 2020 May 5; 133 (9): 1051–6. DOI: 10.1097/CM9.0000000000000797.
 10. Филин К. Н., Берзин И. А., Быков В. Н., Гладких В. Д., Логинова С. Я., Савенко С. В., Щукина В. Н. Экспериментальная оценка активности препарата мефлохин в отношении коронавируса SARS-Cov-2. *Медицина экстремальных ситуаций*. 2020; 3: 13–18. DOI: 10.47183/mes.2020.006.
 11. Ferreira MVD, Vieira JLF, Almeida ED, et al. Pharmacokinetics of mefloquine administered with artesunate in patients with uncomplicated falciparum malaria from the Brazilian Amazon basin. *Malar J*. 2018 Jul 16; 17 (1): 268. DOI: 10.1186/s12936-018-2416-0.
 12. Gautret P, Lagier JC, Parola P, Hoang VT, Meddeb L, Sevestre J, et al. Clinical and microbiological effect of a combination of hydroxychloroquine and azithromycin in 80 COVID 19 patients with at least a six-day follow up: A pilot observational study. *Travel Med Infect Dis*. 2020 Mar–Apr; 34: 101663. DOI: 10.1016/j.tmaid.2020.101663.
 13. Cortegiani A, Ingoglia G, Ippolito M, Giarratano A, Einav S. A systematic review on the efficacy and safety of chloroquine for the treatment of COVID-19. *J Crit Care*. 2020 Jun; 57: 279–83. DOI: 10.1016/j.jcrc.2020.03.005.
 14. Временные методические рекомендации. Профилактика, диагностика и лечение новой коронавирусной инфекции (COVID-19). Версия 5 (08.04.20). Москва: Министерство здравоохранения Российской Федерации. https://static-1.rosminzdrav.ru/system/attachments/attach/000/049/951/original/09042020_MP_COVID-19_v5.pdf.
 15. Sarma P, Kaur H, Kumar H, Mahendru D, Avti P, Bhattacharyya A, et al. Virological and clinical cure in COVID-19 patients treated with hydroxychloroquine: A systematic review and meta-analysis. *J Med Virol*. 2020 Jul; 92 (7): 776–85. DOI: 10.1002/jmv.25898.
 16. Tang W, Cao Z, Han M, Wang Z, Chen J, Sun W, et al. Hydroxychloroquine in patients with mainly mild to moderate coronavirus disease 2019: open label, randomised controlled trial. *BMJ*. 2020 May 14; 369: m1849. DOI: 10.1136/bmj.m1849.
 17. WHO Solidarity Trial Consortium, Pan H, Peto R, Henao-Restrepo AM, Preziosi MP, Sathiyamoorthy V, Abdool Karim Q, et al. Repurposed Antiviral Drugs for Covid-19 — Interim WHO Solidarity Trial Results. *N Engl J Med*. 2021; 384 (6): 497–511. DOI: 10.1056/NEJMoa2023184.
 18. Axfors C, Schmitt AM, Janiaud P, Vant Hooft J, Abd-ElSalm S, Abdo EF, et al. Mortality outcomes with hydroxychloroquine and chloroquine in COVID-19 from an international collaborative meta-analysis of randomized trials. *Nat Commun*. 2021. 12 (1): 2349. DOI: 10.1038/s41467-021-22446-z.
 19. Li R, Yin K, Zhang K, Wang YY, Wu QP, Tang SB, Cheng JD. Application Prospects of Virtual Autopsy in Forensic Pathological Investigations on COVID-19. *Fa Yi Xue Za Zhi*. 2020 Apr; 36 (2): 149–56. DOI: 10.12116/j.issn.1004-5619.2020.02.001.
 20. Филин К. Н., Быков В. Н., Гладких В. Д., Луговик И. А., Гребенюк А. Н.. Оценка токсичности и эффективности противомаларийного препарата мефлохин в отношении SARS-CoV-2 в экспериментах на животных. *Токсикологический вестник*. 2021; 3: 44–49. DOI: 10.36946/0869-7922-2021-29-3-44-49.

COMPARISON OF METHODS FOR PURIFICATION OF BACTERIOPHAGE LYSATES OF GRAM-NEGATIVE BACTERIA FOR PERSONALIZED THERAPY

Gorodnichev RB¹✉, Kornienko MA¹, Kuptsov NS¹, Efimov AD², Bogdan VI², Letarov AV², Shitikov EA¹, Ilna EN¹

¹ Federal Research and Clinical Center of Physical-Chemical Medicine of Federal Medical Biological Agency, Moscow, Russia

² Federal Research Center of Biotechnology, Moscow, Russia

Phage therapy is a promising method of treating antibiotic-resistant infections. To obtain a safe therapeutic formulation, bacterial cell components, including endotoxins, must be removed from the phage lysate. This study was aimed at comparing the efficacy of purification methods for phage lysates intended for therapeutic use. Phages vB_KpnM_Seu621 (*Myoviridae*) and vB_KpnP_Dlv622 (*Autographiviridae*) were grown using the KP9068 strain of *Klebsiella pneumoniae* as a host. The obtained lysates were purified using phage precipitation with polyethylene glycol, CsCl density gradient ultracentrifugation, sucrose density gradient ultracentrifugation, precipitation with 100 kDa centrifugal filter units, and phage concentration on 0.22 µm cellulose filters in the presence of MgSO₄. Endotoxin concentrations were determined by LAL testing. The obtained lysates contained $1.25 \times 10^{12} \pm 7.46 \times 10^{10}$ and $2.25 \times 10^{12} \pm 1.34 \times 10^{11}$ PFU/ml of vB_KpnM_Seu621 and vB_KpnP_Dlv622, respectively, and had endotoxin concentrations of $3,806,056 \pm 429,410$ and $189,456 \pm 12,406$ EU/ml, respectively. CsCl gradient ultracentrifugation was found to be the optimal conventional purification method in terms of reducing endotoxin concentrations and maintaining phage titers (303 ± 20 — 313 ± 35 EU/ml, 1.5 – $2.75 \times 10^{12} \pm 1.71 \times 10^{11}$ PFU/ml). Sucrose gradient ultracentrifugation and filtration in the presence of MgSO₄ were found to be the optimal non-traditional purification methods. A method for phage lysate purification should be selected for each phage preparation individually. Sucrose gradient ultracentrifugation and filtration in the presence of MgSO₄ hold promise as purification methods that can produce phage preparations suitable for intravenous administration.

Keywords: bacteriophage, phage therapy, purification methods, bacterial lysate, microbiology, endotoxin, *Klebsiella pneumoniae*

Funding: all study expenses were covered by the funds allocated for the State Assignment on the Development of a personalized approach to the therapy of infections using virulent bacteriophages (Code: Bacteriophage).

Author contribution: Gorodnichev RB — planned the study, conducted the experiments, and wrote the manuscript; Kornienko MA, Letarov AV, Shitikov EA — planned the study, analyzed its results, and wrote the manuscript; Kuptsov NS, Efimov AD, Bogdan VI — conducted the experiments; Ilna EN — planned the study and wrote the manuscript.

Compliance with ethical standards: the experiments were conducted in full compliance with Biosafety Guidelines for working with risk group III–IV pathogens (SP 1.3.2322-08), Amendment 1 to Biosafety Guidelines for working with risk group III–IV pathogens (SP 1.3.2518-09), medical waste regulations (SanPin 2.1.7.2790-10), and Federal Clinical Guidelines on the rational use of bacteriophages for therapy and prevention of diseases.

✉ **Correspondence should be addressed:** Roman B. Gorodnichev
Malaya Pirogovskaya, 1a, Moscow, 119435; gorodnichev.r.b@gmail.com

Received: 20.07.2021 **Accepted:** 25.08.2021 **Published online:** 22.09.2021

DOI: 10.47183/mes.2021.029

СРАВНЕНИЕ МЕТОДОВ ОЧИСТКИ ФАГОВЫХ ЛИЗАТОВ ГРАМОТРИЦАТЕЛЬНЫХ БАКТЕРИЙ ДЛЯ ПЕРСОНАЛИЗИРОВАННОЙ ТЕРАПИИ

Р. Б. Городничев¹✉, М. А. Корниенко¹, Н. С. Купцов¹, А. Д. Ефимов², В. И. Богдан², А. В. Летаров², Е. А. Шитиков¹, Е. Н. Ильина¹

¹ Федеральный научно-клинический центр физико-химической медицины Федерального медико-биологического агентства, Москва, Россия

² Федеральный исследовательский центр биотехнологии, Москва, Россия

Фаготерапия является перспективным методом лечения инфекций, вызванных устойчивыми к антибактериальным препаратам бактериями. Для получения безопасных терапевтических препаратов бактериофагов необходима глубокая очистка лизатов от компонентов бактериальной клетки, в частности эндотоксинов. Целью работы было исследовать применимость различных методов очистки фаголизатов для получения терапевтических препаратов. Фаги vB_KpnM_Seu621 (*Myoviridae*) и vB_KpnP_Dlv622 (*Autographiviridae*) использовали для получения лизата штамма *Klebsiella pneumoniae* KP9068. Очистку лизатов проводили методом осаждения бактериофагов с использованием полиэтиленгликоля, ультрацентрифугированием в градиенте CsCl, ультрацентрифугированием в градиенте сахарозы, с помощью центрифужных концентраторов (100 кДа), концентрированием на целлюлозных фильтрах 0,22 мкм в присутствии MgSO₄. Уровень эндотоксинов определяли ЛАЛ-тестированием. В результате действия vB_KpnM_Seu621 и vB_KpnP_Dlv622 были получены лизаты с титром $1,25 \times 10^{12} \pm 7,46 \times 10^{10}$ и $2,25 \times 10^{12} \pm 1,34 \times 10^{11}$ БОЕ/мл и концентрацией эндотоксина 3806056 ± 429410 и 189456 ± 12406 ЕЭ/мл соответственно. Из традиционных методов оптимальным по снижению уровня эндотоксина и сохранению концентрации фаговых частиц было ультрацентрифугирование в градиенте CsCl (303 ± 20 — 313 ± 35 ЕЭ/мл, $1,5$ – $2,75 \times 10^{12} \pm 1,71 \times 10^{11}$ БОЕ/мл); из альтернативных — очистка в градиенте сахарозы и фильтрация в присутствии MgSO₄. Метод очистки лизатов следует подбирать для каждого препарата бактериофагов отдельно. Из способов очистки лизатов, пригодных для внутривенного и интратекального введения, перспективны метод ультрацентрифугирования в градиенте сахарозы и фильтрация в присутствии MgSO₄.

Ключевые слова: бактериофаги, бактериофаговая терапия, методы очистки, бактериальные лизаты, микробиология, эндотоксины, *Klebsiella pneumoniae*

Финансирование: исследование выполнено за счет средств, предоставленных для выполнения государственного задания «Разработка персонализированного подхода терапии инфекционных процессов с применением вирулентных бактериофагов» (ШИФР: Бактериофаг).

Вклад авторов: Р. Б. Городничев — план исследований, набор и обработка данных, написание статьи; М. А. Корниенко, А. В. Летаров, Е. А. Шитиков — план исследований, обработка данных, написание статьи; Н. С. Купцов, А. Д. Ефимов, В. И. Богдан — набор данных; Е. Н. Ильина — план исследований, написание статьи.

Соблюдение этических стандартов: вся экспериментальная работа выполнена с соблюдением норм Санитарно-эпидемиологических правил «Безопасность работы с микроорганизмами III–IV групп патогенности (опасности) и возбудителями паразитарных болезней» СП 1.3.2322-08; Санитарно-эпидемиологических правил СП 1.3.2518-09 — «Дополнения и изменения № 1 к санитарно-эпидемиологическим правилам «Безопасность работы с микроорганизмами III–IV групп патогенности (опасности) и возбудителями паразитарных болезней» СП 1.3.2322-08; Санитарно-эпидемиологических правил «Санитарно-эпидемиологические требования к обращению с медицинскими отходами» СанПиН 2.1.7.2790-10, а также Федеральных клинических рекомендаций «Рациональное применение бактериофагов в лечебной и противоэпидемической практике».

✉ **Для корреспонденции:** Роман Борисович Городничев
ул. Малая Пироговская, д. 1а, г. Москва, 119435; gorodnichev.r.b@gmail.com

Статья получена: 20.07.2021 **Статья принята к печати:** 25.08.2021 **Опубликована онлайн:** 22.09.2021

DOI: 10.47183/mes.2021.029

Irrational use of antibiotics has driven the emergence and global dissemination of drug-resistant microorganisms. The World Health Organization has prioritized the search for novel antimicrobial agents against *Acinetobacter baumannii*, *Pseudomonas aeruginosa*, *Klebsiella spp.*, *Escherichia coli*, and *Enterobacter spp.* because the number of multidrug-resistant isolates in this group of microorganisms has been steadily trending upwards [1].

As alternatives to antibiotics, virulent bacteriophages hold promise for the therapy of multidrug-resistant bacterial infections [2]. Phages are naturally occurring antagonists of bacteria, capable of selectively and effectively infecting a bacterial cell. The primary advantage of phage therapy lies in the ability of phages to cause death of the bacterial cell regardless of its sensitivity to antibiotics [3]. Besides, due to remarkable host specificity, phage therapy can eliminate the infectious agent without harming the patient's natural microbiota.

Based on the accumulated clinical experience, the following requirements have been elaborated for therapeutic phages and phage cocktails: phage virulence, the absence of toxin genes and antibiotic resistance determinants in the phage genome, the ability to infect a wide range of hosts, which is determined by the efficiency of plating, high levels of phage particle production per cell, and the effective phage concentration of at least 10^9 PFU/ml [4–7].

However, as typical viruses phages replicate only inside a bacterial cell, usually causing its lysis. So, phage preparations can be contaminated by bacterial cells and their components, including endotoxins [6]. Lipopolysaccharides, which are the main constituent of the outer membrane of gram-negative bacteria, are the most illustrative example of bacterial endotoxins [8]. Endotoxins are highly immunogenic and can provoke septic (endotoxic) shock resulting in intravascular coagulation, organ failure and death [9].

So far, a few approaches to phage cultivation and purification have been proposed; of them, polyethylene glycol (PEG) precipitation and CsCl density gradient ultracentrifugation are the most common [10]. The drawback of these approaches is the presence of harmful compounds (e.g. cesium salts (80 ng/ml) in the end preparation with CsCl centrifugation), which significantly limits its usage as a therapeutic agent [10]. Sucrose density gradient ultracentrifugation exploited by virology studies may offer an alternative [11, 12]. Methods of phage enrichment from environmental sources, too, have been increasingly used for the purification of phage lysates in recent years; among them are 100 kDa filtration and isolation in the presence of salts [10, 12–14]. Several chromatography-based methods for phage purification have been developed, like affinity chromatography-based commercial products for removing endotoxins from phage lysates, for example, EndoTrap® columns (Lionex GmbH; Germany). However, a series of research studies have shown that a single passage of a crude lysate through the column only slightly reduces endotoxin concentrations in the preparation [13, 15, 16]. The aim of this study was to compare the efficacy of purification methods for phage lysates intended for therapeutic use.

METHODS

Bacterial strains, phages, and media

The *K. pneumoniae* strain KP9068 was obtained from the collection of the Laboratory of Molecular Genetics of Microorganisms (Federal Research and Clinical Center of Physical-Chemical Medicine, FMBA; Russia). This strain is

resistant to cephalosporins (cefotaxime, ceftazidime, ceftriaxone, cefixime), fluoroquinolones (ciprofloxacin, ofloxacin), tetracycline, azithromycin, chloramphenicol, gentamicin, and ampicillin and has intermediate sensitivity to meropenem. The strain belongs to sequence type 11. Its capsule type identified by the sequencing of the *wzi* gene is K23 [17]. Bacterial cultures used in our experiment were grown in lysogeny broth (LB, Himedia; India) at 37 °C.

Drawing on the literature data on the phylogenetic diversity of bacteriophages in commercial phage cocktails, we picked 2 lytic phages that represented 2 different families and were active against *K. pneumoniae* strains with K23 capsule type [18].

Bacteriophages vB_KpnM_Seu621 (MT939253.1) and vB_KpnP_Dlv622 (MT939252.1) cause lysis of *K. pneumoniae* and belong to the *Myoviridae* and *Autographiviridae* families, respectively [19]. Phage vB_KpnM_Seu621 has the following morphological characteristics: an isometric head of 75 nm in diameter and a 104 nm long contractile tail. Bacteriophage vB_KpnP_Dlv622 has a smaller isometric head (57 nm) and a 12 nm long non-contractile tail. The genomes of the 2 bacteriophages were analyzed in earlier work and did not encode any toxin and integrase genes that could preclude their use in therapy [19].

The phages were grown using the KP9068 strain of *K. pneumoniae* as a host in a thermoshaker at 100 rpm and 37 °C for 18 h. Briefly, the host strain was grown to the mid-log phase (OD 600 nm = 0.3) and then inoculated with the phage lysate to achieve the multiplicity of infection of 0.001. The obtained phage lysates were clarified from cell debris by 15 min centrifugation at 3,500 g followed by sequential filtering through 0.45 µm (Merck Millipore; USA) and 0.22 µm (Merck Millipore; USA) membrane filters. Phage concentrations in the phage lysate were measured using the standard double-layer agar technique. Phage titers were expressed as the number of plaque forming units per one ml (PFU/ml) [20].

Phage precipitation with PEG

In this step, phage particles were recovered from the lysate by precipitation with PEG 6000 (Dia-M; Russia) using a previously described but slightly modified technique [21]. Ten ml of the phage lysate was combined with 2.5 ml of a sterile solution containing 20% PEG 6000 and 2.5 M NaCl. The samples were mixed by inverting without vortexing, cooled on ice for 1 h and centrifuged at 20,000 g for 20 min. Most of the supernatant was carefully removed. Then the samples were centrifuged again at 20,000 g for 10 min and the supernatant was again removed. The precipitate containing phage particles was resuspended in 1 ml of a sterile SM buffer (100 mM NaCl, 10 mM MgSO₄, 50 mM Tris-HCl, pH 7.5, and 0.01% (w/v) gelatin. The suspension was vortexed, incubated on ice for 1 h, vortexed again to remove PEG, and centrifuged at 13,000 g for 1 min. The supernatant was transferred to a clean testing tube for further experiments.

CsCl density gradient ultracentrifugation

CsCl density gradient ultracentrifugation was performed following the protocol described in [21]. Aliquots (70 ml) of the phage lysates were centrifuged in a Beckman Type 45Ti rotor (Beckman Coulter; USA) at 75,000 g and 20 °C for 1 h. The supernatant was gently removed and the precipitate was resuspended in 800 µl of SM buffer. Next, solutions containing different concentrations of CsCl (1.3–1.4–1.45–1.5–1.6 g/ml)

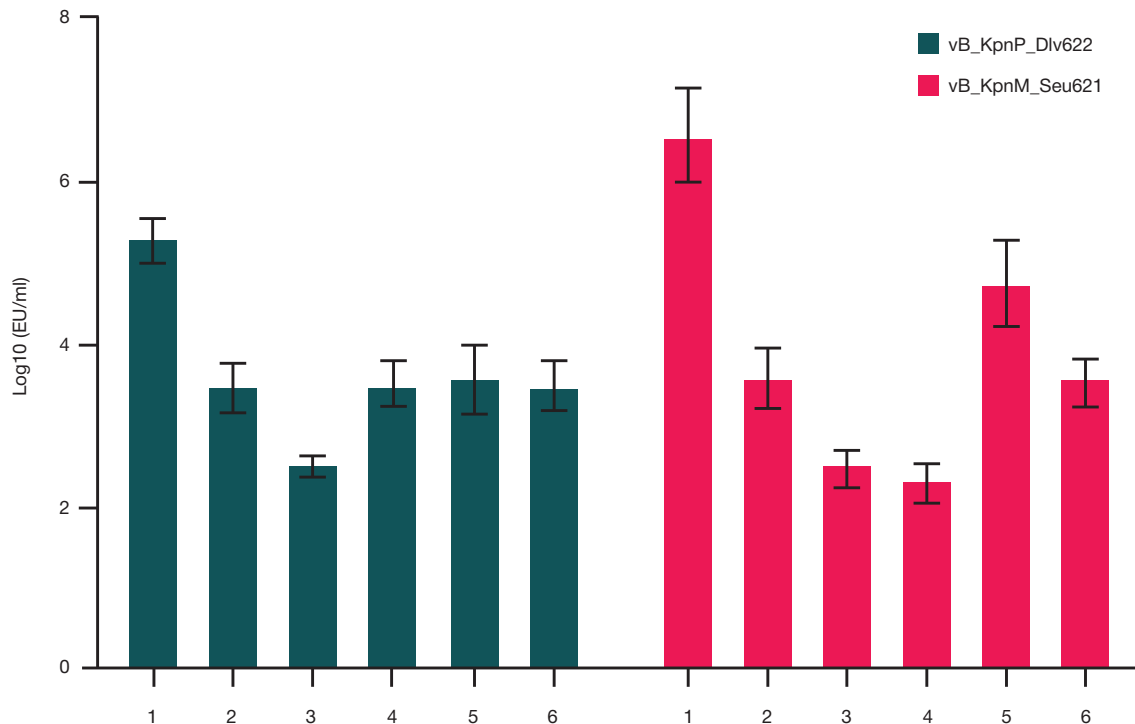


Fig. 1. Endotoxin concentrations in the purified vB_KpnM_Seu621 and vB_KpnP_Dlv622 phage lysates. **1** — crude lysate; **2** — precipitation with PEG; **3** — CsCl density gradient ultracentrifugation; **4** — sucrose density gradient ultracentrifugation; **5** — 100 kDa filtration; **6** — filtration through 0.22 μ m filters in the presence of MgSO₄

and SM buffer were prepared. The solutions (800 μ l) were added to the centrifuge tube layer by layer to create a gradient, starting with the highest CsCl concentration; the top layer solution had the lowest CsCl concentration. A concentrated phage sample (800 μ l) containing only one of the studied phages was applied on top of the last layer of the gradient. The samples were centrifuged in a Beckman SW50.1 rotor (Beckman Coulter; USA) at 75,000 g and 20 °C for 1 h. The opalescent phage band was collected, brought to 1 ml by adding SM buffer, and placed into a dialysis tubing (Thermo FS; USA). Dialysis was performed for 18 h against a tenfold volume of SM buffer at 4 °C and constant stirring of the liquid, replacing the buffer every 4 h. After dialysis, the samples were additionally filtered through 0.22 μ m filters (Merck Millipore; USA).

Sucrose density gradient ultracentrifugation

Sucrose density gradient ultracentrifugation was performed following a standard but slightly modified protocol [11].

Aliquots (70 ml) of the phage lysates were centrifuged in a Beckman Type 45Ti rotor (Beckman Coulter; USA) at 75,000 g and 20 °C for 1 h. Each of the obtained precipitates was resuspended in 800 μ l of SM-buffer. Then sucrose solutions (20, 30, 40, 50 and 60%) were prepared in a buffer containing 50 mM Tris-HCl, 50 mM NaCl, pH 7.5. The solutions (800 μ l) were added to the centrifuge tube layer by layer to create a gradient, starting with the solution that had the highest sucrose concentration (60%); the top layer solution had the lowest sucrose concentration (20%). A concentrated phage sample (800 μ l) containing only one of the studied phages was applied on top of the last layer of the gradient. The samples were centrifuged in a Beckman Type SW50.1 rotor (Beckman Coulter; USA) at 75,000 g and 20 °C for 1 h. Free phage particles formed a visible opalescent band between the 50% and 60% sucrose layers. The phage layer was collected and brought to 1 ml by adding SM buffer.

Phage purification with 100 kDa centrifugal filters

The phage lysates (1 ml) were placed on 100 kDa Microcon centrifugal filters (Millipore; USA) and centrifuged at 10,000 g for 10 min. To recover trapped phage particles, the filter was coated with 300 μ l of sterile SM buffer, placed upside down in a clean sterile centrifuge tube and centrifuged at 1,000 g for 3 min. The purified lysate was brought to 1 ml by adding a sterile SM buffer.

Phage concentration on 0.22 μ m cellulose filters in the presence of MgSO₄

Phage concentration on 0.22 μ m filters in the presence of MgSO₄ was performed on 50 ml aliquots of the lysates cleared of cell debris [14]. Dry reagent-grade MgSO₄ (Dia-M; Russia) was added to the lysates to reach a final concentration of 50 mM. The samples were mixed by inverting without vortexing until complete dissolution of MgSO₄. The obtained suspensions were slowly filtered through 0.22 μ m mixed cellulose ester GSWP membranes (Millipore; USA). The membranes were cut in small pieces (sized ~ 1 mm²) and immersed into 5 ml of a sterile SM buffer. To achieve complete elution of phage particles from the filter surface, the suspension was ultrasonicated treated by ultrasonication for 4 min. Then, large filter fragments were precipitated by 10 min centrifugation at 3,500 g; the supernatant was collected for further experiments.

Measuring endotoxin concentrations in the samples

Endotoxin concentrations were measured using commercial Endosafe® kits for turbidimetric LAL testing (Charles River; USA) following the manufacturer's protocol. Turbidity assays were conducted in a microplate reader (Multiskan Ascent, Thermo; USA) at 405 nm wavelength.

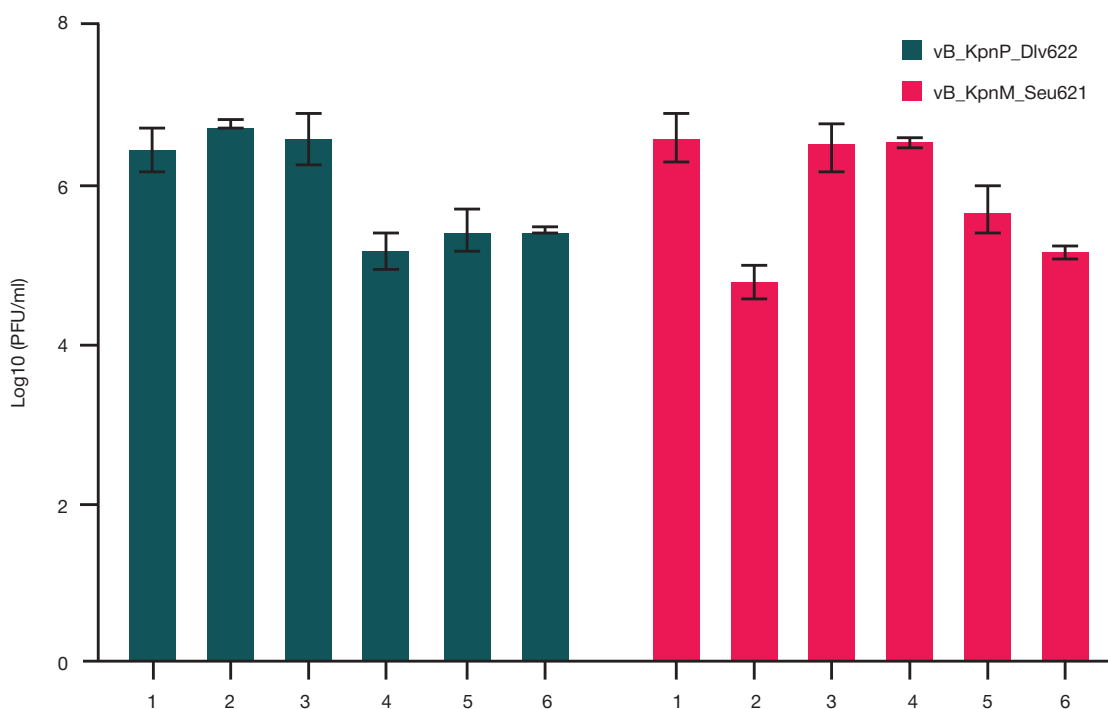


Fig. 2. Concentration of phage particles in purified vB_KpnM_Seu621 and vB_KpnP_Dlv622 lysates after purification. 1 — crude lysates; 2 — precipitation with PEG; 3 — CsCl density gradient ultracentrifugation; 4 — sucrose density gradient ultracentrifugation; 5 — 100 kDa filtration; 6 — filtration through 0.22 µm filters in the presence of MgSO₄

Statistical analysis

Statistical analysis (ANOVA, standard deviations) was carried out in GraphPad Prisma v.8.0.1 (GraphPad Software; USA).

RESULTS

Study design

Five different methods of phage purification were compared: precipitation with PEG, CsCl density gradient ultracentrifugation, sucrose density gradient ultracentrifugation, purification with 100 kDa centrifugal filters, and concentration on 0.22 µm cellulose filters in the presence of MgSO₄. Each of the studied purification procedures was conducted in 3 replicates. Their efficacy was assessed by measuring phage titers and endotoxin concentrations in the purified product.

First, phage lysates were obtained with the following phage titers: $1.25 \times 10^{12} \pm 7.46 \times 10^{10}$ PFU/ml and $2.25 \times 10^{12} \pm 1.34 \times 10^{11}$ PFU/ml for vB_KpnM_Seu621 and vB_KpnP_Dlv622,

respectively. Bacterial debris and live bacterial cells were removed by filtration through 0.22 µm filters (Millipore; USA). Endotoxin concentrations in the non-purified phage lysates were $3,806,056 \pm 429,410$ EU/ml for vB_KpnM_Seu621 and $189,456 \pm 12,406$ EU/ml for B_KpnP_Dlv622 (Fig. 1).

The obtained phage preparations were tested for contamination by seeding their 50 µl aliquots on nutrient agar. Mean values and standard deviations were calculated for the measured phage titers and endotoxin concentrations. We also calculated endotoxin concentrations in a single therapeutic dose of the phage preparation. Drawing on the literature, we assumed the effective therapeutic phage dose to be 10⁹ [22–24].

Changes in endotoxin concentrations after applying different purification methods

In the first part of our study, we analyzed the efficacy of conventional laboratory methods for phage purification: precipitation with PEG and CsCl density gradient ultracentrifugation. Phage precipitation with PEG reduced

Table. Number of doses of therapeutic vB_KpnM_Seu621 and vB_KpnP_Dlv622 phage cocktails and endotoxin content per dose calculated for 100 ml of the initial phage lysate

Purification method	Bacteriophage			
	vB_KpnM_Seu621		vB_KpnP_Dlv622	
	Number of doses	Endotoxin content, EU/dose 10 ⁹ PFU	Number of doses	Endotoxin content, EU/dose 10 ⁹ PFU
Crude lysate	125,000	3045	225,000	84
PEG precipitation	50,000	0.76	10	3000
CsCl density gradient ultracentrifugation	3850	0.11	2100	0.21
Sucrose density gradient ultracentrifugation	7	40	2800	2
100 kDa filtration	15	3743	50	77
Filtration through 0.22 µm filters in the presence of MgSO ₄	150	47	50	128

endotoxin concentrations by 2–3 orders of magnitude ($p < 0.0001$): from $3,000 \pm 324$ to $3,817 \pm 486$ EU/ml. CsCl density gradient ultracentrifugation is the gold standard of phage purification; it resulted in an even greater reduction of endotoxin concentrations: from 303 ± 35 to 313 ± 20 EU/ml ($p < 0.0001$) (see Fig. 1).

Sucrose density gradient ultracentrifugation, 100 kDa filtration and slow filtration through $0.22 \mu\text{m}$ cellulose filters in the presence of MgSO_4 were chosen as alternative purification methods that could produce safe therapeutic formulations suitable for clinical use. Sucrose density gradient ultracentrifugation reduced endotoxin concentrations in the vB_KpnM_Seu621 lysate by 4 orders of magnitude ($p < 0.0001$), to 200 ± 28 EU/ml; for the vB_KpnP_Dlv622 lysate, the reduction was not so pronounced: by only 2 orders of magnitude, to $3,368 \pm 348$ EU/ml ($p < 0.0001$). Using 100 kDa centrifugal filter concentrators, we were able to lower endotoxin concentration by 1.5 orders of magnitude ($p < 0.0001$) in both lysates, bringing them down to $56,148 \pm 7,832$ EU/ml for phage vB_KpnM_Seu621 and $3,850 \pm 593$ EU/ml for phage vB_KpnP_Dlv622. The efficacy of phage isolation in the presence of MgSO_4 was similar to that of PEG precipitation ($p > 0.9999$) and resulted in a reduction in endotoxin concentrations by 2–3 orders of magnitude: from $3,187 \pm 368$ to $3,502 \pm 372$ EU/ml ($p < 0.0001$) (see Fig. 1).

Changes in phage titers after applying different purification methods

A phage titer is an important characteristic of a therapeutic phage formulation; therefore, it needs to be either maintained or increased through purification.

Different purification methods produced different changes in phage titers. Precipitation with PEG did not change vB_KpnM_Seu621 titers significantly. By contrast, vB_KpnP_Dlv622 titers dropped by 3 orders of magnitude ($p < 0.0001$) to $1 \times 10^9 \pm 5.7 \times 10^7$ PFU/ml after PEG precipitation (Fig. 2). The gold standard of purification, CsCl density gradient ultracentrifugation, demonstrated a more uniform result: in both phage preparations, phage titers did not change significantly ($p > 0.9999$) (Fig. 2).

Sucrose density gradient ultracentrifugation led to a reduction ($p < 0.0001$) in vB_KpnM_Seu621 titers to $5 \times 10^9 \pm 2.9 \times 10^8$ PFU/ml but did not change vB_KpnP_Dlv622 titers significantly. Filtration with 100 kDa centrifugal filters reduced ($p < 0.0001$) phage titers in both phage preparations down to $1.5\text{--}5 \times 10^{10} \pm 3.1 \times 10^9$ PFU/ml. Filtration in the presence of MgSO_4 reduced ($p < 0.0001$) phage titers by 2–3 orders of magnitude, to $1.5 \times 10^{10} \pm 1.1 \times 10^9$ PFU/ml and $5 \times 10^9 \pm 2.5 \times 10^8$ PFU/ml for vB_KpnM_Seu621 and vB_KpnP_Dlv622, respectively (see Fig. 2).

DISCUSSION

Phage therapy has been used in clinical practice since the beginning of the 20th century. It is effective against infectious diseases of any etiology, especially against purulent and inflammatory wounds, otitis and bowel infections [25–27]. As more bacteria are acquiring multidrug resistance, the need arises to administer phage preparations intravenously or intrathecally. Phage formulations for intravenous administration must satisfy certain purity and efficacy criteria. According to the pharmacopeial description provided in the Pharmacopoeia Monograph.1.2.4.0006.15 on Bacterial endotoxins, the amount of endotoxin in the formulation cannot exceed 5 EU/kg

per hour for an intravenous formulation and 0.2 EU/kg per hour for an intrathecal formulation [28]. According to the literature, the recommended phage titer ensuring a stable bactericidal effect is at least 10^9 PFU per dose [22–24].

For the purpose of our study, we selected 2 phages from two different families. Both phages vB_KpnM_Seu621 and vB_KpnP_Dlv622 caused lysis of the bacterial host, and the concentrations of phage particles in the lysates were very similar ($1.25\text{--}2.25 \times 10^{12} \pm 1.34 \times 10^{11}$ PFU/ml), but the detected amount of endotoxin in the phage lysates differed twentyfold (see Fig. 1). This finding is consistent with the literature reports: endotoxin concentrations in phage lysates vary considerably ($101\text{--}105$ EU/ 10^9 PFU) depending on the taxonomic position of the phage [10, 12, 13]. Based on the standard guidelines on the minimum phage titer in the therapeutic dose (10^9 PFU/ml) and the maximum allowed endotoxin concentration (325 EU/ml) in an intravenous phage formulation (calculated for a single 1 ml dose administered intravenously to a patient weighing 65 kg), we conclude that the lysate of phage vB_KpnP_Dlv622 can be used for intravenous administration after dilution, unlike the lysate of phage vB_KpnM_Seu621 with endotoxin concentrations being by an order of magnitude higher than the admissible maximum level (Table).

Being the gold standard of phage purification, CsCl density gradient ultracentrifugation turned out to be most effective in comparison with other tested methods (see Table). There are a few reports of successful phage therapy with intravenous phage formulations purified with CsCl density gradient ultracentrifugation [22, 23]. However, this purification method has its own limitations due to the use of cesium salts because the end preparation, even when dialyzed, may contain residual cesium [10]. According to the literature, CsCl density gradient ultracentrifugation can remove up to 99.6% of the total endotoxin amount, but generally its efficacy varies from 18% to 99.6% [13].

Phage precipitation with PEG is a common laboratory method for phage purification. In our study, its efficacy differed between phage families. After PEG purification, the preparation of vB_KpnM_Seu621, the representative of the Myoviridae family, still contained a fairly high vB_KpnM_Seu621 titer. But the titer of phage vB_KpnP_Dlv622 fell significantly after this procedure, showing its low efficacy for the Autographiviridae family. According to the literature, PEG precipitation is not equally effective for morphologically different phages, and it may be necessary to adjust the composition of the salt fraction or the length of the PEG molecule [10, 12, 29]. PEG precipitation removes up to 88% of endotoxin from the lysate of the filamentous *E. coli* phage M13 and reduces the amount of endotoxin twentyfold for the Myoviridae family [12].

Sucrose density gradient ultracentrifugation is widely used for the purification of virus suspension; however, it is rarely exploited to purify phage lysates [11]. In our study, this method generated purified phage preparations suitable for intravenous and even intrathecal administration, as was the case with vB_KpnP_Dlv622. It should be noted that due to the reduction in phage titers, we were able to obtain only 7 doses of vB_KpnM_Seu621 preparations, which may not be sufficient for one complete course of personalized therapy. The problem could be solved by optimizing the protocol by adjusting the concentration of the gradient solution and centrifugation time.

An endotoxin molecule is usually no larger than 10–20 kDa, so 100 kDa filtration may be effective for phage purification. In our study, the efficacy of this method differed between the phages and caused a reduction in phage titers in both preparations. For the *Myoviridae* phage, high endotoxin concentrations might

be explained by the presence of endotoxin micelles that grow to 1,000 kDa and therefore cannot pass the filter [30]. Earlier, tangential flow filtration, a modified version of 100 kDa filtration, was successfully used to effectively eliminate up to 90% of endotoxin from the phage lysate; however, this method was never tested on *Podoviridae* phages [10].

Slow filtration through 0.22 µm cellulose filters in the presence of MgSO₄ is normally used for phage enrichment from natural water sources but can be applied to purify phage lysates, too. Despite the fall in phage titers during purification, this method generated a sufficient number of therapeutic doses suitable for intravenous administration. Importantly, the efficacy of the method was satisfactory for both phages regardless of their taxonomic position and thus was the only alternative for the purification of Myoviridae phages.

Slow filtration in the presence of MgSO₄ and 100 kDa filtration turned out to be the least time-consuming, taking 2 and 1 h, respectively. Sucrose density gradient centrifugation and PEG precipitation took an average of 3.5 h. However, phage lysates purified with CsCl density gradient centrifugation and precipitation with PEG required further purification with dialysis, which extended purification time to 18 h. So, the

most rapid methods for producing purified phage preparations suitable for clinical use were 100 kDa filtration, slow filtration in the presence of MgSO₄, and sucrose density gradient ultracentrifugation.

Our findings were consistent with the literature: the amount of endotoxin after purification and the efficacy of the tested purification methods were different for different phage families. Due to the difference in phage size and/or the value of the sedimentation constant, an optimal purification method or a combination of purification methods will depend on the phylogenetic position of the bacteriophage.

CONCLUSIONS

Phage purification methods or their combination should be selected individually depending on the characteristics of a given phage. Nevertheless, sucrose density gradient centrifugation and slow filtration in the presence of MgSO₄ could be considered as the most promising for the purification of *Myoviridae* and *Autographiviridae* phage lysates. These methods yield safe sufficiently purified phage preparations containing permissible amounts of endotoxins.

References

- Tacconelli E, Carrara E, Savoldi A, Harbarth S, Mendelson M, Monnet DL, et al. Discovery, research, and development of new antibiotics: the WHO priority list of antibiotic-resistant bacteria and tuberculosis. *Lancet Infect Dis*. 2018; 18 (3): 318–27. DOI: 10.1016/S1473-3099(17)30753-3.
- Lin DM, Koskella B, Lin HC. Phage therapy: An alternative to antibiotics in the age of multi-drug resistance. *World J Gastrointest Pharmacol Ther*. 2017; 8 (3): 162. DOI: 10.4292/wjgpt.v8.i3.162.
- Akimkin VG, Darbeeva OS, Kolkov VF. Bakteriofagi: istoricheskie i sovremennye aspekty ih primeneniya: opyt i perspektivy. *Klinicheskaja praktika*. 2010; 4 (4): 48–54. Russian.
- Pirnay JP, Blasdel BG, Bretaudeau L, Buckling A, Chanishvili N, Clark JR, et al. Quality and safety requirements for sustainable phage therapy products. *Pharm Res*. 2015; 32 (7): 2173–9. DOI: 10.1007/s11095-014-1617-7.
- Shkoda AS, Mitrohin SD, Vedjashkina SG, Orlova OE, Bastrikin SYu, Galickij AA, i dr. Personalizirovannaja fagoterapija pacientov, stradajushih infekcijami, svjazannymi s okazaniem medicinskoj pomoshhi: metodicheskie rekomendacii. 2019; 37 s. Dostupno po ssylke: <https://niioz.ru/upload/iblock/259/259f65904e633b948cd2e6a1d04742f0.pdf>. Russian.
- Petrovic-Fabijan A, Khalid A, Maddocks S, Ho J, Gilbey T, Sandaradura I, et al. Phage therapy for severe bacterial infections: a narrative review. *Med J Aust*. 2020; 212 (6): 279–85. DOI: 10.5694/mja2.50355.
- Aleshkin AV, Shkoda AS, Bochkareva SS, Ershova ON, Mitrokhin SD, Kiseleva IA, et al. Concept of individualized medicine based on personalized phage therapy for intensive care unit patients suffering from healthcare-associated infections. *Infektsionnye Bolezni*. 2017; 15 (4): 49–54. DOI: 10.20953/1729-9225-2017-4-49-54.
- Rietschel ET, Kirikae T, Schade FU, Mamat U, Schmidt G, Loppnow H, et al. Bacterial endotoxin: molecular relationships of structure to activity and function. *FASEB J*. 1994; 8 (2): 217–25. DOI: 10.1096/FASEBJ.8.2.8119492.
- Raetz CRH, Whitfield C. Lipopolysaccharide endotoxins. *Annu Rev Biochem*. 2002; 71 (1): 635–700. DOI: 10.1146/annurev.biochem.71.110601.135414.
- Luong T, Salabarria AC, Edwards RA, Roach DR. Standardized bacteriophage purification for personalized phage therapy. *Nat Protoc*. 2020; 15 (9): 2867–90. DOI: 10.1038/s41596-020-0346-0.
- Guo Y, Cheng A, Wang M, Zhou Y. Purification of an atid herpesvirus 1 particles by tangential-flow ultrafiltration and sucrose gradient ultracentrifugation. *J Virol Methods*. 2009; 161 (1): 1–6. DOI: 10.1016/J.JVIROMET.2008.12.017.
- Hietala V, Horsma-Heikkinen J, Carron A, Skurnik M, Kiljunen S. The Removal of Endo- and Enterotoxins From Bacteriophage Preparations. *Front Microbiol*. 2019; 10: 1674. DOI: 10.3389/fmicb.2019.01674.
- Van Belleghem JD, Merabishvili M, Vergauwen B, Lavigne R, Vaneechoutte M. A comparative study of different strategies for removal of endotoxins from bacteriophage preparations. *J Microbiol Methods*. 2017; 132: 153–9. DOI: 10.1016/j.mimet.2016.11.020.
- Van Twest R, Kropinski AM. Bacteriophage enrichment from water and soil. *Methods Mol Biol*. 2009; 501: 15–21. DOI: 10.1007/978-1-60327-164-6_2.
- Cooper CJ, Denyer SP, Maillard J-Y. Stability and purity of a bacteriophage cocktail preparation for nebulizer delivery. *Lett Appl Microbiol*. 2014; 58 (2): 118–22. DOI: 10.1111/lam.12161.
- Merabishvili M, Pirnay J-P, Verbeken G, Chanishvili N, Tediashvili M, Lashkhi N, et al. Quality-controlled small-scale production of a well-defined bacteriophage cocktail for use in human clinical trials. *PLoS One*. 2009; 4 (3): 4944. DOI: 10.1371/JOURNAL.PONE.0004944.
- Brisse S, Passet V, Haugaard AB, Babosan A, Kassis-Chikhani N, Struve C et al. Wzi gene sequencing, a rapid method for determination of capsulartype for klebsiella strains. *J Clin Microbiol*. 2013; 51 (12): 4073–8. DOI: 10.1128/JCM.01924-13.
- Gorodnichev RB, Volozhantsev NV, Krasnikova VM, Bodoev IN, Kornienko MA, Kuptsov NS, et al. Novel Klebsiella pneumoniae K23-specific bacteriophages from different families: similarity of depolymerases and their therapeutic potential. *Front Microbiol*. 2021; 12: 669618. DOI: 10.3389/FMICB.2021.669618.
- Mazzocco A, Waddell TE, Lingohr E, Johnson RP. Enumeration of bacteriophages using the small drop plaque assay system. *Bacteriophages*. 2009; 81–85. DOI: 10.1007/978-1-60327-164-6.
- Maniatis T, Sambrook J, Fritsch EF. *Molecular cloning: a laboratory manual*. 2nd ed. Inglis J. Cold Spring Harbor Laboratory Press. 1984; 2230 p.
- Schooley RT, Biswas B, Gill JJ, Hernandez-Morales A, Lancaster J, Lessor L, et al. Development and use of personalized bacteriophage-based therapeutic cocktails to treat a patient with a disseminated resistant *Acinetobacter baumannii* infection. *Antimicrob Agents Chemother*. 2017; 61 (10): 1–15. DOI:

- 10.1128/AAC.00954-17.
22. Dedrick RM, Guerrero-Bustamante CA, Garland RA, Russell DA, Ford K, Harris K, et al. Engineered bacteriophages for treatment of a patient with a disseminated drug-resistant *Mycobacterium abscessus*. *Nat Med Springer US*. 2019; 25 (5): 730–33. DOI: 10.1038/s41591-019-0437-z.
 23. Rubalskii E, Ruemke S, Salmoukas C, Boyle EC, Warnecke G, Tudorache I, et al. Bacteriophage therapy for critical infections related to cardiothoracic surgery. *Antibiotics*. 2020; 9 (5): 1–12. DOI: 10.3390/ANTIBIOTICS9050232.
 24. Pinto AM, Cerqueira MA, Bañobre-López M, Pastrana LM, Sillankorva S. Bacteriophages for chronic wound treatment: from traditional to novel delivery systems. *Viruses*. 2020; 12 (2): 1–29. DOI: 10.3390/v12020235.
 25. Wills QF, Kerrigan C, Soothill JS. Experimental bacteriophage protection against *Staphylococcus aureus* abscesses in a rabbit model. *Antimicrob Agents Chemother*. 2005; 49 (3): 1220–1. DOI: 10.1128/AAC.49.3.1220-1221.2005.
 26. Fish R, Kutter E, Wheat G, Blasdel B, Kutateladze M, Kuhl S. Bacteriophage treatment of intransigent diabetic toe ulcers: a case series. *Journal of wound care*. 2016; 25 (Sup 7): 27–33. DOI: 10.12968/JOWC.2016.25.SUP7.S27.
 27. OFS.1.2.4.0006.15 Bakterial'nye jendotoksiny. *Farmakopeja. rf [Elektronnyj resurs]*. Dostupno po ssylke: <https://pharmacopoeia.ru/ofs-1-2-4-0006-15-bakterialnye-endotoksiny/> (data obrashhenija: 30.08.2021). Russian.
 28. Zhang ZR, Shen JT, Dai JY, Sun YQ, Dong YS, Xiu ZL. Separation and purification of *Klebsiella* phage by two-step salting-out extraction. *Sep Purif Technol*. 2020; 242 (2): 116784. DOI: 10.1016/j.seppur.2020.116784.
 29. Bergstrand A, Svanberg C, Langton M, Nydén M. Aggregation behavior and size of lipopolysaccharide from *Escherichia coli* O55:B5. *Colloids Surfaces B Biointerfaces*. 2006; 53 (1): 9–14. DOI: 10.1016/J.COLSURFB.2006.06.007.

Литература

1. Tacconelli E, Carrara E, Savoldi A, Harbarth S, Mendelson M, Monnet DL, et al. Discovery, research, and development of new antibiotics: the WHO priority list of antibiotic-resistant bacteria and tuberculosis. *Lancet Infect Dis*. 2018; 18 (3): 318–27. DOI: 10.1016/S1473-3099(17)30753-3.
2. Lin DM, Koskella B, Lin HC. Phage therapy: An alternative to antibiotics in the age of multi-drug resistance. *World J Gastrointest Pharmacol Ther*. 2017; 8 (3): 162. DOI: 10.4292/wjgpt.v8.i3.162.
3. Акимкин В. Г., Дарбеева О. С., Колков В. Ф. Бактериофаги: исторические и современные аспекты их применения: опыт и перспективы. *Клиническая практика*. 2010; 4 (4): 48–54.
4. Pirnay JP, Blasdel BG, Bretaudeau L, Buckling A, Chanishvili N, Clark JR, et al. Quality and safety requirements for sustainable phage therapy products. *Pharm Res*. 2015; 32 (7): 2173–9. DOI: 10.1007/s11095-014-1617-7.
5. Шкода А. С., Митрохин С. Д., Ведяшкина С. Г., Орлова О. Е., Бастрикин С. Ю., Галицкий А. А., и др. Персонализированная фаготерапия пациентов, страдающих инфекциями, связанными с оказанием медицинской помощи: методические рекомендации. 2019; 37 с. Доступно по ссылке: <https://niioz.ru/upload/iblock/259/259f65904e633b948cd2e6a1d04742f0.pdf>.
6. Petrovic-Fabijan A, Khalid A, Maddocks S, Ho J, Gilbey T, Sandaradura I, et al. Phage therapy for severe bacterial infections: a narrative review. *Med J Aust*. 2020; 212 (6): 279–85. DOI: 10.5694/mja2.50355.
7. Aleshkin AV, Shkoda AS, Bochkareva SS, Ershova ON, Mitrokhin SD, Kiseleva IA, et al. Concept of individualized medicine based on personalized phage therapy for intensive care unit patients suffering from healthcare-associated infections. *Infektsionnye Bolezni*. 2017; 15 (4): 49–54. DOI: 10.20953/1729-9225-2017-4-49-54.
8. Rietschel ET, Kirikae T, Schade FU, Mamat U, Schmidt G, Loppnow H, et al. Bacterial endotoxin: molecular relationships of structure to activity and function. *FASEB J*. 1994; 8 (2): 217–25. DOI: 10.1096/FASEBJ.8.2.8119492.
9. Raetz CRH, Whitfield C. Lipopolysaccharide endotoxins. *Annu Rev Biochem*. 2002; 71 (1): 635–700. DOI: 10.1146/annurev.biochem.71.110601.135414.
10. Luong T, Salabarria AC, Edwards RA, Roach DR. Standardized bacteriophage purification for personalized phage therapy. *Nat Protoc*. 2020; 15 (9): 2867–90. DOI: 10.1038/s41596-020-0346-0.
11. Guo Y, Cheng A, Wang M, Zhou Y. Purification of anatid herpesvirus 1 particles by tangential-flow ultrafiltration and sucrose gradient ultracentrifugation. *J Virol Methods*. 2009; 161 (1): 1–6. DOI: 10.1016/J.JVIROMET.2008.12.017.
12. Hietala V, Horsma-Heikkinen J, Carron A, Skurnik M, Kiljunen S. The Removal of Endo- and Enterotoxins From Bacteriophage Preparations. *Front Microbiol*. 2019; 10: 1674. DOI: 10.3389/fmicb.2019.01674.
13. Van Belleghem JD, Merabishvili M, Vergauwen B, Lavigne R, Vaneechoutte M. A comparative study of different strategies for removal of endotoxins from bacteriophage preparations. *J Microbiol Methods*. 2017; 132: 153–9. DOI: 10.1016/j.mimet.2016.11.020.
14. Van Twest R, Kropinski AM. Bacteriophage enrichment from water and soil. *Methods Mol Biol*. 2009; 501: 15–21. DOI: 10.1007/978-1-60327-164-6_2.
15. Cooper CJ, Denyer SP, Maillard J-Y. Stability and purity of a bacteriophage cocktail preparation for nebulizer delivery. *Lett Appl Microbiol*. 2014; 58 (2): 118–22. DOI: 10.1111/lam.12161.
16. Merabishvili M, Pirnay J-P, Verbeken G, Chanishvili N, Tediashvili M, Lashkhi N, et al. Quality-controlled small-scale production of a well-defined bacteriophage cocktail for use in human clinical trials. *PLoS One*. 2009; 4 (3): 4944. DOI: 10.1371/JOURNAL.PONE.0004944.
17. Brisse S, Passet V, Haugaard AB, Babosan A, Kassis-Chikhani N, Struve C et al. Wzi gene sequencing, a rapid method for determination of capsulartype for *klebsiella* strains. *J Clin Microbiol*. 2013; 51 (12): 4073–8. DOI: 10.1128/JCM.01924-13.
18. Gorodnichev RB, Volozhantsev NV, Krasilnikova VM, Bodoev IN, Kornienko MA, Kuptsov NS, et al. Novel *Klebsiella pneumoniae* K23-specific bacteriophages from different families: similarity of depolymerases and their therapeutic potential. *Front Microbiol*. 2021; 12: 669618. DOI: 10.3389/FMICB.2021.669618.
19. Mazzocco A, Waddell TE, Lingohr E, Johnson RP. Enumeration of bacteriophages using the small drop plaque assay system. *Bacteriophages*. 2009; 81–85. DOI: 10.1007/978-1-60327-164-6.
20. Maniatis T, Sambrook J, Fritsch EF. *Molecular cloning: a laboratory manual*. 2nd ed. Inglis J. Cold Spring Harbor Laboratory Press. 1984; 2230 p.
21. Schooley RT, Biswas B, Gill JJ, Hernandez-Morales A, Lancaster J, Lessor L, et al. Development and use of personalized bacteriophage-based therapeutic cocktails to treat a patient with a disseminated resistant *Acinetobacter baumannii* infection. *Antimicrob Agents Chemother*. 2017; 61 (10): 1–15. DOI: 10.1128/AAC.00954-17.
22. Dedrick RM, Guerrero-Bustamante CA, Garland RA, Russell DA, Ford K, Harris K, et al. Engineered bacteriophages for treatment of a patient with a disseminated drug-resistant *Mycobacterium abscessus*. *Nat Med Springer US*. 2019; 25 (5): 730–33. DOI: 10.1038/s41591-019-0437-z.
23. Rubalskii E, Ruemke S, Salmoukas C, Boyle EC, Warnecke G, Tudorache I, et al. Bacteriophage therapy for critical infections related to cardiothoracic surgery. *Antibiotics*. 2020; 9 (5): 1–12. DOI: 10.3390/ANTIBIOTICS9050232.
24. Pinto AM, Cerqueira MA, Bañobre-López M, Pastrana LM, Sillankorva S. Bacteriophages for chronic wound treatment: from traditional to novel delivery systems. *Viruses*. 2020; 12 (2): 1–29. DOI: 10.3390/v12020235.
25. Wills QF, Kerrigan C, Soothill JS. Experimental bacteriophage protection against *Staphylococcus aureus* abscesses in a rabbit model. *Antimicrob Agents Chemother*. 2005; 49 (3): 1220–1. DOI: 10.1128/AAC.49.3.1220-1221.2005.

26. Fish R, Kutter E, Wheat G, Blasdel B, Kutateladze M, Kuhl S. Bacteriophage treatment of intransigent diabetic toe ulcers: a case series. *Journal of wound care*. 2016; 25 (Sup 7): 27–33. DOI: 10.12968/JOWC.2016.25.SUP7.S27.
27. ОФС.1.2.4.0006.15 Бактериальные эндотоксины. Фармакопей. рф [Электронный ресурс]. Доступно по ссылке: <https://pharmacoreia.ru/ofs-1-2-4-0006-15-bakterialnye-endotoksiny/> (дата обращения: 30.08.2021).
28. Zhang ZR, Shen JT, Dai JY, Sun YQ, Dong YS, Xiu ZL. Separation and purification of Klebsiella phage by two-step salting-out extraction. *Sep Purif Technol*. 2020; 242 (2): 116784. DOI: 10.1016/j.seppur.2020.116784.
29. Bergstrand A, Svanberg C, Langton M, Nydén M. Aggregation behavior and size of lipopolysaccharide from *Escherichia coli* O55:B5. *Colloids Surfaces B Biointerfaces*. 2006; 53 (1): 9–14. DOI: 10.1016/J.COLSURFB.2006.06.007.

INTERACTION OF CATIONIC ANTISEPTICS WITH CARDIOLIPIN-CONTAINING MODEL BACTERIAL MEMBRANES

Kholina EG^{1,2}, Bozdaganyan ME^{1,2}, Strakhovskaya MG^{1,2}, Kovalenko IB^{1,2}✉

¹ Federal Scientific and Clinical Center of Specialized Medical Care and Medical Technology of FMBA, Moscow, Russia

² Lomonosov Moscow State University, Moscow, Russia

Plasma membrane is one of the major targets for cationic antiseptics (CA). The study was aimed to assess molecular effects of CAs of different chemical classes on cardiolipin-containing regions of bacterial plasma membranes. The study was carried out using coarse-grained molecular modeling. Interaction of CAs, such as miramistin, chlorhexidine, picloxidine, and octenidine, with cardiolipin-containing bilayer was assessed based on the CA coarse-grained models. CAs reduced lipid lateral diffusion coefficients and increased the membrane area per lipid. All CAs, except miramistin, reduced the lipid fatty acid chain order parameters. Adding octenidine at a CA : lipid ratio of 1 : 4 resulted in cardiolipin clustering with subsequent pulling the neutral phosphatidylethanolamine molecules out of the model bilayer. It was found that CAs have the potential for sorption to lipid bilayer, causing clustering of negatively charged lipids. Antiseptic octenidine causes formation of cardiolipin microdomains. Abnormal lateral lipid distribution together with pulling out phosphatidylethanolamine molecules can result in increased lipid bilayer permeability. The most significant reduction of cardiolipin lateral diffusion coefficient by 2.8 ± 0.4 times was observed in the presence of CA chlorhexidine at an antiseptic : lipid ratio of 1 : 4.

Keywords: antiseptic, bacterial membrane, molecular modeling, miramistin, chlorhexidine, picloxidine, octenidine

Funding: the research was carried out with the financial support of the Russian Foundation for Basic Research (project № 19-34-90045) and the State assignment "The influence of the lipid composition of bacterial membranes on the processes of interaction with antimicrobial compounds" (code: "Membrane").

Author contribution: Kholina EG — constructing molecular models of studied substances, calculations, manuscript writing; Bozdaganyan ME — calculations, manuscript writing; Strakhovskaya MG — study concept, manuscript writing, analysis of the results; Kovalenko IB — study concept, building a computing infrastructure, manuscript writing, analysis of the results.

✉ **Correspondence should be addressed:** Ilya B. Kovalenko
Orehovyi bulvar, 28, Moscow, 115682; ikovalenko78@gmail.com

Received: 19.07.2021 **Accepted:** 21.08.2021 **Published online:** 11.09.2021

DOI: 10.47183/mes.2021.024

ВЗАИМОДЕЙСТВИЕ КАТИОННЫХ АНТИСЕПТИКОВ С КАРДИОЛИПИНСОДЕРЖАЩЕЙ МОДЕЛЬНОЙ БАКТЕРИАЛЬНОЙ МЕМБРАНОЙ

Е. Г. Холина^{1,2}, М. Е. Боздаганян^{1,2}, М. Г. Страховская^{1,2}, И. Б. Коваленко^{1,2}✉

¹ Федеральный научно-клинический центр специализированных видов медицинской помощи и медицинских технологий Федерального медико-биологического агентства, Москва, Россия

² Московский государственный университет имени М. В. Ломоносова, Москва, Россия

Плазматическая мембрана является одной из главных мишеней действия катионных антисептиков (КА). Целью исследования было изучить на молекулярном уровне действие относящихся к разным химическим классам КА на кардиолипинсодержащие участки плазматической бактериальной мембраны. Исследование выполнено с применением крупнозернистого молекулярного моделирования. На основе созданных крупнозернистых молекулярных моделей КА, включая мирамистин, хлоргексидин, пиклоксидин и октенидин, изучено их взаимодействие с липидным кардиолипинсодержащим бислоем. КА снижали коэффициенты латеральной диффузии липидов и увеличивали площадь поверхности мембраны, приходящуюся на липид. Кроме мирамистина, все КА снижали параметры порядка жирнокислотных цепей липидов. Добавление октенидина в соотношении КА : липид как 1 : 4 приводило к кластеризации кардиолипина с последующим вырыванием из модельного бислоя нейтральных молекул фосфатидилэтаноламина. Выявлено, что КА обладают способностью сорбироваться на липидном бислое, вызывая кластеризацию отрицательно заряженных липидов. Антисептик октенидин вызывает образование кардиолипиновых микродоменов. Нарушение латерального распределения липидов и вырывание молекул фосфатидилэтаноламина может привести к повышению проницаемости липидного бислоя. Наиболее значимое уменьшение коэффициента латеральной диффузии липида кардиолипина в $2,8 \pm 0,4$ раза отмечено в присутствии КА хлоргексидина при соотношении антисептик : липид как 1 : 4.

Ключевые слова: антисептик, бактериальная мембрана, молекулярное моделирование, мирамистин, хлоргексидин, пиклоксидин, октенидин

Финансирование: исследование выполнено при финансовой поддержке РФФИ в рамках научного проекта № 19-34-90045 и государственного задания «Влияние липидного состава бактериальных мембран на процессы взаимодействия с антимикробными соединениями», шифр: «Мембрана».

Вклад авторов: Е. Г. Холина — создание молекулярных моделей исследуемых веществ, проведение расчетов, написание текста статьи; М. Е. Боздаганян — проведение расчетов, написание текста статьи; М. Г. Страховская — идея исследования, написание текста статьи, анализ результатов; И. Б. Коваленко — идея исследования, создание вычислительной инфраструктуры, написание текста статьи, анализ результатов.

✉ **Для корреспонденции:** Илья Борисович Коваленко
ул. Ореховый бульвар, д. 28, 115682, г. Москва; ikovalenko78@gmail.com

Статья получена: 19.07.2021 **Статья принята к печати:** 21.08.2021 **Опубликована онлайн:** 11.09.2021

DOI: 10.47183/mes.2021.024

Antiseptics come from one of major groups of compounds extensively used to prevent and combat infectious diseases. Activity of antiseptics is associated with their ability to inhibit the growth (bacteriostatic activity) or inactivate microbial cells (bactericidal activity). Among all antiseptics, cationic compounds, which electrostatically bind to the negatively charged groups of bacterial cell wall components and displace

the stabilizing divalent cations, are one of the most effective. Assessment of antiseptic antimicrobial activity revealed rupture of cell membrane with subsequent leakage of intracellular components [1], impairment of cellular metabolism [2, 3], enzyme inhibition, inhibition of electron transport and oxidative phosphorylation [4, 5]. In particular, electron microscopy showed specific ruptures in bacterial cell walls [6, 7].

Among all CAs, quaternary ammonium compounds (QACs) and biguanides are the largest groups of compounds [8]. The first owe their name to the presence of quaternary nitrogen atom covalently attached to hydrophobic substituent [8]. Miramistin (MIR), carrying single positive charge, is an example of nonheterocyclic QAC. Spatial structure of MIR adopts bent conformation, resembling the hook with its head group tilted back to the long-chain alkyl tail [9]. It is assumed that positively charged nitrogen of MIR interacts with negatively charged phospholipids, which results in abnormal membrane surface charge distribution and incorporation of hydrophobic tails into bacterial membranes, leading to the membrane physical and biological function impairment. Antiseptic octenidine (OCT) is an example of heterocyclic QAC. Here, two pyridinic nitrogen atoms linked via an alkyl bridge have alkylamine substituents in the para-position [10]. OCT, carrying a double positive charge, shows high affinity for lipids forming bacterial membranes, especially for negatively charged cardiolipin (CL). Biguanides are the compounds, in which the amidine group is bonded to the guanidine group to form the $-C=N-C=N-$ conjugated system. Chlorhexidine (CHL) is the best studied representative of biguanides. The symmetric structure of CHL consists of two hydrophilic biguanide groups connected by a hydrophobic linker, each of them bound to chlorphenol ring. Spatial conformation in the form of the bracket is typical for CHL [11]. At physiological pH values, CHL molecule carries a double positive charge [10]. CHL has become widely used due to antimicrobial activity against many microorganisms, including a broad range of gram-positive and gram-negative bacteria, viruses and fungi. However, CHL possesses higher activity against gram-positive bacteria. Some gram-negative species, such as *Proteus mirabilis* (minimum inhibitory concentration (MIC) is 115 mg/L), *Providencia stuartii* (MIC is 102 mg/L), show high resistance to CHL [12].

Bacterial plasma membrane plays an important role in maintaining cell function and has multiple functions, such as regulation of substance transport and involvement in cell division. Lipids, forming the bacterial plasma membrane, differ in the number of fatty acids and their chain length, number and location of double bonds, structure and charge of hydrophilic part [13]. Neutral phosphatidylethanolamine (PE) and negatively charged phospholipids, phosphatidylglycerol (PG) and CL, which make up at least 15% of total content, are common for most bacteria [14]. In contrast to PE and PG, CL has a more massive structure due to the presence of two phosphate residues and four fatty acids.

Bacterial plasma membranes are characterized by heterogenic lipid distribution [15]. PE phospholipid is distributed evenly in the cells of a broad range of gram-negative bacteria (*Escherichia coli*, *Salmonella Typhimurium*, *Pseudomonas putida*, *Azotobacter vinelandii*, *Proteus vulgaris*), however, localization of those in septa was shown for cells of the *Bacillus* species [16]. Microdomain formation was shown for anionic lipids. In particular, there are microdomains formed of CL molecules in the plasma membranes at the cell poles of gram-negative bacteria. It is believed that CL localization at the poles is associated with CL involvement in the cell division processes, in particular, with interaction with cell division proteins DnaA, MinD, FtsA. DnaA is responsible for initiation of DNA replication, MinD, being a part of the MinCDE system, prevents divisome localization to the cell poles, FtsA is a bacterial actin, a protein linker for bacterial tubulin FtsZ, forming the Z ring in the center of the cell. These proteins interact mainly with anionic lipids of bacterial plasma membranes due to the presence of amphipathic motifs enriched in positively

charged amino acids [17]. The other important cellular processes, involving CL due to interaction with proteins, are as follows: energy transfer, osmoadaptation, and protein translocation. X-ray diffraction analysis revealed the presence of CL in the structures of reactive center and cytochrome c oxidase of *Rhodobacter sphaeroides*, formate dehydrogenase and succinate dehydrogenase of *E. coli* [13]. Colocalization of CL with osmosensory transporter ProP [18], which responds to changes in osmolality by increased transport of organic osmolytes to cell, was found in *E. coli*; colocalization with Eps system, responsible for export of cholera toxin, was found in *Vibrio cholera* [19].

Regardless of their amount, experimental data on cationic antiseptic mechanisms of action cannot give a clear answer to the question, what is the root cause of the antiseptics' bactericidal action: membrane disintegration or cell metabolism inhibition. Thus, exact molecular mechanisms of action are poorly understood in this group of antimicrobial substances. Taking into account the earlier suggestion about the potential role of CL molecules as CA binding sites [6], the study was aimed to assess the effects of CAs on the CL-containing bacterial plasma membrane areas by molecular modeling.

METHODS

Coarse-grained molecular models of CAs were described earlier [20]. To assess the effects of CAs on the model bilayer, the following biguanides were selected: CHL, picloxidine (PIC), and QACs (MIR, OCT). All CAs, except MIR, carry double positive charges. CA chemical structures, partitioned to coarse grains using the MARTINI force field, are presented in Fig. 1. Particle type C1 was selected for description of hydrophobic CA fragments by analogy with lipid parameterization; SC2/SC3/SC4 were selected for aromatic fragments, and P5 were selected for fragments containing peptide bonds, by analogy with amino acid parameterization in the second version of MARTINI force field. Antiseptics were added to model bilayer in different ratios: CA : lipid 1 : 8 and 1 : 4, in accordance with the concentrations used in medical solutions.

Coarse-grained molecular model of bilayer was built using the CHARMM-GUI MARTINI Maker [21], developed by the research group of Professor Im at Lehigh University (USA), in the MARTINI force field [22]. Plasma membrane model, simulating lipid composition at the bacterial cell poles, consisted of lipids palmitoyl-oleoyl-PE (POPE), POPG and CL, carrying the charge -2 (CDL2), at a ratio 81 : 7 : 12 by mass. Coarse-grained molecular dynamics (MD) was calculated using the Gromacs 2019.4 software package (developed by Universities of Uppsala and Stockholm, together with the Royal Institute of Technology, Sweden) [23] during 5 μ s for the systems CA : lipid 1 : 8, and during 35 μ s for the systems CA : lipid 1 : 4. Modeling was performed in the NVT ensemble using V-rescale thermostat ($T = 320$ K; $\tau_T = 1$ ps) and Parrinello-Rahman barostat ($p_{ref} = 1$ bar; $\tau_p = 12$ ps) [23]. MD calculation was performed by adding polarized water [24], with dielectric constant $\epsilon_r = 2.5$, and integration step 20 fs. Characteristics of model bilayers in the presence of CAs were calculated using the built-in utilities of the Gromacs 2019.4 software package. Area per lipid was calculated with the *gmx energy* tool, and lateral diffusion coefficients were calculated with the *gmx msd* tool. Density profiles of the molecular dynamic system components relative to the center of bilayer, radial distribution functions, amount of lipids outside the plane of the bilayer were assessed using our *Python* script with the use of MDAnalysis library functions. Model membrane thickness was defined based on the density

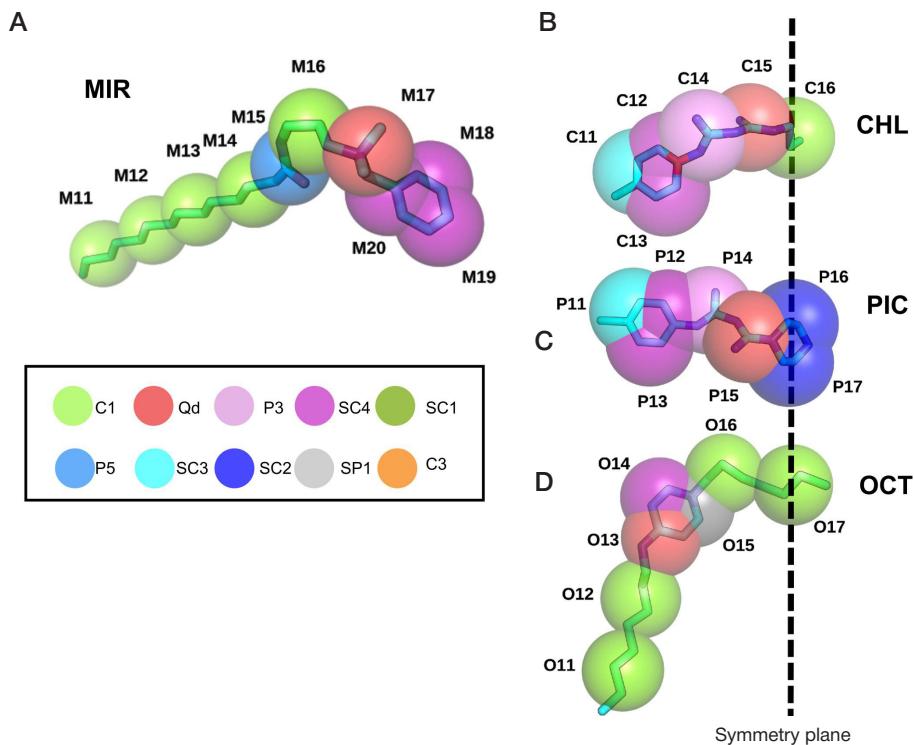


Fig. 1. CA chemical structures with overlapping coarse grains. **A.** Miramistin (MIR). **B.** Chlorhexidine (CHL). **C.** Picloxidine (PIC). **D.** Octenidine (OCT). Coarse grains are highlighted in different colors in accordance with the particle type selected in MARTINI force field (bottom part of A panel)

profiles as the difference between the positions of phosphate density peaks relative to the center of bilayer. Characteristics of model bilayers for each system were calculated based on two last μ s of MD trajectory.

RESULTS

Reduced lipid lateral diffusion coefficients (Fig. 2A), slightly decreased bilayer thickness (Fig. 2B), and increased area per lipid

(Fig. 2C) were observed in the presence of all studied CAs. In the presence of all CA types, except MIR, there was a decrease in lipid fatty acid chain order parameters (no data reported), which could be explained by chemical nature of MIR substantially different from other CAs. Molecules of MIR, having longer hydrophobic regions, penetrated deeper into model bilayer, and their interaction with fatty acid resulted in lipid ordering in the model membrane.

Adding OCT in high concentrations contributed to formation of CL microdomain in the bilayer. Initially, some OCT

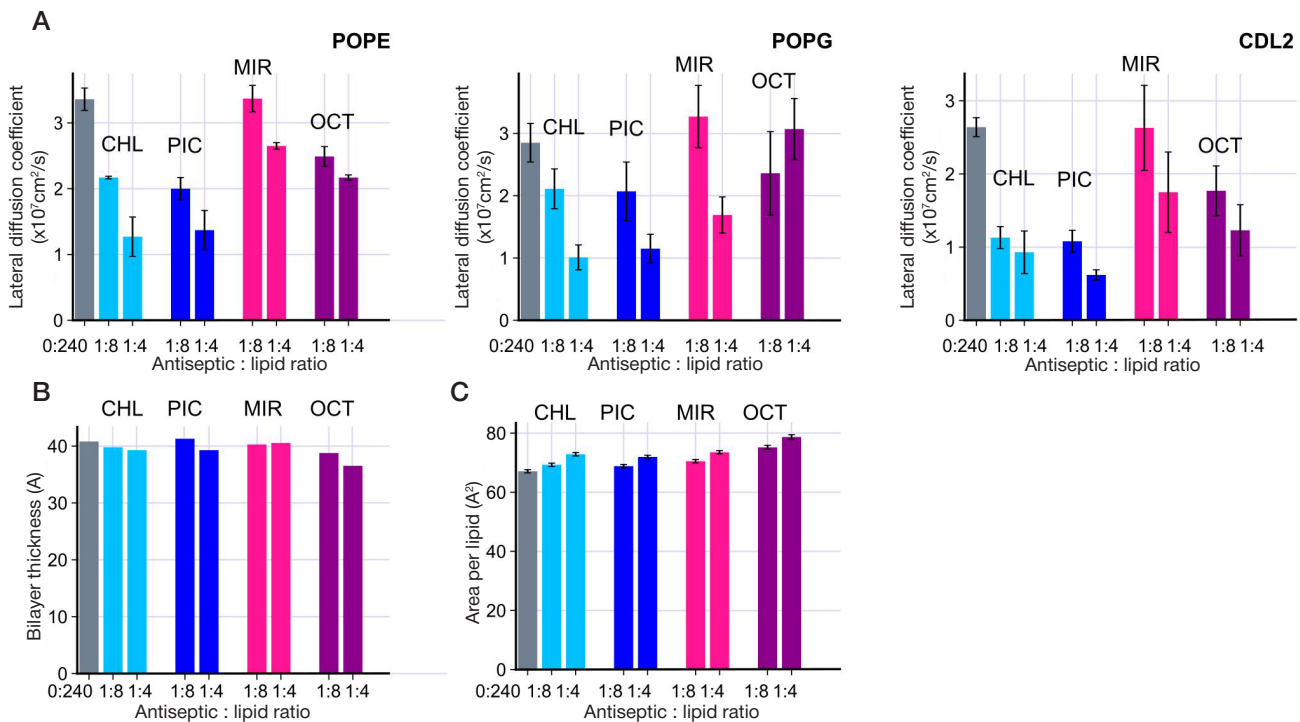


Fig. 2. Characteristics of model membrane comprising POPE:POPG:CDL2 in the presence of various CA concentrations. **A.** Lateral diffusion coefficients for the following lipids: POPE (left), POPG (centre) and CDL2 (right); **B.** Bilayer thickness; **C.** Area per lipid. (Parameter values for model membrane obtained without adding CAs are marked in gray)

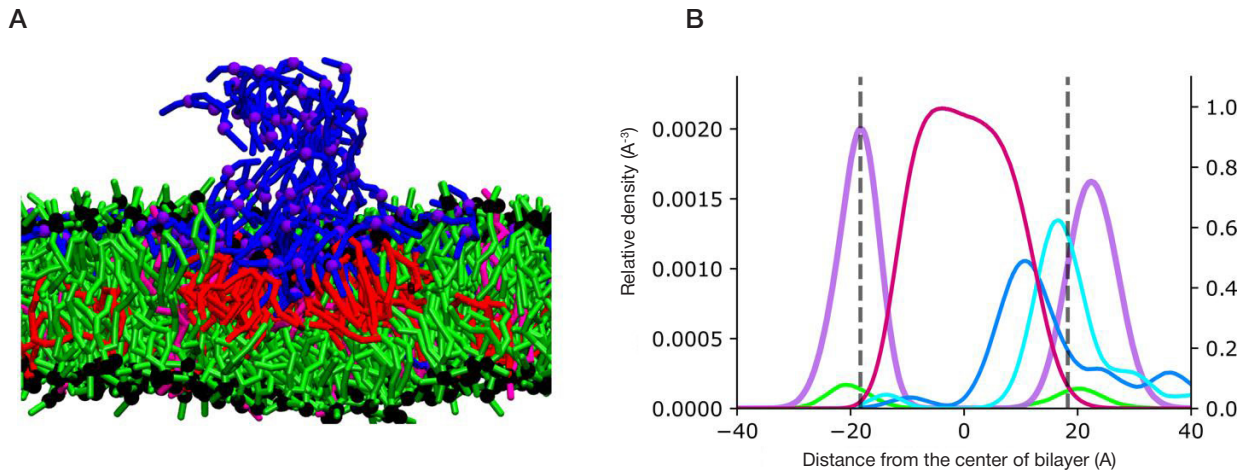


Fig. 3. Effect of CDL2 clustering in the presence of antiseptic OCT at the CA : lipid ratio of 1 : 4. **A.** Image of MD calculation at time 15 μs. POPE lipids are marked in green, POPG in pink, CDL2 in red, and OCT in blue. Phosphate residues are marked in black, and charged particles of OCT molecules are marked in purple. **B.** Density profiles for various components of model membrane. Density profile for lipid fatty acid chains is marked in pink, charged particles of OCT are marked in cyan, terminal OCT particles are marked in light blue, NH₃ particle (ethanol) of POPE lipid is marked in purple, GL0 particle (glycerol) of POPG lipid is marked in green. Position of phosphates is represented by the dotted lines going through the centers of corresponding peaks. Density profiles for fatty acid chains normalized to the maximum peak value are shown on the second Y axis (right)

molecules integrated itself into the bilayer with subsequent clustering of negatively charged lipids CL and PG. Some OCT molecules, which remained in the “solution”, formed a single micellar aggregate quite fast. Such behavior of molecules was due to large number of hydrophobic regions in the molecule of OCT (in addition to terminal end regions, there was a long

hydrophobic linker between pyridine fragments). Micellar aggregate sorbed to OCT molecules found on the formed CL microdomain (Fig. 3A), and remained in this state for a few microseconds. In this case, the symmetry of POPE molecules in outer and inner monolayers was disturbed. The latter was confirmed by displacement of POPE lipid polar head peaks in

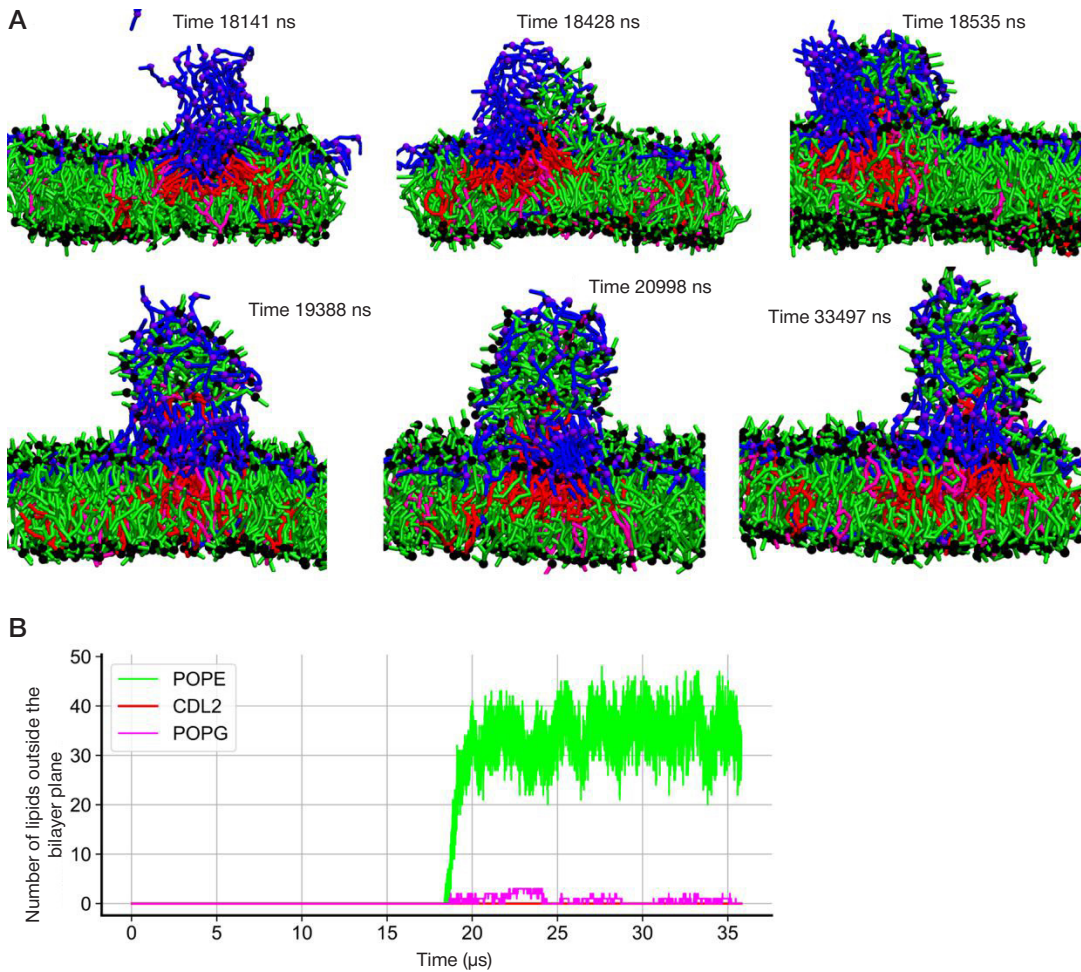


Fig. 4. Effect of pulling lipids out of the model bilayer by OCT molecules. CA : lipid ratio of 1 : 4. **A.** Consecutive images of MD calculation obtained at different times. POPE lipids are marked in green, POPG in pink, CDL2 in red, and OCT in blue. Phosphate residues are marked in black, and charged particles of OCT molecules are marked in purple. **B.** Number of lipids pulled out of the bilayer as a function on MD calculation time

Table. Ratios of phosphatidylethanolamine (PE), phosphatidylglycerol (PG), cardiolipin (CL) in plasma membranes of some species of gram-negative (-) and gram-positive (+) bacteria [13, 14]

Species	PE, %	PG, %	CL, %
<i>Escherichia coli</i> (-)	80	15	5
<i>Yersinia kristensenii</i> (-)	60	20	20
<i>Proteus mirabilis</i> (-)	80	10	5
<i>Klebsiella pneumoniae</i> (-)	82	5	6
<i>Pseudomonas aeruginosa</i> (-)	60	21	11
<i>Caulobacter crescentus</i> (-)	0	78	9
<i>Staphylococcus aureus</i> (+)	0	58	42
<i>Streptococcus pneumoniae</i> (+)	0	50	50
<i>Bacillus cereus</i> (+)	43	40	17
<i>Bacillus polymyxa</i> (+)	60	3	8

the outer monolayer relative to central position of phosphates in the relative density profiles of system components (Fig. 3B). This was due to the fact that phosphates of POPE lipid heads located close to CL domain were attracted to micellar aggregate formed by OCT molecules. From the moment after about 18 μ s of MD calculation, POPE molecules located close to CL domain were pulled out gradually (Fig. 4A). The pulling out process lasted approximately 2 μ s (Fig. 4B).

DISCUSSION

Plasma membranes of gram-negative and gram-positive bacteria have a different composition. Table presents ratios of three predominant lipids for best studied model species. These data show that PE lipid is the most abundant in the membranes of the majority of species of gram-negative cells compared to gram-positive cells. Usually, CL accounts for no more than 20% of the total amount, with the exception of species, containing no PE. The contents of CL in plasma membranes of such species can reach 50%.

Coarse-grained MD calculations showed that all studied CAs were incorporated into the model lipid bilayer. All studied CAs reduced lateral diffusion coefficients both in neutral POPE and in negatively charged lipids POPG and CDL2 (see Fig. 2A). Lipid mobility in fluid mosaic biological membranes [25] plays a vital part in maintaining activity of membrane proteins involved in all cellular processes, such as cell growth and differentiation, transport of substances, and cellular respiration. Lipid mobility is a measure of how easily these biomolecules can move along the plane of bilayer, it is assessed based on lateral diffusion coefficients [26], which could be obtained from the molecular dynamics results [27]. Reduction of lateral diffusion coefficients to 20% of baseline is observed with the antimicrobial substance : lipid concentration ratio of 1 : 5 [28, 29], which can adversely affect the membrane function.

The most significant reduction of lateral diffusion was observed with respect to CDL2 lipid, having a larger negative charge (-2 compared to -1 in POPG) and a more massive structure. MIR showed the slightest effect of lateral diffusion reduction. This could be due to the fact that, unlike other studied CAs, molecules of MIR carry a single negative charge and therefore are unable to bind several lipids and form long regions relative to immobilized lipids. Pronounced lateral lipid diffusion slowdown in the presence of biguanides CHL and PIC can be also attributed to their chemical nature. CHL and PIC, having the +2 charge and the short linker between

the charged particles, contributed to formation of semi-rigid frame, linking the lipids to form the structured areas of the membrane.

When adding all studied CAs, the average thickness of model membrane declined slightly, and the area per lipid molecule increased (see Fig. 2). All antiseptics, except MIR, disrupted packing of lipid fatty acids due to pushing apart acyl chains by their terminal ends embedded in the membrane. Long tail of the MIR molecule is chemically similar to fatty acids of lipids. That is why adding MIR resulted in lipid ordering in the model membrane. The detected changes in the model bilayer may explain the disruptive effect of antiseptics on the bacterial cell plasma membrane function and barrier properties.

Antiseptic OCT contributed to formation of CL microdomain in the bilayer. Molecules of antiseptic sorbed to this microdomain in the form of micellar aggregate, pulling the adjacent neutral POPE lipids out of the bilayer. Such effects may result in the increased permeability of vesicles after adding OCT, observed during the experiment. The following molecular mechanism of the OCT bactericidal activity was proposed based on the obtained experimental results [30]. Initially, OCT binds to the outer bacterial membrane, causing the surface charge neutralization. Hydrophobic regions of OCT interact with acyl chains of lipid A, which results in hydrophobic mismatch, together with disrupted membrane structure and integrity. Likewise, OCT molecules affect plasma membrane, causing membrane depolarization, together with fluidity and phospholipid acyl chain packing impairment. As a result of this nonspecific action, both membranes of cell wall become disrupted, and intracellular fluid flows out of the cell. Our molecular modeling data on the OCT sorption to lipid bilayer, as well as reduced lipid lateral diffusion coefficients and acyl chain order parameters in the presence of OCT support the reported [30] mechanism of this antiseptic bactericidal activity.

CONCLUSIONS

Interaction of CAs belonging to biguanides (CHL, PIC) and QACs (MIR, OCT) with the CL-containing model bilayer, simulating the plasma membrane at the cell poles of bacilliform bacteria, was studied based on the constructed coarse-grain models of these substances. MD modeling results revealed both similarities and differences between the effects of various CAs on the model bilayer. Adding all studied CAs resulted in reduced lipid lateral diffusion coefficients, slightly reduced average membrane thickness and increased area per lipid.

High concentrations of OCT contributed to CL microdomain formation with subsequent pulling the POPE lipids out of the model plasma membrane. Studying the CA interaction with the model plasma membrane using computer modeling made

it possible to confirm the experimental findings at the molecular level. Comparison of chemically different CAs may contribute to development of effective new medications and enable rational use of antiseptics.

References

- Denyer SP, Hugo WB. Biocide-induced damage to the bacterial cytoplasmic membrane. *Soc Appl Bacteriol Tech Ser.* 1991; 27: 171–87.
- Kroll RG, Patchett RA. Biocide-induced perturbations of aspects of cell homeostasis : intracellular pH, membrane potential and solute transport. *Soc Appl Bacteriol Tech Ser.* 1991; 27: 189–202.
- Russell AD, Hugo WB. Perturbation of homeostatic mechanisms in bacteria by pharmaceuticals. In: Whittenbury R, Gould GW, Banks JG, Board RG, editors. *Homeostatic mechanisms in microorganisms.* Bath University Press, Bath, England. 1988; p. 206–19.
- Fuller SJ. Biocide-induced enzyme inhibition. *Soc Appl Bacteriol Tech Ser.* 1991; 27: 235–49.
- Kuyyakanond T, Quesnel LB. The mechanism of action of chlorhexidine. *FEMS Microbiol Lett Oxford Academic.* 1992; 100 (1–3): 211–15.
- Cheung, HY, Wong MM, Cheung SH, Liang LY, Lam YW, Chiu SK. Differential actions of chlorhexidine on the cell wall of *Bacillus subtilis* and *Escherichia coli*. *PLoS One.* 2012; 7 (5): e36659.
- Strakhovskaya MG, Khalatyan AS, Budzinskaya MV, Kholina EG, Kolyshkina NA, Kovalenko IB, Zhukhovitsky VG. Chuvstvitel'nost' antibiotikorezistentnyh koagulazonegativnyh stafilokokkov k antiseptiku pikloksidinu. *Klinicheskaja praktika.* 2020; 11 (1): 42–48. Russian.
- Gilbert P, Moore LE. Cationic antiseptics: diversity of action under a common epithet. *J Appl Microbiol.* 2005; 99 (4): 703–15.
- Dolgushin FM, Goloveshkin AS, Ananyev IV, Osintseva SV, Torubaev YV, Krylov SS, et al. Interplay of noncovalent interactions in antiseptic quaternary ammonium surfactant Miramistin. *Acta Crystallogr Sect C International Union of Crystallography (IUCr).* 2019; 75 (4): 402–11.
- Vereshchagin AN, Frolov NA, Egorova KS, Seitkaliyeva MM, Ananikov VP. Quaternary Ammonium Compounds (QACs) and Ionic Liquids (ILs) as Biocides: From Simple Antiseptics to Tunable Antimicrobials. *Int J Mol Sci.* 2021; 22 (13): 67–93.
- Van Oosten B, Marquardt D, Komljenović I, Bradshaw JP, Sternin E, Harroun TA. Small molecule interaction with lipid bilayers: a molecular dynamics study of chlorhexidine. *J Mol Graph Model.* 2014; 48: 96–104.
- Amsterdam D, Ostrov BE. Disinfectants and antiseptics: Modes of action, mechanisms of resistance, and testing regimens. *Antibiotics in Laboratory Medicine.* Wolters Kluwer Health Adis (ESP), 2014; p. 1135–230.
- Lin TY, Weibel DB. Organization and function of anionic phospholipids in bacteria. *Appl Microbiol Biotechnol.* 2016; 100 (10): 4255–67.
- Epand RM, Epand RF. Bacterial membrane lipids in the action of antimicrobial agents. *J Pept Sci.* 2011; 17 (5): 298–305.
- Matsumoto K, Kusaka J, Nishibori A, Hara H. Lipid domains in bacterial membranes. *Mol Microbiol.* 2006; 61 (5): 1110–17.
- Strahl H, Errington J. Bacterial Membranes: Structure, Domains, and Function. *Annu Rev Microbiol.* 2017; 71: 519–38.
- Mileykovskaya E, Dowhan W. Cardiolipin membrane domains in prokaryotes and eukaryotes. *Biochim Biophys Acta — Biomembr Elsevier B.V.* 2009; 1788 (10): 2084–91.
- Romantsov T, Battle AR, Hendel JL, Martinac B, Wood JM. Protein localization in *Escherichia coli* cells: comparison of the cytoplasmic membrane proteins ProP, LacY, ProW, AqpZ, MscS, and MscL. *Journal of bacteriology.* 2010; 192 (4): 912–24.
- Camberg JL, Johnson TL, Patrick M, Abendroth J, Hol WG, Sandkvist M. Synergistic stimulation of EpsE ATP hydrolysis by EpsL and acidic phospholipids. *The EMBO journal.* 2007; 26 (1): 19–27.
- Kholina EG, Kovalenko IB, Bozdaganyan ME, Strakhovskaya MG, Orekhov PS. Cationic antiseptics facilitate pore formation in model bacterial membranes. *The Journal of Physical Chemistry B.* 2020; 124 (39): 8593–600.
- Qi Y, Inglyfsson HI, Cheng X, Lee J, Marrink SJ, Im W. CHARMM-GUI martini maker for coarse-grained simulations with the martini force field. *Journal of chemical theory and computation.* 2015; 11 (9): 4486–94.
- Marrink SJ, Risselada HJ, Yefimov S, Tieleman DP, De Vries AH, et al. The MARTINI Force Field: Coarse Grained Model for Biomolecular Simulations. *J Phys Chem B.* 2007; 111 (27): 7812–24.
- Abraham MJ, Murtola T, Schulz R, Pall S, Smith JC, Hess B, et al. GROMACS: High performance molecular simulations through multi-level parallelism from laptops to supercomputers. *Software X.* 2015; 1: 19–25.
- Yesylevskyy SO, Schäfer LV, Sengupta D, Marrink SJ. Polarizable water model for the coarse-grained MARTINI force field. *PLoS computational biology.* 2010; 6 (6): e1000810.
- Singer SJ, Nicolson GL. The Fluid Mosaic Model of the Structure of Cell Membranes. *Science.* 1972; 175 (4023): 720–31.
- Macháň R, Hof M. Lipid diffusion in planar membranes investigated by fluorescence correlation spectroscopy. *Biochimica et Biophysica Acta (BBA)-Biomembranes.* 2010; 1798 (7): 1377–91.
- Moradi S, Nowroozi A, Shahlaei M. Shedding light on the structural properties of lipid bilayers using molecular dynamics simulation: a review study. *RSC Adv. The Royal Society of Chemistry.* 2019; 9 (8): 4644–58.
- John T, Thomas T, Abel B, Wood BR, Chalmers DK, Martin LL. How kanamycin A interacts with bacterial and mammalian mimetic membranes. *Biochimica et Biophysica Acta (BBA)-Biomembranes.* 2017; 1859 (11): 2242–52.
- Berglund NA, Piggot TJ, Jefferies D, Sessions RB, Bond PJ, Khalid S. Interaction of the antimicrobial peptide polymyxin B1 with both membranes of *E. coli*: a molecular dynamics study. *PLoS computational biology.* 2005; 11 (4): e1004180.
- Malanovic N, ÖN A, Pabst G, Zellner A, Lohner K. Octenidine: Novel insights into the detailed killing mechanism of Gram-negative bacteria at a cellular and molecular level. *Int J Antimicrob Agents.* 2020; 56 (5): 106146.

Литература

- Denyer SP, Hugo WB. Biocide-induced damage to the bacterial cytoplasmic membrane. *Soc Appl Bacteriol Tech Ser.* 1991; 27: 171–87.
- Kroll RG, Patchett RA. Biocide-induced perturbations of aspects of cell homeostasis : intracellular pH, membrane potential and solute transport. *Soc Appl Bacteriol Tech Ser.* 1991; 27: 189–202.
- Russell AD, Hugo WB. Perturbation of homeostatic mechanisms in bacteria by pharmaceuticals. In: Whittenbury R, Gould GW, Banks JG, Board RG, editors. *Homeostatic mechanisms in microorganisms.* Bath University Press, Bath, England. 1988; p.

- 206–19.
4. Fuller SJ. Biocide-induced enzyme inhibition. *Soc Appl Bacteriol Tech Ser.* 1991; 27: 235–49.
 5. Kuyyakanond T, Quesnel LB. The mechanism of action of chlorhexidine. *FEMS Microbiol Lett Oxford Academic.* 1992; 100 (1–3): 211–15.
 6. Cheung, HY, Wong MM, Cheung SH, Liang LY, Lam YW, Chiu SK. Differential actions of chlorhexidine on the cell wall of *Bacillus subtilis* and *Escherichia coli*. *PLoS One.* 2012; 7 (5): e36659.
 7. Страховская М. Г., Халатян А. С., Будзинская М. В., Холина Е. Г., Колышкина Н. А., Коваленко И. Б. и др. Чувствительность антибиотикорезистентных коагулазонегативных стафилококков к антисептику пиклоксидину. *Клиническая практика.* 2020; 11 (1): 42–48.
 8. Gilbert P, Moore LE. Cationic antiseptics: diversity of action under a common epithet. *J Appl Microbiol.* 2005; 99 (4): 703–15.
 9. Dolgushin FM, Goloveshkin AS, Ananyev IV, Osintseva SV, Torubaev YV, Krylov SS, et al. Interplay of noncovalent interactions in antiseptic quaternary ammonium surfactant Miramistin. *Acta Crystallogr Sect C International Union of Crystallography (IUCr).* 2019; 75 (4): 402–11.
 10. Vereshchagin AN, Frolov NA, Egorova KS, Seitkalieva MM, Ananikov VP. Quaternary Ammonium Compounds (QACs) and Ionic Liquids (ILs) as Biocides: From Simple Antiseptics to Tunable Antimicrobials. *Int J Mol Sci.* 2021; 22 (13): 67–93.
 11. Van Oosten B, Marquardt D, Komljenović I, Bradshaw JP, Sterin E, Harroun TA. Small molecule interaction with lipid bilayers: a molecular dynamics study of chlorhexidine. *J Mol Graph Model.* 2014; 48: 96–104.
 12. Amsterdam D, Ostrov BE. Disinfectants and antiseptics: Modes of action, mechanisms of resistance, and testing regimens. *Antibiotics in Laboratory Medicine.* Wolters Kluwer Health Adis (ESP), 2014; p. 1135–230.
 13. Lin TY, Weibel DB. Organization and function of anionic phospholipids in bacteria. *Appl Microbiol Biotechnol.* 2016; 100 (10): 4255–67.
 14. Epanand RM, Epanand RF. Bacterial membrane lipids in the action of antimicrobial agents. *J Pept Sci.* 2011; 17 (5): 298–305.
 15. Matsumoto K, Kusaka J, Nishibori A, Hara H. Lipid domains in bacterial membranes. *Mol Microbiol.* 2006; 61 (5): 1110–17.
 16. Strahl H, Errington J. Bacterial Membranes: Structure, Domains, and Function. *Annu Rev Microbiol.* 2017; 71: 519–38.
 17. Mileyskovskaya E, Dowhan W. Cardiolipin membrane domains in prokaryotes and eukaryotes. *Biochim Biophys Acta — Biomembr.* Elsevier B.V. 2009; 1788 (10): 2084–91.
 18. Romantsov T, Battle AR, Hendel JL, Martinac B, Wood JM. Protein localization in *Escherichia coli* cells: comparison of the cytoplasmic membrane proteins ProP, LacY, ProW, AqpZ, MscS, and MscL. *Journal of bacteriology.* 2010; 192 (4): 912–24.
 19. Camberg JL, Johnson TL, Patrick M, Abendroth J, Hol WG, Sandkvist M. Synergistic stimulation of EpsE ATP hydrolysis by EpsL and acidic phospholipids. *The EMBO journal.* 2007; 26 (1): 19–27.
 20. Kholina EG, Kovalenko IB, Bozdoganyan ME, Strakhovskaya MG, Orekhov PS. Cationic antiseptics facilitate pore formation in model bacterial membranes. *The Journal of Physical Chemistry B.* 2020; 124 (39): 8593–600.
 21. Qi Y, Inglyfsson HI, Cheng X, Lee J, Marrink SJ, Im W. CHARMM-GUI martini maker for coarse-grained simulations with the martini force field. *Journal of chemical theory and computation.* 2015; 11 (9): 4486–94.
 22. Marrink SJ, Risselada HJ, Yefimov S, Tieleman DP, De Vries AH, et al. The MARTINI Force Field: Coarse Grained Model for Biomolecular Simulations. *J Phys Chem B.* 2007; 111 (27): 7812–24.
 23. Abraham MJ, Murtola T, Schulz R, Pall S, Smith JC, Hess B, et al. GROMACS: High performance molecular simulations through multi-level parallelism from laptops to supercomputers. *Software X.* 2015; 1: 19–25.
 24. Yesylevskyy SO, Schäfer LV, Sengupta D, Marrink SJ. Polarizable water model for the coarse-grained MARTINI force field. *PLoS computational biology.* 2010; 6 (6): e1000810.
 25. Singer SJ, Nicolson GL. The Fluid Mosaic Model of the Structure of Cell Membranes. *Science.* 1972; 175 (4023): 720–31.
 26. Macháň R, Hof M. Lipid diffusion in planar membranes investigated by fluorescence correlation spectroscopy. *Biochimica et Biophysica Acta (BBA)-Biomembranes.* 2010; 1798 (7): 1377–91.
 27. Moradi S, Nowroozi A, Shahlaei M. Shedding light on the structural properties of lipid bilayers using molecular dynamics simulation: a review study. *RSC Adv. The Royal Society of Chemistry.* 2019; 9 (8): 4644–58.
 28. John T, Thomas T, Abel B, Wood BR, Chalmers DK, Martin LL. How kanamycin A interacts with bacterial and mammalian mimetic membranes. *Biochimica et Biophysica Acta (BBA)-Biomembranes.* 2017; 1859 (11): 2242–52.
 29. Berglund NA, Piggot TJ, Jefferies D, Sessions RB, Bond PJ, Khalid S. Interaction of the antimicrobial peptide polymyxin B1 with both membranes of *E. coli*: a molecular dynamics study. *PLoS computational biology.* 2005; 11 (4): e1004180.
 30. Malanovic N, Ön A, Pabst G, Zellner A, Lohner K. Octenidine: Novel insights into the detailed killing mechanism of Gram-negative bacteria at a cellular and molecular level. *Int J Antimicrob Agents.* 2020; 56 (5): 106146.

ASSESSING HEPATOPROTECTIVE EFFECTS OF ANTIOXIDANTS ON AMIODARONE-INDUCED CYTOTOXICITY IN HUMAN HEPATOMA *HEPARG* CELL LINE

Filimonova KS, Rogovskaya NYu, Belyukov PP, Babakov VN ✉

Research Institute of Hygiene, Occupational Pathology and Human Ecology of the Federal Medical Biological Agency, Leningrad Region, Russia

Effective therapy of amiodarone-induced hepatotoxicity requires studying the mechanisms of the toxic effects of amiodarone on hepatocytes and assessing the potential impact of hepatoprotective agents. The study was aimed to assess hepatoprotective effects of antioxidants on the amiodarone-induced hepatotoxicity with the use of immortalized human hepatoma cells of the *HepaRG* cell line. Cell viability was evaluated upon exposure to amiodarone and in the mixture with vitamin E, N-acetylcysteine and S-adenosylmethionine by impedance measurement; the levels of some hepatotoxicity biomarkers were defined using the Luminex xMAP technology. As a result of the research, the dose-dependent toxic effects of amiodarone were established. The IC_{50} value of amiodarone in the *HepaRG* cell line was 3.5 μ M. It is shown that cytotoxic effects decrease and the IC_{50} value increases in the presence of vitamin E, N-acetylcysteine and S-adenosylmethionine. Amiodarone reduces the activity of cell cycle regulators: AKT, JNK kinases, and p53 protein. Exposure to amiodarone results in reduced intracellular ATP levels and the release of intracellular enzymes (malate dehydrogenase 1, glutathione S-transferase, sorbitol dehydrogenase, 5'-nucleotidase) into conditioned medium, indicating the necrotic cell death. Thus, vitamin E, S-adenosylmethionine and N-acetylcysteine reduce amiodarone cytotoxicity in the model of amiodarone-induced damage to hepatocytes and can be considered as hepatoprotective agents in case of the need to protect liver against the hepatotoxic effects of amiodarone.

Keywords: *HepaRG*, amiodarone, drug hepatotoxicity, vitamin E, N-acetylcysteine, S-adenosylmethionine

✉ **Correspondence should be addressed:** Vladimir N. Babakov
Kapitolovo, 93, p/o Kuzmolovsky, Leningradskaja oblast, 188663; babakov@gpech.ru

Received: 20.07.2021 **Accepted:** 11.08.2021 **Published online:** 23.09.2021

DOI: 10.47183/mes.2021.030

ОЦЕНКА ГЕПАТОПРОТЕКТОРНОГО ЭФФЕКТА АНТИОКСИДАНТОВ НА АМИОДАРОН-ИНДУЦИРОВАННУЮ ЦИТОТОКСИЧНОСТЬ В КЛЕТКАХ ГЕПАТОМЫ ЧЕЛОВЕКА ЛИНИИ *HEPARG*

К. С. Филимонова, Н. Ю. Роговская, П. П. Бельюков, В. Н. Бабаков ✉

Научно-исследовательский институт гигиены, профпатологии и экологии человека Федерального медико-биологического агентства, Ленинградская область, Россия

Для эффективной терапии амиодарон-индуцированной гепатотоксичности необходимы изучение механизмов токсического действия амиодарона на гепатоциты и оценка возможного влияния гепатопротекторов. Целью работы было исследовать гепатопротекторный эффект антиоксидантов на амиодарон-индуцированную цитотоксичность с использованием immortalized гепатомы человека линии *HepaRG*. Жизнеспособность клеток оценивали при действии амиодарона и в смеси с витамином E, N-ацетилцистеином и S-аденозилметионином методом импедансометрии, а также определяли содержание некоторых биомаркеров гепатотоксичности с использованием технологии Luminex xMAP. В результате исследования установлен дозозависимый эффект токсического действия амиодарона, IC_{50} амиодарона для линии *HepaRG* составил 3,5 мкМ. Показано, что в присутствии витамина E, N-ацетилцистеина и S-аденозилметионина снижается цитотоксический эффект и увеличивается значение IC_{50} . Амиодарон снижает активность регуляторов клеточного цикла: киназ AKT, JNK и белка p53. В результате действия амиодарона уменьшается содержание АТФ в клетках и наблюдается выход внутриклеточных ферментов (малатдегидрогеназы 1, глутатион-S-трансферазы, сорбитолдегидрогеназы, 5'-нуклеотидазы) в кондиционную среду, что свидетельствует о клеточной гибели по типу некроза. Таким образом, витамин E, S-аденозилметионин и N-ацетилцистеин снижают цитотоксичность амиодарона в модели амиодарон-индуцированного повреждения гепатоцитов и могут быть рассмотрены в качестве гепатопротекторов при необходимости защиты тканей печени от гепатотоксических эффектов амиодарона.

Ключевые слова: *HepaRG*, амиодарон, лекарственная гепатотоксичность, витамин E, N-ацетилцистеин, S-аденозилметионин

✉ **Для корреспонденции:** Владимир Николаевич Бабаков
ст. Капитолово, к. 93, п. Кузьмолловский, Ленинградская область, 188663; babakov@gpech.ru

Статья получена: 20.07.2021 **Статья принята к печати:** 11.08.2021 **Опубликована онлайн:** 23.09.2021

DOI: 10.47183/mes.2021.030

The symptoms of drug-induced liver injury constitute about 10% of adverse reactions, caused by medications, and are considered the main reason for clinical trial termination or for withdrawal of medications already used in therapy. Drugs of various pharmacological classes possess hepatotoxic effects: antibiotics (amoxicillin/clavulanate), analgesics (acetaminophen), antiepileptic drugs (valproate), etc. [1].

Drug dosage reduction or permanent discontinuation of the drug allows for prevention of irreversible liver damage. However, in some cases it is necessary to continue using hepatotoxic drug in parallel with the use of hepatoprotective drugs. The efficiency of hepatoprotective drugs used in clinical practice results from the presence of components, having various mechanisms of action. There remains a need for developing new pharmaceutical products to protect the liver against the

possible toxic effects, since hepatoprotective drugs are not always able to minimize the adverse effects of xenobiotics, and the use of specific antidotes is limited to the use of N-acetylcysteine in paracetamol overdose [2]. Developing the efficient methods for the drug-induced liver injury treatment requires studying the toxin-induced hepatic cell damage mechanisms, and selecting the potential hepatoprotective agents and specific antidotes.

Amiodarone, being the anti-arrhythmic agent, is characterized by the frequent side effects, manifested by the symptoms of drug-induced liver injury. Amiodarone is one of the most frequently prescribed anti-arrhythmic medication due to high efficiency and broad spectrum of action [3].

In 10–15% of cases, administration of amiodarone is compounded by side effects in the form of elevated serum

transaminase levels, phospholipidosis and steatohepatitis. The long-term use of amiodarone may result in acute liver failure, which is sometimes fatal [4].

Liver injury, resulting from administration of amiodarone, is due to cytotoxic effects of the medication. It is known that amiodarone and its metabolites (mostly mono- and di-N-desethylamiodarone) inhibit the electron transport chain function and uncouple oxidative phosphorylation, which should be complemented by the reactive oxygen species accumulation and the development of oxidative stress [5, 6]. Oxidative stress is indicated by the elevated lipid peroxidation marker levels after exposure to amiodarone [7]. Furthermore, amiodarone is able to inhibit phospholipase A and β -oxidation of long-chain fatty acids, which promotes lipid accumulation in hepatic cells [8, 9]. There is also a decline in the intracellular ATP levels and calcium ions; endoplasmic reticulum is damaged [10].

Earlier, the study involving the L929 mouse fibroblast cell line showed that the use of antioxidant agents, vitamin C and N-acetylcysteine, contributed to reduced amiodarone cytotoxicity [11]. We have studied the ability of nonspecific hepatoprotective compounds, possessing antioxidant activity (vitamin E and the sulfur-containing N-acetylcysteine and S-adenosylmethionine), to affect cytotoxic properties of amiodarone.

Vitamin E has long been known as a cytoprotective agent and recommended for therapy of inflammatory and degenerative liver diseases, such as non-alcoholic fatty liver disease and steatohepatitis [12]. N-acetyl-L-cysteine (NAC) is the effective antidote to treat paracetamol overdose. NAC is also proposed to be used in management of non-paracetamol drug-induced

liver injury [13]. S-adenosyl-L-methionine (SAM) is the main donor of methyl groups in the body, it also plays an important role in the xenobiotic metabolism in the liver. Therefore, SAM is also viewed as a hepatoprotective agent for various liver diseases. However, in clinical practice, hepatoprotective effects of SAM has not been supported by randomized placebo-controlled trials [14].

Test systems based on primary human hepatocyte culture or immortalized cell lines are used for *in vitro* investigation of cytotoxic effects on hepatocytes. During the study, we used the human hepatoma *HepaRG* cell line. Cells of this cell line ensure the expression of biotransformation enzymes (in particular, cytochromes P450) and transport proteins at the levels close to those of primary human hepatocytes. This gives us ground to consider this cell line to be the optimal choice for *in vitro* hepatotoxicity modeling [15, 16]. The *HepaRG* cell line has shown maximum sensitivity in assessing the potential hepatotoxicity of medications with the use of multiparametric assay [17, 18].

Thus, the study was aimed to assess cytoprotective effects of antioxidants in the human hepatoma *HepaRG* cell line-based model of amiodarone-induced cytotoxicity.

METHODS

Human hepatoma cells of the *HepaRG* cell line (Gibco; USA) were cultured in the complete growth medium, consisting of William's E medium with 10% fetal bovine serum, 5 $\mu\text{g}/\text{mL}$ of insulin, 10 U/mL of penicillin, 100 $\mu\text{g}/\text{mL}$ of streptomycin, 50 μM of hydrocortisone hemisuccinate, and 2 mM of L-glutamine, in

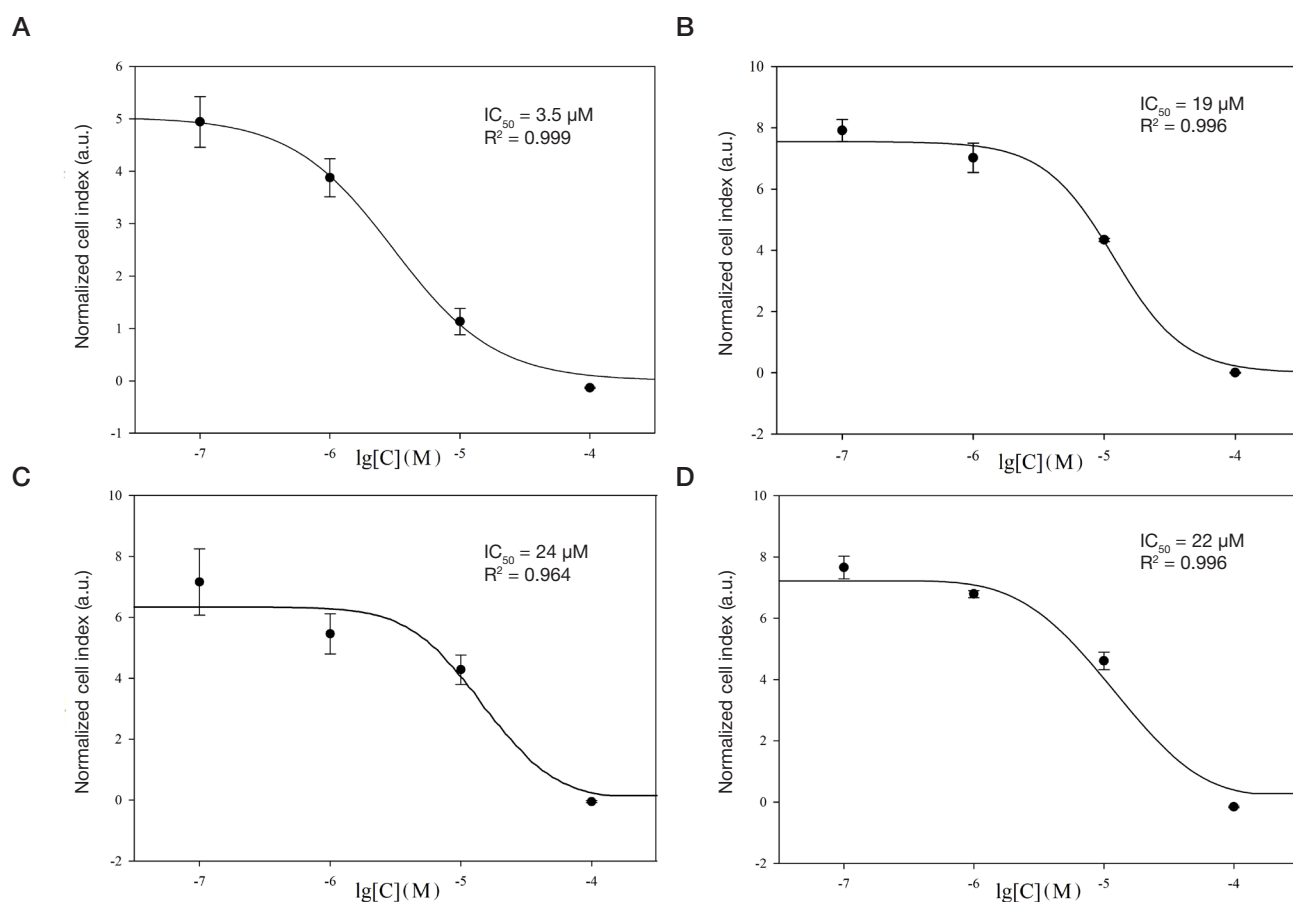


Fig. 1. Relationship between cell index of *HepaRG* cells and log concentration of amiodarone (cell index has been normalized in terms of the time when the medium containing the studied substance has been added). **A.** Changes in cell index upon exposure to amiodarone at a concentration of 0.1, 1, 10 and 100 μM . **B.** Changes in cell index upon exposure to amiodarone dilution series in the presence of 100 μM of vitamin E. **C.** Changes in cell index upon exposure to amiodarone dilution series in the presence of 100 μM of N-acetylcysteine. **D.** Changes in cell index upon exposure to amiodarone dilution series in the presence of 100 μM of S-adenosylmethionine

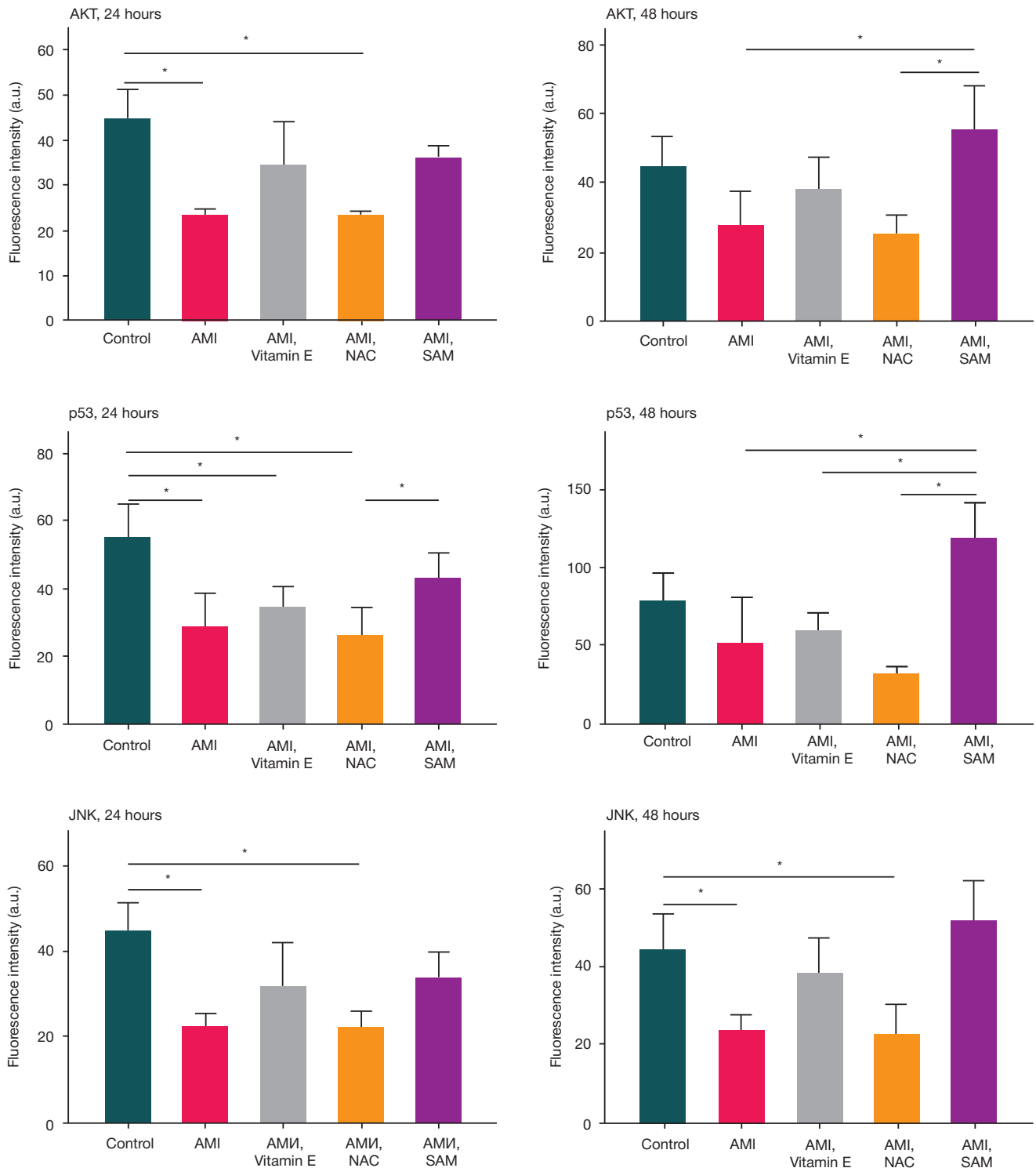


Fig. 2. Phosphorylated AKT kinase (Ser473), p53 protein (Ser46), JNK kinase (Thr183/Tyr185) fluorescence intensity in the *HepaRG* cell lysates after exposure to amiodarone at a concentration of 10 μM (AMI), and against the effects of 100 μM of vitamin E, 100 μM of N-acetylcysteine (NAC), 100 μM of S-adenosylmethionine (SAM) during the 24- and 48-hour incubation. * — $p < 0.05$

the atmosphere of CO_2 incubator (5% CO_2) at a temperature of 37 $^\circ\text{C}$ and saturation humidity.

The xCELLigence RTCA system (ACEA; USA) was used to define amiodarone cytotoxicity. Cell index, being the indicator of cell viability, was calculated with the RTCA Software 2.0 (ACEA; USA) based on the analysis of changes in impedance over time. Prior to the experiment, the impedance of the growth medium in the absence of cells was measured. Next, a total of 10,000 *HepaRG* cells were added to each well of the 96-well plate and cultured for 24 hours. After that amiodarone (at a

concentration of 0.1–100 μM) and studied antioxidants (vitamin E, NAC and SAM at a concentration of 100 μM) were added to the medium. Cells cultured in complete growth medium were used as a control.

Molecular markers of cell damage were assessed with the Bio-Plex 200 suspension array system (Bio-Rad; USA). Markers of apoptosis were assessed in cell lysates, and markers of hepatocyte damage were assessed in conditioned media. In order to obtain conditioned media and lysates, human hepatoma cells of the *HepaRG* cell line were added to the 24-well plate

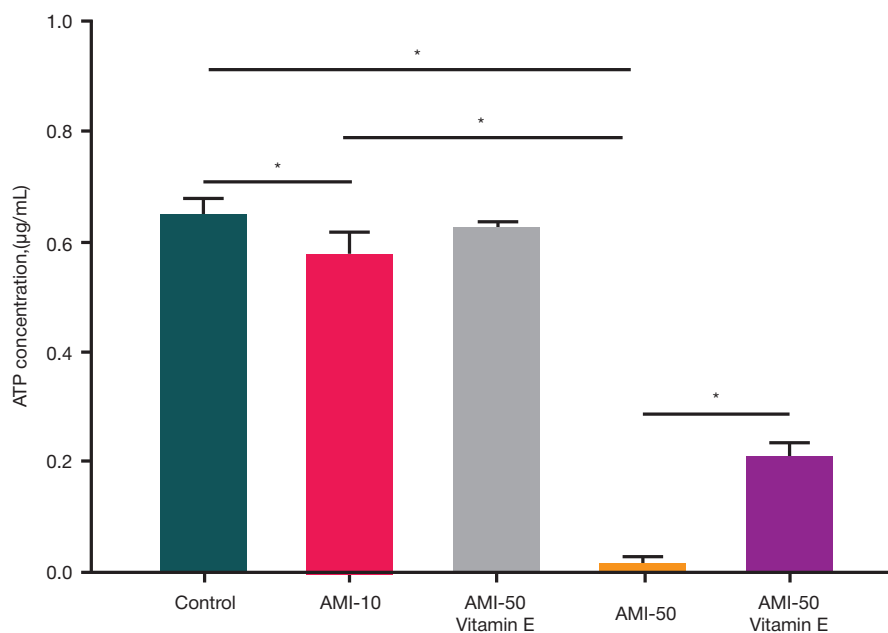


Fig. 3. ATP levels in HepaRG cell lysates after the 24-hour exposure to amiodarone at a concentration of 10 µM (AMI-10) and 50 µM (AMI-50) against the background of exposure to vitamin E. * — $p < 0.05$

(400,000 cells per well) and cultured in the complete growth medium. The next day after passage, the medium was replaced with the medium, containing amiodarone at a concentration of 10 µM together with the studied antioxidants at a concentration of 100 µM. The samples were incubated for 24 and 48 hours. Each experimental concentration of the studied substances was added in at least three iterations. The following kits were used for the multiplex analysis: MILLIPLEX MAP Human Liver Injury Magnetic Bead Panel (Cat. HLNJMAG-75K; Merck, USA), MILLIPLEX MAP Human Early Apoptosis Magnetic Bead 6-Plex Kit (Cat. 48-669MAG; Merck, USA), and Bio-PlexPro™ Human Cytokine 27-plex Screening Panel (Cat. M500KCAFOY; Bio-Rad, USA).

ATP was assessed in the HepaRG cell lysates using the ATP Bioluminescent Assay Kit (Cat. FLASC; Sigma-Aldrich, USA). The intensity of luminescent emission was measured with the FLx800 Microplate Fluorescence Reader (BioTek; USA). Data preprocessing was performed with the Gen5 1.10 software (BioTek; USA).

Statistical analysis and charting were carried out using the SigmaPlot 12.5 software (SystatSoftware Inc; USA). The sample was tested for normality with the Shapiro–Wilk test. The significance of differences between means was assessed by univariate analysis of variance for normal distributions and Kruskal–Wallis test for distributions other than normal. The differences were considered significant when $p < 0.05$. The results were presented as mean \pm standard deviation.

RESULTS

The IC_{50} value, calculated based on the monitoring of amiodarone cytotoxicity for the human hepatoma cells of the HepaRG cell line, was 3.5 µM (Fig. 1). The use of hepatoprotective agents, possessing antioxidant activity, resulted in significantly increased cell index compared to amiodarone. Thus, the IC_{50} value obtained for amiodarone in the presence of vitamin E was 19 µM; the value for N-acetylcysteine was 24 µM, and the value for S-adenosylmethionine was 22 µM.

The levels of some kinases involved in the cell cycle regulation in cell lysates, and the levels of intracellular enzymes in the conditioned media were analyzed in order to

assess the mechanisms of cytotoxicity. The exposure of cells to amiodarone (10 µM) during 24 and 48 hours resulted in reduced levels of phosphorylated AKT and JNK kinases together with the p53 protein (Fig. 2). In other words, amiodarone contributes the decreased activity of enzymes, involved in the cell cycle regulation, and triggers cell death. This can explain high cytotoxicity of amiodarone. The levels of AKT and JNK kinase active forms in the cell lysates after treating with amiodarone (10 µM) in the presence of vitamin E or S-adenosylmethionine were the same as in control samples.

The study found that amiodarone concentrations of 10 and 50 µM caused a significant decline in the ATP levels in the HepaRG cell lysates; the decline in the ATP levels was dose dependent (Fig. 3). Vitamin E provided a significant increase in the intracellular ATP levels upon amiodarone cell treatment.

Assessment of extracellular enzyme levels showed that there was no significant increase in the levels of arginase 1 after treating cells with amiodarone (Fig. 4). After the 24 hour incubation with amiodarone, elevated levels of malate dehydrogenase 1, glutathione S-transferase and sorbitol dehydrogenase in the conditioned medium were observed (Fig. 4, 5). The levels of 5'-nucleotidase significantly increased in 48 hours. In the presence of vitamin E and S-adenosylmethionine, decline in the levels of MDH1, GST α and SDH intracellular enzymes in the conditioned medium was detected.

Analysis of cytokine levels after the HepaRG line cells' incubation in the medium with amiodarone (10 µM) showed the significant and the most prominent increase in the levels of IL1 β , IL6, IL8, IFN γ , TNF α pro-inflammatory factors, resulting from exposure to amiodarone (Fig. 6). At the same time, elevated levels of anti-inflammatory cytokine IL10 were noted. The effects of antioxidants were reflected in the reduced levels of the assessed cytokines in the conditioned media.

DISCUSSION

Side effects of amiodarone were reported in the late 20th century, after the beginning of its widespread use as an antiarrhythmic agent [19]. Based on its structure, amiodarone belongs to the class of cationic amphiphilic substances. Moreover, amiodarone has a long half-life in the terminal elimination phase, which can

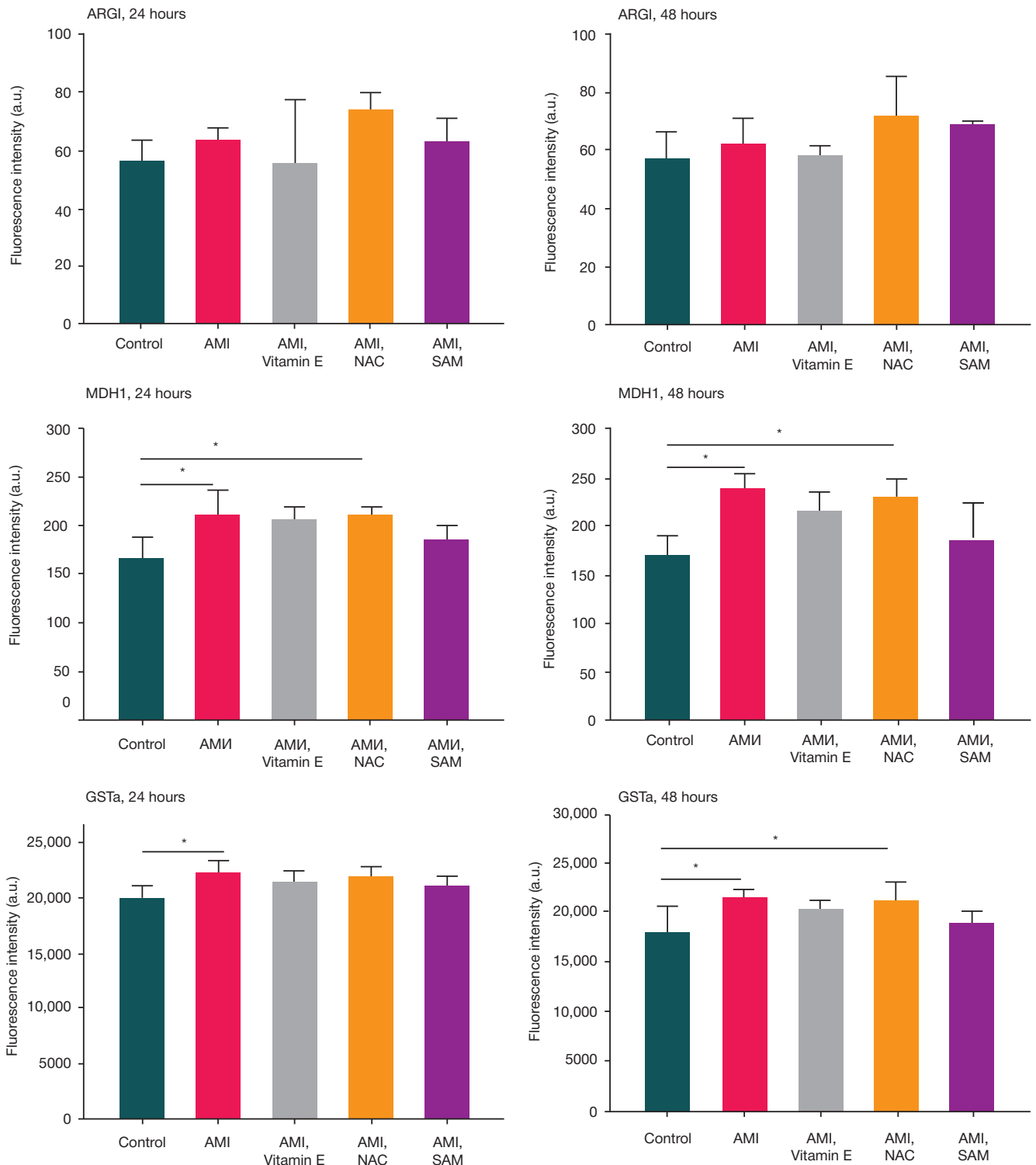


Fig. 4. Arginase 1 (ARG1), malate dehydrogenase 1 (MDH1), glutathione S-transferase (GSTα) fluorescence intensity in the conditioned medium of the *HepaRG* cells after exposure to amiodarone at a concentration of 10 μM (AMI), and against the effects of 100 μM of vitamin E, 100 μM of N-acetylcysteine (NAC), 100 μM of S-adenosylmethionine (SAM) during the 24- and 48-hour incubation. * — $p < 0.05$

be up to 150 days [8]. Amiodarone and its metabolites can accumulate in lungs, skeletal muscles, adipose tissue, liver, and exhibit toxic effects. Meanwhile, the degree of liver injury varies significantly from slightly increased serum transaminase levels to acute liver failure [4].

The long-term oral (per os) administration of amiodarone results in accumulation of fatty acids and polar lipids in hepatocytes due to inhibition of phospholipase A and enzymes for β -oxidation of fatty acids. Accumulation of amiodarone in lysosomal lipid bilayers has been reported, which interferes with

the normal intracellular degradation of membrane phospholipids and results in phospholipidosis [8, 20]. Accumulation of triglycerides and lipid droplets after the 14-day incubation of the human hepatoma *HepaRG* cell line with amiodarone at a concentration of 20 μM has been reported [21].

However, the mechanisms of amiodarone-induced hepatotoxicity are still poorly understood.

We defined the dose-dependent cytotoxic effects of amiodarone on the *HepaRG* cell line for three days and calculated the IC_{50} value, which was 3.5 μM . Earlier, amiodarone

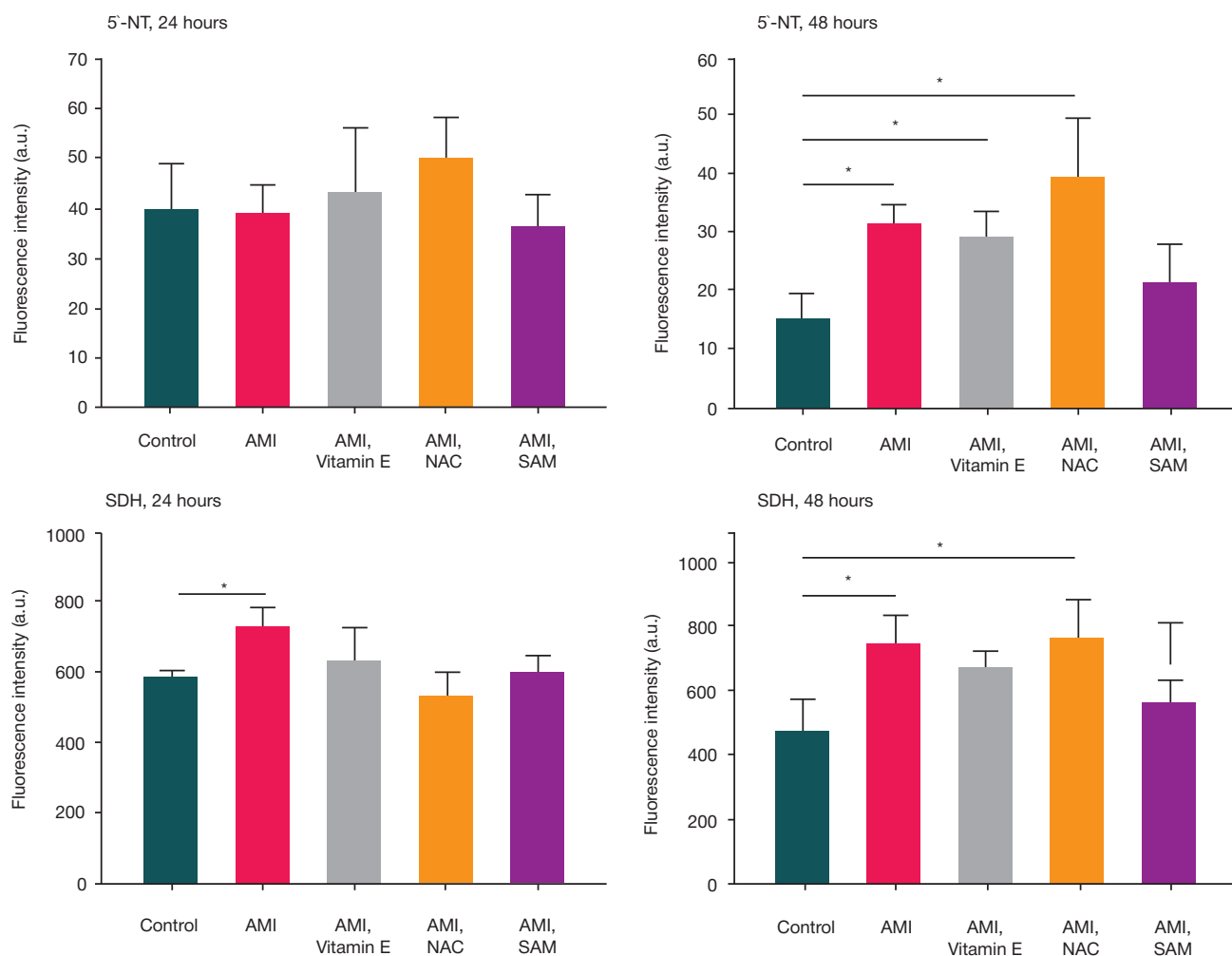


Fig. 5. Nucleotidase (5'-NT), sorbitol dehydrogenase (SDH) fluorescence intensity in the conditioned medium of the *HepaRG* cells after exposure to amiodarone at a concentration of 10 μ M (AMI), and against the effects of 100 μ M of vitamin E, 100 μ M of N-acetylcysteine (NAC), 100 μ M of S-adenosylmethionine (SAM) during the 24- and 48-hour incubation. * — $p < 0.05$

cytotoxicity was demonstrated during the study, involving the *HepG2* cell line, where the IC_{50} value was 105 μ M [7]. However, *HepaRG* cells show higher expression of the cytochrome P450 system enzymes compared to the *HepG2* cell line. Amiodarone metabolites (mono- and di-N-desethylamiodarone), formed after transformation by cytochromes, can exhibit higher hepatotoxicity compared to amiodarone [18].

The increased intracellular levels of active (phosphorylated) forms of kinases, involved in the cell cycle regulation, indicate the type of cell death and the pathways of cell death process activation [22]. During our study, exposure to amiodarone resulted in reduced levels of active forms of AKT and JNK kinases and p53 protein. This indicates that mitochondrial damage is the main mechanism, triggering cell death when exposed to amiodarone. The levels of active initiator caspase-8 are also reduced after threatening cell culture with amiodarone, which makes it possible to speak of necrotic cell death instead of apoptosis.

It is known that intracellular levels of ATP are the measure of cell viability [23]. Depletion of intracellular ATP reserves is considered one of the characteristic features of necrosis [24]. The detected decline in intracellular ATP levels, and the release of intracellular enzymes into conditioned medium also demonstrate the necrotic cell death.

It has been also found that exposure to amiodarone results in elevated levels of pro-inflammatory cytokines IL1 β , IL6, IL8, IFN γ , TNF α and anti-inflammatory cytokine IL10 in the conditioned medium.

Intracellular enzymes, cytokines and danger associated molecular patterns (DAMPs), released when the cells are damaged, activate the innate immunity cells [25]. Activated Kupffer cells and neutrophils together with other resident liver cells secrete various cytokines, which can result in triggering apoptosis through death receptors and the development of inflammatory response [22]. Thus, the exposure to amiodarone may cause both necrosis and apoptosis, which is consistent with the previously published data on cytostatic effects of amiodarone [26, 27].

Thus, the human hepatoma *HepaRG* cell line model has shown that cell death, occurring after the 48-hour exposure to amiodarone, is the result of necrosis.

It is anticipated that oxidative stress is one of the root causes of amiodarone cytotoxicity [7]. Earlier, with the use of various cell models (primary rat hepatocytes, *HepG2*, *L929* cells), it has been shown that antioxidants protect cells against cytotoxic effects of amiodarone [7, 11, 28]. We have assessed the impact of compounds with antioxidant properties on the amiodarone-induced cytotoxicity in the human hepatoma cells of the *HepaRG* cell line. Vitamin E, S-adenosylmethionine and N-acetylcysteine reduce cytotoxicity of amiodarone and increase the IC_{50} value. Vitamin E and S-adenosylmethionine ensure amiodarone-induced reduction of the key pro-inflammatory IL1 β and IL6 cytokine secretion.

The listed above results confirm that amiodarone is able to induce oxidative stress in cells. The studied vitamin E,

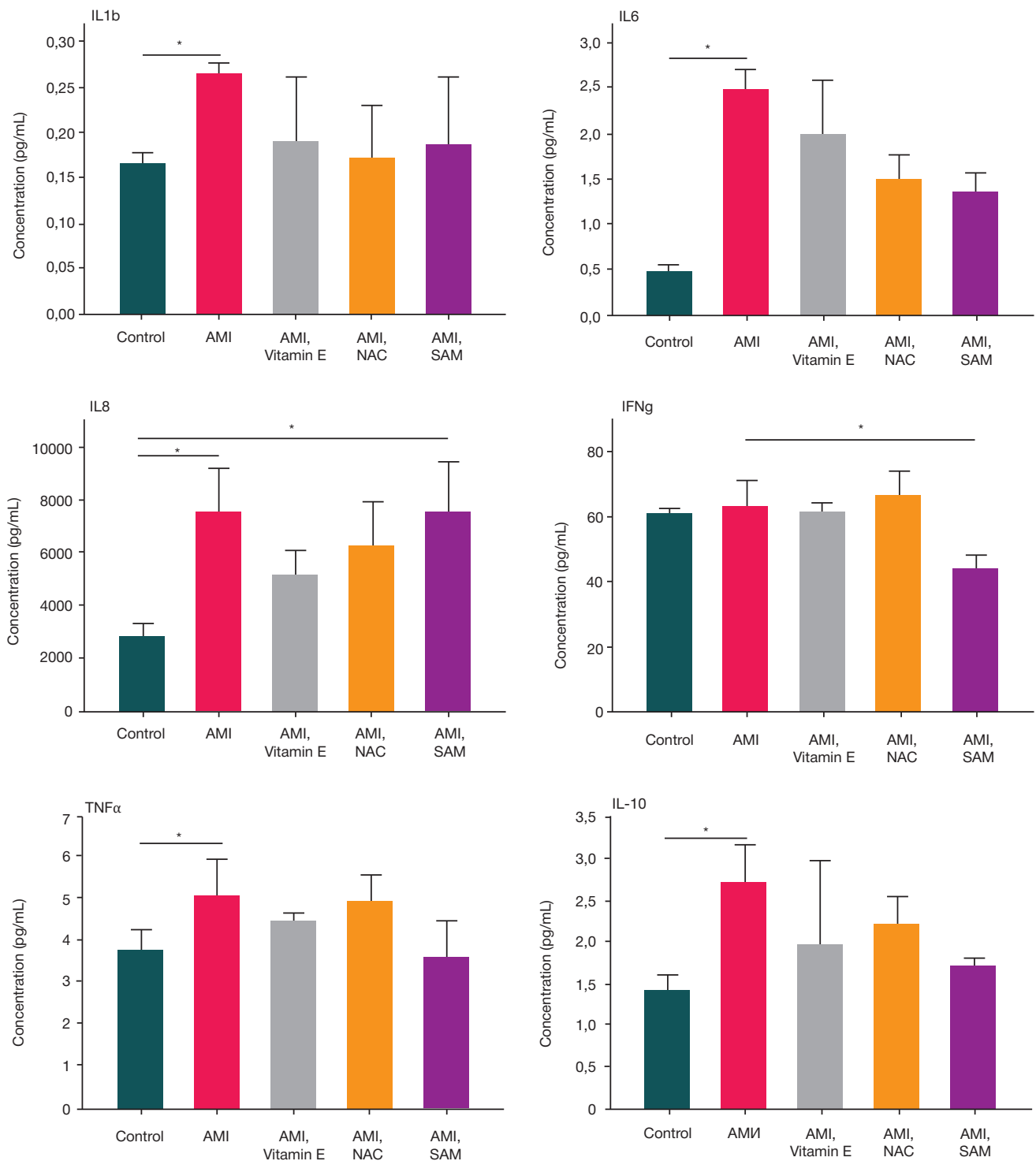


Fig. 6. Concentration of cytokines IL1 β , IL6, IL8, IFN γ , TNF α and IL10 in the conditioned medium of *HepaRG* cells, incubated during 48 hours and exposed to amiodarone at a concentration of 10 μ M (AMI), and against the effects of 100 μ M of vitamin E, 100 μ M of N-acetylcysteine (NAC), 100 μ M of S-adenosylmethionine (SAM). * — $p < 0.05$

S-adenosylmethionine and N-acetylcysteine are the registered medicinal products and could be recommended as hepatoprotective agents during amiodarone therapy.

CONCLUSIONS

Amiodarone has a cytotoxic effect on the human hepatoma cells of the *HepaRG* cell line (IC_{50} 3.5 μ M). Cell death occurs with underlying reduction in the levels of active forms of factors,

involved in cell cycle regulation, such as AKT, JNK kinases, and p53 protein. The effects of amiodarone result in cytolysis accompanied by the increase in the levels of intracellular enzymes (MDH1, GST α , SDH and 5'-NT) in the conditioned medium. The studied compounds possessing antioxidant properties, Vitamin E, N-acetylcysteine and S-adenosylmethionine, reduce amiodarone-induced cytotoxicity in the human hepatoma cells of the *HepaRG* cell line and can be considered as potential hepatoprotective agents during treatment with amiodarone.

References

- Ivashkin VT, Baranovsky AY, Raikhelson KL, et al. Lekarstvennyye porazheniya pecheni (klinicheskie rekomendatsii dlja vrachej). Rossijskij zhurnal gastrojenterologii, gepatologii, koloproktologii. 2019; 29 (1): 101–31. Russian.
- Stine JG, Lewis JH. Current and future directions in the treatment and prevention of drug-induced liver injury: a systematic review. *Expert Rev Gastroenterol Hepatol*. 2016; 10 (4): 517–36.
- Mujović N, Dobrev D, Marinković M, et al. The role of amiodarone in contemporary management of complex cardiac arrhythmias. *Pharmacol Res*. 2020; 151: 104521.
- Hashmi A, Keswani NR, Kim S, et al. Hepatic dysfunction in patients receiving intravenous amiodarone. *South Med J*. 2016; 109 (2): 83–6.
- Waldhauser KM, Török M, Ha H-R, et al. Hepatocellular toxicity and pharmacological effect of amiodarone and amiodarone derivatives. *J Pharmacol Exp Ther*. 2006; 319 (3): 1413–23.
- Serviddio G, Bellanti F, Giudetti AM, et al. Mitochondrial oxidative stress and respiratory chain dysfunction account for liver toxicity during amiodarone but not dronedarone administration. *Free Radic Biol Med*. 2011; 51 (12): 2234–42.
- Golli-Bennour EE, Bouslimi A, Zouaoui O, et al. Cytotoxicity effects of amiodarone on cultured cells. *Exp Toxicol Pathol*. 2012; 64 (5): 425–30.
- Schumacher JD, Guo GL. Mechanistic review of drug-induced steatohepatitis. *Toxicol Appl Pharmacol*. 2015; 289 (1): 40–7.
- Grünig D, Duthaler U, Krähenbüh S. Effect of Toxicants on Fatty Acid Metabolism in HepG2 Cells. *Front Pharmacol*. 2018; 9: 257.
- Erez N, Hubel E, Avraham R, et al. Hepatic amiodarone lipotoxicity is ameliorated by genetic and pharmacological inhibition of endoplasmic reticulum stress. *Toxicol Sci*. 2017; 159 (2): 402–12.
- Durukan AB, Erdem B, Durukan E, et al. May toxicity of amiodarone be prevented by antioxidants? A cell-culture study. *J Cardiothorac Surg*. 2012; 7 (1): 61.
- Galli F, Azzi A, Birringer M, et al. Vitamin E: Emerging aspects and new directions. *Free Radic Biol Med*. 2017; 102: 16–36.
- Chughlay MF, Kramer N, Spearman CW, et al. N-acetylcysteine for non-paracetamol drug-induced liver injury: a systematic review. *Br J Clin Pharmacol*. 2016; 81: 1021–9.
- Anstee QM, Day CP. S-adenosylmethionine (SAMe) therapy in liver disease: A review of current evidence and clinical utility. *J Hepatol*. 2012; 57 (5): 1097–109.
- Aninat C, Piton A, Glaise D, et al. Expression of cytochromes P450, conjugating enzymes and nuclear receptors in human hepatoma HepaRG cells. *Drug Metab Dispos*. 2006; 34 (1): 75–83.
- Yokoyama Y, Sasaki Y, Terasaki N, et al. Comparison of drug metabolism and its related hepatotoxic effects in HepaRG, cryopreserved human hepatocytes, and HepG2 cell cultures. *Biol Pharm Bull*. 2018; 41 (5): 722–32.
- Tomida T, Okamura H, Yokoi T, et al. A modified multiparametric assay using HepaRG cells for predicting the degree of drug-induced liver injury risk. *J Appl Toxicol*. 2017; 37 (3): 382–90.
- Wu Y, Geng X, Wang J, et al. The HepaRG cell line, a superior in vitro model to L-02, HepG2 and hiHeps cell lines for assessing drug-induced liver injury. *Cell Biol Toxicol*. 2016; 32 (1): 37–59.
- McGovern B, Garan H, Ruskin JN. Serious adverse effects of amiodarones. *Clin Cardiol*. 1984; 7 (3): 131–7.
- Pessayre D, Fromenty B, Berson A, et al. Central role of mitochondria in drug-induced liver injury. *Drug Metab Rev*. 2012; 44 (1): 34–87.
- Anthérieu S, Rogue A, Fromenty B, et al. Induction of vesicular steatosis by amiodarone and tetracycline is associated with up-regulation of lipogenic genes in heparg cells. *Hepatology*. 2011; 53 (6): 1895–905.
- Ye H, Nelson LJ, Gómez del Moral M, et al. Dissecting the molecular pathophysiology of drug-induced liver injury. *World J Gastroenterol*. 2018; 24 (13): 1373–85.
- Yuan L, Kaplowitz N. Mechanisms of drug induced liver injury. *Clin Liver Dis*. 2013; 17 (4): 507–18.
- Iorga A., Dara L. Cell death in drug-induced liver injury. *Adv Pharmacol*. 2019; 85: 31–74.
- Ali SE, Waddington JC, Park BK, et al. Definition of the Chemical and Immunological Signals Involved in Drug-Induced Liver Injury. *Chem Res Toxicol*. 2020; 33 (1): 61–76.
- Bognar Z, Fekete K, Antus C, et al. Desethylamiodarone — A metabolite of amiodarone — Induces apoptosis on T24 human bladder cancer cells via multiple pathways. *PLoS One*. 2017; 12 (12): e0189470.
- Steinberg E, Fluksman A, Zemmour C, et al. Low dose amiodarone reduces tumor growth and angiogenesis. *Sci Rep*. 2020; 10 (1): 18034.
- Abdulkhaleq F, Alhussainy T, Badr M, et al. Antioxidative stress effects of vitamins C, E, and B12, and their combination can protect the liver against acetaminophen-induced hepatotoxicity in rats. *Drug Des Devel Ther*. 2018; 12: 3525–33.

Литература

- Ивашкин В. Т., Барановский А. Ю., Райхельсон К. Л. и др. Лекарственные поражения печени (клинические рекомендации для врачей). Российский журнал гастроэнтерологии, гепатологии, колопроктологии. 2019; 29 (1): 101–31.
- Stine JG, Lewis JH. Current and future directions in the treatment and prevention of drug-induced liver injury: a systematic review. *Expert Rev Gastroenterol Hepatol*. 2016; 10 (4): 517–36.
- Mujović N, Dobrev D, Marinković M, et al. The role of amiodarone in contemporary management of complex cardiac arrhythmias. *Pharmacol Res*. 2020; 151: 104521.
- Hashmi A, Keswani NR, Kim S, et al. Hepatic dysfunction in patients receiving intravenous amiodarone. *South Med J*. 2016; 109 (2): 83–6.
- Waldhauser KM, Török M, Ha H-R, et al. Hepatocellular toxicity and pharmacological effect of amiodarone and amiodarone derivatives. *J Pharmacol Exp Ther*. 2006; 319 (3): 1413–23.
- Serviddio G, Bellanti F, Giudetti AM, et al. Mitochondrial oxidative stress and respiratory chain dysfunction account for liver toxicity during amiodarone but not dronedarone administration. *Free Radic Biol Med*. 2011; 51 (12): 2234–42.
- Golli-Bennour EE, Bouslimi A, Zouaoui O, et al. Cytotoxicity effects of amiodarone on cultured cells. *Exp Toxicol Pathol*. 2012; 64 (5): 425–30.
- Schumacher JD, Guo GL. Mechanistic review of drug-induced steatohepatitis. *Toxicol Appl Pharmacol*. 2015; 289 (1): 40–7.
- Grünig D, Duthaler U, Krähenbüh S. Effect of Toxicants on Fatty Acid Metabolism in HepG2 Cells. *Front Pharmacol*. 2018; 9: 257.
- Erez N, Hubel E, Avraham R, et al. Hepatic amiodarone lipotoxicity is ameliorated by genetic and pharmacological inhibition of endoplasmic reticulum stress. *Toxicol Sci*. 2017; 159 (2): 402–12.
- Durukan AB, Erdem B, Durukan E, et al. May toxicity of amiodarone be prevented by antioxidants? A cell-culture study. *J Cardiothorac Surg*. 2012; 7 (1): 61.
- Galli F, Azzi A, Birringer M, et al. Vitamin E: Emerging aspects and new directions. *Free Radic Biol Med*. 2017; 102: 16–36.
- Chughlay MF, Kramer N, Spearman CW, et al. N-acetylcysteine for non-paracetamol drug-induced liver injury: a systematic review. *Br J Clin Pharmacol*. 2016; 81: 1021–9.
- Anstee QM, Day CP. S-adenosylmethionine (SAMe) therapy in liver disease: A review of current evidence and clinical utility. *J Hepatol*. 2012; 57 (5): 1097–109.
- Aninat C, Piton A, Glaise D, et al. Expression of cytochromes P450, conjugating enzymes and nuclear receptors in human hepatoma HepaRG cells. *Drug Metab Dispos*. 2006; 34 (1): 75–83.
- Yokoyama Y, Sasaki Y, Terasaki N, et al. Comparison of drug metabolism and its related hepatotoxic effects in HepaRG, cryopreserved human hepatocytes, and HepG2 cell cultures. *Biol Pharm Bull*. 2018; 41 (5): 722–32.

17. Tomida T, Okamura H, Yokoi T, et al. A modified multiparametric assay using HepaRG cells for predicting the degree of drug-induced liver injury risk. *J Appl Toxicol*. 2017; 37 (3): 382–90.
18. Wu Y, Geng X, Wang J, et al. The HepaRG cell line, a superior in vitro model to L-02, HepG2 and hiHeps cell lines for assessing drug-induced liver injury. *Cell Biol Toxicol*. 2016; 32 (1): 37–59.
19. McGovern B, Garan H, Ruskin JN. Serious adverse effects of amiodarones. *Clin Cardiol*. 1984; 7 (3): 131–7.
20. Pessayre D, Fromenty B, Berson A, et al. Central role of mitochondria in drug-induced liver injury. *Drug Metab Rev*. 2012; 44 (1): 34–87.
21. Anthérieu S, Rogue A, Fromenty B, et al. Induction of vesicular steatosis by amiodarone and tetracycline is associated with up-regulation of lipogenic genes in heparg cells. *Hepatology*. 2011; 53 (6): 1895–905.
22. Ye H, Nelson LJ, Gómez del Moral M, et al. Dissecting the molecular pathophysiology of drug-induced liver injury. *World J Gastroenterol*. 2018; 24 (13): 1373–85.
23. Yuan L, Kaplowitz N. Mechanisms of drug induced liver injury. *Clin Liver Dis*. 2013; 17 (4): 507–18.
24. Iorga A., Dara L. Cell death in drug-induced liver injury. *Adv Pharmacol*. 2019; 85: 31–74.
25. Ali SE, Waddington JC, Park BK, et al. Definition of the Chemical and Immunological Signals Involved in Drug-Induced Liver Injury. *Chem Res Toxicol*. 2020; 33 (1): 61–76.
26. Bogнар Z, Fekete K, Antus C, et al. Desethylamiodarone — A metabolite of amiodarone — Induces apoptosis on T24 human bladder cancer cells via multiple pathways. *PLoS One*. 2017; 12 (12): e0189470.
27. Steinberg E, Fluksman A, Zemmour C, et al. Low dose amiodarone reduces tumor growth and angiogenesis. *Sci Rep*. 2020; 10 (1): 18034.
28. Abdulkhaleq F, Alhussainy T, Badr M, et al. Antioxidative stress effects of vitamins C, E, and B12, and their combination can protect the liver against acetaminophen-induced hepatotoxicity in rats. *Drug Des Devel Ther*. 2018; 12: 3525–33.

RESPIRATORY MUSCLE STRENGTH IN PATIENTS AFTER COVID-19

Savushkina OI^{1,2}✉, Malashenko MM², Cherniak AV¹, Kryukov EV², Sinitsyn EA¹, Zykov KA¹¹ Pulmonology Scientific Research Institute under Federal Medical Biological Agency, Moscow, Russia² Main Military Clinical Hospital named after academician N. N., Ministry of Defense, Moscow, Russia

Respiratory muscles (RM) are a very important part of the respiratory system that enables pulmonary ventilation. This study aimed to assess the post-COVID-19 strength of RM by estimating maximum static inspiratory (MIP or PImax) and expiratory (MEP or PEmax) pressures and to identify the relationship between MIP and MEP and the parameters of lung function. We analyzed the data of 36 patients (72% male; median age 47 years) who underwent spirometry, and body plethysmography, diffusion test for carbon monoxide (DLCO) and measurement of MIP and MEP. The median time between the examinations and onset of COVID-19 was 142 days. The patients were divided into two subgroups. In subgroup 1, as registered with computed tomography, the median of the maximum lung tissue damage volume in the acute period was 27%, in subgroup 2 it reached 76%. The most common functional impairment was decreased DLCO, detected in 20 (55%) patients. Decreased MIP and MEP were observed in 5 and 11 patients, respectively. The subgroups did not differ significantly in MIP and MEP values, but decreased MIP was registered in the second subgroup more often (18%). There were identified no significant dependencies between MIP/MEP and the parameters of ventilation and pulmonary gas exchange. Thus, in patients after COVID-19, MIP and MEP were reduced in 14 and 31% of cases, respectively. It is reasonable to add RM tests to the COVID-19 patient examination plan in order to check them for dysfunction and carry out medical rehabilitation.

Keywords: respiratory muscle strength, spirometry, body plethysmography, diffusion test, post-COVID-19, new coronavirus infection

Funding: ordered by the state under the research topic "Impact of the new coronavirus infection SARS-CoV-2 on the functional parameters of respiratory system during the convalescence period" (code: "Post-COVID functional diagnostics").

Acknowledgements: we would like to thank Zaitov M. R., engineer of ZAO Meditsinskoye Sistemy, for technical support.

Author contribution: Savushkina OI — study design development, clinical material collection, analysis and interpretation of the results, article authoring; Malashenko MM — clinical material collection, interpretation of the results; Cherniak AV — study design development, clinical material collection, analysis and interpretation of the results, article editing; Kryukov EV — article concept development, editing; Sinitsyn EA — interpretation of the results, article editing; Zykov KA — article editing, approval of the final version of the manuscript.

Compliance with ethical standards: the study was approved by the Ethics Committee of the Pulmonology Scientific Research Institute of the FMBA of Russia (minutes № 01-21 of May 14, 2021). All study participants signed informed consent.

✉ **Correspondence should be addressed:** Olga I. Savushkina
Orekhovy bulvar, 28, Moscow, 115682; olga-savushkina@yandex.ru

Received: 19.07.2021 **Accepted:** 09.08.2021 **Published online:** 16.09.2021

DOI: 10.47183/mes.2021.025

ИССЛЕДОВАНИЕ СИЛЫ ДЫХАТЕЛЬНЫХ МЫШЦ У БОЛЬНЫХ, ПЕРЕНЕСШИХ COVID-19

О. И. Савушкина^{1,2}✉, М. М. Малашенко², А. В. Черняк¹, Е. В. Крюков², Е. А. Синицын¹, К. А. Зыков¹¹ Научно-исследовательский институт пульмонологии Федерального медико-биологического агентства, Москва, Россия² Главный военный клинический госпиталь имени Н. Н. Бурденко, Москва, Россия

Дыхательные мышцы (ДМ) — важнейшее звено респираторной системы, обеспечивающее легочную вентиляцию. Целью исследования было оценить силу инспираторных (MIP) и экспираторных (MEP) ДМ после COVID-19 и выявить взаимосвязь показателей MIP и MEP с функциональными показателями системы дыхания. Проанализированы данные 36 пациентов (72% мужчин; медиана возраста — 47 лет), которым проводили спирометрию и бодиплетизмографию, определяли диффузионную способность легких (DLCO) и измеряли MIP/MEP. Медиана срока проведения исследований от начала COVID-19 составила 142 дня. Пациенты были разделены на две подгруппы. Медиана максимального объема поражения легочной ткани в острый период заболевания по КТ в подгруппе 1 составила 27%, в подгруппе 2 — 76%. Наиболее частым функциональным нарушением было снижение DLCO (выявлено у 20 (55%) пациентов). Снижение MIP и MEP было отмечено у 5 и 11 пациентов соответственно. Статистически значимых различий по показателям MIP и MEP между подгруппами выявлено не было, однако частота снижения MIP во второй подгруппе была выше (18%). Статистически значимых связей показателей MIP и MEP с параметрами вентиляции и легочного газообмена выявлено не было. Таким образом, у пациентов, перенесших COVID-19, обнаружено снижение MIP и MEP в 14 и 31% случаев соответственно. Исследование силы ДМ целесообразно включать в план обследования пациентов, перенесших COVID-19, для выявления их дисфункции и проведения медицинской реабилитации.

Ключевые слова: сила дыхательных мышц, спирометрия, бодиплетизмография, диффузионный тест, пост-COVID-19, новая коронавирусная инфекция, SARS-CoV-2

Финансирование: в рамках выполнения государственного задания по теме: «Влияние новой коронавирусной инфекции SARS-CoV-2 на функциональные показатели системы дыхания в период реконвалесценции» (шифр: «Пост-COVID-функциональная диагностика»).

Благодарности: инженеру ЗАО «Медицинские системы» М. Р. Зайтову за техническую поддержку.

Вклад авторов: О. И. Савушкина — разработка дизайна исследования, набор клинического материала, анализ и интерпретация результатов, написание текста; М. М. Малашенко — набор клинического материала, интерпретация результатов; А. В. Черняк — разработка дизайна исследования, набор клинического материала, анализ и интерпретация результатов, редактирование текста; Е. В. Крюков — концепция статьи, редактирование текста; Е. А. Синицын — интерпретация результатов, редактирование текста; К. А. Зыков — редактирование текста, утверждение итогового варианта текста рукописи.

Соблюдение этических стандартов: исследование одобрено этическим комитетом НИИ пульмонологии ФМБА России (протокол № 01-21, от 14 мая 2021 г.). Все участники исследования подписали информированное согласие.

✉ **Для корреспонденции:** Ольга Игоревна Савушкина
Ореховый бульвар, д. 28, 115682, г. Москва; olga-savushkina@yandex.ru

Статья получена: 19.07.2021 **Статья принята к печати:** 09.08.2021 **Опубликована онлайн:** 16.09.2021

DOI: 10.47183/mes.2021.025

COVID-19 is a highly contagious infectious disease caused by the new coronavirus SARS-CoV-2. The virus attacks respiratory system as one of its main targets, and this attack is the main reason that brought such patients to the hospital. The research efforts focused on COVID-19 mainly aimed to investigate the pathogenesis of the disease and find ways to treat it at the acute phase in order to minimize mortality. However, with the accumulation of knowledge, it became clear that COVID-19 is a multisystem disease, the consequences of which are currently not well understood.

From the point of view of damage to the respiratory system, the main functional disorder in the post-COVID period is the reduced lung diffusion capacity; less common are restrictive ventilation disorders, and even less so are obstructive ventilation disorders [1–3]. The data obtained are taken into account when drawing up individual post-disease medical rehabilitation programs for COVID-19 patients. However, it is not just the respiratory system that needs medical rehabilitation after COVID-19 but also the cardiovascular system, as well as the peripheral skeletal muscles, which grow weak and fatigued in severe and extremely severe COVID-19 cases.

Respiratory muscles (RM), which are the most important component of the respiratory system that enabled pulmonary ventilation, also belong to the skeletal muscles. Pathological changes in the respiratory muscles that occur after community-acquired pneumonia (CAP) [4, 5] and thoracic interventions [6] have been studied well. A comparative analysis of the strength of RM in CAP cases of varying severity of endogenous intoxication showed that, causing local inflammation and damaging myofibrils [5], this intoxication is the dominant extrapulmonary mechanism triggering RM dysfunction. In addition, there is hyperventilation syndrome caused by arterial hypoxemia that also contributes to RM fatigue. Moreover, glucocorticosteroids may also be the reason of weakness [7, 8]. However, there are just a few publications that investigate respiratory muscles strength after COVID-19 [9, 10].

The most common method for assessing RM strength is measurement of the maximum static mouth pressure when the person's airways are closed. This pressure may be expiratory (MEP) and inspiratory (MIP). Thus, this study aimed to assess the post-COVID-19 strength of RM and identify the relationship between MIP and MEP and other lung function parameters.

METHODS

The observational cross-sectional study included 36 patients (26 of them male, median age 47 years) admitted to hospitals with a diagnosed interstitial lung disease caused by the new coronavirus infection (J98.4). The inclusion criteria were: confirmed recovery from moderate or severe case of COVID-19, bilateral viral lung damage. In all patients the diagnosis was confirmed by polymerase chain reaction. The exclusion criterion was a recorded history of chronic lung disease. In the context of a single visit, all participants of this study underwent functional examinations of the respiratory system, including spirometry, body plethysmography, diffusion test and RM strength measurement. The system used for the examinations was the MasterScreen Body/Diff system (Viasys Healthcare / ErichJager, Vyair Medical / ErichJager; Germany).

All procedures were carried out in accordance with national and international standards [11–14] and recommendations of the Russian Respiratory Society for conducting lung function tests during the COVID-19 pandemic [15].

The lung diffusing capacity was assessed for carbon monoxide measured by means of the single-breath test through the use of rapidly responding gas analyser (RGA).

Analyzed parameters:

1) spirometry (forced vital capacity (FVC), forced expiratory volume in 1 sec (FEV_1), FEV_1/FVC , maximal mid-expiratory flow between 25% and 75% of the FVC expiration ($MMEF_{25-75}$));

2) body plethysmography (slow vital capacity (VC), total lung capacity (TLC), residual volume (RV) and its ratio to TLC (RV/TLC), thoracic gas volume (TGV), inspiratory capacity (IC), total airways resistance (Raw_{tot}));

3) diffusion test (transfer factor CO (DLCO) adjusted for hemoglobin value and its ratio to alveolar volume (VA) — $DLCO/VA$);

4) MIP and MEP.

The analyzed data were presented as a percentage of the predicted values ($\%_{pred}$), which were calculated using the equations of the European Coal and Steel Community [16] for patient's gender, age and height. The predicted MIP and MEP values were calculated by the equations recommended the European Respiratory Society [17]. Values greater than $75\%_{pred}$ were considered normal [18].

As registered with high-resolution chest computed tomography (CT), there was post-inflammatory damage of varying severity in the lungs of the patients at the time of the study. The cohort was divided into two subgroups depending on the maximum area of lung damage caused by SARS-CoV-2 in the acute period of the disease. Patients whose lungs had $\leq 50\%$ of tissue damaged were included in subgroup 1, those with lung damage exceeding 50% made up subgroup 2.

Sixteen (44%) patients had concomitant diseases: 7 patients — hypertension, 4 patients — hypertension and type 2 diabetes mellitus, one patient each — type 1 diabetes, varicose veins, myocarditis, psoriasis, iron deficiency anemia.

We employed STATISTICA 10.0 software (StatSoft Inc.; USA) for statistical analysis and Shapiro–Wilk test to assess the normality of distribution of the variables. Quantitative variables, the distribution of which differed from normal, were presented as medians (Me) and interquartile range (Q_1-Q_3), nominative variables — number of patients (n). Comparison of nonparametric quantitative indicators of the two groups relied on the nonparametric Mann–Whitney U test, that of qualitative variables — Fisher's exact test. Correlation analysis was performed using Spearman's rank correlation. The differences were considered significant at $p < 0.05$.

RESULTS

The median duration of the lung function examination from the onset of COVID-19 was 142 (108–186) days.

Table 1 presents characteristics of all the patients participating in the study and their characteristics by subgroups.

There were no significant differences established between the subgroups by age, gender, height, body mass index.

The majority of patients in both subgroups were nonsmokers; only subgroup 1 had a small number of smokers.

The median value of the maximum lung damage area (CT_{max}) in the acute period of the disease was 27% in the 1st subgroup and 76% in the 2nd subgroup, which is a significant difference. The length of hospital stay for COVID-19 was significantly longer in subgroup 2.

Table 2 summarizes the functional examination data analysis overall and by subgroups.

For all the patients, the medians of all analyzed lung function parameters were within normal range, apart from the decreased DLCO in 20 (55%) patients. In addition, 5 (14%) patients had impairment of TLC, one patient had impairment of VC and FEV_1/VC ($FEV_1/VC < 0.7$), 5 (14%) and 11 (31%)

Table 1. Patient characteristics

Parameter	Overall <i>n</i> = 36	Subgroup 1 <i>n</i> = 14	Subgroup 2 <i>n</i> = 22	<i>p</i> *
Gender, men, <i>n</i> (%)	26 (72)	8 (57)	18 (82)	NS
Age, years	47 (40–58)	46 (39–59)	48 (42–57)	NS
Height, cm	174 (165–181)	170 (165–183)	174 (165–179)	NS
BMI, kg/m ²	29 (26–32)	30 (25–32)	29 (27–31)	NS
Tobacco smoking, no/ex-smoker/smoker, %	69/28/3	72/21/7	68/32	–
Length of hospital stay for COVID-19	18 (13–25)	14 (8–16)	23 (15–27)	0,01

Note: the data are presented as quantity (*n*) or median (lower quartile — upper quartile). BMI — body mass index; * — subgroups 1 and 2 compared with Mann-Whitney test; NS — no significant differences found between subgroups 1 and 2.

patients had impairment of MIP and MEP, respectively. It should be noted that decreased TLC was found mainly in patients of subgroup 2, with only one such case registered in subgroup 1. Eight patients had the RV decreased, and 3 of them had the RV decreased isolated without impairment of TLC.

We found significant differences in TLC and DLCO values between the subgroups, these values being lower in subgroup 2. The subgroups did not differ significantly in MIP and MEP values, but decreased MIP was registered in the second subgroup more often (18%), while the frequency of decreased MEP was similar.

Correlation analysis did not reveal significant dependencies between MIP/MEP and the studied parameters of ventilation and pulmonary gas exchange.

DISCUSSION

Observation of COVID-19 convalescents indicates that after discharge from the hospital they do not fully recover functionally for a long time. Patients continue to experience shortness of breath, general weakness, increased fatigue and deteriorating quality of life. Besides, there are functional impairments of the respiratory system, cardiovascular system, as well as neuropathy and myopathy registered, which are primarily caused the extremely severe course of COVID-19 that required intensive care.

At the same time, even mild and moderate COVID-19 course brings the same symptoms with varying intensity of manifestation. The reduced RM strength is part of COVID-19-induced neuropathy and myopathy, which indicates the need for medical rehabilitation interventions to remedy the symptoms.

The Experts Consensus concerning respiratory techniques which are recommended for inclusion in post-COVID-19 medical rehabilitation programs draws special attention to training of inspiratory muscles aimed at improving ventilation-perfusion ratios and oxygenation [19]. However, this study shows that the reduced MEP registers twice as often as reduced MIP, that points out to justify breathing techniques in the context of training expiratory RM.

At the same time, physiotherapy methods such as electrical stimulation, chest massage with correction of muscle triggers and myofascial release, infrared laser therapy and magnetic therapy in the chest zones, help improve microcirculation and functional state of both inspiratory and expiratory RM.

Among the other findings of this study that draw attention is the lack of significant differences in MIP and MEP values between the subgroups, i.e., lack of confirmation the changes

in these parameters depend on the lung damage severity during the acute period of the disease. The results obtained are consistent with those reported in the previously published studies [9, 10], which allows considering other factors, possibly biochemical, including those affecting the central mechanisms of respiration regulation and, accordingly, the functional state of RM after COVID-19.

The median duration of this study from the onset of COVID-19 was 142 days, and the most common functional impairment registered was decreased diffusion capacity (55% of cases), mainly found in patients who had over 50% of their lungs damaged by the disease (subgroup 2), and restrictive ventilation disorders were diagnosed in 5 (14%) patients, 4 of whom (18%) were also in subgroup 2, while airways obstruction was only discovered in 1 patient. The meta-analysis that covered early post-COVID-19 period (1 to 3 months) showed that the prevalence of decreased diffusion capacity is 39% (CI: 24–56%; $p < 0.01$; heterogeneity index (I^2) — 86%), whereas restrictive ventilation disorders is 15% (CI: 9–22%; $p = 0.03$; $I^2 = 59%$), airways obstruction — 7% (CI: 4–11%; $p = 0.31$; $I^2 = 16%$) [3].

The results of this study are consistent with the data of the meta-analysis, however, the present study addressed later post-COVID-19 recovery periods, which may indicate that, after this disease, the functions of the respiratory system recover slowly.

No statistically significant correlations were found between the maximum static mouth pressure and the lung function parameters, which once again confirms the importance of measuring RM strength, especially in patients who experience shortness of breath and rapid fatigue while having the traditional pulmonary functional tests return normal values.

The effect COVID-19 has on RM strength should be investigated further in order to uncover the relationship between MIP/MEP values and the quantitative assessment of muscle strength by the MRC Weakness scale, as well as the severity of dyspnea by the mMRC scale.

Particular attention to RM strength should be paid when COVID-19 takes extreme form and causes post-intensive care syndrome (PICS), including general muscle weakness, decreased muscle mass, reduced physical performance and muscle strength, and reduced strength of the inspiratory muscles that may result in diaphragm atrophy and dysfunction. Measurement of the MIP and MEP values over time in such patients will allow adjustment of the medical rehabilitation program and prediction of the outcomes of identified impairments.

Table 2. Spirometry, body plethysmography, diffusion test, respiratory muscle strength test data

Parameter	Overall <i>n</i> = 36	Subgroup 1 <i>n</i> = 14	Subgroup 2 <i>n</i> = 22	<i>p</i>
VC, % _{pred}	106 (95–120)	111 (103–123)	104 (92–112)	NS
VC < 80% _{pred} , <i>n</i>	1	0	1	NS
FVC, % _{pred}	109 (99–123)	116 (106–125)	107 (96–114)	NS
FEV ₁ , % _{pred}	105 (98–125)	119 (102–128)	103 (97–116)	NS
FEV ₁ < 80% _{pred} , <i>n</i>	1	0	1	NS
FEV ₁ /VC, %	82 (78–84)	82 (78–84)	83 (78–86)	NS
FEV ₁ /VC < 0.7, <i>n</i>	1	0	1	NS
FEV ₁ /FVC, %	83 (80–85)	82 (80–84)	83 (80–86)	NS
MMEF _{25–75} , % _{pred}	109 (93–123)	110 (103–121)	105 (92–125)	NS
TLC, % _{pred}	100 (90–109)	108 (98–114)	97 (85–105)	NS
TLC < 80% _{pred} , <i>n</i>	5	1	4	NS
TGV, % _{pred}	87 (75–101)	93 (75–105)	85 (75–95)	NS
IC, % _{pred}	114 (102–126)	114 (109–137)	114 (95–125)	NS
RV, % _{pred}	88 (81–97)	89 (81–97)	85 (73–89)	0.03
RV < 80% _{pred} , <i>n</i>	8	0	8	0.011
RV/TLC, % _{pred}	83 (78–89)	108 (98–119)	82 (79–86)	NS
Raw _{tot} , kPa·s/L	0.22 (0.17–0.29)	0.23 (0.19–0.30)	0.2 (0.17–0.29)	NS
DLCO, % _{pred}	77 (68–89)	87 (76–95)	72 (67–83)	0.014
DLCO < 80% _{pred} , <i>n</i>	20	5	15	0.058
DLCO/VA, % _{pred}	90 (82–98)	96 (86–103)	87 (79–93)	NS
MIP, % _{pred}	108 (89–135)	114 (91–137)	102 (85–129)	NS
MIP decreased, <i>n</i>	5	1	4	NS
MEP, % _{pred}	87 (72–105)	86 (74–108)	87 (71–103)	NS
MEP decreased, <i>n</i>	11	4	7	NS

Note: data are presented as median (lower quartile — upper quartile); * — Mann-Whitney test applied to comparison of subgroups 1 and 2; NS — no significant differences found between subgroups 1 and 2.

In addition, given that muscle strength directly depends on protein metabolism, it is advisable to analyze the relationship of total blood protein with MIP and MEP values, and in case of their decrease, consider nutritional support for the patients.

Thus, RM strength test is an important addition to the traditional pulmonary function tests in terms of information concerning the functional state of the RM that can be used in the context of prevention of pathological conditions and adequate clinical treatment.

CONCLUSIONS

Patients that recovered from COVID-19 of varying severity exhibit decreased maximum static mouth pressure, specifically, expiratory pressure in 31% of cases and inspiratory pressure in 14% of cases. There were identified no significant dependencies between MIP/MEP values and the parameters of ventilation and pulmonary gas exchange. It is reasonable to add RM tests to the COVID-19 patient examination plan in order to detect their dysfunction and timely initiate a medical rehabilitation intervention.

References

- Savushkina OI, Cherniak AV, Kryukov EV, Kulagina ITs, Samsonova MV, Kalmanova EN et al. Pulmonary function after COVID-19 in early convalescence phase. Medical alphabet. 2020; (25): 7–12. DOI: 10.33667/2078-5631-2020-25-7-12. Russian.
- Zaitsev AA, Savushkina OI, Cherniak AV, Kulagina ITs, Kryukov EV. Clinical and functional characteristics of patients who recovered from the novel coronavirus infection (COVID-19). Practical pulmonology. 2020; 1: 78–81. Russian.
- Torres-Castro R, Vasconcello-Castillo L, Alsina-Restoy X, Solis-Navarro L, Burgos F, Puppo H, et al. Respiratory function in patients post-infection by COVID-19: a systematic review and meta-analysis. Pulmonology. 2021; 27 (4): 328–37. DOI: 10.1016/j.pulmoe.2020.10.013.
- Dei AA, Kozhanov AG, Geltser BI. Results of respiratory muscle strength study in young persons with community-acquired pneumonia. Bulletin Physiology and Pathology of Respiration. 2020; 77: 34–40. DOI: 10.36604/1998-5029-2020-77-34-40. Russian.
- Geltser BI, Dej AA, Titorenko IN, Kotelnikov VN. Comparative analysis of the strength of the respiratory muscles in community-acquired pneumonia with different severity of endogenous intoxication. Terapevticheskii arkhiv. 2020; 92 (3): 19–24. DOI: 10.26442/00403660.2020.03.000372. Russian.
- Kozhanov AG, Kopaev VA, Geltser BI. Assessment of the strength of the respiratory muscles in the early stages after thoracic interventions. Bulletin Physiology and Pathology of Respiration. 2020; Issue 75: 32–39. DOI: 10.36604/1998-5029-2020-75-32-39. Russian.
- Avdeev SN. Assessment of the strength of the respiratory muscles in the clinical practice. Pulmonology and allergology. 2008; 4: 12–17. Russian.

8. Segizbaeva MO, Aleksandrova NP. Assessment of the functional status of respiratory muscles: methodical aspects and interpretation of data. *Human Physiology*. 2019; 45 (2): 115–27. DOI: 10.1134/S0131164619010120. Russian.
9. Huang Y, Tan C, Wu J, Chen M, Wang Z, Luo L, et al. Impact of coronavirus disease 2019 on pulmonary function in early convalescence phase. *Respir Res*. 2020; 21 (1): 163. DOI: 10.1186/s12931-020-01429-6.
10. Guler SA, Ebner L, Beigelman C, Bridevaux P, Brutsche M, Clarenbach C, et al. Pulmonary function and radiological features four months after COVID-19: first results from the national prospective observational Swiss COVID-19 lung study. *Eur Respir J*. 2021; 57 (4): 2003690. DOI: 10.1183/13993003.03690-2020.
11. Chuchalin AG, Aysanov ZR, Chikina SYu, Chernyak AV, Kalmanova EN. Federal guidelines of Russian Respiratory Society on spirometry. *Pulmonology*. 2014; (6): 11–23. Russian.
12. Graham BL, Steenbruggen I, Miller MR, Barjaktarevic IZ, Cooper BG, Hall GL, et al. Standardization of spirometry 2019 update an official American thoracic society and European respiratory society technical statement. *Am J Respir Crit Care Med*. 2019; 200 (8): 70–88. DOI: 10.1164/rccm.201908-1590ST.
13. Wanger J, Clausen JL, Coates A, Pedersen OF, Brusasco V, Burgos F, et al. Standardisation of the measurement of lung volumes. *Eur Respir J*. 2005; 26 (3): 511–22. DOI: 10.1183/09031936.05.00035005.
14. Graham BL, Brusasco V, Burgos F, Cooper BG, Jensen R, Kendrick A, et al. 2017 ERS/ATS standards for single-breath carbon monoxide uptake in the lung. *Eur Respir J*. 2017; 49: 1600016. DOI: 10.1183/13993003.00016-2016.
15. Aysanov ZR, Kalmanova EN, Kameneva MYu, Kirukhina LD, Lukina OF, Naumenko JK, et al. Guideline of the Russian Respiratory Society for functional diagnostics of the respiratory system during the COVID-19 pandemic. Ver. 1.1. from 19.05.2020. Available from: https://spulmo.ru/upload/rekomendacii_rro_fvd_COVID_19_rev1_1_01062020.pdf. Russian.
16. Quanjer PH, Tammeling GJ, Cotes JE, Pedersen OF, Peslin R, Yernault JC. Lung volumes and forced ventilatory flows. Report Working Party Standardization of Lung Function Tests, European Community for Steel and Coal. Official Statement of the European Respiratory Society. *Eur Respir J*. 1993; 6 (Suppl.16): 5–40. PMID: 8499054.
17. Laveneziana P, Albuquerque A, Aliverti A, Babb T, Barreiro E, Dreset M, et al. ERS statement on respiratory muscle testing at rest and during exercise. *Eur Respir J*. 2019; 53: 1801214. DOI: 10.1183/13993003.01214-2018.
18. Evans JA, Whitelaw W. The assessment of maximal respiratory mouth pressures in adults. *Respir Care*. 2009; 54 (10): 1348–59.
19. Bubnova MG, Shlyakhto EV, Aronov DM, Belevsky AS, Gerasimenko MYu, Glezer MG et al. Coronavirus disease 2019: features of comprehensive cardiac and pulmonary rehabilitation. *Russian Journal of Cardiology*. 2021; 26 (5): 4487. DOI: 10.15829/1560-4071-2021-4487.

Литература

1. Савушкина О. И., Черняк А. В., Крюков Е. В., Кулагина И. Ц., Самсонова М. В., Калманова Е. Н. и др. Функциональные нарушения системы дыхания в период раннего выздоровления после COVID-19. *Медицинский алфавит*. 2020; 25: 7–12. DOI: 10.33667/2078-5631-2020-25-7-12.
2. Зайцев А. А., Савушкина О. И., Черняк А. В., Кулагина И. Ц., Крюков Е. В. Клинико-функциональная характеристика пациентов, перенесших новую коронавирусную инфекцию COVID-19. *Практическая пульмонология*. 2020; 1: 78–81.
3. Torres-Castro R, Vasconcello-Castillo L, Alsina-Restoy X, Solis-Navarro L, Burgos F, Puppo H, et al. Respiratory function in patients post-infection by COVID-19: a systematic review and meta-analysis. *Pulmonology*. 2021; 27 (4): 328–37. DOI: 10.1016/j.pulmoe.2020.10.013.
4. Дей А. А., Кожанов А. Г., Гельцер Б. И. Результаты исследования силы дыхательных мышц у лиц молодого возраста с внебольничной пневмонией. *Бюллетень физиологии и патологии дыхания*. 2020; 77: 34–40. DOI: 10.36604/1998-5029-2020-77-34-40.
5. Гельцер Б. И., Дей А. А., Титоренко И. Н., Котельников В. Н. Сравнительный анализ силы дыхательных мышц при внебольничной пневмонии с различной тяжестью эндогенной интоксикации. *Терапевтический архив*. 2020; 92 (3): 19–24. DOI: 10.26442/00403660.2020.03.000372.
6. Кожанов А. Г., Копаев В. А., Гельцер Б. И. Оценка силы дыхательных мышц в ранние сроки после торакальных вмешательств. *Бюллетень физиологии и патологии дыхания*. 2020; 75: 32–39. DOI: 10.36604/1998-5029-2020-75-32-39.
7. Авдеев С. Н. Оценка силы дыхательных мышц в клинической практике. *Пульмонология и аллергология*. 2008; 4: 12–17.
8. Сегизбаева М. О., Александрова Н. П. Оценка функционального состояния дыхательных мышц: методические аспекты и интерпретация данных. *Физиология человека*. 2019; 45 (2): 115–27. DOI: 10.1134/S0131164619010120.
9. Huang Y, Tan C, Wu J, Chen M, Wang Z, Luo L, et al. Impact of coronavirus disease 2019 on pulmonary function in early convalescence phase. *Respir Res*. 2020; 21 (1): 163. DOI: 10.1186/s12931-020-01429-6.
10. Guler SA, Ebner L, Beigelman C, Bridevaux P, Brutsche M, Clarenbach C, et al. Pulmonary function and radiological features four months after COVID-19: first results from the national prospective observational Swiss COVID-19 lung study. *Eur Respir J*. 2021; 57 (4): 2003690. DOI: 10.1183/13993003.03690-2020.
11. Чучалин А. Г., Айсанов З. Р., Чикина С. Ю., Черняк А. В., Калманова Е. Н. Федеральные клинические рекомендации Российского респираторного общества по использованию метода спирометрии. *Пульмонология*. 2014; 6: 11–23.
12. Graham BL, Steenbruggen I, Miller MR, Barjaktarevic IZ, Cooper BG, Hall GL, et al. Standardization of spirometry 2019 update an official American thoracic society and European respiratory society technical statement. *Am J Respir Crit Care Med*. 2019; 200 (8): 70–88. DOI: 10.1164/rccm.201908-1590ST.
13. Wanger J, Clausen JL, Coates A, Pedersen OF, Brusasco V, Burgos F, et al. Standardisation of the measurement of lung volumes. *Eur Respir J*. 2005; 26 (3): 511–22. DOI: 10.1183/09031936.05.00035005.
14. Graham BL, Brusasco V, Burgos F, Cooper BG, Jensen R, Kendrick A, et al. 2017 ERS/ATS standards for single-breath carbon monoxide uptake in the lung. *Eur Respir J*. 2017; 49: 1600016. DOI: 10.1183/13993003.00016-2016.
15. Айсанов З. Р., Калманова Е. Н., Каменева М. Ю., Кирюхина Л. Д., Луккина О. Ф., Науменко Ж. К. и др. Рекомендации Российского респираторного общества по проведению функциональных исследований системы дыхания в период пандемии COVID-19. Версия 1.1. от 19.05.2020. Доступно по ссылке: https://spulmo.ru/upload/rekomendacii_rro_fvd_COVID_19_rev1_1_01062020.pdf.
16. Quanjer PH, Tammeling GJ, Cotes JE, Pedersen OF, Peslin R, Yernault JC. Lung volumes and forced ventilatory flows. Report Working Party Standardization of Lung Function Tests, European Community for Steel and Coal. Official Statement of the European Respiratory Society. *Eur Respir J*. 1993; 6 (Suppl.16): 5–40. PMID: 8499054.
17. Laveneziana P, Albuquerque A, Aliverti A, Babb T, Barreiro E, Dreset M, et al. ERS statement on respiratory muscle testing at rest and during exercise. *Eur Respir J*. 2019; 53: 1801214. DOI: 10.1183/13993003.01214-2018.
18. Evans JA, Whitelaw W. The assessment of maximal respiratory mouth pressures in adults. *Respir Care*. 2009; 54 (10): 1348–59.
19. Бубнова М. Г., Шляхто Е. В., Аронов Д. М., Белевский А. С., Герасименко М. Ю., Глезер М. Г. и др. Новая коронавирусная инфекционная болезнь COVID-19: особенности комплексной кардиологической и респираторной реабилитации. *Российский кардиологический журнал*. 2021; 26 (5): 4487. DOI: 10.15829/1560-4071-2021-4487.

ENVIRONMENTAL IMPACT ASSESSMENT OF THE TERRITORIES IN THE VICINITY OF COMMISSIONING REGIONAL RADIOACTIVE WASTE MANAGEMENT FACILITY

Zozul YuN , Kiselev SM, Laschenova TN, Shlygin VV, Akhromeev SV, Gimadova TI, Malakhova AN, Shashkova OB, Oskina KYu

Burnasyan Federal Medical Biophysical Center, Moscow, Russia

The Regional center of conditioning and long-term storage of radioactive waste is being constructed in Primorsky Krai, where radioactive waste (RW) management concerns have been especially acute. The project involves intensification of activities related to RW management, as well as to building the new technology block for RW reprocessing, storage facility and boiler house. The study was aimed to perform environmental impact assessment of the territories in the vicinity of the Regional center of conditioning and long-term storage of radioactive waste prior to the facility commissioning. Radiation situation was assessed by radiometric and spectrometric methods; the levels of heavy metals were evaluated by atomic absorption spectrometry. Heavy metal (lead, nickel, copper, etc.) and arsenic levels exceeding or, in certain cases, similar to maximum permissible concentration (MPC) were found in soil and ground. Radiation situation is characterized by background levels of artificial radionuclides ^{137}Cs and ^{90}Sr in environmental media. Quality of water in wells and boreholes was largely compliant with the requirements established for groundwater used in decentralized water supply systems, with the exception of boreholes, in which the arsenic levels exceeding MPC were detected. The average annual public dose was 0.046 mSv excluding natural regional background radiation, which was below the dose limit. Carcinogenic health risks induced by radiation and chemical factors was 4×10^{-6} and 6×10^{-6} respectively. The obtained results form the basis for setting reference values of environmental contamination prior to the Regional center of conditioning and long-term storage of radioactive waste commissioning and can be used for regulatory supervision during the facility operation.

Keywords: nuclear legacy site, radiological monitoring, carcinogenic risk, artificial radionuclides, heavy metals, public health, radiation situation

Author contribution: Zozul YuN — preparation and analysis of research data; Kiselev SM, Laschenova TN — overall management, analysis of research data; Shlygin VV — assessment of radiological situation, data processing; Akhromeev SV — spectrometry, data acquisition; Gimadova TI — thermoluminescence dosimetry; Malakhova AN — data acquisition, working with TL-dosimeters; Shashkova OB — atomic absorption spectrometry; Oskina KYu — radiochemistry research.

Compliance with ethical standards: the study was carried out in full compliance with radiation safety measures and labour protection requirements. No research involving human subjects or animals was performed.

 **Correspondence should be addressed:** Yilia N. Zozul
Zhivopisnaya, 46, 123098, Moscow; julnik@list.ru

Received: 15.07.2021 **Accepted:** 11.08.2021 **Published online:** 27.08.2021

DOI: 10.47183/mes.2021.022

КОМПЛЕКСНАЯ ГИГИЕНИЧЕСКАЯ ОЦЕНКА ТЕРРИТОРИЙ В РАЙОНЕ РАЗМЕЩЕНИЯ СТРОЯЩЕГОСЯ РЕГИОНАЛЬНОГО ЦЕНТРА ПО ОБРАЩЕНИЮ С РАДИОАКТИВНЫМИ ОТХОДАМИ

Ю. Н. Зозуль , С. М. Киселев, Т. Н. Лашенцова, В. В. Шлыгин, С. В. Ахромеев, Т. И. Гимадова, А. Н. Малахова, О. Б. Шашкова, К. Ю. Оськина

Федеральный медицинский биофизический центр имени А. И. Бурназяна, Москва, Россия

В Приморском крае, где вопросы обращения с радиоактивными отходами (РАО) стоят весьма остро, ведется строительство Регионального центра кондиционирования и долговременного хранения радиоактивных отходов (РЦКДХ). Проект предполагает интенсификацию работ по обращению с РАО, а также строительство нового технологического корпуса по переработке РАО, пункта хранения и котельной. Целью исследования было дать комплексную гигиеническую оценку территорий в районе расположения РЦКДХ перед вводом его в эксплуатацию. Оценку радиационных параметров выполняли с использованием методов радиометрии и спектрометрии, содержания тяжелых металлов — методом атомно-абсорбционной спектрометрии. В почвах и грунтах выявлено присутствие тяжелых металлов (свинец, никель, медь и др.) и мышьяка в концентрациях, превышающих фоновые значения и в ряде случаев предельно допустимую концентрацию (ПДК). Радиационную обстановку характеризуют фоновые значения активности техногенных радионуклидов ^{137}Cs и ^{90}Sr в объектах окружающей среды. Качество воды колодцев и скважин в основном соответствует требованиям для подземных вод, используемых для децентрализованного водоснабжения, за исключением скважин, где присутствует мышьяк в концентрации выше ПДК. Среднегодовая интегральная доза облучения населения за вычетом естественного регионального фона составила 0,046 мЗв, что ниже предела дозы. Канцерогенный риск для здоровья населения от воздействия радиационного и химического фактора составил 4×10^{-6} и 6×10^{-6} соответственно. Полученные результаты являются основой для установления референсных значений состояния загрязнения окружающей среды перед вводом в эксплуатацию РЦКДХ и могут быть использованы в практике регулирующего надзора в процессе его эксплуатации.

Ключевые слова: объект ядерного наследия, радиационно-гигиенический мониторинг, канцерогенный риск, техногенные радионуклиды, тяжелые металлы, здоровье населения, радиационная обстановка

Вклад авторов: Ю. Н. Зозуль — анализ и подготовка материалов исследования; С. М. Киселев, Т. Н. Лашенцова — общее руководство, анализ материалов исследования; В. В. Шлыгин — проведение исследований радиационной обстановки, обработка данных; С. В. Ахромеев — проведение исследований методом спектрометрии, сбор информации; Т. И. Гимадова — проведение исследований методом интегральной ТЛ-дозиметрии; А. Н. Малахова — сбор информации, работа с ТЛ-дозиметрами; О. Б. Шашкова — проведение исследований методом атомно-абсорбционной спектрометрии; К. Ю. Оськина — проведение радиохимических исследований.

Соблюдение этических стандартов: все работы проведены с соблюдением мер радиационной безопасности и требований охраны труда.

 **Для корреспонденции:** Юлия Николаевна Зозуль
ул. Живописная, д. 46, 123098, г. Москва; julnik@list.ru

Статья получена: 15.07.2021 **Статья принята к печати:** 11.08.2021 **Опубликована онлайн:** 27.08.2021

DOI: 10.47183/mes.2021.022

A modern technological platform for radioactive waste management is being constructed in the Russian Federation. As part of the implementation of this platform, regional facilities for the accumulated and new radioactive waste collection, reprocessing and detoxification are being established. The Regional center of conditioning and long-term storage of radioactive waste is constructed in Primorsky Krai since 2016. It is located in the vicinity of the Sysoev Bay industrial site of the Fokino branch of the Far Eastern Center for Radioactive Waste Management (Sysoev Bay site). According to the project, the production structure under construction is designed for reprocessing and detoxification of radioactive waste (RW) accumulated on the Sysoev Bay site and produced during the facilities' use and decommission. Regional status of the facility also entails collection and reprocessing of radioactive materials produced by other plants of the Far East region, i.e. plants engaged in decommissioning of Russian nuclear-powered vessels. Federal Medical Biological Agency of the Russian Federation is responsible for state sanitary and epidemiological supervision on the territories where the RW management is carried out [1].

The studied radiation-hazardous facility is located on the southeastern tip of the Dunay peninsula. There is a private sector of the Dunay urban-type settlement (Staryi Dunay settlement) in the area of the Sysoev Bay site, inhabited by permanent residents. Private sector is located along the railway down to Konushkov Bay and the state route, which had been used for transportation of containers with spent nuclear fuel to the facility. The local population lives in wooden and stone-built one-storey houses and practices subsistence farming. Water supply is decentralized; water for drinking and household needs is taken from underground sources (wells and boreholes). The inhabitants' diet includes local milk and vegetables grown in the garden. The population of the Staryi Dunay settlement is a critical group living in the area of potential impact exerted by the facility.

The territory of Regional center of conditioning and long-term storage of radioactive waste lies within the health protection zone (HPZ) of the Sysoev Bay site in the vicinity of the production facility. The health physics situation on the territory of the newly built facility is conditioned by the production activities in the Sysoev Bay site. It has been working on managing RW, accumulated during military activities of the former coastal technical base for maintenance of nuclear submarines, for more than 20 years [2]. Currently, the stationary sources of artificial radionuclide emissions to atmosphere are the existing facilities of the Sysoev Bay site, liquid radioactive waste treatment facility, radiochemical laboratory and vehicle decontamination site (VD-8) [3]. According to Roshydromet, in 2017–2019 the content of artificial radionuclides in the atmospheric fall-out on the territory of Primorsky Krai reached the method detection limit. Maximum ambient air pollution (^{137}Cs — 0.9×10^{-7} Bq/m³; ^{90}Sr — 2.7×10^{-7} Bq/m³) was many orders of magnitude below the permissible average annual activity levels [4]. The average annual gamma dose rate in Primorsky Krai was 0.13 $\mu\text{Sv/h}$ [5]. After the Regional center of conditioning and long-term storage of radioactive waste once completed, there would be another source of chemical and radioactive emissions, namely the exhaust vent of the technology block responsible for RW reprocessing and conditioning. The composition of collected RW included radioactive waste produced during the nuclear submarine disposal and RW rehabilitation. The dominant radionuclides were ^{60}Co , ^{137}Cs , ^{90}Sr .

Given the current situation and the planned intensification of activities related to RW management in the region, assessment

of anthropogenic impact on the environment and population at the current stage of production activities in the Sysoev Bay site is an urgent task. The obtained data would be used as reference values for comparative environmental impact assessment in the further RW management production activities.

The study was aimed to perform environmental impact assessment of the territories in the vicinity of the Regional center of conditioning and long-term storage of radioactive waste in Primorsky Krai prior to the facility commissioning.

METHODS

Measurements, sampling, and sample analysis were performed following the conventional procedures approved by the certified Laboratory Centre at the Burnasyan Federal Medical Biophysical Center (Certificate No. RA.RU.21BY01).

Environmental radiation was assessed based on the gamma dose measurements with a Multirad-M detector (NTTs Amplituda; Russia) using the method of pedestrian gamma radiation survey.

Artificial radionuclide composition and specific activity were determined by gamma spectrometry with the use of gamma-ray spectrometer with germanium-based semiconductor detector (CANBERRA; USA) and radiometry with the use of UMF-200 radiometer (SPC "DOZA"; Russia), together with preliminary radiochemical separation.

Public dose assessment was performed for the situation of actual radiation exposure taking into account the regional background levels. Annual public dose was calculated as the sum of external radiation doses for the current year and the committed dose resulting from annual intake of radionuclides [4].

The average annual effective dose (hereinafter called AAED) of external exposure, both indoors and outdoors, was conservatively assessed based on the exposure of thermoluminescent dosimeter (TL-dosimeter) with lithium fluoride detector (DTG-4) in the tissue-equivalent cassette with a total thickness of 1 g/cm² [7].

Internal exposure doses due to oral intake of radionuclides with water and food were calculated based on the specific activity of artificial radionuclides [8].

Environmental heavy metal contamination was assessed by atomic absorption spectrometry using the Kvant 2 AT system (CORTEC; Russia). Of certain chemical elements, the paper reports data on heavy metal content for metals, which have been found in the samples in significant quantities.

Chemical contamination of soil was evaluated in accordance with the Guidelines [9] based on MPC (TPC) with the use of concentration factor (Kc) relative to regional background value and cumulative pollution index (Zc) [10].

Heavy metal contamination of drinking water was assessed based on MPC stipulated in statutory documents [10].

Health risk was evaluated under the conservative scenario for a hypothetical person exposed to existing maximum levels throughout his/her life. Individual carcinogenic risk was calculated based on the exposure pathways for artificial radionuclides and heavy metals found in soil, drinking water and local food.

Health risk caused by radiation exposure was calculated based on AAED using the linear risk coefficient for malignant neoplasms for the overall population (5.5×10^{-2}) [11]. The risk, taking into account the exposure pathways, was evaluated in accordance with the Guidelines based on specific content of artificial radionuclides in soil, drinking water and food [12].

The risk caused by exposure to heavy metals was assessed under the permanent residence scenario based on the data

on exposure and estimated carcinogenic potential values characteristic of additional individual carcinogenic risk or the risk of cancer depending on the carcinogen routes of intake [13].

Statistical processing of the results was performed using Microsoft Excel 2010 (Microsoft Corporation; USA). Median and its confidence limits (CL) with $P = 0.95$ were used as the central tendency indicators due to the measured values' inconsistency with normal or log-normal distribution [6]. According to the principle of conservatism, the values are reported taking into account the expanded uncertainty of measurements.

RESULTS

Environmental impact assessment of the territory in the area of Regional center of conditioning and long-term storage of radioactive waste construction

According to the results of assessment performed in the HPZ of the Sysoev Bay site in 2018–2020, the gamma dose rate in the area of the Regional center of conditioning and long-term storage of radioactive waste construction varies within the range of 0.03–0.23 $\mu\text{Sv/h}$, and the median is 0.09 $\mu\text{Sv/h}$, which is consistent with typical values registered in Primorsky Krai (0.09–0.18 $\mu\text{Sv/h}$), resulting from the regional background levels [5]. The dominant artificial radionuclides in the environment (soil, underground water) are ^{137}Cs and ^{90}Sr [14].

Specific activity of artificial radionuclides in soil is significantly below the requirements established for unlimited use of solid materials A_{UU} [15]: the median content of ^{137}Cs is 17 Bq/kg (maximum value is 63 Bq/kg), and the median content of ^{90}Sr is 3 Bq/kg (maximum value is 4 Bq/kg). Excessive heavy metal concentrations with excessive quantities exceeding MPC for arsenic, lead, zinc, nickel, copper, vanadium and manganese have been detected (Table 1). Maximum values of cumulative pollution index (Z_c) derived from regional backgrounds values do not exceed 16, which characterizes soil contamination level as "permissible".

Environmental impact assessment of the residential area located in the vicinity of Regional center of conditioning and long-term storage of radioactive waste (Staryi Dunay settlement)

Radiation situation on the territory of Staryi Dunay settlement characterized by gamma dose rate being within the range of

0.05–0.21 $\mu\text{Sv/h}$ (the median value is 0.10 $\mu\text{Sv/h}$) corresponds to background levels registered in Shkotovsky District (the median value 0.10 is $\mu\text{Sv/h}$; CI 0.07–0.13 $\mu\text{Sv/h}$) and typical values registered in Primorsky Krai (0.09–0.18 $\mu\text{Sv/h}$) [5]. The main dose-forming artificial radionuclides in the environment and food are ^{137}Cs and ^{90}Sr .

Concentrations of ^{137}Cs and ^{90}Sr in soil of Staryi Dunay settlement correspond mostly to the regional background levels typical for Shkotovsky District (the median specific activity value for ^{137}Cs is 6 Bq/kg, and for ^{90}Sr it is 2 Bq/kg). Exceeding regional background levels for ^{137}Cs specific activity (median specific activity value for ^{137}Cs is 46 Bq/kg) elevated to the levels established for unlimited use of solid materials ($A_{\text{UU}} = 100$ Bq/kg) are detected in soil samples taken from the roadsides. Based on artificial radionuclide specific activity (the median specific activity value for ^{137}Cs is 9 Bq/kg, and the value for ^{90}Sr is 2 Bq/kg), soils of home gardens meet the requirements established for unlimited use of solid materials [15].

Based on artificial radionuclide contents, drinking water from underground sources meets the requirements established for drinking water quality (Table 2) [4]. Specific activity of ^{137}Cs and ^{90}Sr in groundwater (wells, boreholes) is 3–4 orders of magnitude below the interventional level (IL).

Specific activity of artificial radionuclides in local food (milk, vegetables grown in the garden) is 2–4 orders of magnitude below the permissible level (PL) established for food (Table 2) [16].

Assessment of external exposure of the population to artificial radionuclides based on the radionuclide contents in drinking water and local food has shown that exposure due to consumption of drinking water, milk and potato provides a key contribution (see Table 2). External exposure AAED for the population due to artificial radionuclides is 0.008 mSv (0.0005 mSv due to ^{137}Cs , and 0.007 mSv due to ^{90}Sr).

Assessment of external exposure of the population by dosimetry measuring the cumulative dose is based on the data obtained with TL-dosimeters installed outdoors and in residential buildings in Staryi Dunay settlement throughout the year. According to obtained results, AAED of external exposure measured outdoors does not exceed 1.70 mSv with a median value of 1.03 mSv (Table 3), which corresponds to background levels resulting from natural background radiation. External exposure of the population in the houses exceeds the outdoor values by 20%. Based on the standard time spent

Table 1. Levels of heavy metals and arsenic in soils in the area of Regional center of conditioning and long-term storage of radioactive waste construction in 2017 and 2019

Element	Chemical hazard class	Levels of heavy metals, mg/kg		Assessment criteria, mg/kg		
		Median	Maximum	Regional background level*	MPC/TPC**	k_{max} ***
Pb	1	66 (38–180)	180	62	65	260
Cd	1	0,17 (0,17–0,18)	0,18	0,2	1	–
As	1	8 (8–9)	9	12	5	15
Zn	1	200 (100–350)	350	130	110	–
Ni	2	46 (27–100)	100	35	40	–
Cu	2	74 (22–230)	230	18	66	–
Cr	2	130 (110–170)	170	110	–	–
V	3	180 (130–310)	310	110	150	350
Mn	3	2200 (770–2700)	2700	1000	1500	15000
Ba	3	890 (570–1400)	1400	700	–	–
Sr	3	180 (150–500)	500	200	–	–
Zc		6 (5–8)	13	–	–	–

Note: * — results of original research; ** — hygienic standards are provided for total forms for clayey and loamy soil with $\text{pH} < 5.5$ [10]; *** — maximum permissible content of the element based on one of four hazard indicators.

Table 2. Internal exposure AAED in the population of Staryi Dunay settlement due to drinking water and local food intake

Item	Specific activity, Bq/L (kg)				Consumption, kg/year	Internal exposure AAED, mSv		
	¹³⁷ Cs		⁹⁰ Sr			Due to ¹³⁷ Cs	Due to ⁹⁰ Sr	Total
	Staryi Dunay settlement *	IL/ PL **	Staryi Dunay settlement *	IL/PL **				
Ground drinking water	$\frac{0,005 \div 0,040}{0,012}$	11	$0,002 \div 0,143$ 0,051	4,9	730	4×10^{-5}	9×10^{-4}	9×10^{-4}
Milk	$\frac{0,02 \div 0,62}{0,24}$	100	$0,03 \div 0,64$ 0,24	25	136,5	3×10^{-4}	1×10^{-3}	2×10^{-3}
Potato	$\frac{0,02 \div 0,38}{0,11}$	80	$0,01 \div 7,3$ 0,63	40	50,4	1×10^{-4}	4×10^{-3}	4×10^{-3}
Cucumbers	$\frac{0,01 \div 0,16}{0,06}$	60	$0,04 \div 0,19$ 0,12	25	5,6	8×10^{-6}	8×10^{-5}	1×10^{-4}
Beets, carrots	$\frac{0,01 \div 0,06}{0,04}$	60	$0,04 \div 0,28$ 0,12	25	10	9×10^{-6}	5×10^{-4}	5×10^{-4}

Note: * numerator — range of variation, * denominator — median; ** drinking water — interventional level (IL) [4]; ** food — permissible level (PL) [16].

by the population indoors (6,600 h) and outdoors (2,200 h), the median external exposure AAED value for the population, living close to the Regional center of conditioning and long-term storage of radioactive waste, is 1.18 mSv (the regional background level is 1.15 mSv).

The total AAED for the population of Staryi Dunay settlement is 0.046 mSv excluding regional background radiation, which is two orders of magnitude below the dose limits established by radiation safety standards [4]. External exposure, 0.030 mSv, makes a major contribution (over 65%). Internal exposure AAED is 0.008 mSv (0.007 mSv due to food, 0.0009 mSv due to drinking water).

Concentrations of metals and arsenic in soil and water on the territory of Staryi Dunay settlement are presented in Table 4.

Comparison of heavy metal contents in the soil of Staryi Dunay settlement with the regional background levels has revealed elevated levels of lead, copper, chromium, zinc and manganese. The highest MPC excess has been found for zinc, lead and copper. Elevated levels of zinc that exceed MPC have been also registered for regional background levels, which characterize specific regional features of the territory. According to assessment of soil contamination by heavy metals based on the cumulative pollution index (Zc), the majority of soil samples (78%) taken from the settlement are considered as having a "permissible" contamination level ($Zc < 16$). A total of 22% soil samples are considered as having a "moderately hazardous" contamination level ($16 < Zc < 32$) due to elevated copper, lead and zinc levels.

The results of groundwater contamination by heavy metals have shown that the quality of water in the wells and the majority of boreholes meets the requirements established for drinking water quality based on the concentrations of heavy metals and arsenic [10] (see Table 4).

The levels of elements from hazard classes 1 and 2 in drinking water do not exceed 0.1 MPC. MPC values exceeded for iron (hazard class 3) has been found in 40% of water samples

taken from the wells. The levels of arsenic (hazard class 1), reaching or exceeding MPC, have been found in 30–40 m deep boreholes being the sources of private drinking water supply.

DISCUSSION

Health physics situation in the area of the Regional center of conditioning and long-term storage of radioactive waste built at the base of Sysoev Bay temporary storage facility has a number of features. Based on artificial radionuclide specific activity, soils in the area of the Regional center of conditioning and long-term storage of radioactive waste construction meet the requirements established for unlimited use of solid materials in accordance with OSPORB-99/2010. Gamma dose rate corresponds to the regional background level typical for the natural background radiation. Hygienic situation is compounded by the hazard class 1 element (lead, arsenic) levels exceeding MPC. Radiation situation in the residential area located in the vicinity of the Regional center of conditioning and long-term storage of radioactive waste corresponds to the regional background levels. The same situation is observed in the areas of RW storage facilities of the former coastal technical bases of the Northern Fleet in North-Western Russia [17]. Groundwater contamination with radioactive and chemical contaminants is an essential parameter for monitoring.

Analysis of carcinogenic risk for population resulting from exposure to radiation and chemical factors has been performed based on the field and laboratory research data.

Calculation of radiation risk for the population of Staryi Dunay settlement based on exposure pathways for artificial radionuclides contained in soil, drinking water and food, has shown that external exposure due to artificial radionuclides contained in soil provides a key contribution (Table 5). The risk of malignant neoplasms caused by radiation from artificial sources for the overall population, assessed based on the total AAED values [11], is 3×10^{-6} , which is considered the acceptable level.

Table 3. Average annual external exposure AAED in the population of Staryi Dunay settlement

Territory	Number of measurements	External exposure AAED, mSv		
		Minimum	Maximum	Median (CL)
Regional background level:				
– outdoors	19	0,46	1,5	1,00 (0,50–1,48)
– inside houses	7	0,49	2,07	1,20 (0,57–1,25)
Staryi Dunay settlement:				
– outdoors	37	0,49	1,7	1,03 (0,55–1,51)
– inside houses	18	0,6	2,13	1,23 (0,67–1,70)

Table 4. Concentrations of heavy metals and arsenic in soil and underground water in the vicinity of Regional center of conditioning and long-term storage of radioactive waste

Element	Chemical hazard class	Levels of heavy metals, mg/kg (L)			Assessment criteria, mg/kg (L)		K _c
		Minimum	Maximum	Median	Regional background level	MPC/TPC	
Soil							
Pb	1	41	250	110 (67–180)*	62	65	2
Cd	1	< 0,12	0,51	0,23 (0,12–0,51)*	0,2	1	1
As	1	< 1	3	2 (1–3)*	12	5	< 1
Zn	1	100	820	215 (140–460)*	130	110	2
Ni	2	22	47	42 (34–45)*	35	40	1
Cu	2	19	260	67 (41–130)*	18	66	4
Cr	2	55	300	155 (130–160)*	110	–	1
V	3	83	180	125 (120–130)*	110	150	1
Mn	3	670	2000	1300 (1200–1400)*	1000	1500	1
Ba	3	510	1200	635 (560–720)*	700	–	1
Sr	3	130	310	160 (140–220)*	200	–	1
Zc		2	21	6 (3–9)*	–	–	–
Groundwater (boreholes, wells)							
As	1	< 0,005	0,025	< 0,005 / 0,010** < 0,005	< 0,005	0,01	–
Ba	2	0,01	0,04	0,02 / 0,01** 0,02	0,03	0,7	–
Cd	2	< 0,0001	0,0005	0,0001 / < 0,0001** 0,0001"	< 0,0001	0,001	–
Cr	2	0,001	0,005	0,002 / 0,003** 0,002	0,001	0,05	–
Pb	2	< 0,001	0,008	0,001 / 0,007** 0,001	< 0,001	0,1	–
Sr	2	0,1	0,4	0,19 / < 0,10** 0,12	0,36	7	–
Al	3	0,05	0,33	0,05 / 0,05** 0,06	0,12	0,2	–
Cu	3	< 0,01	0,11	0,01 / 0,02** 0,04	< 0,01	1	–
Fe	3	0,01	1,36	0,02 / 0,06** 0,10	0,36	0,3	–
Mn	3	0,01	0,64	0,02 / 0,01** 0,02	0,33	0,1	–
Zn	3	0,01	1,5	0,05 / 0,01** 0,01	0,01	1	–

Note: * — median and its confidence limits; ** numerator — median concentration in boreholes (70 m/30–40 m deep); ** denominator — median concentration in wells.

Carcinogenic risk of exposure to chemicals due to heavy metal contamination of soil is considered acceptable (1×10^{-6}) (Table 6). The risk of using drinking water taken from wells and boreholes of 5×10^{-6} meets the requirements established for acceptable risk to the population. The exception is drinking water from the 30–40 m deep boreholes, since the risk reaches 5×10^{-4} due to presence of arsenic, which is unacceptable to the overall population [13] and therefore requires further investigation. As mentioned above, the water sources for drinking and household water supply available in Staryi Dunay settlement are quite far from the Sysoev Bay temporary storage facility and are not exposed to the anthropogenic impact of the industrial site emissions and discharges. The presence of arsenic levels exceeding MPC in the water obtained from 30–40 m deep boreholes may be due to physical features of the water-bearing horizon in the studied area.

The study has shown that health risk caused by exposure to radiation for the population of Staryi Dunay settlement living in the vicinity of the Regional center of conditioning and long-

term storage of radioactive waste is 4×10^{-6} . It does not exceed the risk caused by exposure to chemicals, which is 6×10^{-6} (taking into account arsenic contained in water, the risk reaches 5×10^{-4}).

CONCLUSIONS

The paper presents the results of the complex environmental impact assessment of the Regional center of conditioning and long-term storage of radioactive waste, performed prior to the Facility commissioning. It has been shown that radiation situation on the construction site and in adjacent residential area is characterized by background γ -dose rate and background concentrations of artificial radionuclides ^{137}Cs and ^{90}Sr in environmental media. At the same time, contamination with heavy metals and arsenic have been found in the ground of the production complex construction site and in the soil of home gardens located in the residential area. Qualitative composition of chemical contamination in the area of the Regional center

Table 5. Individual radiation risk for the population of Staryi Dunay settlement

Parameter	Specific activity, Bq/kg (L)	Individual radiation risk		
		Exposure		Total
		internal	external	
Soil		3×10^{-8}	3×10^{-6}	3×10^{-6}
^{137}Cs	89	3×10^{-10}	2×10^{-6}	2×10^{-6}
^{90}Sr	160	3×10^{-8}	2×10^{-6}	2×10^{-6}
Water		4×10^{-7}	–	4×10^{-7}
^{137}Cs	0,04	2×10^{-8}	–	2×10^{-8}
^{90}Sr	0,14	4×10^{-7}	–	4×10^{-7}
Food		8×10^{-7}	–	8×10^{-7}
^{137}Cs		7×10^{-8}	–	7×10^{-8}
^{90}Sr		7×10^{-7}	–	7×10^{-7}
Total risk		1×10^{-6}	3×10^{-6}	4×10^{-6}

Table 6. Individual carcinogenic risk caused by chemical pollution for the population of Staryi Dunay settlement

Parameter	Concentration, mg/kg (L)	Individual carcinogenic risk			Total
		Intake			
		Ingestion	Inhalation	Dermal	
Soil		4×10^{-8}	9×10^{-7}	3×10^{-8}	1×10^{-6}
Cr	300	–	9×10^{-7}	–	9×10^{-7}
Pb	250	4×10^{-8}	8×10^{-10}	3×10^{-8}	7×10^{-8}
Ni	47	–	2×10^{-9}	–	3×10^{-9}
Drinking water*		4×10^{-6}	–	8×10^{-7}	5×10^{-6}
As	0,025	5×10^{-4}	–	1×10^{-5}	5×10^{-4}
Cd	0,00052	2×10^{-6}	–	6×10^{-7}	3×10^{-6}
Pb	0,02	2×10^{-6}	–	2×10^{-7}	2×10^{-6}
Total carcinogenic risk* (water + soil)		4×10^{-6}	9×10^{-7}	8×10^{-7}	6×10^{-6}

Note: * — calculated without taking into account the 30–40 m deep boreholes.

of conditioning and long-term storage of radioactive waste construction is characterized by high levels of arsenic, lead, zinc, nickel, copper, vanadium and manganese, and in the residential area it is characterized by high levels of zinc, lead and copper. In general, based on the results of soil contamination with heavy metals in the examined territories, soil has a “permissible” chemical contamination level. The excess of MPC has been found in a number of samples. The quality of drinking water in the residential area meets the requirements established for groundwater used in decentralized water supply systems, except for local boreholes, in which the arsenic levels exceeding MPC have been detected. The presence of arsenic in studied groundwater and soil may be due to specific regional features related to high levels of the element in environmental media. This fact requires clarification and further investigation. Comparative evaluation of carcinogenic risks caused by radiation exposure

and chemical pollutants demonstrates comparable results: the approximate risk does not exceed 10^{-6} and therefore is considered negligible. The study results make it clear that hygienic situation determined by past and ongoing production activities in the facility (before commissioning of the Regional center of conditioning and long-term storage of radioactive waste does not pose any additional health risks caused by the impact of artificial radionuclides and heavy metals on the environment and the population living in the area of the Facility.

The results of complex environmental impact assessment, obtained prior to the Regional center of conditioning and long-term storage of radioactive waste commissioning, provide the basis for setting reference values of artificial radionuclide and heavy metal levels in environmental media and can be used for regulatory supervision aimed to ensure public safety during the facility operation.

References

1. Udalova AA, Geraskin SA, Aleksahin RM, Kiselev SM, Sovremennye podhody k ocenke radiacionnogo vozdejstviya na okruzhajushhuyu sredu. Medicinskaja radiologija i radiacionnaja bezopasnost'. 2013; 58 (4): 23–33. Russian.
2. Shandala NK, Kiselev SM, Titov AV, Serjogin VA, Isaev DV, Ahromeev SV, i dr. Regulirujushhij nadzor i oценка radiacionnoj obstanovki v rajonah razmeshhenija byvshih voennyh tehnikeskikh baz. Gigiena i sanitarija. 2013; 92 (3): 15–19. Russian.
3. Otchet po jekologicheskoj bezopasnosti Dal'nevostochnogo centra po obrashheniju s radioaktivnymi othodami — filiala federal'nogo gosudarstvennogo unitarnogo predpriyatija «Predpriyatije po obrashheniju s radioaktivnymi othodami «RosRAO» (DVC «Dal'RAO» — filiala FGUP «RosRAO»). 2019 g. Dostupno po ssylke: <https://www.rosatom.ru/upload/iblock/109/109b27982c8cfd90a72224db545c17be.pdf>. Russian.
4. Normy radiacionnoj bezopasnosti (NRB-99/2009) ot 02.07.2009.

- SanPiN 2.6.1.2523-09. Dostupno po sсылке: https://www.np-ciz.ru/userfiles/2_6_1_2523-09.pdf. Russian.
- Radiacionnaja obstanovka na territorii Rossii i sopredel'nyh gosudarstv v 2019 g. Ezhegodnik. Ministerstvo prirodnyh resursov i jekologii Rossijskoj Federacii. Obninsk, 2020; 343 s. Dostupno po sсылке: https://www.rpatyphoon.ru/upload/medialibrary/187/ezhegodnik_ro_2019.pdf. Russian.
 - Statisticheskie metody. Statisticheskoe predstavlenie dannyh. Mediana. Opredelenie tochechnoj ocenki i doveritel'nyh intervalov. GOST R ISO 16269-7-2004. Dostupno po sсылке: <https://docs.cntd.ru/document/1200035332>. Russian.
 - Ionizirujushhee izluchenie, radiacionnaja bezopasnost'. Provedenie kompleksnogo jekspedicionnogo radiacionno-gigienicheskogo obsledovanija naselennogo punkta dlja ocenki doz oblucheniya naselenija. Metodicheskie rekomendacii. MR 2.6.1.0006-10. Dostupno po sсылке: <https://docs.cntd.ru/document/1200085909>. Russian.
 - Ionizirujushhee izluchenie, radiacionnaja bezopasnost'. Kontrol' doz oblucheniya naselenija, prozhivajushhego v zone nabljudeniya radiacionnogo ob'ekta, v uslovijah ego normal'noj jekspluatacii i radiacionnoj avarii. Metodicheskie rekomendacii. MR 2.6.1.0063-12. Dostupno po sсылке: <https://docs.cntd.ru/document/1200095229>. Russian.
 - Pochva, ochistka naselennyh mest, bytovye i promyshlennye othody, sanitarnaja ohrana pochvy. Gigienicheskaja ocenka kachestva pochvy naselennyh mest. Metodicheskie ukazaniya. MU 2.1.7.730-99. Dostupno po sсылке: <https://docs.cntd.ru/document/1200003852>. Russian.
 - Gigienicheskie normativy i trebovanija k obespecheniju bezopasnosti i (ili) bezvrednosti dlja cheloveka faktorov sredy obitanija. SanPiN 1.2.3685-21. Dostupno po sсылке: <https://docs.cntd.ru/document/573500115>. Russian.
 - Ocenka radiacionnogo riska u naselenija za schet dlitel'nogo ravnomernogo tehnogenного oblucheniya v malyh dozah. Metodicheskie ukazaniya. MU 2.1.10.3014-12. Dostupno po sсылке: <https://docs.cntd.ru/document/1200095241>. Russian.
 - Metodika ocenki radiacionnyh riskov na osnove dannyh monitoringa radiacionnoj obstanovki. Rekomendacii. R 52.18.787-2013. Obninsk: FGBU «VNIIGMI-MCD», 2014; 116 s. Dostupno po sсылке: <https://files.stroyinf.ru/Data2/1/4293754/4293754569.pdf>. Russian.
 - Rukovodstvo po ocenke riska dlja zdorov'ja naselenija pri vozdeystvii himicheskikh veshhestv, zagryaznjajushhh okruzhajushhuju sredu. Rekomendacii. R 2.1.10.1920-04. Dostupno po sсылке: <https://docs.cntd.ru/document/1200037399>. Russian.
 - Akhromeev SV, Kiselev SM, Titov AV, Seregin VA, Shlygin VV, Starinskaja RA. Issledovanie radiacionnoj obstanovki na ob'ektah jadernogo nasledija v Dal'nevostochnom regione Rossii. ANRI. 2016; 1 (84): 65–71. Russian.
 - Osnovnye sanitarnye pravila obespechenija radiacionnoj bezopasnosti (OSPORB-99/2010). SP 2.6.1.2612-10. Dostupno po sсылке: https://orfi.ru/files/doc/uchcenter/osporb_2612612-10.pdf.
 - Gigienicheskie trebovanija k bezopasnosti i pishhevoj cennosti pishhevych produktov. SanPiN 2.3.21078-01. Dostupno po sсылке: <https://docs.cntd.ru/document/901806306>. Russian.
 - Shandala NK, Sneve MK, Titov AV, Smith GM, Novikova NYa, Romanov VV, et al. Radiological criteria for the remediation of sites for spent fuel and radioactive waste storage in the Russian Northwest. Journal of Radiological Protection. 2008; 28: 479–97.

Литература

- Удалова А. А., Гераськин С. А., Алексахин Р. М., Киселев С. М., Современные подходы к оценке радиационного воздействия на окружающую среду. Медицинская радиология и радиационная безопасность. 2013; 58 (4): 23–33.
- Шандала Н. К., Киселёв С. М., Титов А. В., Серёгин В. А., Исаев Д. В., Ахромеев С. В. и др. Регулирующий надзор и оценка радиационной обстановки в районах размещения бывших военных технических баз. Гигиена и санитария. 2013; 92 (3): 15–19.
- Отчет по экологической безопасности Дальневосточного центра по обращению с радиоактивными отходами — филиала федерального государственного унитарного предприятия «Предприятие по обращению с радиоактивными отходами «РосРАО» (ДВЦ «ДальРАО» — филиала ФГУП «РосРАО»). 2019 г. Dostupno po sсылке: <https://www.rosatom.ru/upload/iblock/109/109b27982c8cfd90a72224db545c17be.pdf>.
- Нормы радиационной безопасности (НРБ-99/2009) от 02.07.2009. СанПиН 2.6.1.2523-09. Dostupno po sсылке: https://www.np-ciz.ru/userfiles/2_6_1_2523-09.pdf.
- Радиационная обстановка на территории России и сопредельных государств в 2019 г. Ежегодник. Министерство природных ресурсов и экологии Российской Федерации. Обнинск, 2020; 343 с. Dostupno po sсылке: https://www.rpatyphoon.ru/upload/medialibrary/187/ezhegodnik_ro_2019.pdf.
- Статистические методы. Статистическое представление данных. Медиана. Определение точечной оценки и доверительных интервалов. ГОСТ Р ИСО 16269-7-2004. Dostupno po sсылке: <https://docs.cntd.ru/document/1200035332>.
- Ионизирующее излучение, радиационная безопасность. Проведение комплексного экспедиционного радиационно-гигиенического обследования населенного пункта для оценки доз облучения населения. Методические рекомендации. МР 2.6.1.0006-10. Dostupno po sсылке: <https://docs.cntd.ru/document/1200085909>.
- Ионизирующее излучение, радиационная безопасность. Контроль доз облучения населения, проживающего в зоне наблюдения радиационного объекта, в условиях его нормальной эксплуатации и радиационной аварии. Методические рекомендации. МР 2.6.1.0063-12. Dostupno po sсылке: <https://docs.cntd.ru/document/1200095229>.
- Почва, очистка населенных мест, бытовые и промышленные отходы, санитарная охрана почвы. Гигиеническая оценка качества почвы населенных мест. Методические указания. МУ 2.1.7.730-99. Dostupno po sсылке: <https://docs.cntd.ru/document/1200003852>.
- Гигиенические нормативы и требования к обеспечению безопасности и (или) безвредности для человека факторов среды обитания. СанПиН 1.2.3685-21. Dostupno po sсылке: <https://docs.cntd.ru/document/573500115>.
- Оценка радиационного риска у населения за счет длительного равномерного техногенного облучения в малых дозах. Методические указания. МУ 2.1.10.3014-12. Dostupno po sсылке: <https://docs.cntd.ru/document/1200095241>.
- Методика оценки радиационных рисков на основе данных мониторинга радиационной обстановки. Рекомендации. Р 52.18.787-2013. Обнинск: ФГБУ «ВНИИГМИ-МЦД», 2014; 116 с. Dostupno po sсылке: <https://files.stroyinf.ru/Data2/1/4293754/4293754569.pdf>.
- Руководство по оценке риска для здоровья населения при воздействии химических веществ, загрязняющих окружающую среду. Рекомендации. Р 2.1.10.1920-04. Dostupno po sсылке: <https://docs.cntd.ru/document/1200037399>.
- Ахромеев С. В., Киселев С. М., Титов А. В., Серегин В. А., Шлыгин В. В., Старинская Р. А. Исследование радиационной обстановки на объектах ядерного наследия в Дальневосточном регионе России. АНРИ. 2016; 1 (84): 65–71.
- Основные санитарные правила обеспечения радиационной безопасности (ОСПОРБ-99/2010). СП 2.6.1.2612-10. Dostupno po sсылке: https://orfi.ru/files/doc/uchcenter/osporb_2612612-10.pdf.
- Гигиенические требования к безопасности и пищевой ценности пищевых продуктов. СанПиН 2.3.21078-01. Dostupno po sсылке: <https://docs.cntd.ru/document/901806306>.
- Shandala NK, Sneve MK, Titov AV, Smith GM, Novikova NYa, Romanov VV, et al. Radiological criteria for the remediation of sites for spent fuel and radioactive waste storage in the Russian Northwest. Journal of Radiological Protection. 2008; 28: 479–97.

CURRENT TRENDS IN ANTICANCER DRUG PROTOTYPE *IN VITRO* PHARMACOLOGY: BIBLIOMETRIC ANALYSIS 2019–2021

Ershov PV , Makarova AS

Centre for Strategic Planning and Management of Biomedical Health Risks of the Federal Medical Biological Agency, Moscow, Russia

Identification of novel low molecular weight compounds with antitumor activity is the first important step towards the development of candidate drugs and a popular trend in *in vitro* pharmacology. The aim of the study was to assess the key trends and rank the scientific priorities in anticancer drug design using bibliometric analysis. The protocol involved using the panel of bibliographic databases (PubMed, Scopus, Cortellis) and analytical web-based tools PubChem, FACTA+, ClustVis, Reaxys, PathwayStudio and VOSviewer software to review a sample of 1657 papers issued 2020–2021. The work was also focused on 70 new promising basic structures and derivatives targeted at inhibiting both individual pro-tumor proteins and signaling cascades. It was found that serine-threonine protein kinases, receptor tyrosine kinases, DNA topoisomerases and tubulins as well as signaling pathways PI3K, mTOR, AKT1, STAT3, HIF-1 α , and p53 account for up to 60% of the total structure of cellular targets for the design of anticancer drugs. The increasing scientific interest in innovative inhibitors of tumor-associated protein complexes, transcription factors and metabolic enzymes has been found. The compounds, which belong to heterocycles, glycosides, quinones and terpenes, were mentioned in 71% of papers as the basic structures for antitumor derivatives design. Papers, published in 2019, in which the compounds, such as lapachone, luteolin, quercetin, monastrol, and crizosplenol D are studied in the context of the design of new drug prototypes, have the highest citation rate. The systematic bibliometric approach involving the use of a panel of analytical resources makes it possible to assess R&D trends and scientific priorities in anticancer drug design, thus organically complementing the classic reviews in periodicals.

Keywords: cancer, drugs, pharmacology, bibliometric analysis, publication activity, protein target

Author contribution: Ershov PV — literature search, manuscript writing and formatting, conceptualization of the paper; Makarova AS — literature search, manuscript editing.

 **Correspondence should be addressed:** Pavel V. Ershov
Pogodinskaya, 10, korp 1, Moscow, 119121; pavel79@inbox.ru

Received: 21.07.2021 **Accepted:** 18.08.2021 **Published online:** 27.09.2021

DOI: 10.47183/mes.2021.033

СОВРЕМЕННЫЕ ТЕНДЕНЦИИ *IN VITRO* ФАРМАКОЛОГИИ ПРОТОТИПОВ ПРОТИВООПУХОЛЕВЫХ ЛЕКАРСТВ: БИБЛИОМЕТРИЧЕСКИЙ АНАЛИЗ ЗА 2020–2021 ГГ.

П. В. Ершов , А. С. Макарова

Центр стратегического планирования и управления медико-биологическими рисками Федерального медико-биологического агентства, Москва, Россия

Выявление новых низкомолекулярных соединений, обладающих противоопухолевой активностью, является первым важным шагом на пути создания кандидатных лекарств и популярным направлением в *in vitro* фармакологии. Целью исследования было оценить ключевые тенденции и ранжировать научные приоритеты в области дизайна противоопухолевых лекарств с применением библиометрического анализа. Протокол предполагал использование панели библиографических баз данных (PubMed, Scopus, Cortellis) и аналитических ресурсов PubChem, FACTA+, ClustVis, Reaxys, PathwayStudio и VOSviewer для исследования выборки из 1657 публикаций за 2020–2021 гг. В работе также систематизирован материал по 70 новым перспективным производным на основе базовых химических структур, нацеленных на ингибирование отдельных про-опухолевых белковых молекул и сигнальных каскадов. Установлено, что серин-треониновые протеинкиназы, рецепторные тирозинкиназы, ДНК-топоизомеразы и тубулины, а также сигнальные пути PI3K, mTOR, AKT1, STAT3, HIF-1 α и p53 составляют до 60% в общей структуре клеточных мишеней для дизайна противоопухолевых лекарств. Отмечен рост научного интереса к инновационным ингибиторам опухоль-ассоциированных белковых комплексов, факторов транскрипции и метаболических ферментов. Соединения из класса гетероциклов, гликозидов, хинонов и терпенов в 71% работ служат базовыми структурами для дизайна противоопухолевых производных. Лидирующие позиции по цитированию занимают вышедшие в 2019 г. публикации, в которых рассмотрены такие соединения, как лапахон, лутеолин, кверцетин, монастрол и кризоспленол D, в контексте дизайна новых прототипов лекарств. Системный библиометрический подход с использованием панели аналитических ресурсов позволяет оценить тенденции в области разработки и дизайна противоопухолевых лекарств и выявить приоритеты научного интереса, органично дополняя классические обзорные работы в периодических изданиях.

Ключевые слова: рак, лекарства, фармакология, библиометрический анализ, публикационная активность, белковые мишени

Вклад авторов: П. В. Ершов — поиск литературы, написание и оформление текста статьи, концептуализация статьи; А. С. Макарова — поиск литературы, редактирование статьи.

 **Для корреспонденции:** Павел Викторович Ершов
ул. Погодинская, д. 10, стр. 1, г. Москва, 119121; pavel79@inbox.ru

Статья получена: 21.07.2021 **Статья принята к печати:** 18.08.2021 **Опубликована онлайн:** 27.09.2021

DOI: 10.47183/mes.2021.033

Progress in the therapy of socially significant diseases, including malignant neoplasms (MN), is organically linked to success in research and development (R&D) of the new drug prototypes, the pharmacologically active molecules, having the greatest antitumor effect and maximum conformity of physical and chemical parameters to canonical drug-like structures [1]. One of the evidence-based approaches to the drug discovery consists in design of molecules, which possess the desired properties and affect the cancer-related proteins [2–4]. Defining the mechanism of action of anticancer drug prototypes and the whole range of on-target and off-target proteins is essential

for design of the highly selective drugs with minimal side effects. The development of the improved anticancer drugs follows from the properties of the tumor itself: intertumor and intratumor heterogeneity, and the diversity of mechanisms for resistance [5]. On the other hand, many pharmacotherapeutic approaches require improving the benefit–harm balance, since many existing anticancer drugs can cause severe side effects [6].

The number of annual publications dedicated to identification of the novel peptide and non-peptide molecules with anticancer activity, repositioning effects and prescriptions, is about 2700–3400 (over the five-year period, according to

PubMed (accession on May 20, 2021). It should be noted that the review papers are focused mostly on systematizing the data on the anticancer drug prototypes, either belonging to a certain chemical taxon, or a spectrum of synthesized derivatives with the same chemical scaffold. Papers are also focused on discussing the range of biologically active substances with respect to the only molecular target. Nevertheless, reviews are a major source of scientific analysis in describing the current trends in drug discovery. Thus, the works [7, 8] cover the actual cancer-associated molecular targets, assessment of biological effects and concepts of the drug design, which in recent years has been intrinsically linked to computer-aided modeling (QSAR and others) [9]. At the same time, the search for current trends in drug prototypes, together with the interpretation of medical and biological effects of various anticancer compounds, results in the need for prompt data analysis from the multiple literature and biomedical sources. When performing without the use of customized algorithms and automated methods of data extraction (known as text mining), such an analysis can be very time-consuming. However, the application of the bibliometric analysis with adapted algorithms for creating an up-to-date "analytical portrait", which includes a more diversified repertoire of research data on drug prototypes and their molecular targets, has proved to be effective in defining the current trends in molecular oncology and pharmacology [10–13]. The aim of the study was to assess the key trends and rank the scientific priorities in anticancer drug design using bibliometric analysis.

METHODS

PubMed (<https://pubmed.ncbi.nlm.nih.gov/>) was used to search for journal papers (issued from May 20, 2020 to May 19, 2021) by keywords "antitumor and anticancer activity". Inclusion criteria was "original research" reporting the new data on identification of anticancer drug prototypes and the best relevancy of search. Exclusion criteria was paper types "Books and Documents", "Clinical Trial", "Meta-Analysis", "Randomized Controlled Trial", "Review" and "Systematic Review". A total of 1902 papers were found, from which 240 reviews and five clinical trials were subsequently excluded. 402 papers were selected from the remaining 1657 experimental papers, based on the abstracts analysis, and included in the target sample.

VOSviewer software [14] was used for keyword co-occurrence analysis in the papers from the target sample, as well as for keyword frequency analysis of MeSH terms and authors' terms in the papers' abstracts.

Names of low molecular weight non-peptide compounds were extracted from papers' abstracts and keyword listings. Their MeSH classification groups (Classification/Ontologie/MeSH-Tree) were defined using PubChem database (<https://pubchem.ncbi.nlm.nih.gov/>).

Analysis of research trends and publication activity over the five-year period (2016–2020) was performed using the Scopus database (<https://www.scopus.com/>) (Elsevier; Netherlands). The key "compound name and tumor" (for example, "magnolol and tumor") was used as a search query. The scientific interest to papers, issued in 2019, was assessed by the total number of citations for papers issued before May 19, 2021, being corrected for self-citation of all co-authors of the paper. Another parameter was the average number of citations per paper, issued in 2019.

Associations between protein targets, their cancer significance and drug prototypes were analyzed using the Pathway Studio and Reaxys (Elsevier; Netherlands). These

resources enable extracting the links between different molecular entities from biomedical data containing in twenty million abstracts and several million full-text papers with the help of Medscan software. They adapted for comprehensive search and prediction of drug targets as well as constructing of signaling pathways from the internal curated database. Associations found between molecular targets and key biological processes as "malignant transformation" and "cancer progression" was used to create the interaction map.

Web-based tool FACTA+ v.0.9 (accession on June 29, 2019) (<http://www.nactem.ac.uk/facta/>) was used to find biomedical associations in the full-text papers of the MEDLINE database.

Cortellis database (<https://www.cortellis.com/intelligence>) (Clarivate Analytics; UK) was used for patent search.

Principal component analysis (PCA) using k-means clustering and creating a heat map were performed using the ClustVis web-base tool [15]. The singular values decomposition method with imputation was used for PCA. It allows to generate and visualize the numeric data set geometric structure while imputing the missing values (imputation). Data preprocessing options included the following options: data transformation – "no transformation"; row scaling – "no scaling". The heat map options were as follows: cluster distance for rows and columns – Pearson correlation or "correlation", clustering method for rows and columns – "average".

RESULTS

Analysis of abstracts from the target sample (402 papers) made it possible to define distribution of the occurrence frequency for keywords, which were related to identification of anticancer drug prototype and were mentioned in the text massive more than 10 times (Fig. 1). Fig. 1 allows one to see the focus in studying the pharmacological targeting of signaling pathways involving RAC- α serine/threonine-protein kinase (AKT1), signal transducer and activator of transcription (STAT)-3, hypoxia-inducible factor 1- α (HIF-1 α), and p53-dependent pathways. Cancer-associated protein targets can be also distinguished: protein kinases (PKC and AMPK), tubulin, matrix metalloproteinases (MMP), poly (ADP-ribose) polymerase 1 (PARP1), epidermal growth factor receptor (EGFR), vascular endothelial growth factor (VEGFR). Furthermore, targeting of caspases, aimed at activation of apoptotic programs in tumor cells, provides another important field of research.

Visual representation of keyword co-occurrence, mentioned in more than three papers, is provided in Fig. 2. The figure presents five clusters with semantic links between the keywords. Thus, the pronounced co-occurrence was observed in the following keywords pairs: histone deacetylase–quinolines, topoisomerase inhibitors–indoles (or pyrazoles, or pyrimidines), tubulin modulators–chalcones (or naphthalenes). Thus, the analysis of papers abstracts and keyword co-occurrence (Fig. 1 and 2) made it possible to identify the studies focused on the design of chalcone and licochalcone (flavonoids with opened pyran ring), naphthalene, saponin, indole, quinolone, sesquiterpene, pyrazole, pyridine (pyrimidine), steroid, curcumin and britanin derivatives exhibiting anticancer activity. It is interesting to note that a sufficient number of papers were focused in the design optimization of tubulin polymerization inhibitors [16]. According to 10-year PubMed statistics, the number of new studies in this field remained stable, with a slight decline, observed in 2019–2020, which could demonstrate the decrease in scientific interest. Fig. 1 and 2 also show that

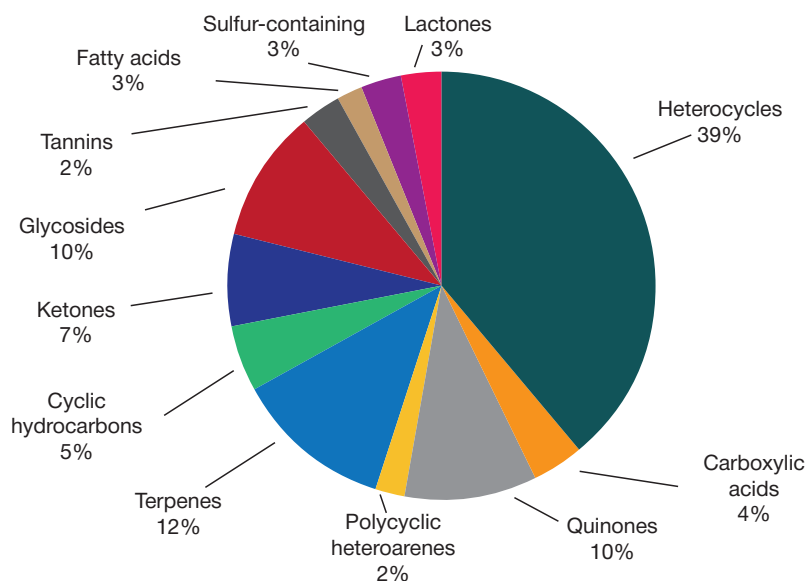


Fig. 3. The distribution of major groups of non-peptide organic compounds as new anticancer drug prototypes

stilbene, phenanthridine, pyranocarbazole, benzopyran, imidazolo-pyridine, indole, indolizine, naphthyridine, phthalazine, chinazoline) used for organic synthesis of new derivatives with anticancer activity and other spectrum [18, 19]. Thus, indole, quinazoline, acridine and pyridine derivatives in total account for 35% of all ones.

The trends of publication activity over the 5-year period (2016–2020) performed for 150 compounds, including the names of synthetic (46%) and natural (54%) chemical

scaffolds, is presented in Fig. 4. It is reasonable to distinguish a discrete group of compounds (for example, derivatives of 1,6-naphthypyridone, sulfonylaspirodienone, N-acyl-phenylenediamine and scabioside C), in which the anticancer activity was found for the first time. Fig. 4 also shows the re-emerging scientific interest in dioscin, cinnoline, indolizine, nargenicin A1 derivatives and quercetin. It follows from the growing number of publications, issued in 2020, describing the new anticancer effects for these compounds. On the other

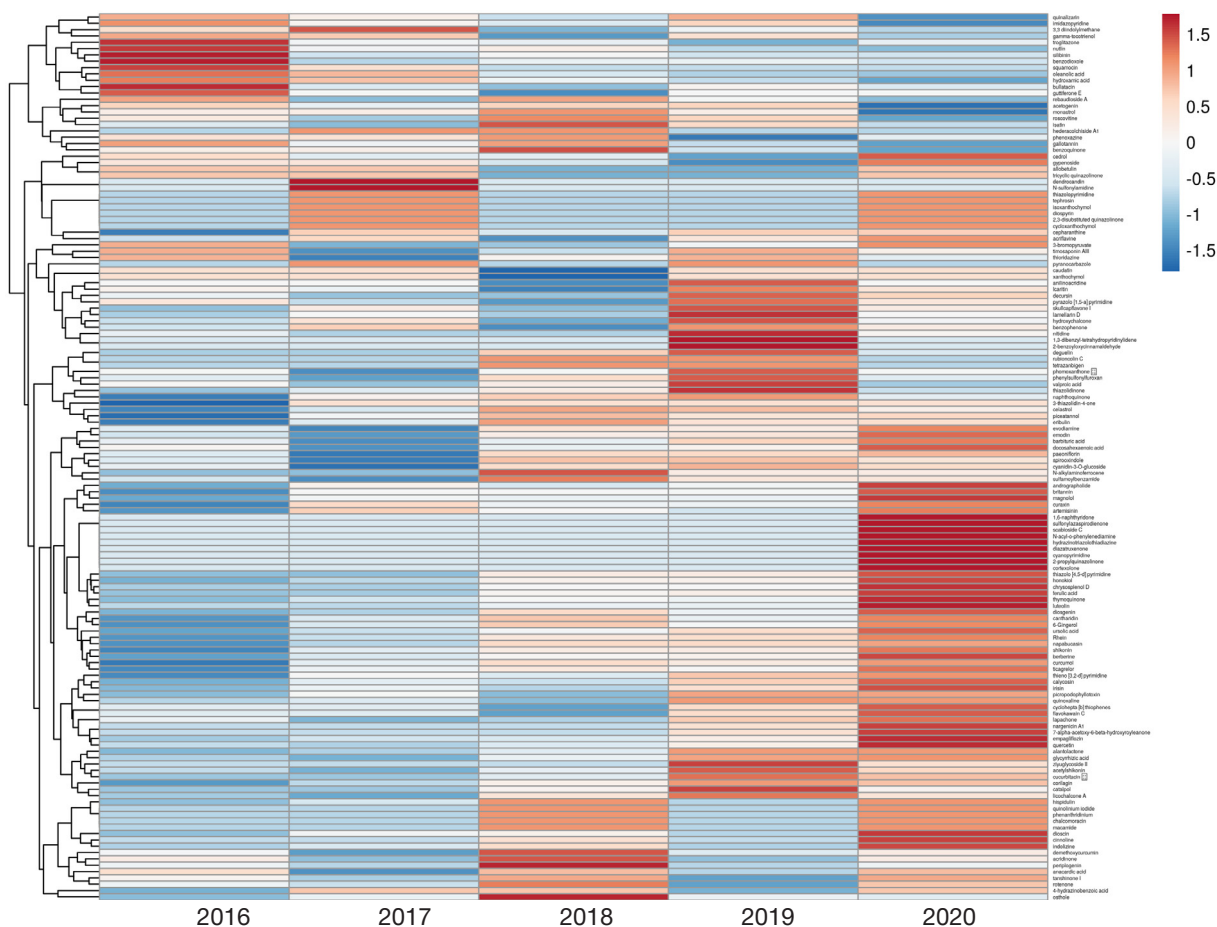


Fig. 4. Heat map of changes in publication activities (2016–2020) on identifying the new anticancer drug prototypes. Note: legend scale — cluster distance; decrease and increase in the number of papers are highlighted in red and blue colors, respectively

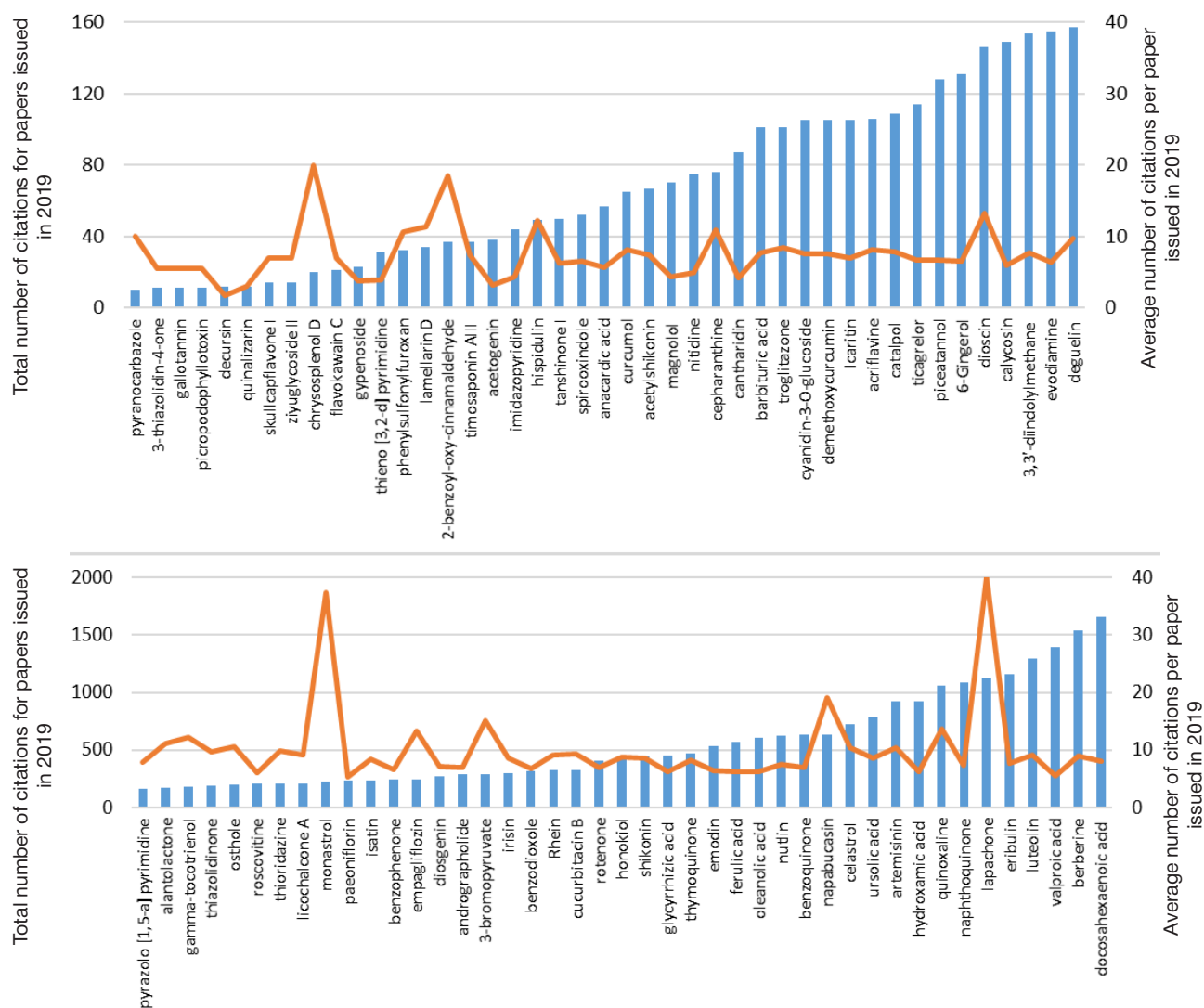


Fig. 5. Citations of papers issued in 2019 and focused on the anticancer drug prototype identification. Original names of compounds are provided

hand, publication activity with a reference to derivatives of thiazolidinedione (troglitazone), nutlin, silybin, squamocin, and derivatives of benzodioxole, oleanolic acid, and hydroxamic acid declined gradually in 2018–2020 compared to 2016–2017 period.

In addition to assessment of dynamic changes in the papers number, citing the papers, issued in 2019, was also analyzed. Fig. 5 shows that, citation rate in 2019–2021 (minimum threshold: 1000 citations) was observed for studies referring quinoxaline, naphthoquinone, berberine, valproic acid and docosahexaenoic acid derivatives, as well as on lapachone, luteolin and quercetin. The latter is the “cite leader”, which is mentioned 4200 times. However, based on the average number of citations per paper, issued in 2019, (minimum threshold: 15 citations), publications referring to crisosplenol D, 2-benzoyl-oxy-cinnamaldehyde, monastrol and lapachone ranked first in the context of new anticancer drug prototypes development.

The effective anticancer drug design is intrinsically linked with the related biomedical area of identifying the molecular targets. Efforts in this complementary area involve identification of mechanisms of action of drugs, which is critically important for differentiation of their on-target and off-target effects, as well as for design of highly selective compounds affecting the desired range of molecular targets. The vast majority of the clinically significant targets are the monomeric proteins or,

more rarely, the oligomeric protein complexes [20]. Thus, the search for protein targets for a number of the priority anticancer drug prototypes (Fig. 5), contained in the Reaxys database, has helped to find out molecular targets has been mapped for the other three compounds, except crisosplenol D. As it turns out, the 2-benzoyloxycinnamaldehyde structure similar, ((E)-2-(3-oxoprop-1-en-1-yl) phenyl benzoate), inhibits cyclin-dependent kinase 4, CDK4 (Target ID: 820056979) enzymatic activity, glutathione reductase (Target ID: 820106479) and farnesyltransferase (Target ID: 470858527). However, the monastrol and lapachone derivatives exhibit more optimal drug-like properties (compliance with the “rule of five” parameters [21]) compared to 2-benzoyl-oxy-cinnamaldehyde, and have a greater potential for identification of their molecular target. Reaxys database contains 31 and 117 records (accession on May 29, 2021) about the monastrol and lapachone targets, respectively. Among them, it can be found Aurora A protein kinase (Reaxys Target ID: 818366617), M-phase inducer phosphatase 2 (Target ID: 820046846), DNA topoisomerase I (Target ID: 818289566), DNA topoisomerase II (Target ID: 824645880), glutathione S-transferase P (Target ID: 820104166), K-Ras GTPase variants (Target ID: 819104337) with G12C and Q61R substitutions, NAD(P)H quinone dehydrogenase 1 (Target ID: 820009294).

In Table, the new experimental synthetic and natural compounds, exhibiting anticancer activity [22–92] were shown with respect to molecular target mapping and the mechanisms

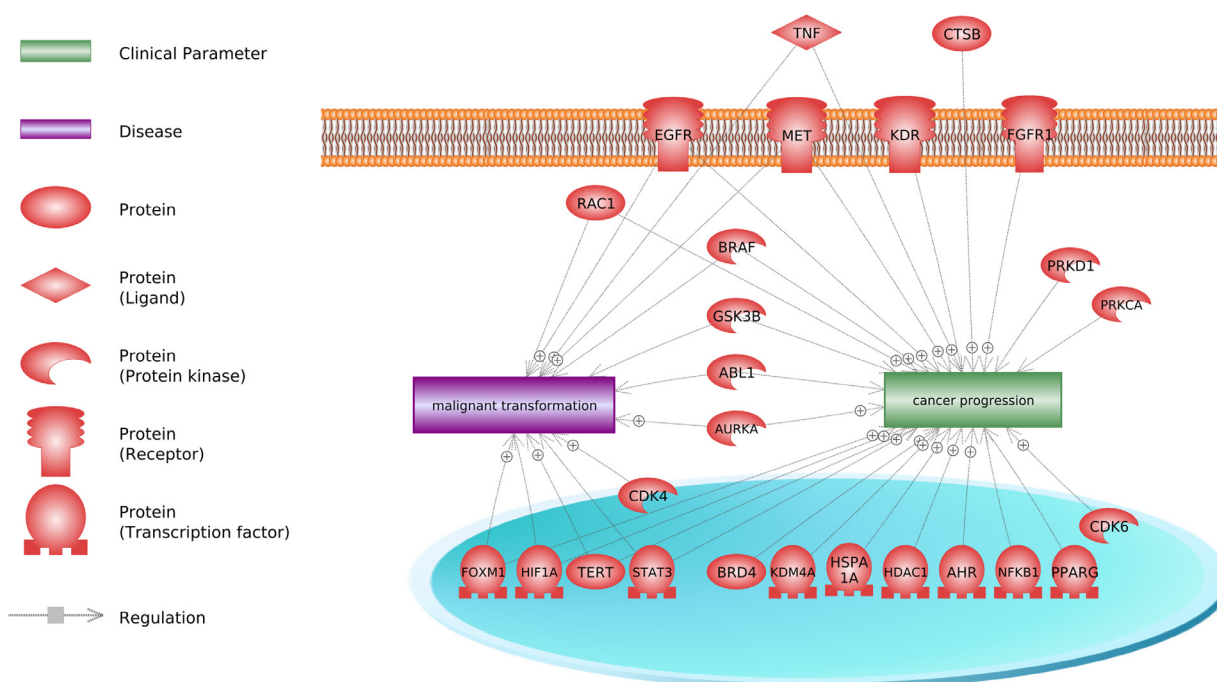


Fig. 6. Associations between the protein targets of anticancer drug prototypes returned by the queries "malignant transformation" and "cancer progression" in the Pathway Studio

of action studies. Scientific interest in such compounds follows from increased citation numbers and existence of patent potential. Furthermore, the newly identified chemical scaffolds, exhibiting a broad spectrum of anticancer activity, may later be used for design and synthesis of their derivatives. It is worth noting that papers on drug target mapping currently represent the great scientific demand and have a high citation rate in experimental pharmacology area.

DISCUSSION

Analysis of data presented in Table revealed the following quantitative distribution of the new anticancer drug protein targets: protein kinases (38%), DNA topoisomerases I and II (10%), transcription factors (9%), clinically significant protein-protein complexes (7%), cytoskeleton proteins (tubulin) (5%), and, finally, the rest of the diverse targets' group accounted for 40%. It is noteworthy that the latter group included phosphodiesterase 5A (PDE5A), Na⁺-glucose cotransporter 2 (SGLT2), and glutathione S-transferase (GSTP1) and dihydrofolate reductase (DHFR) enzymes, associated with chemotherapy drug metabolism and involved in the drug-resistant tumor phenotype formation [93]. Therefore, blockade of such enzymes may be considered a complementary pharmacological strategy, enabling to decrease chemoresistance. Analysis of papers' abstracts made it possible to determine the mechanism of action of anticancer drug prototypes (Table) which represent, mainly, competitive or noncompetitive reversible inhibition of the enzymes' catalytic activity.

Table demonstrates scientific interest in low molecular weight compounds that capable of modulating the function of transcription factors (for example, HIF-1a, FOXM1, ATF4). This is a group of intracellular nuclear proteins, which have been considered the extremely complicated molecular objects for drug design for a long time [94]. The search for new compounds disturbing signal transduction in the classic cancer-associated signaling pathways remains the traditional approach for carcinogenesis inhibition. Based on bibliometric analysis over 2020–2021, it should be pointed out that references to

the PI3K, mTOR, AKT1, STAT3, HIF-1a and p53 signaling cascades were most often found among the pharmacologically targeted signaling pathways.

One more group can be seen in Table, including the compounds (LQFM126, E7386, britanin) and miconazole, which have the potential to selectively modulate the protein complex affinity. This approach to drug prototype design is innovative, since it is based on the pharmacological targeting of conservative interfaces of protein-protein interactions (PPI) with low mutation rate [95, 96]. However, there is a number of polemical papers [97, 98], reporting the opposite, namely, predominant accumulation of mutations, associated with carcinogenesis, in the PPI interfaces of clinically significant protein complexes. This point is needed for in-depth study of the mutation factors' significance for drug targeted protein interfaces.

Then, we searched for information of involvement in carcinogenesis of the protein targets (listed in Table) using Pathway Studio. The assessment was performed based on the presence of links between proteins, and terms "malignant transformation" and "cancer progression". The results were selected on the availability of at least five papers, reporting the association of each protein target with each of these parameters. Thus, the visualization (Fig. 6) has revealed many evidence on the cancer involvement of majority of protein targets (Table).

The table also demonstrates that, on the one hand, STAT3 has been identified as a new protein target for the well-known anticancer drug napabucasin. On the other hand, studying the repositioning effects of miconazole, troglitazone, dexamethasone, vinpocetine and empagliflozin has made it possible to determine one more type of their biological activity, that is the anticancer activity. It can be assumed that such activity results from the modulating of signal transduction in the pro-oncogene pathways.

Pathway Studio can help to found out that the main type of interaction between the protein targets, was a post-translational modification by means of phosphorylation. The identified binary protein-protein interactions, where the first protein of a pair phosphorylates the second protein, are as follows: EGFR/STAT3, MET/STAT3, GSK3B/HIF1A, ABL1/

Table. Relationship between the biological activity of new anticancer drug prototypes and their molecular targets

Biologically active compound	Description	Source
Protein targets		
LQFM126	PPI* inhibitor between MDM2 and p53	[22]
E7386	PPI inhibitor between β -catenin and CREB	[23]
Britanin	PPI inhibitor between HIF-1 α and Myc	[24]
<i>Miconazole*</i>	PPI inhibitor between DDIAS and STAT3	[25]
5F-203	Activator of aryl hydrocarbon receptor (AHR)	[26]
Emodin	Activator of AHR	[27]
3/4-(pyrimidin-2-ylamino) benzoyl)-based hydrazine-1-carboxamide/carbothioamide derivatives	Antagonist of retinoic acid receptor α (RXR α)	[28]
Epigallocatechin and podophyllotoxin conjugates (epigallocatechin-3-gallate-4 β -triazolopodophyllotoxin)	Inhibitor of DNA topoisomerase II (TOP2)	[29]
Tricyclic quinazolinone derivatives	Inhibitor of DNA topoisomerase I (TOP1)	[30]
5(or 6)-nitro-2-(substitutedphenyl) benzo xazole, 2-(substitutedphenyl) oxazolo[4,5-b] pyridine derivatives	Inhibitor of TOP1 and TOP2	[31]
Lamellarin D	Inhibitor of TOP1	[32]
Hoechst 33342	Inhibitor of TOP1	[33]
3-(1H-indol-3-yl)-2,3,3a,4-tetrahydrothio chromeno[4,3-c] pyrazole derivatives	Inhibitor of TOP2	[34]
2,3-dihydropyrazino[1,2-a] indole-1,4-dione derivatives	Inhibitor of EGFR tyrosine kinase and mutant variant of serine/threonine kinase BRAF V600E	[35]
4-hydroxyquinazoline derivatives	Inhibitor of VEGFR2 tyrosine kinase	[36]
DW14383	Inhibitor of FGFR tyrosine kinase	[37]
Chimeric compounds containing piperazine and chalcone	Inhibitor of VEGFR tyrosine kinase	[38]
1,6-naphthyridone derivatives	Inhibitor of c-MET tyrosine kinase	[39]
N-sulfonylamidine derivatives	Inhibitor of c-MET tyrosine kinase	[40]
Di-2-pyridylketone 4,4-dimethyl-3-thiosemicarbazone (Dp44mT)	Inhibitor of AMPK protein kinase	[41]
Tigilanol tiglate	Activator of protein kinase C (PKC)	[42]
Epoxytigiliane derivatives	Activators of protein kinase C (PKC)	[42]
Isoxazolo[4,5-e] [1,2,4] triazepine derivatives	Inhibitor of protein kinase C (PKC)	[43]
Pyrazolo[3,4-d]pyrimidine derivatives	Inhibitor of protein kinase D (PKD)	[44]
TAS-119	Inhibitor of AURKA protein kinase	[45]
Spirobibenzopyran derivatives	Inhibition of CDK4 protein kinase	[46]
Pyrazolo [3,4-d] pyrimidine derivatives (Si306 and Si113)	Inhibitor of CDK 1/2 protein kinases	[47]
7H-[1,2,4]triazolo[3,4- b] [1,3,4] thiadiazine derivatives	Inhibitor of GSK-3 β protein kinase	[48]
<i>Vinpocetine</i>	Activator of GSK-3 β protein kinase	[49]
Thiazolyl hydrazone derivatives	Inhibitor of ABL1 protein kinase	[50]
5-(3-chlorophenylamino) benzo[c][2,6] naphthyridine derivatives	Inhibitor Casein kinase 2 (CK2) 2	[51]
WZ4003	Inhibitor of AMPK-related kinase 5	[52]
N2817	Inhibitor of BET1vesicular membrane trafficking protein	[53]
Tetrazanbigen	Regulation of PPAR γ expression	[54]
Calycosin	Regulation of apoptosis and miR-375 expression	[55]
3-bromopyruvate	Regulation of CTSB protease activity	[56]
Decursin	Regulation of HIF-1 α transcription factor expression and degradation	[57]
<i>Troglitazone</i>	Inhibitor of FOXM1 transcription factor activity	[58]
<i>Napabucasin</i>	Inhibitor of STAT3 transcription factor	[59]
N-substituted sulfamoylbenzamide derivatives	Inhibitor of Il-6/STAT3 activity	[60]
Andrographolide	Regulation of ATF4 transcription factor activity	[61]
Quinoline derivatives	Inhibitor of phosphodiesterase (PDE5)	[62]
Osthole	Inhibitor of histone deacetylase (HDAC)	[63]
<i>Empagliflozin</i>	Inhibitor of SGLT2 (SLC5A2) ion transporter	[64]
Amb4269951	Inhibitor of choline transporter-like protein CTL1	[65]
Evodiamine	Inhibitor of HSP70 chaperone	[66]

Table continued

6-(7-nitro-2,1,3-benzoxadiazol-4-ylthio) hexanol (NBDHEX) derivatives	Inhibitor of GSTP1 glutathione transferase	[67]
BIBR1532	Regulation of TERT telomerase activity	[68]
Acetylshikonin	Inhibitor of DHFR dihydrofolate reductase	[69]
Docosahexaenoic acid derivatives	Inhibitor of bromodomain-containing protein 4 (BRD4)	[70]
Licochalcone A	Regulation of PD-L1 expression	[71]
2-amino-pyrrole-carboxamide derivatives	Inhibitor of tubulin polymerization	[72]
2,3-diaryl-2H-azirine derivatives	Inhibitor of tubulin polymerization	[73]
Indolizine derivatives	Potential inhibitor of tubulin polymerization	[74]
Rhein derivatives	Inhibitor of small GTPase Rac1	[75]
<i>Dexamethasone</i>	<i>Regulation of p65 activity</i>	[76]
Signaling cascades as targets		
Oleanolic acid and its semi-synthetic derivatives	PI3K/AKT/mTOR	[77]
Gypenoside derivatives	PI3K/AKT/mTOR	[78]
Cyanidin-3-O-glucoside derivatives	PI3K/AKT/mTOR	[79]
IPM712	PI3K/AKT	[80]
Thieno[3,2-d]pyrimidine	PI3K/mTOR	[81]
Artemisinin	Wnt/ β -catenin	[82]
PRI-724	Wnt/ β -catenin	[83]
Celastral derivatives	HIF-1 α	[84]
Decursin	HIF-1 α	[85]
Ursolic acid	JAK2/STAT3/EGFR	[86]
Skullcapflavone I	JAK/STAT/MAPK	[87]
Gallothanin	JAK/STAT	[88]
Licochalcone A	MAPK	[89]
Chrysin-chromene-spiroxyindole derivatives	p53	[90]
Picropodophyllotoxin	JNK/p38	[91]
Luteolin	ERK/FOXO3a	[92]

Note: PPI — protein-protein interaction; * — approved medications are shown in italics.

STAT3, EGFR/GSK3B, ABL1/TERT, EGFR/MET, PRKCA/GSK3B, ABL1/STAT3, AURKA/GSK3B, PRKD1/EGFR, GSK3B/HSPA1A, GSK3B/NFKB1. It should be emphasized that the above mentioned interactions include proteins, which are involved in carcinogenesis regulation and are the targets for the approved anticancer drugs [99, 100].

Thus, bibliometric analysis of papers, issued in 2020–2021, focused on the identification and development of the novel non-peptide anticancer drug prototypes revealed the following findings: i) a significant proportion (71%) of compounds belong to the chemical class of heterocycles, glycosides, quinones and terpenes; ii) indole, quinazoline, acridine and pyridine scaffolds were up to 35% from all used in organic synthesis of derivatives. Trend analysis of publication activity made it possible to define the scientific interest in the distinct groups of anticancer compounds and the progress in mapping their molecular targets. Among them, were proteins, associated with carcinogenesis, such as serine/threonine protein kinases,

receptor tyrosine kinases, DNA topoisomerases and tubulins, which still remain the most studied anticancer drug targets. However, there are the increasing growth of the scientific interest in the design of inhibitors targeted to cancer-associated protein-protein complexes, transcription factors and metabolic enzymes, involved in the drug-resistant tumor phenotype.

CONCLUSIONS

Bibliometric approach with the using of Scopus, Reaxys, Pathway Studio and Cortellis databases together with VOS Viewer software enables prompt monitoring of the trends in the anticancer drug research and development (R&D) as well as defining the priorities in current scientific interest. At the same time, it can be said that there emerges a growing number a growing number of novel molecular modalities associated with carcinogenesis processes, which encourages the studies discovery of more efficient pharmacotherapeutic agents.

References

- Kiriiri GK, Njogu PM, Mwangi AN. Exploring different approaches to improve the success of drug discovery and development projects: a review. *Futur J Pharm Sci.* 2020; 6: 27. DOI: 10.1186/s43094-020-00047-9.
- Gibbs JB. Mechanism-based target identification and drug discovery in cancer research. *Science.* 2000; 287 (5460): 1969–73. DOI: 10.1126/science.287.5460.1969.
- Druker BJ. Perspectives on the development of a molecularly targeted agent. *Cancer Cell.* 2002 Feb; 1 (1): 31–6. DOI: 10.1016/s1535-6108(02)00025-9.
- Nam NH, Parang K. Current targets for anticancer drug discovery. *Curr Drug Targets.* 2003; 4 (2): 159–79. DOI: 10.2174/1389450033346966.
- Haider T, Pandey V, Banjare N, Gupta PN, Soni V. Drug resistance

- in cancer: mechanisms and tackling strategies. *Pharmacol Rep.* 2020; 72 (5): 1125–51. DOI:10.1007/s43440-020-00138-7.
6. Devlin EJ, Denson LA, Whitford HS. Cancer treatment side effects: A meta-analysis of the relationship between response expectancies and experience. *J Pain Symptom Manage.* 2017; 54 (2): 245–58.e2. DOI:10.1016/j.jpainsymman.2017.03.017.
 7. Kumar B, Singh S, Skvortsova I, Kumar V. Promising targets in anti-cancer drug development: recent updates. *Curr Med Chem.* 2017; 24 (42): 4729–52. DOI: 10.2174/0929867324666170331123648.
 8. Magalhaes LG, Ferreira LLG, Andricopulo AD. Recent advances and perspectives in cancer drug design. *An Acad Bras Cienc.* 2018; 90 (1 Suppl 2): 1233–50. DOI: 10.1590/0001-3765201820170823.
 9. Cui W, Aouidate A, Wang S, Yu Q, Li Y, Yuan S. Discovering anti-cancer drugs via computational methods. *Front Pharmacol.* 2020; 11: 733. DOI: 10.3389/fphar.2020.00733.
 10. Özen Çınar İ. Bibliometric analysis of breast cancer research in the period 2009–2018. *Int J Nurs Pract.* 2020; 26 (3): e12845. DOI:10.1111/ijn.12845.
 11. Didion CA, Henne WA. A bibliometric analysis of folate receptor research. *BMC Cancer.* 2020; 20 (1): 1109. DOI:10.1186/s12885-020-07607-5.
 12. Jin B, Wu XA, Du SD. Top 100 most frequently cited papers in liver cancer: a bibliometric analysis. *ANZ J Surg.* 2020; 90 (1–2): 21–6. DOI:10.1111/ans.15414.
 13. Liu W, Wu L, Zhang Y, Shi L, Yang X. Bibliometric analysis of research trends and characteristics of oral potentially malignant disorders. *Clin Oral Investig.* 2020; 24 (1): 447–54. DOI: 10.1007/s00784-019-02959-0.
 14. Van Eck NJ, Waltman L. Text mining and visualization using VOSviewer. *ISSI Newsletter.* 2011; 7 (3): 50–4.
 15. Tauno M, Jaak V. Clustvis: a web tool for visualizing clustering of multivariate data using Principal Component Analysis and heatmap. *Nucleic Acids Research.* 2015; 43 (W1): W566–W570, 2015. DOI: 10.1093/nar/gkv468.
 16. Arnst KE, Banerjee S, Chen H, Deng S, Hwang DJ, Li W, et al. Current advances of tubulin inhibitors as dual acting small molecules for cancer therapy. *Med Res Rev.* 2019; 39 (4): 1398–426. DOI:10.1002/med.21568.
 17. Chopra B, Dhingra AK, Dhar KL, Nepali K. Emerging role of terpenoids for the treatment of cancer: a review. *Mini Rev Med Chem.* 2021. Available from: <https://www.eurekaselect.com/190215/article>. DOI: 10.2174/1389557521666210112143024.
 18. Kirsch P, Hartman AM, Hirsch AKH, Empting M. Concepts and core principles of fragment-based drug design. *Molecules.* 2019; 24 (23): 4309. DOI: 10.3390/molecules24234309.
 19. Giacomini E, Rupiani S, Guidotti L, Recanatini M, Roberti M. The use of stilbene scaffold in medicinal chemistry and multi-target drug design. *Curr Med Chem.* 2016; 23 (23): 2439–89. DOI: 10.2174/0929867323666160517121629.
 20. Hughes JP, Rees S, Kalindjian SB, Philpott KL. Principles of early drug discovery. *Br J Pharmacol.* 2011; 162 (6): 1239–49. DOI: 10.1111/j.1476-5381.2010.01127.x.
 21. Lipinski CA, Lombardo F, Dominy BW, Feeney PJ. Experimental and computational approaches to estimate solubility and permeability in drug discovery and development settings. *Adv Drug Deliv Rev.* 1997; 23 (1–3): 3–25. DOI: 10.1016/S0169-409X(96)00423-1.
 22. Garcia da Silva AC, Rodrigues BDS, Andrade WM, Marques Dos Santos TR, de Carvalho FS, Sanz G, et al. Antiangiogenic and antitumoral activity of LQFM126 prototype against B16F10 melanoma cells. *Chem Biol Interact.* 2020; 325: 109127. DOI: 10.1016/j.cbi.2020.109127.
 23. Yamada K, Hori Y, Inoue S, Yamamoto Y, Iso K, Kamiyama H, et al. E7386, a selective inhibitor of the interaction between β -catenin and CBP, exerts antitumor activity in tumor models with activated canonical Wnt signaling. *Cancer Res.* 2021; 81 (4): 1052–62. DOI: 10.1158/0008-5472.CAN-20-0782.
 24. Zhang YF, Zhang ZH, Li MY, Wang JY, Xing Y, Ri M, et al. Britannin stabilizes T cell activity and inhibits proliferation and angiogenesis by targeting PD-L1 via abrogation of the crosstalk between Myc and HIF-1 α in cancer. *Phytomedicine.* 2021; 81: 153425. DOI: 10.1016/j.phymed.2020.153425
 25. Yoon SH, Kim BK, Kang MJ, Im JY, Won M. Miconazole inhibits signal transducer and activator of transcription 3 signaling by preventing its interaction with DNA damage-induced apoptosis suppressor. *Cancer Sci.* 2020 Jul; 111 (7): 2499–507. DOI: 10.1111/cas.14432. Epub 2020 May 31. PMID: 32476221; PMCID: PMC7385363.
 26. Osmaniye D, Korkut Çelikeleş B, Sağlık BN, Levent S, Acar Çevik U, Kaya Çavuşoğlu B, et al. Synthesis of some new benzoxazole derivatives and investigation of their anticancer activities. *Eur J Med Chem.* 2021; 210: 112979. DOI: 10.1016/j.ejmech.2020.112979.
 27. Zhang N, Wang J, Sheng A, Huang S, Tang Y, Ma S, et al. Emodin inhibits the proliferation of MCF-7 human breast cancer cells through activation of aryl hydrocarbon receptor (AhR). *Front Pharmacol.* 2021; 11: 622046. DOI: 10.3389/fphar.2020.622046.
 28. Qin J, Liu J, Wu C, Xu J, Tang B, Guo K, et al. Synthesis and biological evaluation of (3/4-(pyrimidin-2-ylamino) benzoyl)-based hydrazine-1 carboxamide/carbothioamide derivatives as novel RXR α antagonists. *J Enzyme Inhib Med Chem.* 2020; 35 (1): 880–96. DOI: 10.1080/14756366.2020.1740692.
 29. Zi CT, Yang L, Hu Y, Zhang P, Tang H, Zhang BL, et al. Synthesis, antitumor activity, and molecular docking of (-)-epigallocatechin-3-gallate-4 β -triazolopodophyllotoxin conjugates. *J Asian Nat Prod Res.* 2020; 1–9. DOI: 10.1080/10286020.2020.1786066.
 30. Huang WY, Zhang XR, Lyu L, Wang SQ, Zhang XT. Pyridazino[1,6-b]quinazolinones as new anticancer scaffold: synthesis, DNA intercalation, topoisomerase I inhibition and antitumor evaluation in vitro and in vivo. *Bioorg Chem.* 2020; 99: 103814. DOI: 10.1016/j.bioorg.2020.103814.
 31. Karatas E, Foto E, Ertan-Bolelli T, Yalcin-Ozkat G, Yilmaz S, Ataei S, et al. Discovery of 5-(or 6)-benzoxazoles and oxazolo[4,5-b]pyridines as novel candidate antitumor agents targeting hTopo II α . *Bioorg Chem.* 2021; 112: 104913. DOI: 10.1016/j.bioorg.2021.104913.
 32. Fukuda T, Nanjo Y, Fujimoto M, Yoshida K, Natsui Y, Ishibashi F, et al. Lamellarin-inspired potent topoisomerase I inhibitors with the unprecedented benzo[g][1]benzopyrano[4,3-b]indol-6(13H)-one scaffold. *Bioorg Med Chem.* 2019; 27 (2): 265–77. DOI: 10.1016/j.bmc.2018.11.037.
 33. Acar Çevik U, Sağlık BN, Osmaniye D, Levent S, Kaya Çavuşoğlu B, Karaduman AB, et al. Synthesis, anticancer evaluation and molecular docking studies of new benzimidazole-1,3,4-oxadiazole derivatives as human topoisomerase types I poison. *J Enzyme Inhib Med Chem.* 2020; 35 (1): 1657–73. DOI: 10.1080/14756366.2020.1806831.
 34. Song Y, Feng S, Feng J, Dong J, Yang K, Liu Z, et al. Synthesis and biological evaluation of novel pyrazoline derivatives containing indole skeleton as anti-cancer agents targeting topoisomerase II. *Eur J Med Chem.* 2020; 200: 112459. DOI: 10.1016/j.ejmech.2020.112459.
 35. Al-Wahaibi LH, Gouda AM, Abou-Ghadir OF, Salem OIA, Ali AT, Farghaly HS, et al. Design and synthesis of novel 2,3-dihydropyrazino[1,2-a]indole-1,4-dione derivatives as antiproliferative EGFR and BRAFV600E dual inhibitors. *Bioorg Chem.* 2020; 104: 104260. DOI: 10.1016/j.bioorg.2020.104260.
 36. Eissa IH, Ibrahim MK, Metwaly AM, Belal A, Mehany ABM, Abdelhady AA, et al. Design, molecular docking, in vitro, and in vivo studies of new quinazolin-4(3H)-ones as VEGFR-2 inhibitors with potential activity against hepatocellular carcinoma. *Bioorg Chem.* 2021; 107: 104532. DOI: 10.1016/j.bioorg.2020.104532.
 37. Dai MD, Wang YL, Fan J, Dai Y, Ji YC, Sun YM, et al. DW14383 is an irreversible pan-FGFR inhibitor that suppresses FGFR-dependent tumor growth in vitro and in vivo. *Acta Pharmacol Sin.* 2020. Available from: <https://www.nature.com/articles/s41401-020-00567-3>. DOI: 10.1038/s41401-020-00567-3.
 38. Ahmed MF, Santali EY, El-Haggag R. Novel piperazine-chalcone hybrids and related pyrazoline analogues targeting VEGFR-2 kinase; design, synthesis, molecular docking studies, and anticancer evaluation. *J Enzyme Inhib Med Chem.* 2021; 36 (1): 307–18. DOI: 10.1080/14756366.2020.1861606.
 39. Zhuo LS, Wu FX, Wang MS, Xu HC, Yang FP, Tian YG, et al. Structure-activity relationship study of novel quinazoline-based 1,6-naphthyridinones as MET inhibitors with potent antitumor efficacy. *Eur J Med Chem.* 2020; 208: 112785. DOI: 10.1016/j.

- ejmech.2020.112785.
40. Nan X, Zhang J, Li HJ, Wu R, Fang SB, Zhang ZZ, et al. Design, synthesis and biological evaluation of novel N-sulfonylamidine-based derivatives as c-Met inhibitors via Cu-catalyzed three-component reaction. *Eur J Med Chem.* 2020; 200: 112470. DOI: 10.1016/j.ejmech.2020.112470.
 41. Krishan S, Sahni S, Richardson DR. The anti-tumor agent, Dp44mT, promotes nuclear translocation of TFEB via inhibition of the AMPK-mTORC1 axis. *Biochim Biophys Acta Mol Basis Dis.* 2020; 1866 (12): 165970. DOI: 10.1016/j.bbadis.2020.165970.
 42. Cullen JK, Boyle GM, Yap PY, Elmlinger S, Simmons JL, Broit N, et al. Activation of PKC supports the anticancer activity of tigilanol tiglate and related epoxytiglanes. *Sci Rep.* 2021; 11 (1): 207. DOI: 10.1038/s41598-020-80397-9.
 43. Wagner E, Wietrzyk J, Psurski M, Becan L, Turlej E. Synthesis and anticancer evaluation of novel derivatives of isoxazolo[4,5-e] [1,2,4]triazepine derivatives and potential inhibitors of protein kinase C. *ACS Omega.* 2020; 6 (1): 119–34. DOI:10.1021/acsomega.0c03801.
 44. Gilles P, Kashyap RS, Freitas MJ, Ceusters S, Van Asch K, Janssens A, et al. Design, synthesis and biological evaluation of pyrazolo[3,4-d]pyrimidine-based protein kinase D inhibitors. *Eur J Med Chem.* 2020; 205: 112638. DOI: 10.1016/j.ejmech.2020.112638.
 45. Sootome H, Miura A, Masuko N, Suzuki T, Uto Y, Hirai H, et al. Inhibitor TAS-119 enhances antitumor efficacy of taxanes in vitro and in vivo: preclinical studies as guidance for clinical development and trial design. *Mol Cancer Ther.* 2020; 19 (10): 1981–91. DOI: 10.1158/1535-7163.MCT-20-0036.
 46. Kar S, Ramamoorthy G, Mitra K, Shivalingegowda N, Mahesha, Mavileti SK, et al. Synthesis of novel spirobenzopyrans as potent anticancer leads inducing apoptosis in HeLa cells. *Bioorg Med Chem Lett.* 2020; 30 (12): 127199. DOI: 10.1016/j.bmcl.2020.127199.
 47. Massaro M, Barone G, Barra V, Cancemi P, Di Leonardo A, Grossi G, et al. Pyrazole[3,4-d]pyrimidine derivatives loaded into halloysite as potential CDK inhibitors. *Int J Pharm.* 2021; 599: 120281. DOI: 10.1016/j.ijpharm.2021.120281.
 48. Ismail MI, Mohamady S, Samir N, Abouzid KAM. Design, synthesis, and biological evaluation of novel 7H-[1,2,4]triazolo[3,4-b][1,3,4]thiadiazine inhibitors as antitumor agents. *ACS Omega.* 2020; 5 (32): 20170–86. DOI: 10.1021/acsomega.0c01829.
 49. Zhang ZY, Dong SM, Liu YH, Zhang MM, Zhang JK, Zhu HJ, et al. Enhanced anticancer activity by the combination of vinpocetine and sorafenib via PI3K/AKT/GSK-3 β signaling axis in hepatocellular carcinoma cells. *Anticancer Drugs.* 2021. Available from: https://journals.lww.com/anti-cancerdrugs/Abstract/2021/09000/Enhanced_antitumor_activity_by_the_combination_of.7.aspx. DOI: 10.1097/CAD.0000000000001056.
 50. Zeytün E, Altıntop MD, Sever B, Özdemir A, Ellakwa DE, Ocak Z, et al. A new series of antileukemic agents: design, synthesis, in vitro and in silico evaluation of thiazole-based abl1 kinase inhibitors. *Anticancer Agents Med Chem.* 2021; 21 (9): 1099–109. DOI: 10.2174/1871520620666200824100408.
 51. Wang Y, Lv Z, Chen F, Wang X, Gou S. Discovery of 5-(3-chlorophenylamino) benzo[c][2,6] naphthyridine derivatives as highly selective ck2 inhibitors with potent cancer cell stemness inhibition. *J Med Chem.* 2021; 64 (8): 5082–98. DOI: 10.1021/acs.jmedchem.1c00131.
 52. Yang H, Wang X, Wang C, Yin F, Qu L, Shi C et al. Optimization of WZ4003 as NUAk inhibitors against human colorectal cancer. *Eur J Med Chem.* 2021; 210: 113080. DOI: 10.1016/j.ejmech.2020.113080.
 53. Wu Q, Chen DQ, Sun L, Huan XJ, Bao XB, Tian CQ et al. Novel bivalent BET inhibitor N2817 exhibits potent anticancer activity and inhibits TAF1. *Biochem Pharmacol.* 2021; 185: 114435. DOI: 10.1016/j.bcp.2021.114435.
 54. Gan L, Gan Z, Dan Y, Li Y, Zhang P, Chen S, et al. Tetrazanbigen derivatives as peroxisome proliferator-activated receptor gamma (ppary) partial agonists: design, synthesis, structure-activity relationship, and anticancer activities. *J Med Chem.* 2021; 64 (2): 1018–36. DOI: 10.1021/acs.jmedchem.0c01512.
 55. Zhang D, Sun G, Peng L, Tian J, Zhang H. Calycosin inhibits viability, induces apoptosis, and suppresses invasion of cervical cancer cells by upregulating tumor suppressor miR-375. *Arch Biochem Biophys.* 2020; 691: 108478. DOI: 10.1016/j.abb.2020.108478.
 56. Szczuka I, Wiśniewski J, Kustrzeba-Wójcicka I, Terlecki G. The effect of 3-bromopyruvate on the properties of cathepsin B in the aspect of metastatic potential of colon cancer cells. *Adv Clin Exp Med.* 2020; 29 (8): 949–57. DOI: 10.17219/acem/123622. PMID: 32820873.
 57. Ge Y, Yoon SH, Jang H, Jeong JH, Lee YM. Decursin promotes HIF-1 α proteasomal degradation and immune responses in hypoxic tumour microenvironment. *Phytomedicine.* 2020; 78: 153318. DOI: 10.1016/j.phymed.2020.153318.
 58. Tabatabaei Dakhili SA, Pérez DJ, Gopal K, Haque M, Ussher JR, Kashfi K, et al. SP1-independent inhibition of FOXM1 by modified thiazolidinediones. *Eur J Med Chem.* 2021; 209: 112902. DOI: 10.1016/j.ejmech.2020.112902.
 59. Liu Y, Peng X, Li H, Jiao W, Peng X, Shao J, et al. STAT3 inhibitor napabucasin inhibits tumor growth and cooperates with proteasome inhibition in human ovarian cancer cells. *Recent Pat Anticancer Drug Discov.* 2021. DOI: 10.2174/1574892816666210224155403.
 60. Wang X, Wu K, Fang L, Yang X, Zheng N, Du Z, et al. Discovery of N-substituted sulfamoylbenzamide derivatives as novel inhibitors of STAT3 signaling pathway based on Niclosamide. *Eur J Med Chem.* 2021; 218:113362. DOI: 10.1016/j.ejmech.2021.113362.
 61. Zhang J, Li C, Zhang L, Heng Y, Xu T, Zhang Y, et al. Andrographolide induces noxa-dependent apoptosis by transactivating atf4 in human lung adenocarcinoma cells. *Front Pharmacol.* 2021; 12: 680589. DOI:10.3389/fphar.2021.680589.
 62. Ibrahim TS, Hawwas MM, Taher ES, Alhakamy NA, Alfaleh MA, Elagawany M, et al. Design and synthesis of novel pyrazolo[3,4-d]pyrimidin-4-one bearing quinoline scaffold as potent dual PDE5 inhibitors and apoptotic inducers for cancer therapy. *Bioorg Chem.* 2020; 105: 104352. DOI: 10.1016/j.bioorg.2020.104352.
 63. Abosharaf HA, Diab T, Atlam FM, Mohamed TM. Osthole extracted from a citrus fruit that affects apoptosis on A549 cell line by histone deacetylase inhibition (HDACs). *Biotechnol Rep (Amst).* 2020; 28: e00531. DOI: 10.1016/j.btre.2020.e00531.
 64. Xie Z, Wang F, Lin L, Duan S, Liu X, Li X, et al. An SGLT2 inhibitor modulates SHH expression by activating AMPK to inhibit the migration and induce the apoptosis of cervical carcinoma cells. *Cancer Lett.* 2020; 495: 200–10. DOI: 10.1016/j.canlet.2020.09.005.
 65. Watanabe S, Nishijima N, Hirai K, Shibata K, Hase A, Yamanaka T, et al. Anticancer activity of amb4269951, a choline transporter-like protein 1 inhibitor, in human glioma cells. *Pharmaceuticals (Basel).* 2020; 13 (5): 104. DOI: 10.3390/ph13050104.
 66. Hyun SY, Le HT, Min HY, Pei H, Lim Y, Song I, et al. Evodiamine inhibits both stem cell and non-stem-cell populations in human cancer cells by targeting heat shock protein 70. *Theranostics.* 2021; 11 (6): 2932–52. DOI: 10.7150/thno.49876.
 67. Tentori L, Dorio AS, Mazzon E, Muzi A, Sau A, Cuzzocrea S, et al. The glutathione transferase inhibitor 6-(7-nitro-2,1,3-benzoxadiazol-4-ylthio)hexanol (NBDHEX) increases temozolomide efficacy against malignant melanoma. *Eur J Cancer.* 2011; 47(8): 1219–30. DOI: 10.1016/j.ejca.2010.12.008.
 68. Altamura G, Degli Uberti B, Galiero G, De Luca G, Power K, Licenziato L, et al. The small molecule BIBR1532 exerts potential anti-cancer activities in preclinical models of feline oral squamous cell carcinoma through inhibition of telomerase activity and down-regulation of TERT. *Front Vet Sci.* 2021; 7: 620776. DOI: 10.3389/fvets.2020.620776.
 69. Wang J, Iannarelli R, Pucciarelli S, Laudadio E, Galeazzi R, Giangrossi M, et al. Acetylshikonin isolated from *Lithospermum erythrorhizon* roots inhibits dihydrofolate reductase and hampers autochthonous mammary carcinogenesis in Δ 16HER2 transgenic mice. *Pharmacol Res.* 2020; 161: 105123. DOI: 10.1016/j.phrs.2020.105123.
 70. Ding W, Zhang H, Mei G. Synergistic antitumor activity of DHA and JQ1 in colorectal carcinoma. *Eur J Pharmacol.* 2020; 885: 173500. DOI: 10.1016/j.ejphar.2020.173500.
 71. Yuan LW, Jiang XM, Xu YL, Huang MY, Chen YC, Yu WB, et al.

- Licochalcone A inhibits interferon-gamma-induced programmed death-ligand 1 in lung cancer cells. *Phytomedicine*. 2021; 80: 153394. DOI:10.1016/j.phymed.2020.153394.
72. Boichuk S, Galembikova A, Bikinieva F, Dunaev P, Aukhadieva A, Syuzov K, et al. 2-APCAs, the novel microtubule targeting agents active against distinct cancer cell lines. *Molecules*. 2021; 26 (3): 616. DOI: 10.3390/molecules26030616.
 73. Lin S, Liang Y, Cheng J, Pan F, Wang Y. Novel diaryl-2H-azirines: Antitumor hybrids for dual-targeting tubulin and DNA. *Eur J Med Chem*. 2021; 214: 113256. DOI: 10.1016/j.ejmech.2021.113256.
 74. Sardaru MC, Craciun AM, Al Matarneh CM, Sandu IA, Amarandi RM, Popovici L, et al. Cytotoxic substituted indolizines as new colchicine site tubulin polymerisation inhibitors. *J Enzyme Inhib Med Chem*. 2020; 35 (1): 1581–95. DOI: 10.1080/14756366.2020.1801671.
 75. Li X, Liu Y, Zhao Y, Tian W, Zhai L, Pang H, et al. Rhein derivative 4f inhibits the malignant phenotype of breast cancer by downregulating Rac1 protein. *Front Pharmacol*. 2020; 11: 754. DOI: 10.3389/fphar.2020.00754.
 76. Yao Y, Yao QY, Xue JS, Tian XY, An QM, Cui LX, et al. Dexamethasone inhibits pancreatic tumor growth in preclinical models: Involvement of activating glucocorticoid receptor. *Toxicol Appl Pharmacol*. 2020; 401: 115118. DOI: 10.1016/j.taap.2020.115118.
 77. Wang SS, Zhang QL, Chu P, Kong LQ, Li GZ, Li YQ, et al. Synthesis and antitumor activity of α,β -unsaturated carbonyl moiety-containing oleanolic acid derivatives targeting PI3K/AKT/mTOR signaling pathway. *Bioorg Chem*. 2020; 101: 104036. DOI: 10.1016/j.bioorg.2020.104036.
 78. Liu H, Li X, Duan Y, Xie JB, Piao XL. Mechanism of gypenosides of *Gynostemma pentaphyllum* inducing apoptosis of renal cell carcinoma by PI3K/AKT/mTOR pathway. *J Ethnopharmacol*. 2021; 271: 113907. DOI: 10.1016/j.jep.2021.113907.
 79. Li X, Zhao J, Yan T, Mu J, Lin Y, Chen J, et al. Cyanidin-3-O-glucoside and cisplatin inhibit proliferation and downregulate the PI3K/AKT/mTOR pathway in cervical cancer cells. *J Food Sci*. 2021. Available from: <https://onlinelibrary.wiley.com/doi/10.1111/1750-3841.15740>. DOI: 10.1111/1750-3841.15740.
 80. Ma W, Zhang Q, Li X, Ma Y, Liu Y, Hu S, et al. IPM712, a vanillin derivative as potential antitumor agents, displays better antitumor activity in colorectal cancers cell lines. *Eur J Pharm Sci*. 2020; 152: 105464. DOI: 10.1016/j.ejps.2020.105464.
 81. Han Y, Tian Y, Wang R, Fu S, Jiang J, Dong J, et al. Design, synthesis and biological evaluation of thieno[3,2-d]pyrimidine derivatives containing aroyl hydrazone or aryl hydrazide moieties for PI3K and mTOR dual inhibition. *Bioorg Chem*. 2020; 104: 104197. DOI: 10.1016/j.bioorg.2020.104197.
 82. Wang T, Wang J, Ren W, Liu ZL, Cheng YF, Zhang XM. Combination treatment with artemisinin and oxaliplatin inhibits tumorigenesis in esophageal cancer EC109 cell through Wnt/ β -catenin signaling pathway. *Thorac Cancer*. 2020; 11 (8): 2316–24. DOI: 10.1111/1759-7714.13570.
 83. Gabata R, Harada K, Mizutani Y, Ouchi H, Yoshimura K, Sato Y, et al. Anti-tumor activity of the small molecule inhibitor PRI-724 against β -catenin-activated hepatocellular carcinoma. *Anticancer Res*. 2020; 40 (9): 5211–19. DOI: 10.21873/anticancerres.14524.
 84. Shang FF, Wang JY, Xu Q, Deng H, Guo HY, Jin X, et al. Design, synthesis of novel celastrol derivatives and study on their antitumor growth through HIF-1 α pathway. *Eur J Med Chem*. 2021; 220: 113474. Available from: <https://www.sciencedirect.com/science/article/abs/pii/S0223523421003238?via%3Dihub>. DOI: 10.1016/j.ejmech.2021.113474.
 85. Ge Y, Yoon SH, Jang H, Jeong JH, Lee YM. Decursin promotes HIF-1 α proteasomal degradation and immune responses in hypoxic tumour microenvironment. *Phytomedicine*. 2020; 78: 153318. DOI:10.1016/j.phymed.2020.153318.
 86. Kang DY, Sp N, Lee JM, Jang KJ. Antitumor effects of ursolic acid through mediating the inhibition of STAT3/PD-L1 signaling in non-small cell lung cancer cells. *Biomedicines*. 2021; 9 (3): 297. DOI:10.3390/biomedicines9030297.
 87. Cui J, Li H, Wang Y, Tian T, Liu C, Wang Y, et al. Skullcapflavone I has a potent anti-pancreatic cancer activity by targeting miR-23a. *Biofactors*. 2020; 46 (5): 821–30. DOI: 10.1002/biof.1621.
 88. Houssein M, Abi Saab W, Khalil M, Khalife H, Fatfat M. Cell death by galloylation is associated with inhibition of the JAK/STAT pathway in human colon cancer cells. *Curr Ther Res Clin Exp*. 2020; 92: 100589. DOI: 10.1016/j.curtheres.2020.100589.
 89. Luo W, Sun R, Chen X, Li J, Jiang J, He Y, et al. ERK activation-mediated autophagy induction resists licochalcone a-induced anticancer activities in lung cancer cells in vitro. *Oncotargets Ther*. 2021; 13: 13437–50. DOI: 10.2147/OTT.S278268.
 90. Zhang WH, Chen S, Liu XL, Bing-Lin, Liu XW, Zhou Y. Study on antitumor activities of the chrysin-chromene-spirooxindole on Lewis lung carcinoma C57BL/6 mice in vivo. *Bioorg Med Chem Lett*. 2020; 30 (17): 127410. DOI: 10.1016/j.bmcl.2020.127410.
 91. Kwak AW, Yoon G, Lee MH, Cho SS, Shim JH, Chae JI. Picropodophyllotoxin, an epimer of podophyllotoxin, causes apoptosis of human esophageal squamous cell carcinoma cells through ROS-mediated JNK/P38 MAPK pathways. *Int J Mol Sci*. 2020; 21 (13): 4640. DOI: 10.3390/ijms21134640.
 92. Potočnjak I, Šimić L, Gobin I, Vukelić I, Domitrović R. Antitumor activity of luteolin in human colon cancer SW620 cells is mediated by the ERK/FOXO3a signaling pathway. *Toxicol In Vitro*. 2020; 66: 104852. DOI:10.1016/j.tiv.2020.104852.
 93. Brooks JD, Teraoka SN, Bernstein L, Mellemkjær L, Malone KE, Lynch CF, et al. Common variants in genes coding for chemotherapy metabolizing enzymes, transporters, and targets: a case-control study of contralateral breast cancer risk in the WECARE Study. *Cancer Causes Control*. 2013; 24 (8): 1605–14. DOI: 10.1007/s10552-013-0237-6.
 94. Bushweller JH. Targeting transcription factors in cancer — from undruggable to reality. *Nat Rev Cancer*. 2019; 19 (11): 611–24. DOI: 10.1038/s41568-019-0196-7.
 95. Lu H, Zhou Q, He J, Jiang Z, Peng C, Tong R, et al. Recent advances in the development of protein-protein interactions modulators: mechanisms and clinical trials. *Signal Transduct Target Ther*. 2020; 5 (1): 213. DOI: 10.1038/s41392-020-00315-3.
 96. Ivanov AA, Khuri FR, Fu H. Targeting protein-protein interactions as an anticancer strategy. *Trends Pharmacol Sci*. 2013; 34 (7): 393–400. DOI: 10.1016/j.tips.2013.04.007.
 97. Engin HB, Kreisberg JF, Carter H. Structure-based analysis reveals cancer missense mutations target protein interaction interfaces. *PLoS One*. 2016; 11 (4): e0152929. DOI: 10.1371/journal.pone.0152929.
 98. Porta-Pardo E, Garcia-Alonso L, Hrabe T, Dopazo J, Godzik A. A pan-cancer catalogue of cancer driver protein interaction interfaces. *PLoS Comput Biol*. 2015; 11 (10): e1004518. DOI: 10.1371/journal.pcbi.1004518.
 99. Duffy MJ, Crown J. Drugging "undruggable" genes for cancer treatment: Are we making progress? *Int J Cancer*. 2021; 148 (1): 8–17. DOI: 10.1002/ijc.33197.
 100. Santos R, Ursu O, Gaulton A, Bento AP, Donadi RS, Bologa CG, et al. A comprehensive map of molecular drug targets. *Nat Rev Drug Discov*. 2017; 16 (1): 19–34. DOI: 10.1038/nrd.2016.230.

Литература

1. Kiriiri GK, Njogu PM, Mwangi AN. Exploring different approaches to improve the success of drug discovery and development projects: a review. *Futur J Pharm Sci*. 2020; 6: 27. DOI: 10.1186/s43094-020-00047-9.
2. Gibbs JB. Mechanism-based target identification and drug discovery in cancer research. *Science*. 2000; 287 (5460): 1969–73. DOI: 10.1126/science.287.5460.1969.
3. Druker BJ. Perspectives on the development of a molecularly targeted agent. *Cancer Cell*. 2002 Feb; 1 (1): 31–6. DOI: 10.1016/s1535-6108(02)00025-9.
4. Nam NH, Parang K. Current targets for anticancer drug discovery. *Curr Drug Targets*. 2003; 4 (2): 159–79. DOI:

- 10.2174/1389450033346966.
- Haider T, Pandey V, Banjare N, Gupta PN, Soni V. Drug resistance in cancer: mechanisms and tackling strategies. *Pharmacol Rep.* 2020; 72 (5): 1125–51. DOI:10.1007/s43440-020-00138-7.
 - Devlin EJ, Denson LA, Whitford HS. Cancer treatment side effects: A meta-analysis of the relationship between response expectancies and experience. *J Pain Symptom Manage.* 2017; 54 (2): 245–58.e2. DOI:10.1016/j.jpainsymman.2017.03.017.
 - Kumar B, Singh S, Skvortsova I, Kumar V. Promising targets in anti-cancer drug development: recent updates. *Curr Med Chem.* 2017; 24 (42): 4729–52. DOI: 10.2174/0929867324666170331123648.
 - Magalhaes LG, Ferreira LLG, Andricopulo AD. Recent advances and perspectives in cancer drug design. *An Acad Bras Cienc.* 2018; 90 (1 Suppl 2): 1233–50. DOI: 10.1590/0001-3765201820170823.
 - Cui W, Aouidate A, Wang S, Yu Q, Li Y, Yuan S. Discovering anti-cancer drugs via computational methods. *Front Pharmacol.* 2020; 11: 733. DOI: 10.3389/fphar.2020.00733.
 - Özen Çınar İ. Bibliometric analysis of breast cancer research in the period 2009–2018. *Int J Nurs Pract.* 2020; 26 (3): e12845. DOI:10.1111/ijn.12845.
 - Didion CA, Henne WA. A bibliometric analysis of folate receptor research. *BMC Cancer.* 2020; 20 (1): 1109. DOI:10.1186/s12885-020-07607-5.
 - Jin B, Wu XA, Du SD. Top 100 most frequently cited papers in liver cancer: a bibliometric analysis. *ANZ J Surg.* 2020; 90 (1–2): 21–6. DOI:10.1111/ans.15414.
 - Liu W, Wu L, Zhang Y, Shi L, Yang X. Bibliometric analysis of research trends and characteristics of oral potentially malignant disorders. *Clin Oral Investig.* 2020; 24 (1): 447–54. DOI: 10.1007/s00784-019-02959-0.
 - Van Eck NJ, Waltman L. Text mining and visualization using VOSviewer. *ISSI Newsletter.* 2011; 7 (3): 50–4.
 - Tauno M, Jaak V. Clustvis: a web tool for visualizing clustering of multivariate data using Principal Component Analysis and heatmap. *Nucleic Acids Research.* 2015; 43 (W1): W566–W570, 2015. DOI: 10.1093/nar/gkv468.
 - Arnst KE, Banerjee S, Chen H, Deng S, Hwang DJ, Li W, et al. Current advances of tubulin inhibitors as dual acting small molecules for cancer therapy. *Med Res Rev.* 2019; 39 (4): 1398–426. DOI:10.1002/med.21568.
 - Chopra B, Dhingra AK, Dhar KL, Nepali K. Emerging role of terpenoids for the treatment of cancer: a review. *Mini Rev Med Chem.* 2021. Available from: <https://www.eurekaselect.com/190215/article>. DOI: 10.2174/1389557521666210112143024.
 - Kirsch P, Hartman AM, Hirsch AKH, Empting M. Concepts and core principles of fragment-based drug design. *Molecules.* 2019; 24 (23): 4309. DOI: 10.3390/molecules24234309.
 - Giacomini E, Rupiani S, Guidotti L, Recanatini M, Roberti M. The use of stilbene scaffold in medicinal chemistry and multi-target drug design. *Curr Med Chem.* 2016; 23 (23): 2439–89. DOI: 10.2174/0929867323666160517121629.
 - Hughes JP, Rees S, Kalindjian SB, Philpott KL. Principles of early drug discovery. *Br J Pharmacol.* 2011; 162 (6): 1239–49. DOI: 10.1111/j.1476-5381.2010.01127.x.
 - Lipinski CA, Lombardo F, Dominy BW, Feeney PJ. Experimental and computational approaches to estimate solubility and permeability in drug discovery and development settings. *Adv Drug Deliv Rev.* 1997; 23 (1–3): 3–25. DOI: 10.1016/S0169-409X(96)00423-1.
 - Garcia da Silva AC, Rodrigues BDS, Andrade WM, Marques Dos Santos TR, de Carvalho FS, Sanz G, et al. Antiangiogenic and antitumoral activity of LQFM126 prototype against B16F10 melanoma cells. *Chem Biol Interact.* 2020; 325: 109127. DOI: 10.1016/j.cbi.2020.109127.
 - Yamada K, Hori Y, Inoue S, Yamamoto Y, Iso K, Kamiyama H, et al. E7386, a selective inhibitor of the interaction between β -catenin and CBP, exerts antitumor activity in tumor models with activated canonical Wnt signaling. *Cancer Res.* 2021; 81 (4): 1052–62. DOI: 10.1158/0008-5472.CAN-20-0782.
 - Zhang YF, Zhang ZH, Li MY, Wang JY, Xing Y, Ri M, et al. Britannin stabilizes T cell activity and inhibits proliferation and angiogenesis by targeting PD-L1 via abrogation of the crosstalk between Myc and HIF-1 α in cancer. *Phytomedicine.* 2021; 81: 153425. DOI: 10.1016/j.phymed.2020.153425
 - Yoon SH, Kim BK, Kang MJ, Im JY, Won M. Miconazole inhibits signal transducer and activator of transcription 3 signaling by preventing its interaction with DNA damage-induced apoptosis suppressor. *Cancer Sci.* 2020 Jul; 111 (7): 2499–507. DOI: 10.1111/cas.14432. Epub 2020 May 31. PMID: 32476221; PMCID: PMC7385363.
 - Osmaniye D, Korkut Çelikeleş B, Sağlık BN, Levent S, Acar Çevik U, Kaya Çavuşoğlu B, et al. Synthesis of some new benzoxazole derivatives and investigation of their anticancer activities. *Eur J Med Chem.* 2021; 210: 112979. DOI: 10.1016/j.ejmech.2020.112979.
 - Zhang N, Wang J, Sheng A, Huang S, Tang Y, Ma S, et al. Emodin inhibits the proliferation of MCF-7 human breast cancer cells through activation of aryl hydrocarbon receptor (AhR). *Front Pharmacol.* 2021; 11: 622046. DOI: 10.3389/fphar.2020.622046.
 - Qin J, Liu J, Wu C, Xu J, Tang B, Guo K, et al. Synthesis and biological evaluation of (3/4-(pyrimidin-2-ylamino) benzoyl)-based hydrazine-1 carboxamide/carbothioamide derivatives as novel RXR α antagonists. *J Enzyme Inhib Med Chem.* 2020; 35 (1): 880–96. DOI: 10.1080/14756366.2020.1740692.
 - Zi CT, Yang L, Hu Y, Zhang P, Tang H, Zhang BL, et al. Synthesis, antitumor activity, and molecular docking of (-)-epigallocatechin-3-gallate-4 β -triazolopodophyllotoxin conjugates. *J Asian Nat Prod Res.* 2020; 1–9. DOI: 10.1080/10286020.2020.1786066.
 - Huang WY, Zhang XR, Lyu L, Wang SQ, Zhang XT. Pyridazino[1,6-b]quinazolinones as new anticancer scaffold: synthesis, DNA intercalation, topoisomerase I inhibition and antitumor evaluation in vitro and in vivo. *Bioorg Chem.* 2020; 99: 103814. DOI: 10.1016/j.bioorg.2020.103814.
 - Karatas E, Foto E, Ertan-Bolelli T, Yalcin-Ozkat G, Yilmaz S, Ateci S, et al. Discovery of 5-(or 6)-benzoxazoles and oxazolo[4,5-b]pyridines as novel candidate antitumor agents targeting hTopo II α . *Bioorg Chem.* 2021; 112: 104913. DOI: 10.1016/j.bioorg.2021.104913.
 - Fukuda T, Nanjo Y, Fujimoto M, Yoshida K, Natsui Y, Ishibashi F, et al. Lamellarin-inspired potent topoisomerase I inhibitors with the unprecedented benzo[g][1]benzopyrano[4,3-b]indol-6(13H)-one scaffold. *Bioorg Med Chem.* 2019; 27 (2): 265–77. DOI: 10.1016/j.bmc.2018.11.037.
 - Acar Çevik U, Sağlık BN, Osmaniye D, Levent S, Kaya Çavuşoğlu B, Karaduman AB, et al. Synthesis, anticancer evaluation and molecular docking studies of new benzimidazole-1,3,4-oxadiazole derivatives as human topoisomerase types I poison. *J Enzyme Inhib Med Chem.* 2020; 35 (1): 1657–73. DOI: 10.1080/14756366.2020.1806831.
 - Song Y, Feng S, Feng J, Dong J, Yang K, Liu Z, et al. Synthesis and biological evaluation of novel pyrazoline derivatives containing indole skeleton as anti-cancer agents targeting topoisomerase II. *Eur J Med Chem.* 2020; 200: 112459. DOI: 10.1016/j.ejmech.2020.112459.
 - Al-Wahaibi LH, Gouda AM, Abou-Ghadir OF, Salem OIA, Ali AT, Farghaly HS, et al. Design and synthesis of novel 2,3-dihydropyrazino[1,2-a]indole-1,4-dione derivatives as antiproliferative EGFR and BRAFV600E dual inhibitors. *Bioorg Chem.* 2020; 104: 104260. DOI: 10.1016/j.bioorg.2020.104260.
 - Eissa IH, Ibrahim MK, Metwaly AM, Belal A, Mehany ABM, Abdelhady AA, et al. Design, molecular docking, in vitro, and in vivo studies of new quinazolin-4(3H)-ones as VEGFR-2 inhibitors with potential activity against hepatocellular carcinoma. *Bioorg Chem.* 2021; 107: 104532. DOI: 10.1016/j.bioorg.2020.104532.
 - Dai MD, Wang YL, Fan J, Dai Y, Ji YC, Sun YM, et al. DW14383 is an irreversible pan-FGFR inhibitor that suppresses FGFR-dependent tumor growth in vitro and in vivo. *Acta Pharmacol Sin.* 2020. Available from: <https://www.nature.com/articles/s41401-020-00567-3>. DOI: 10.1038/s41401-020-00567-3.
 - Ahmed MF, Santali EY, El-Hagggar R. Novel piperazine-chalcone hybrids and related pyrazoline analogues targeting VEGFR-2 kinase; design, synthesis, molecular docking studies, and anticancer evaluation. *J Enzyme Inhib Med Chem.* 2021; 36 (1): 307–18. DOI: 10.1080/14756366.2020.1861606.
 - Zhuo LS, Wu FX, Wang MS, Xu HC, Yang FP, Tian YG, et al. Structure-activity relationship study of novel quinazoline-based

- 1,6-naphthylidines as MET inhibitors with potent antitumor efficacy. *Eur J Med Chem.* 2020; 208: 112785. DOI: 10.1016/j.ejmech.2020.112785.
40. Nan X, Zhang J, Li HJ, Wu R, Fang SB, Zhang ZZ, et al. Design, synthesis and biological evaluation of novel N-sulfonylamidine-based derivatives as c-Met inhibitors via Cu-catalyzed three-component reaction. *Eur J Med Chem.* 2020; 200: 112470. DOI: 10.1016/j.ejmech.2020.112470.
41. Krishan S, Sahni S, Richardson DR. The anti-tumor agent, Dp44mT, promotes nuclear translocation of TFEB via inhibition of the AMPK-mTORC1 axis. *Biochim Biophys Acta Mol Basis Dis.* 2020; 1866 (12): 165970. DOI: 10.1016/j.bbdis.2020.165970.
42. Cullen JK, Boyle GM, Yap PY, Elminger S, Simmons JL, Broit N, et al. Activation of PKC supports the anticancer activity of tigilanol tiglate and related epoxytigilanes. *Sci Rep.* 2021; 11 (1): 207. DOI: 10.1038/s41598-020-80397-9.
43. Wagner E, Wietrzyk J, Psurski M, Becan L, Turlej E. Synthesis and anticancer evaluation of novel derivatives of isoxazolo[4,5-e][1,2,4]triazepine derivatives and potential inhibitors of protein kinase C. *ACS Omega.* 2020; 6 (1): 119–34. DOI:10.1021/acsomega.0c03801.
44. Gilles P, Kashyap RS, Freitas MJ, Ceusters S, Van Asch K, Janssens A, et al. Design, synthesis and biological evaluation of pyrazolo[3,4-d]pyrimidine-based protein kinase D inhibitors. *Eur J Med Chem.* 2020; 205: 112638. DOI: 10.1016/j.ejmech.2020.112638.
45. Sootome H, Miura A, Masuko N, Suzuki T, Uto Y, Hirai H, et al. Inhibitor TAS-119 enhances antitumor efficacy of taxanes in vitro and in vivo: preclinical studies as guidance for clinical development and trial design. *Mol Cancer Ther.* 2020; 19 (10): 1981–91. DOI: 10.1158/1535-7163.MCT-20-0036.
46. Kar S, Ramamoorthy G, Mitra K, Shivalingegowda N, Mahesha, Mavileti SK, et al. Synthesis of novel spirobenzopyrans as potent anticancer leads inducing apoptosis in HeLa cells. *Bioorg Med Chem Lett.* 2020; 30 (12): 127199. DOI: 10.1016/j.bmcl.2020.127199.
47. Massaro M, Barone G, Barra V, Cancemi P, Di Leonardo A, Grossi G, et al. Pyrazole[3,4-d]pyrimidine derivatives loaded into halloysite as potential CDK inhibitors. *Int J Pharm.* 2021; 599: 120281. DOI: 10.1016/j.ijpharm.2021.120281.
48. Ismail MI, Mohamady S, Samir N, Abouzid KAM. Design, synthesis, and biological evaluation of novel 7H-[1,2,4]triazolo[3,4-b][1,3,4]thiadiazine inhibitors as antitumor agents. *ACS Omega.* 2020; 5 (32): 20170–86. DOI: 10.1021/acsomega.0c01829.
49. Zhang ZY, Dong SM, Liu YH, Zhang MM, Zhang JK, Zhu HJ, et al. Enhanced anticancer activity by the combination of vinpocetine and sorafenib via PI3K/AKT/GSK-3 β signaling axis in hepatocellular carcinoma cells. *Anticancer Drugs.* 2021. Available from: https://journals.lww.com/anti-cancerdrugs/Abstract/2021/09000/Enhanced_antitumor_activity_by_the_combination_of.7.aspx. DOI: 10.1097/CAD.0000000000001056.
50. Zeytün E, Altıntop MD, Sever B, Özdemir A, Ellakwa DE, Ocak Z, et al. A new series of antileukemic agents: design, synthesis, in vitro and in silico evaluation of thiazole-based abl1 kinase inhibitors. *Anticancer Agents Med Chem.* 2021; 21 (9): 1099–109. DOI: 10.2174/1871520620666200824100408.
51. Wang Y, Lv Z, Chen F, Wang X, Gou S. Discovery of 5-(3-chlorophenylamino) benzo[c][2,6] naphthyridine derivatives as highly selective ck2 inhibitors with potent cancer cell stemness inhibition. *J Med Chem.* 2021; 64 (8): 5082–98. DOI: 10.1021/acs.jmedchem.1c00131.
52. Yang H, Wang X, Wang C, Yin F, Qu L, Shi C et al. Optimization of WZ4003 as NUAk inhibitors against human colorectal cancer. *Eur J Med Chem.* 2021; 210: 113080. DOI: 10.1016/j.ejmech.2020.113080.
53. Wu Q, Chen DQ, Sun L, Huan XJ, Bao XB, Tian CQ et al. Novel bivalent BET inhibitor N2817 exhibits potent anticancer activity and inhibits TAF1. *Biochem Pharmacol.* 2021; 185: 114435. DOI: 10.1016/j.bcp.2021.114435.
54. Gan L, Gan Z, Dan Y, Li Y, Zhang P, Chen S, et al. Tetrazanbigen derivatives as peroxisome proliferator-activated receptor gamma (ppary) partial agonists: design, synthesis, structure-activity relationship, and anticancer activities. *J Med Chem.* 2021; 64 (2): 1018–36. DOI: 10.1021/acs.jmedchem.0c01512.
55. Zhang D, Sun G, Peng L, Tian J, Zhang H. Calycosin inhibits viability, induces apoptosis, and suppresses invasion of cervical cancer cells by upregulating tumor suppressor miR-375. *Arch Biochem Biophys.* 2020; 691: 108478. DOI: 10.1016/j.abb.2020.108478.
56. Szczuka I, Wiśniewski J, Kustrzeba-Wójcicka I, Terlecki G. The effect of 3-bromopyruvate on the properties of cathepsin B in the aspect of metastatic potential of colon cancer cells. *Adv Clin Exp Med.* 2020; 29 (8): 949–57. DOI: 10.17219/acem/123622. PMID: 32820873.
57. Ge Y, Yoon SH, Jang H, Jeong JH, Lee YM. Decursin promotes HIF-1 α proteasomal degradation and immune responses in hypoxic tumour microenvironment. *Phytomedicine.* 2020; 78: 153318. DOI: 10.1016/j.phymed.2020.153318.
58. Tabatabaei Dakhili SA, Pérez DJ, Gopal K, Haque M, Ussher JR, Kashfi K, et al. SP1-independent inhibition of FOXM1 by modified thiazolidinediones. *Eur J Med Chem.* 2021; 209: 112902. DOI: 10.1016/j.ejmech.2020.112902.
59. Liu Y, Peng X, Li H, Jiao W, Peng X, Shao J, et al. STAT3 inhibitor napabucasin inhibits tumor growth and cooperates with proteasome inhibition in human ovarian cancer cells. *Recent Pat Anticancer Drug Discov.* 2021. DOI: 10.2174/1574892816666210224155403.
60. Wang X, Wu K, Fang L, Yang X, Zheng N, Du Z, et al. Discovery of N-substituted sulfamoylbenzamide derivatives as novel inhibitors of STAT3 signaling pathway based on Niclosamide. *Eur J Med Chem.* 2021; 218:113362. DOI: 10.1016/j.ejmech.2021.113362.
61. Zhang J, Li C, Zhang L, Heng Y, Xu T, Zhang Y, et al. Andrographolide induces noxa-dependent apoptosis by transactivating atf4 in human lung adenocarcinoma cells. *Front Pharmacol.* 2021; 12: 680589. DOI:10.3389/fphar.2021.680589.
62. Ibrahim TS, Hawwas MM, Taher ES, Alhakamy NA, Alfaleh MA, Elagawany M, et al. Design and synthesis of novel pyrazolo[3,4-d]pyrimidin-4-one bearing quinoline scaffold as potent dual PDE5 inhibitors and apoptotic inducers for cancer therapy. *Bioorg Chem.* 2020; 105: 104352. DOI: 10.1016/j.bioorg.2020.104352.
63. Abosharaf HA, Diab T, Atlam FM, Mohamed TM. Osteone extracted from a citrus fruit that affects apoptosis on A549 cell line by histone deacetylase inhibition (HDACs). *Biotechnol Rep (Amst).* 2020; 28: e00531. DOI: 10.1016/j.btre.2020.e00531.
64. Xie Z, Wang F, Lin L, Duan S, Liu X, Li X, et al. An SGLT2 inhibitor modulates SHH expression by activating AMPK to inhibit the migration and induce the apoptosis of cervical carcinoma cells. *Cancer Lett.* 2020; 495: 200–10. DOI: 10.1016/j.canlet.2020.09.005.
65. Watanabe S, Nishijima N, Hirai K, Shibata K, Hase A, Yamanaka T, et al. Anticancer activity of amb4269951, a choline transporter-like protein 1 inhibitor, in human glioma cells. *Pharmaceuticals (Basel).* 2020; 13 (5): 104. DOI: 10.3390/ph13050104.
66. Hyun SY, Le HT, Min HY, Pei H, Lim Y, Song I, et al. Evodiamine inhibits both stem cell and non-stem-cell populations in human cancer cells by targeting heat shock protein 70. *Theranostics.* 2021; 11 (6): 2932–52. DOI: 10.7150/thno.49876.
67. Tentori L, Dorio AS, Mazzon E, Muzi A, Sau A, Cuzzocrea S, et al. The glutathione transferase inhibitor 6-(7-nitro-2,1,3-benzoxadiazol-4-ylthio)hexanol (NBDHEX) increases temozolomide efficacy against malignant melanoma. *Eur J Cancer.* 2011; 47(8): 1219–30. DOI: 10.1016/j.ejca.2010.12.008.
68. Altamura G, Degli Uberti B, Galiero G, De Luca G, Power K, Licenziato L, et al. The small molecule BIBR1532 exerts potential anti-cancer activities in preclinical models of feline oral squamous cell carcinoma through inhibition of telomerase activity and down-regulation of TERT. *Front Vet Sci.* 2021; 7: 620776. DOI: 10.3389/fvets.2020.620776.
69. Wang J, Iannarelli R, Pucciarelli S, Laudadio E, Galeazzi R, Giangrossi M, et al. Acetylshikonin isolated from *Lithospermum erythrorhizon* roots inhibits dihydrofolate reductase and hampers autochthonous mammary carcinogenesis in Δ 16HER2 transgenic mice. *Pharmacol Res.* 2020; 161: 105123. DOI: 10.1016/j.phrs.2020.105123.
70. Ding W, Zhang H, Mei G. Synergistic antitumor activity of DHA and JQ1 in colorectal carcinoma. *Eur J Pharmacol.* 2020; 885:

173500. DOI: 10.1016/j.ejphar.2020.173500.
71. Yuan LW, Jiang XM, Xu YL, Huang MY, Chen YC, Yu WB, et al. Licochalcone A inhibits interferon-gamma-induced programmed death-ligand 1 in lung cancer cells. *Phytomedicine*. 2021; 80: 153394. DOI:10.1016/j.phymed.2020.153394.
 72. Boichuk S, Galebikova A, Bikinieva F, Dunaev P, Aukhadieva A, Syuzov K, et al. 2-APCAs, the novel microtubule targeting agents active against distinct cancer cell lines. *Molecules*. 2021; 26 (3): 616. DOI: 10.3390/molecules26030616.
 73. Lin S, Liang Y, Cheng J, Pan F, Wang Y. Novel diaryl-2H-azirines: Antitumor hybrids for dual-targeting tubulin and DNA. *Eur J Med Chem*. 2021; 214: 113256. DOI: 10.1016/j.ejmech.2021.113256.
 74. Sardaru MC, Craciun AM, Al Matarneh CM, Sandu IA, Amarandi RM, Popovici L, et al. Cytotoxic substituted indolizines as new colchicine site tubulin polymerisation inhibitors. *J Enzyme Inhib Med Chem*. 2020; 35 (1): 1581–95. DOI: 10.1080/14756366.2020.1801671.
 75. Li X, Liu Y, Zhao Y, Tian W, Zhai L, Pang H, et al. Rhein derivative 4f inhibits the malignant phenotype of breast cancer by downregulating Rac1 protein. *Front Pharmacol*. 2020; 11: 754. DOI: 10.3389/fphar.2020.00754.
 76. Yao Y, Yao QY, Xue JS, Tian XY, An QM, Cui LX, et al. Dexamethasone inhibits pancreatic tumor growth in preclinical models: Involvement of activating glucocorticoid receptor. *Toxicol Appl Pharmacol*. 2020; 401: 115118. DOI: 10.1016/j.taap.2020.115118.
 77. Wang SS, Zhang QL, Chu P, Kong LQ, Li GZ, Li YQ, et al. Synthesis and antitumor activity of α,β -unsaturated carbonyl moiety-containing oleanolic acid derivatives targeting PI3K/AKT/mTOR signaling pathway. *Bioorg Chem*. 2020; 101: 104036. DOI: 10.1016/j.bioorg.2020.104036.
 78. Liu H, Li X, Duan Y, Xie JB, Piao XL. Mechanism of gypenosides of *Gynostemma pentaphyllum* inducing apoptosis of renal cell carcinoma by PI3K/AKT/mTOR pathway. *J Ethnopharmacol*. 2021; 271: 113907. DOI: 10.1016/j.jep.2021.113907.
 79. Li X, Zhao J, Yan T, Mu J, Lin Y, Chen J, et al. Cyanidin-3-O-glucoside and cisplatin inhibit proliferation and downregulate the PI3K/AKT/mTOR pathway in cervical cancer cells. *J Food Sci*. 2021. Available from: <https://onlinelibrary.wiley.com/doi/10.1111/1750-3841.15740>. DOI: 10.1111/1750-3841.15740.
 80. Ma W, Zhang Q, Li X, Ma Y, Liu Y, Hu S, et al. IPM712, a vanillin derivative as potential antitumor agents, displays better antitumor activity in colorectal cancers cell lines. *Eur J Pharm Sci*. 2020; 152: 105464. DOI: 10.1016/j.ejps.2020.105464.
 81. Han Y, Tian Y, Wang R, Fu S, Jiang J, Dong J, et al. Design, synthesis and biological evaluation of thieno[3,2-d]pyrimidine derivatives containing aroyl hydrazone or aryl hydrazide moieties for PI3K and mTOR dual inhibition. *Bioorg Chem*. 2020; 104: 104197. DOI: 10.1016/j.bioorg.2020.104197.
 82. Wang T, Wang J, Ren W, Liu ZL, Cheng YF, Zhang XM. Combination treatment with artemisinin and oxaliplatin inhibits tumorigenesis in esophageal cancer EC109 cell through Wnt/ β -catenin signaling pathway. *Thorac Cancer*. 2020; 11 (8): 2316–24. DOI: 10.1111/1759-7714.13570.
 83. Gabata R, Harada K, Mizutani Y, Ouchi H, Yoshimura K, Sato Y, et al. Anti-tumor activity of the small molecule inhibitor PRI-724 against β -catenin-activated hepatocellular carcinoma. *Anticancer Res*. 2020; 40 (9): 5211–19. DOI: 10.21873/anticancer.14524.
 84. Shang FF, Wang JY, Xu Q, Deng H, Guo HY, Jin X, et al. Design, synthesis of novel celastrol derivatives and study on their antitumor growth through HIF-1 α pathway. *Eur J Med Chem*. 2021; 220: 113474. Available from: <https://www.sciencedirect.com/science/article/abs/pii/S0223523421003238?via%3Dihub>. DOI: 10.1016/j.ejmech.2021.113474.
 85. Ge Y, Yoon SH, Jang H, Jeong JH, Lee YM. Decursin promotes HIF-1 α proteasomal degradation and immune responses in hypoxic tumour microenvironment. *Phytomedicine*. 2020; 78: 153318. DOI:10.1016/j.phymed.2020.153318.
 86. Kang DY, Sp N, Lee JM, Jang KJ. Antitumor effects of ursolic acid through mediating the inhibition of STAT3/PD-L1 signaling in non-small cell lung cancer cells. *Biomedicine*. 2021; 9 (3): 297. DOI:10.3390/biomedicine9030297.
 87. Cui J, Li H, Wang Y, Tian T, Liu C, Wang Y, et al. Skullcapflavone I has a potent anti-pancreatic cancer activity by targeting miR-23a. *Biofactors*. 2020; 46 (5): 821–30. DOI: 10.1002/biof.1621.
 88. Houssein M, Abi Saab W, Khalil M, Khalife H, Fattat M. Cell death by gallotannin is associated with inhibition of the JAK/STAT pathway in human colon cancer cells. *Curr Ther Res Clin Exp*. 2020; 92: 100589. DOI: 10.1016/j.curtheres.2020.100589.
 89. Luo W, Sun R, Chen X, Li J, Jiang J, He Y, et al. ERK activation-mediated autophagy induction resists licochalcone a-induced anticancer activities in lung cancer cells in vitro. *Onco Targets Ther*. 2021; 13: 13437–50. DOI: 10.2147/OTT.S278268.
 90. Zhang WH, Chen S, Liu XL, Bing-Lin, Liu XW, Zhou Y. Study on antitumor activities of the chrysin-chromene-spirooxindole on Lewis lung carcinoma C57BL/6 mice in vivo. *Bioorg Med Chem Lett*. 2020; 30 (17): 127410. DOI: 10.1016/j.bmcl.2020.127410.
 91. Kwak AW, Yoon G, Lee MH, Cho SS, Shim JH, Chae JI. Picropodophyllotoxin, an epimer of podophyllotoxin, causes apoptosis of human esophageal squamous cell carcinoma cells through ROS-mediated JNK/P38 MAPK pathways. *Int J Mol Sci*. 2020; 21 (13): 4640. DOI: 10.3390/ijms21134640.
 92. Potočnjak I, Šimić L, Gobin I, Vukelić I, Domitrović R. Antitumor activity of luteolin in human colon cancer SW620 cells is mediated by the ERK/FOXO3a signaling pathway. *Toxicol In Vitro*. 2020; 66: 104852. DOI:10.1016/j.tiv.2020.104852.
 93. Brooks JD, Teraoka SN, Bernstein L, Mellekmjær L, Malone KE, Lynch CF, et al. Common variants in genes coding for chemotherapy metabolizing enzymes, transporters, and targets: a case-control study of contralateral breast cancer risk in the WECARE Study. *Cancer Causes Control*. 2013; 24 (8): 1605–14. DOI: 10.1007/s10552-013-0237-6.
 94. Bushweller JH. Targeting transcription factors in cancer — from undruggable to reality. *Nat Rev Cancer*. 2019; 19 (11): 611–24. DOI: 10.1038/s41568-019-0196-7.
 95. Lu H, Zhou Q, He J, Jiang Z, Peng C, Tong R, et al. Recent advances in the development of protein-protein interactions modulators: mechanisms and clinical trials. *Signal Transduct Target Ther*. 2020; 5 (1): 213. DOI: 10.1038/s41392-020-00315-3.
 96. Ivanov AA, Khuri FR, Fu H. Targeting protein-protein interactions as an anticancer strategy. *Trends Pharmacol Sci*. 2013; 34 (7): 393–400. DOI: 10.1016/j.tips.2013.04.007.
 97. Engin HB, Kreisberg JF, Carter H. Structure-based analysis reveals cancer missense mutations target protein interaction interfaces. *PLoS One*. 2016; 11 (4): e0152929. DOI: 10.1371/journal.pone.0152929.
 98. Porta-Pardo E, Garcia-Alonso L, Hrabe T, Dopazo J, Godzik A. A pan-cancer catalogue of cancer driver protein interaction interfaces. *PLoS Comput Biol*. 2015; 11 (10): e1004518. DOI: 10.1371/journal.pcbi.1004518.
 99. Duffy MJ, Crown J. Drugging "undruggable" genes for cancer treatment: Are we making progress? *Int J Cancer*. 2021; 148 (1): 8–17. DOI: 10.1002/ijc.33197.
 100. Santos R, Ursu O, Gaulton A, Bento AP, Donadi RS, Bologa CG, et al. A comprehensive map of molecular drug targets. *Nat Rev Drug Discov*. 2017; 16 (1): 19–34. DOI: 10.1038/nrd.2016.230.

EVALUATION OF AVIAN ADENOVIRUS INACTIVATION METHODS USED IN THE PRODUCTION OF INFLUENZA VACCINES

Savina NN¹✉, Ekimov AA¹, Trukhin VP¹, Evtushenko AE¹, Zhirenkina EN¹, Sinegubova EO², Slita AV²

¹ Saint Petersburg Research Institute of Vaccines and Serums, FMBA, Russia

² Saint Petersburg Pasteur Research Institute of Epidemiology and Microbiology, Saint Petersburg, Russia

Inactivation of influenza virus and other potential contaminants like avian adenoviruses coming from embryonated chicken eggs is a critical step in the production of inactivated influenza vaccines. Inactivation must lead to a guaranteed reduction in contaminant titers by at least 4 lg (PFU)/ml. The aim of this study was to identify an optimum cell line for adenovirus propagation and to estimate a reduction in adenovirus titers in vaccine intermediates after inactivation. In a series of experiments, we identified the optimum conditions and the optimum cell line for the propagation of avian adenovirus (strains CELO and Fontes). The most commonly used inactivation methods were analyzed, including inactivation by β -propiolactone and UV light. Viral titers were measured by plaque assays. After 10 h of inactivation with β -propiolactone, CELO titers fell by 4.12 ± 0.06 lg, whereas Fontes titers, by 4.20 ± 0.19 lg, suggesting that β -propiolactone is an effective inactivating agent. Exposure to UV light led to a reduction in CELO titers by 4.69 ± 0.89 lg and a reduction in Fontes titers by 4.44 ± 1.06 lg after 5 min. N-octyl- β -D-glucopyranoside added at the splitting step reduced CELO titers by 0.93 ± 0.15 lg and Fontes titers by 1.04 ± 0.12 lg, whereas tetradecyltrimethylammonium bromide led to a reduction in CELO and Fontes titers by 1.18 ± 0.17 lg and 1.12 ± 0.38 lg, respectively.

Keywords: influenza vaccine, inactivation, avian adenovirus, propiolactone, UV radiation

Author contribution: all authors have equally contributed to the methodology of the study, analysis and interpretation of the results and manuscript preparation.

Compliance with ethical standards: the study complied with the principles of the Declaration of Helsinki (1964) and its revisions.

✉ **Correspondence should be addressed:** Natalya N. Savina
Svobody, 52, Krasnoye Selo, Saint Petersburg, 198320; n.n.savina@spbniivs.ru

Received: 18.08.2021 **Accepted:** 12.09.2021 **Published online:** 26.09.2021

DOI: 10.47183/mes.2021.032

ОЦЕНКА МЕТОДОВ ИНАКТИВИРОВАНИЯ АДЕНОВИРУСА ПТИЦ ПРИ ПРОИЗВОДСТВЕ ГРИППОЗНЫХ ВАКЦИН

Н. Н. Савина¹✉, А. А. Екимов¹, В. П. Трухин¹, А. Э. Евтушенко¹, Е. Н. Жиренкина¹, Е. О. Синегубова², А. В. Слита²

¹ Санкт-Петербургский научно-исследовательский институт вакцин и сывороток и предприятие по производству бактериальных препаратов Федерального медико-биологического агентства, Санкт-Петербург, Россия

² Санкт-Петербургский научно-исследовательский институт эпидемиологии и микробиологии имени Пастера, Санкт-Петербург, Россия

При производстве инактивированных гриппозных вакцин на стадии инактивации должен быть инактивирован как вирус гриппа, так и возможные вирусные контаминанты (например, аденовирус птиц), которые могут попасть в вакцину из сырья (куриных эмбрионов). Инактиваторы должны обеспечивать гарантированное снижение вирусной нагрузки контаминанта не менее чем на 4 lg (БОЕ)/мл, что обеспечит его отсутствие в готовой вакцине. Целью работы было выбрать клеточную линию для наработки аденовируса и оценить снижение титра аденовируса в полупродуктах гриппозных вакцин при воздействии инактиваторов. Были подобраны оптимальные условия наработки аденовируса птиц штаммов CELO и Fontes в культуре клеток, в качестве оптимальной выбрана культура клеток Vero; рассмотрены основные используемые инактиваторы: β -пропиолактон и УФ-излучение. Титры аденовируса определяли методом бляшкообразования. Спустя 10 ч инактивации β -пропиолактоном аденовирус штамма CELO показал снижение вирусной нагрузки на $4,12 \pm 0,06$ lg, а аденовирус штамма Fontes — на $4,20 \pm 0,19$ lg, что указывает на эффективное действие β -пропиолактона при инактивации. Проведение инактивации УФ-излучением позволяет снизить вирусную нагрузку штамма CELO на $4,69 \pm 0,89$ lg, а штамма Fontes — на $4,44 \pm 1,06$ lg за 5 мин. Отмечено, что добавление детергента на стадии расщепления также снижает вирусную нагрузку на $0,93 \pm 0,15$ lg и $1,04 \pm 0,12$ lg для штаммов CELO и Fontes соответственно при использовании н-октил- β -D-глюкопиранозиды и на $1,18 \pm 0,17$ lg и $1,12 \pm 0,38$ lg при использовании тетрадецилтриметиламмоний бромида.

Ключевые слова: гриппозные вакцины, инактивация, аденовирус птиц, пропиолактон, УФ-излучение

Вклад авторов: все авторы внесли равнозначный вклад в разработку методики исследования, получение, анализ и интерпретацию данных, в написание и редактирование статьи.

Соблюдение этических стандартов: исследование проведено с соблюдением этических принципов Хельсинкской декларации Всемирной медицинской ассоциации 1964 г. и последующих ее пересмотров.

✉ **Для корреспонденции:** Наталья Николаевна Савина
ул. Свободы, д. 52, г. Красное Село, г. Санкт-Петербург, 198320; n.n.savina@spbniivs.ru

Статья получена: 18.08.2021 **Статья принята к печати:** 12.09.2021 **Опубликована онлайн:** 26.09.2021

DOI: 10.47183/mes.2021.032

One of the key steps in the production of inactivated influenza vaccines is influenza virus inactivation for the safety of the final product. The World Health Organization and the European Medicines Agency [1, 2] require that influenza virus should be completely inactivated during this step. It is known that vaccine intermediates can potentially contain other contaminants like avian leukosis virus, avian adenoviruses and mycoplasmas. So, the guidelines prescribe that the inactivation step should be effective against these pathogens, too.

Technologically, inactivation can be achieved by physical or chemical methods. The most widespread physical method is irradiation with ultraviolet light; one of the commonly used chemical methods is exposure to alkylating agents, such as β -propiolactone [3].

Avian adenoviruses cause a chronic infection in birds and are lethal for chicken embryos (CE). Avian adenoviruses are members of the Aviadenovirus genus. So far, 12 serologically distinct types of avian adenoviruses from CELO (Chicken

Embryo Lethal Orphan) and GAL (Gallus Adeno-Like) virus groups are recognized; one more serotype is represented by the causative agent of the egg drop syndrome (EDS-76) [4].

In chickens, adenovirus infection manifests as inclusion body hepatitis, hepatitis-hydropericardium syndrome, gizzard erosion, respiratory conditions, growth retardation, and joint inflammation [5].

Avian adenovirus infection often develops as a secondary infection in poultry with infectious bronchitis, mycoplasma infection and other respiratory diseases.

Now and then, outbreaks of avian adenovirus infection occur on poultry farms across Russia [6, 7].

According to the literature, adenoviruses can be inactivated with formaldehyde [8]; however, the efficacy of this method has been tested on influenza virus and adenoviruses propagated in MDCK cells; therefore, the results cannot be extrapolated to the egg-based technology of influenza vaccine production. It is known that formaldehyde reduces the immunogenicity of the final vaccine to a much greater extent than β -propiolactone; besides, β -propiolactone inactivates influenza more effectively [9].

As an inactivating agent, β -propiolactone is preferred over formaldehyde because β -propiolactone hydrolyzes to 3-hydroxypropionic acid, an intermediate product of lipid metabolism in humans [10]; this has a beneficial effect on vaccine safety.

The aim of this study was to find an optimum virucidal agent for the inactivation of influenza vaccine contaminants (CELO and GAL viruses) and to determine the minimum inactivation time needed for a guaranteed reduction in viral titers by at least 4 lg (PFU)/ml [11].

METHODS

Material

The avian adenovirus from the Adenoviridae family, Aviadenovirus, Fowl adenovirus A, Fowl adenovirus 1, strain: Phelps (CELO), ATCC VR-432 (ATCC collection; USA).

The avian adenovirus from the Adenoviridae family, Aviadenovirus, Fowl adenovirus D, Fowl adenovirus 2, strain: Fontes, ATCC VR-280 (ATCC collection; USA).

HEp-2 cells (collection of cell cultures of Saint Petersburg Pasteur Research Institute of Epidemiology and Microbiology; Russia).

MA-104 cells (collection of cell cultures of Saint Petersburg Pasteur Research Institute of Epidemiology and Microbiology; Russia).

Vero cells (collection of cell cultures of Saint Petersburg Pasteur Research Institute of Epidemiology and Microbiology; Russia).

Cultivation of CELO and Fontes viruses and measurement of infectious titers

The optimum cell culture for the propagation of adenoviruses was selected from 3 candidate cell lines: Vero B, MA-104 and HEp-2. The cells were cultured in the alpha-MEM growth medium supplemented with Gibco's heat-inactivated

fetal bovine serum (10%), 2 mM L-glutamine and 100 μ g/ml gentamicin. The maintenance medium used in the experiment contained 2% FBS, as opposed to 10% FBS in the growth medium. The cells were seeded at 500,000 cells/ml and grown overnight in culture flasks (surface area: 25 cm²) at 37 °C and 5% CO₂ until a monolayer was formed.

The cell cultures were infected with Phelps or Fontes strains and grown at 37 °C and 5% CO₂ until 80–90% of the monolayer was destroyed. The flasks were frozen at –20 °C; after thawing, adenovirus titers were determined as described below.

The cells were plated in 24-well plates at 500,000 cells/ml and cultured overnight at 37 °C and 5% CO₂ until a monolayer was formed. Then, the cells were infected with serial tenfold dilutions (from 10⁻¹ to 10⁻⁷) of the viral stocks and incubated for 30 min at room temperature. After that, the cells were washed in culture medium; MEM was mixed with Avicel (SigmaAldrich; USA) at a 1 : 1 ratio and added to the washed cells. Then, the cells were incubated for 96 h at 37 °C and 5% CO₂. After that, the cells were stained with 1 ml of 0.1% alcohol crystal violet for 15 min, washed with distilled water, dried at room temperature, and viral plaques were counted in each well. Based on the obtained counts, viral titers were determined using a method proposed by Reed and Muench [12]; the titers were expressed as PFU/ml.

Virus-containing allantoic fluid

Influenza virus was cultured in 9–11-day old embryonated chicken eggs. The embryos were challenged with 102,0–104,5 EID₅₀/0.2 ml. The eggs inoculated with type A influenza virus were incubated at 35 °C for 48 h; those infected with type B influenza virus were incubated for 72 h. After incubation, the eggs were cooled and the virus-containing allantoic fluid (AF) was harvested.

Viral concentrates (VC)

AF was filtered through a cascade of 10, 6 and 1 μ m filters and run through a 300 kDa ultrafiltration unit. The obtained concentrate was centrifuged in a sucrose density gradient (60–20%). Then, 40–25% gradient fractions were collected.

Statistical analysis

Statistical analysis was conducted in Microsoft Excel 365 (Microsoft corp.; USA) and Minitab 19 (Minitab Inc.; USA) and involved calculation of 95% confidence intervals.

RESULTS

Optimum cell line for avian adenovirus production

Three candidate cell lines were tested: Vero, MA-104 and HEp-2. These are the most commonly used cell lines for the propagation of adenoviruses. The infectious titers of CELO and Fontes viruses cultured in these cell lines are provided in Table 1.

Both adenoviruses propagated in Vero cells more effectively than in MA-104 and HEp-2: their titers in Vero cells were by at

Table 1. Infectious titers of CELO and Fontes adenoviruses cultured in different cell lines

Virus	Infectious titers, PFU/ml		
	Vero	HEp-2	MA-104
CELO	4.3 ± 2.3 × 10 ⁶	6.5 ± 3.0 × 10 ³	1.1 ± 0.2 × 10 ³
Fontes	3.3 ± 1.5 × 10 ⁶	9.7 ± 3.8 × 10 ³	2.0 ± 0.7 × 10 ³

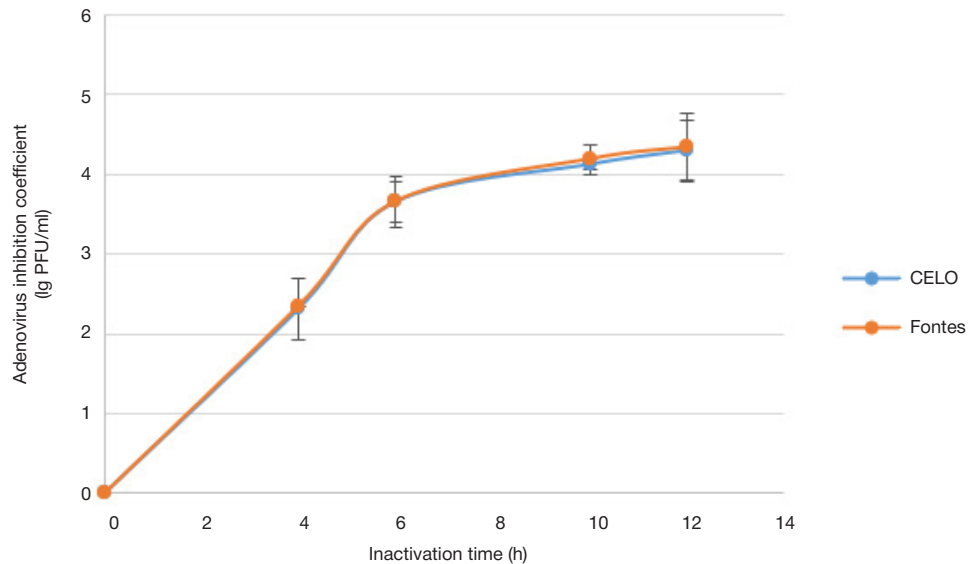


Fig. 1. Dynamics of CELO and Fontes inactivation in the presence of β-propiolactone

least 2 lg higher. In other words, Vero cells turned out to be the most permissive cells for both studied avian adenoviruses.

Dynamics of avian adenovirus inactivation in allantoic fluid by β-propiolactone

To model inactivation of avian adenoviruses in allantoic fluid by β-propiolactone, the titrated viral stock (10% of the AF volume) was added to AF so that the final viral titer was at least 10⁵ PFU/ml. The mixture was inactivated with β-propiolactone (0.09% in the final mixture) and viral titers were measured in the samples. Inactivation dynamics are shown in Fig. 1.

A reduction in viral titers by at least 4 lg PFU/ml occurred no sooner than 10 h after adding β-propiolactone; in other words, allantoic fluid used in the production of influenza vaccines should be exposed to β-propiolactone for inactivation for at least 10 h.

Dynamics of avian adenovirus inactivation in virus concentrates by exposure to UV light

To model inactivation of avian adenoviruses in VC by irradiation with UV light, the titrated viral stock (10% of the VC volume) was added to VC so that the final viral titer was at least 10⁵

PFU/ml. Contaminated VC was placed in 90 mm Petri dishes. The dishes were exposed to 4 UV lamps (total power: 60 W) installed at a 20 cm distance from the dishes. The following UV irradiation protocol was applied:

- Dish 1 — 0 s;
- Dish 2 — 30 s;
- Dish 3 — 1 min;
- Dish 4 — 2 min;
- Dish 5 — 5 min.

After time points specified in the protocol, 1ml samples of VC were collected from the dishes to quantify the number of plaques and thus determine the viral titer. Inactivation dynamics are shown in Fig. 2

A reduction in viral titers by at least 4 lg PFU/ml occurred no sooner than after 5 min of exposure; in other words, exposure to UV light for the inactivation of viral particles in allantoic fluid during the production of influenza vaccines should last at least 5 min.

Dynamics of avian adenovirus inactivation in virus concentrates by detergents

To model inactivation of avian adenoviruses in VC by exposure to detergents, the titrated viral stock (10% of the VC volume)

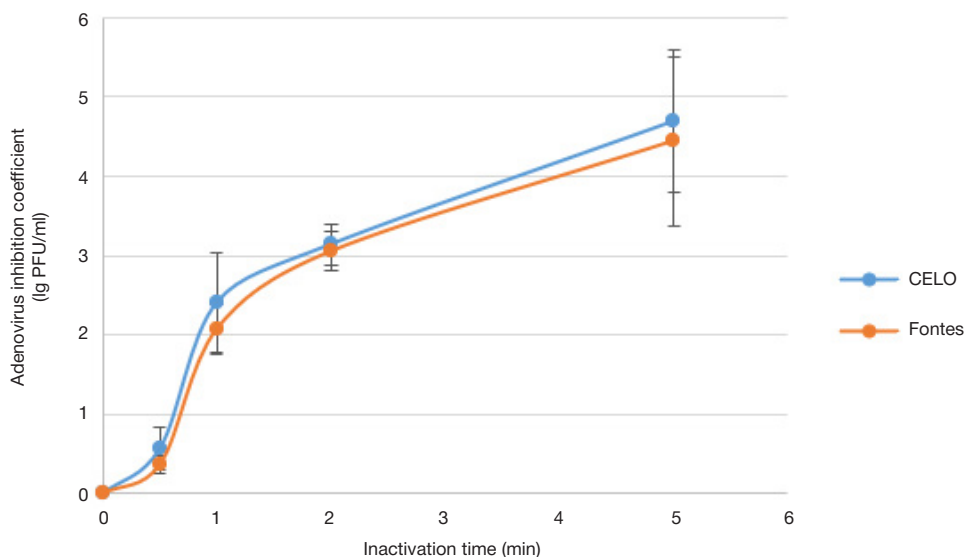


Fig. 2. Dynamics of CELO and Fontes inactivation by UV light

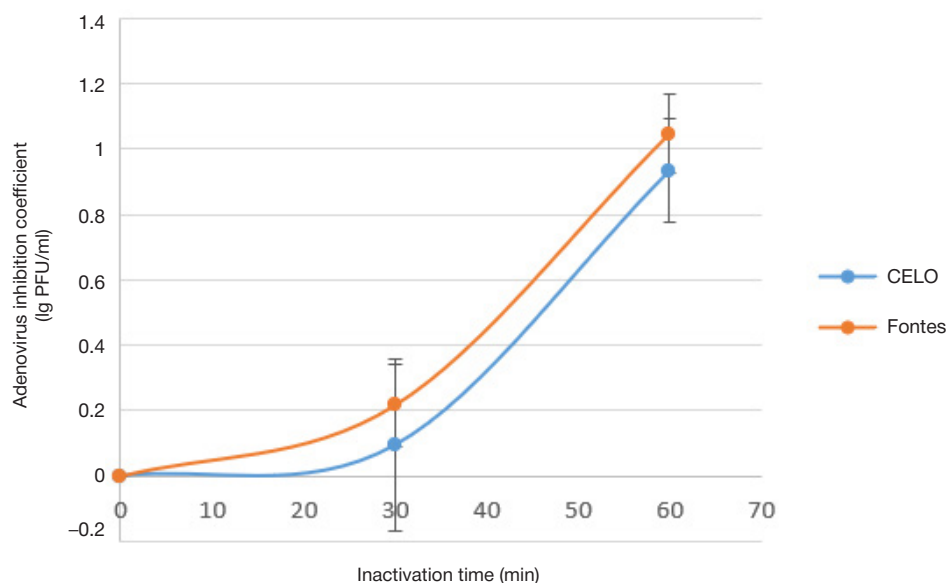


Fig. 3. Dynamics of CELO and Fontes inactivation by n-octyl-β-D-glucopyranoside

was added to VC so that the final viral titer was at least 10^5 PFU/ml. Then, contaminated VC samples were combined with the solutions of n-octyl-β-D-glucopyranoside (total protein to detergent ratio: 1 : 8) or tetradecyltrimethylammonium bromide (total protein to detergent ratio: 1 : 0.5) in PBS, and viral titers were determined. Inactivation dynamics are shown in Fig. 3 and 4.

A reduction in viral titers by at least 1 lg PFU/ml occurred after 1 h of exposure to the detergents. Following exposure to n-octyl-β-D-glucopyranoside, CELO titers fell by 0.93 ± 0.15 lg and Fontes titers fell by 1.04 ± 0.12 lg. With tetradecyltrimethylammonium bromide, CELO titers fell by 1.18 ± 0.17 lg and Fontes titers fell by 1.12 ± 0.38 lg.

DISCUSSION

Inactivation by β-propiolactone and by exposure to UV light is effective against the avian adenovirus strains Fontes and CELO. However, the variability of the results is greater for UV irradiation (Table 2).

These findings may indicate that the UV-based inactivation method is less reliable and may increase the risk of producing a

poor-quality influenza vaccine. Most pharmaceutical companies in Russia and abroad employ chemical methods of inactivation. For example, Novartis, ID Biomedical Corp of Quebec and Saint Petersburg Research Institute of Vaccines and Serums (FMBA, Russia) use β-propiolactone as an inactivating agent in the production of influenza vaccines [13–15]. Apart from influenza virus, β-propiolactone can inactivate avian adenoviruses, which are potential contaminants of influenza vaccine intermediates.

CONCLUSIONS

We have selected the optimum cell line for the propagation of Fontes and CELO adenoviruses: Vero cells allow more effective propagation (~ by 2 lg) of these adenovirus strains than Hep-2 and MA-104 cells. Virus-containing allantoic fluid used in the production of influenza vaccines should be exposed to β-propiolactone for inactivation for at least 10 h to ensure a reduction in avian adenovirus titers by 4 lg PFU/ml. If inactivation is performed with UV light, exposure should last at least 5 min to reduce viral titers by 4 lg PFU/ml. In the production of split influenza vaccines, an additional reduction in viral titers by 1 lg PFU/ml can be achieved by using detergents.

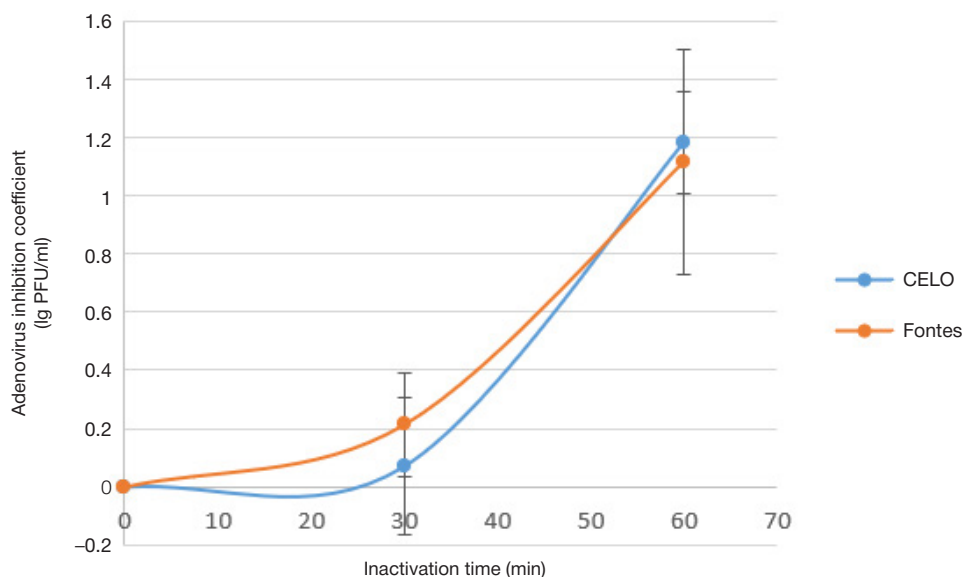


Fig. 4. Dynamics of CELO and Fontes inactivation by tetradecyltrimethylammonium bromide

Table 2. A reduction in adenovirus titers following exposure to different inactivating agents

Inactivating agent	Strain	
	CELO	Fontes
β -propiolactone (inactivation time: 10 h)	4.12 \pm 0,06 lg	4.20 \pm 0.19 lg
UV light (inactivation time: 5 min)	4.69 \pm 0,89 lg	4.44 \pm 1.06

So, the technology of influenza vaccine production that involves inactivation of allantoic fluid by β -propiolactone for 10 h followed by inactivation with detergents for 1 h guarantees complete inactivation of avian adenoviruses in

the vaccine. However, avian adenoviruses are not the only vaccincontaminants, and further research is needed to study the kinetics of β -propiolactone-based inactivation of avian leukosis virus and mycoplasmas.

References

- Guideline on Influenza vaccines — Quality module. EMA/CHMP/BWP/310834/2012 Rev.1 Committee for Medicinal Products for Human use (CHMP), 2017. Available from: https://www.ema.europa.eu/en/documents/scientific-guideline/guideline-influenza-vaccines-quality-module-revision-1_en.pdf.
- Seriya tehniceskikh dokladov VOZ, # 927, 2005 god. Prilozhenie 3. Rekomendacii po proizvodstvu i kontrolju vakcin protiv gripa (inaktivirovannyh). Russian.
- Sabbaghi A, Miri SM, Keshavarz M, Zargar M, Ghaemi A. Inactivation methods for whole influenza vaccine production. *Rev Med Virol.* 2019 Nov; 29 (6): e2074.
- King AMQ, Adams MJ, Carstens EB, Leftkowitz EJ, editors. *Virus Taxonomy: Classification and Nomenclature of Viruses*. Ninth Report of the International Committee on Taxonomy of Viruses. Elsevier, 2012; 1327 p.
- Qing Pan, Jing Wang, Yulong Gao, Qi Wang, Hongyu Cui, Changjun Liu, et al. Identification of chicken CAR homology as a cellular receptor for the emerging highly pathogenic fowl adenovirus 4 via unique binding mechanism, *Emerging Microbes & Infections.* 2020; 9 (1): 586–96.
- Bakulin V. A., Murj V. A. Adenovirusnyj gepatit s vključenijami gidroperekardit kur: jepizootologija, diagnostika i specificheskaja profilaktika. *Bio.* 2011; 12: 28–30. Russian.
- Borisov VV. Razrabotka sredstv i metodov diagnostiki i specificheskoi profilaktiki adenovirusnyh boleznej kur [dissertacija]. Ivanovo, 2007.
- Kap M, Arron GI, Loibner M, Hausleitner A, Siaulyte G, Zatloukal K, Riegman P. Inactivation of Influenza A virus, Adenovirus, and Cytomegalovirus with PAXgene Tissue Fixative and Formalin. *Biopreservation and Biobanking.* 2013; 11 (4): 229–34.
- Herrera-Rodriguez J, Signorazzi A, Holtrop M, de Vries-Idema J, Huckriede A. Inactivated or damaged? Comparing the effect of inactivation methods on influenza virions to optimize vaccine production. *Vaccine.* 2019; 37 (12): 1630–7.
- Shuo Lei, Xun Gao, Yang Sun, Xiangyong Yu, Longshan Zhao. Gas chromatography-mass spectrometry method for determination of β -propiolactone in human inactivated rabies vaccine and its hydrolysis analysis, *Journal of Pharmaceutical Analysis.* 2018; 8 (6): 373–7.
- Rukovodstvo po issledovaniju validacii virusnoj ochistki: proektirovanie, vklad i interpretacija issledovanij, ispol'zujushchih inaktivaciju i udalenie virusov. EMA CPMP/BWP/268/95; 1996. Russian.
- Reed LJ, Muench H. A simple method of estimating fifty percent endpoints. *The American Journal of Hygiene.* 1938; 27: 493–7.
- Hausmann C, Hauschild F, Jobst B, Novartis AG, assignee. Improvements in preparation of influenza virus vaccine antigens. United States patent US № US6986808P. 18.03.2008.
- Burt DS, Jones DH, Lowell GH, White GL, Torossian K, Fries LF, assignee. ID Biomedical Corp of Quebec. Proteosome influenza vaccine. United States patent US № US18247600P. 15.02.2000.
- Truhin VP, Evtushenko AY, Krasinikov IV, Savina NN, Bykov DG, Ujba SV, Vasilev AN, Ryskova EV, Nacharova EP, Arakelov SA, avtory; Federal'noe gosudarstvennoe unitarnoe predpriatie «Sankt-Peterburgskij nauchno-issledovatel'skij institut vakcin i syvorotok i predpriatie po proizvodstvu bakterijnyh preparatov» Federal'nogo mediko-biologicheskogo agentstva (FGUP SPbNIIVS FMBA Rossii), patentoobladatel'. Sposob poluchenija antigena ili antigenov dlja proizvodstva protivogrippoznoj vakciny i vakcina na ego osnove. Patent RF # RU2019118695A. 14.06.2019. Russian.

Литература

- Guideline on Influenza vaccines — Quality module. EMA/CHMP/BWP/310834/2012 Rev.1 Committee for Medicinal Products for Human use (CHMP), 2017. Available from: https://www.ema.europa.eu/en/documents/scientific-guideline/guideline-influenza-vaccines-quality-module-revision-1_en.pdf.
- Seriya tehniceskikh dokladov VOZ, № 927, 2005 god. Prilozhenie 3. Rekomendacii po proizvodstvu i kontrolju vakcin protiv gripa (inaktivirovannyh).
- Sabbaghi A, Miri SM, Keshavarz M, Zargar M, Ghaemi A. Inactivation methods for whole influenza vaccine production. *Rev Med Virol.* 2019 Nov; 29 (6): e2074.
- King AMQ, Adams MJ, Carstens EB, Leftkowitz EJ, editors. *Virus Taxonomy: Classification and Nomenclature of Viruses*. Ninth Report of the International Committee on Taxonomy of Viruses. Elsevier, 2012; 1327 p.
- Qing Pan, Jing Wang, Yulong Gao, Qi Wang, Hongyu Cui, Changjun Liu, et al. Identification of chicken CAR homology as a cellular receptor for the emerging highly pathogenic fowl adenovirus 4 via unique binding mechanism, *Emerging Microbes & Infections.* 2020; 9 (1): 586–96.
- Бакулин В. А., Мурый В. А. Аденовирусный гепатит с включениями-гидроперикардит кур: эпизоотология, диагностика и специфическая профилактика. *Био.* 2011; 12: 28–30.
- Борисов В. В. Разработка средств и методов диагностики и специфической профилактики аденовирусных болезней кур [диссертация]. Иваново, 2007.
- Kap M, Arron GI, Loibner M, Hausleitner A, Siaulyte G, Zatloukal K, Riegman P. Inactivation of Influenza A virus, Adenovirus, and Cytomegalovirus with PAXgene Tissue Fixative and Formalin. *Biopreservation and Biobanking.* 2013; 11 (4): 229–34.
- Herrera-Rodriguez J, Signorazzi A, Holtrop M, de Vries-Idema J, Huckriede A. Inactivated or damaged? Comparing the effect of inactivation methods on influenza virions to optimize vaccine production. *Vaccine.* 2019; 37 (12): 1630–7.
- Shuo Lei, Xun Gao, Yang Sun, Xiangyong Yu, Longshan Zhao. Gas chromatography-mass spectrometry method for determination

- of β -propiolactone in human inactivated rabies vaccine and its hydrolysis analysis, *Journal of Pharmaceutical Analysis*. 2018; 8 (6): 373–7.
11. Руководство по исследованию валидации вирусной очистки: проектирование, вклад и интерпретация исследований, использующих инактивацию и удаление вирусов. EMA CPMP/BWP/268/95; 1996.
 12. Reed LJ, Muench H. A simple method of estimating fifty percent endpoints. *The American Journal of Hygiene*. 1938; 27: 493–7.
 13. Haussmann C, Hauschild F, Jobst B, Novartis AG, assignee. Improvements in preparation of influenza virus vaccine antigens. United States patent US № US6986808P. 18.03.2008.
 14. Burt DS, Jones DH, Lowell GH, White GL, Torossian K, Fries LF, assignee. ID Biomedical Corp of Quebec. Proteosome influenza vaccine. United States patent US № US18247600P. 15.02.2000.
 15. Трухин В. П., Евтушенко А. Э., Красильников И. В., Савина Н. Н., Быков Д. Г., Уйба С. В., Васильев А. Н., Рыськова Е. В., Начарова Е. П., Аракелов С. А., авторы; Федеральное государственное унитарное предприятие «Санкт-Петербургский научно-исследовательский институт вакцин и сывороток и предприятие по производству бактериальных препаратов» Федерального медико-биологического агентства (ФГУП СПбНИИВС ФМБА России), патентообладатель. Способ получения антигена или антигенов для производства противогриппозной вакцины и вакцина на его основе. Патент РФ № RU2019118695A. 14.06.2019.

MOLECULAR GENETIC CHARACTERIZATION OF THREE NEW *KLEBSIELLA PNEUMONIAE* BACTERIOPHAGES SUITABLE FOR PHAGE THERAPY

Gorodnichev RB , Kornienko MA, Kuptsov NS, Malakhova MV, Bespiatykh DA, Veselovsky VA, Shitikov EA, Iliina EN

Federal Research and Clinical Center of Physical-Chemical Medicine of Federal Medical Biological Agency, Moscow, Russia

The *Klebsiella pneumoniae* bacterium is capable of causing the broad range of human nosocomial infections associated with antibiotic resistance and high mortality. Virulent bacteriophage therapy is one of the promising alternatives to antibiotic treatment of such infections. The study was aimed to isolate virulent bacteriophages effective against the relevant clinical *K. pneumoniae* strains, and to perform the molecular genetic characterization of these phages. Bacteriophages were isolated from the river water samples using the enrichment method. The whole-genome sequencing was performed on the MiSeq platform (Illumina). Three novel *K. pneumoniae* bacteriophages belonging to families *Autographiviridae* (vB_KpnP_NER40, GenBank MZ602146) and *Myoviridae* (vB_KpnM_VIK251, GenBank MZ602147; vB_KpnM_FRZ284, GenBank MZ602148) have been isolated and characterized. On the collection of 105 *K. pneumoniae* clinical strains, it has been found that bacteriophages vB_KpnP_NER40 and vB_KpnM_VIK251 have a narrow lytic spectrum (22% and 11%), which is limited to strains of the capsular types K2 and K20 respectively. In contrast, bacteriophage vB_KpnM_FRZ284 has a broad lytic spectrum (37%), causing the lysis of strains with different types of capsular polysaccharide. The phages are strictly virulent and have no genes encoding integrases, toxins or pathogenicity factors in their genomes. Genes of depolymerases, encoding the potential receptor binding proteins, have been found in the genomes of the capsular-specific bacteriophages vB_KpnP_NER40 and vB_KpnM_VIK251. The cocktail of three bacteriophages has lysed about 65% of the studied collection of *K. pneumoniae* strain and is potentially applicable for therapeutic purposes.

Keywords: virulent bacteriophages, *Klebsiella pneumoniae*, antibiotic resistance, phage therapy, depolymerases

Funding: the study was carried out within the framework of the State Assignment "Development of a Personalized Approach to the Therapy of Infections Using Virulent Bacteriophages" (CODE: Bacteriophage).

Acknowledgements: the authors thank the Center for Precision Genome Editing and Genetic Technologies for Biomedicine, the Federal Research and Clinical Center of Physical-Chemical Medicine of the Russian Federal Medical Biological Agency, for their help with bacteriophage genome sequencing.

Author contribution: Gorodnichev RB, Kornienko MA, Shitikov EA — study plan, data processing, manuscript writing; Kuptsov NS — data acquisition and processing, manuscript writing; Malakhova MV, Veselovsky VA — data acquisition; Bespiatykh DA — data processing, Iliina EN — study plan, manuscript writing.

Compliance with ethical standards: experimental work was carried out in strict compliance with the guidelines SP 1.3.2322-08 "Safety of Working With Microorganisms of III–IV Groups of Pathogenicity (Danger) and Causative Agents of Parasitic Diseases"; guidelines SP 1.3.2518-09 "Additions and Amendments № 1 to the guidelines SP 1.3.2322-08 "Safety of Working With Microorganisms of III–IV Groups of Pathogenicity (Danger) and Causative Agents of Parasitic Diseases"; guidelines "Sanitary and Epidemiologic Requirements for the Handling of Medical Waste" (SanPIN 2.1.7.2790-10), and Federal Clinical Guidelines "Rational Use of Bacteriophages in Clinical and Epidemiological Practice".

✉ **Correspondence should be addressed:** Roman B. Gorodnichev
Malaya Pirogovskaya, 1a, Moscow, 119435; gorodnichev.r.b@gmail.com

Received: 21.07.2021 **Accepted:** 26.08.2021 **Published online:** 29.09.2021

DOI: 10.47183/mes.2021.035

МОЛЕКУЛЯРНО-ГЕНЕТИЧЕСКАЯ ХАРАКТЕРИСТИКА ТРЕХ НОВЫХ БАКТЕРИОФАГОВ *KLEBSIELLA PNEUMONIAE*, ПЕРСПЕКТИВНЫХ ДЛЯ ПРИМЕНЕНИЯ В ФАГОВОЙ ТЕРАПИИ

Р. Б. Городничев , М. А. Корниенко, Н. С. Купцов, М. В. Малахова, Д. А. Беспятых, В. А. Веселовский, Е. А. Шитиков, Е. Н. Ильина

Федеральный научно-клинический центр физико-химической медицины Федерального медико-биологического агентства, Москва, Россия

Бактерия *Klebsiella pneumoniae* способна вызывать широкий спектр внутрибольничных инфекций человека, ассоциированных с антибиотикорезистентностью и высокой смертностью. Одна из перспективных альтернатив применению антибиотиков для лечения таких инфекций — терапия вирулентными бактериофагами. Целью работы было выделить из внешней среды вирулентные бактериофаги, эффективные против актуальных клинических штаммов *K. pneumoniae*, и дать их молекулярно-генетическую характеристику. Бактериофаги выделяли из проб речной воды методом накопительных культур. Полногеномное секвенирование бактериофагов выполняли на платформе MiSeq (Illumina). Выделено и описано три новых бактериофага *K. pneumoniae*, принадлежащих к семействам *Autographiviridae* (vB_KpnP_NER40, GenBank MZ602146) и *Myoviridae* (vB_KpnM_VIK251, GenBank MZ602147; vB_KpnM_FRZ284, GenBank MZ602148). На коллекции из 105 клинических штаммов *K. pneumoniae* установлено, что бактериофаги vB_KpnP_NER40 и vB_KpnM_VIK251 обладают узким спектром литической активности (22% и 11%), ограниченными штаммами с капсульным типом K2 и K20 соответственно. Бактериофаг vB_KpnM_FRZ284, напротив, имел широкий спектр литической активности (37%), вызывая лизис штаммов с различным типом капсульного полисахарида. Фаги обладают строго вирулентной природой и не несут в составе генома гены интеграз, токсинов или факторов патогенности. В составе геномов капсулоспецифичных бактериофагов vB_KpnP_NER40 и vB_KpnM_VIK251 обнаружены гены деполимераз, кодирующие потенциальные рецепторсвязывающие белки. Коктейль из трех бактериофагов лизировал около 65% штаммов исследуемой коллекции *K. pneumoniae* и потенциально применим в терапевтических целях.

Ключевые слова: вирулентные бактериофаги, *Klebsiella pneumoniae*, антибиотикорезистентность, фаготерапия, деполимераза

Финансирование: исследование выполнено за счет средств, предоставленных для выполнения государственного задания «Разработка персонализированного подхода терапии инфекционных процессов с применением вирулентных бактериофагов» (ШИФР: Бактериофаг).

Благодарности: авторы благодарят Центр высокоточного редактирования и генетических технологий для биомедицины ФГБУ ФНКЦ ФХМ ФМБА России за секвенирование геномов бактериофагов.

Вклад авторов: Р. Б. Городничев, М. А. Корниенко, Е. А. Шитиков — план исследований, обработка данных, написание статьи; Н. С. Купцов — набор и обработка данных, написание статьи; М. В. Малахова, В. А. Веселовский — набор данных; Д. А. Беспятых — обработка данных, Е. Н. Ильина — план исследований, написание статьи.

Соблюдение этических стандартов: вся экспериментальная работа выполнена с соблюдением норм Санитарно-эпидемиологических правил «Безопасность работы с микроорганизмами III–IV групп патогенности (опасности) и возбудителями паразитарных болезней» СП 1.3.2322-08; Санитарно-эпидемиологических правил СП 1.3.2518-09 — «Дополнения и изменения № 1 к санитарно-эпидемиологическим правилам «Безопасность работы с микроорганизмами III–IV групп патогенности (опасности) и возбудителями паразитарных болезней» СП 1.3.2322-08; Санитарно-эпидемиологических правил «Санитарно-эпидемиологические требования к обращению с медицинскими отходами» СанПин 2.1.7.2790-10, а также Федеральных клинических рекомендаций «Рациональное применение бактериофагов в лечебной и противозидемической практике».

✉ **Для корреспонденции:** Роман Борисович Городничев
ул. Малая Пироговская, д. 1а, г. Москва, 119435; gorodnichev.r.b@gmail.com

Статья получена: 21.07.2021 **Статья принята к печати:** 26.08.2021 **Опубликована онлайн:** 29.09.2021

DOI: 10.47183/mes.2021.035

Klebsiella pneumoniae is a Gram-negative, non-motile, facultative anaerobic bacterium, widely spread in the environment. Microorganisms of this species have traditionally been regarded as commensals, they can be found on human skin, in the gastrointestinal and respiratory tract [1]. This is the second most common nosocomial pathogen in the world capable of causing a wide range of infections, such as abscesses, purulent wounds, septicemia, pneumonia, infections of urinary tract and gastrointestinal tract [2].

Inappropriate use of antibiotics all over the world resulted in emergence and spread of drug resistant bacteria. Among the members of the genus *Klebsiella*, the isolates, carrying genes encoding extended spectrum beta-lactamases or carbapenemase-encoding genes, are the most dangerous [3]. According to the antibiotic resistance map of Russia, 30–60% of nosocomial isolates can be resistant to carbapenems, and 60–80% can be resistant to the third generation cephalosporins [4].

As a consequence of the crisis caused by dissemination of resistant bacteria, searching for new approaches to antimicrobial therapy is especially relevant. Virulent bacteriophage (phage) therapy is one of the promising alternatives [5]. Phages are natural antagonists of bacteria in wild populations, which are capable of quick selective lysis of pathogens, including the *K. pneumoniae* isolates associated with antibiotic resistance. Phage therapy has been used in clinical practice since the early 20th century. No significant side effects of phage therapy have been detected throughout history [6]. To date, the phage therapy safety and efficiency have been confirmed by mammal and *Galleria mellonella* models, as well as by clinical data [7, 8]. The narrow host range of distinct phages is the natural limitation of this approach. As a result, phage cocktails of active bacteriophages targeting various bacterial species have to be used to combat the undefined pathogen [9].

The host range of *K. pneumoniae* phages strongly correlates with the capsular polysaccharide (CPS) type [10]. To date, at least 130 CPS types have been described. CPS is the key virulence factor protecting the bacteria against the human immune system and the effects of some antibiotics [11]. Strains, characterized by the increased CPS expression, are often more virulent, and belong to the hypervirulent *K. pneumoniae* group [12].

The majority of *K. pneumoniae* phages encode depolymerases: the enzymes capable of breaking down the polysaccharide capsule through glycosidic bond cleavage [10, 13]. The diversity of phage depolymerases is of particular interest, since studying the enzymes may lead to developing the new class of antimicrobial agents. It has been shown that phage depolymerases can accelerate inactivation of bacteria with the serum *in vitro* and significantly increase the survival rate in murine and *Galleria mellonella* larvae models [14, 15]. Moreover, phage depolymerases can be used for the express microbial capsular type identification or the bacterial biofilm destruction [16].

The study was aimed to isolate the virulent bacteriophages, active against the relevant clinical *K. pneumoniae* strains, perform bacteriophage characterization, and assess the viability of using the bacteriophages as the agents for phage therapy.

METHODS

Bacterial strains and their characteristics

The collection of 105 *K. pneumoniae* strains was compiled in 2018–2019 at the Clinical Hospital № 123 of the Federal

Research and Clinical Center of Physical-Chemical Medicine of the FMBA of Russia. All bacteria were grown in the lysogeny broth (LB) (Himedia; India) at 37 °C. The bacteria were identified by MALDI-TOF mass spectrometry as described previously [17]. Antimicrobial susceptibility was tested by the disk-diffusion method in accordance with the guidelines issued by the Clinical and Laboratory Standards Institute [18].

Molecular genetic characterization of bacterial strains

Genomic DNA was extracted using the DNA-Express kit (Lytech; Russia) following the manufacturer's instructions. Multilocus sequence typing (MLST) of *K. pneumoniae* strains was performed by sequencing of seven housekeeping genes in accordance with the standard scheme as described previously [19]. The capsular type was defined by the *wzi* gene Sanger sequencing [20]. Amplification of genes, included in the molecular genetic typing schemes, was carried out in the TETRAD DNA ENGINE (MJ Research; USA). Sanger sequencing was performed with the 3730 DNA Analyzer (Thermo Fisher Scientific; UK).

Bacteriophage isolation and purification

Three *K. pneumoniae* strains, Kp40, Kp25-1 and Kp284, were used as the hosts for bacteriophage isolation. Phages vB_KpnP_NER40, vB_KpnM_VIK251 and vB_KpnM_FRZ284 were isolated from the water samples taken from the Chernyanka River in accordance with the previously reported method [21]. The 15 mL river water sample was centrifuged at 10,000 g for 15 min; supernatant was filtered through the 0.22 µm membrane sterile syringe filter (Millipore; USA). The filtered supernatant and 0.2 mL of the host strain culture being in the logarithmic growth phase (OD 600 nm = 0.3) were combined with 15 mL of the double concentration LB broth and incubated overnight while stirring (200 rpm) at 37 °C to enrich the phage fraction. Then the culture was centrifuged at 10,000 g for 15 min and filtered through the 0.22 µm filters. The resulting lysates were serially diluted in LB, the phage titer was determined by the method of agar layers according to Grazia in order to detect and isolate individual phages [22]. Monoisolates were obtained by sequential (three-fold) extraction from the distinct phage plaque.

Lytic spectrum determination

The lytic spectrum of the phages was defined by the spot test assay with the use of 105 *K. pneumoniae* strains. The 100 µl aliquot of the culture of each strain being in the logarithmic growth phase (OD 600 nm = 0.3) was added to 5 mL of semi-solid agar (0.6%), which was later applied on the bottom agar layer to form the top layer. Phage lysate, 5 mL with a titer of 10⁶ pfu/mL, was applied drop by drop onto the fresh bacterial lawn and left to dry until completely absorbed. The results were assessed after the overnight incubation at 37 °C by the presence of lysis zones at the sites of the applied bacteriophage drops. In case of solid lysis zone or sporadic phage plaques, the bacterial strain was considered sensitive to bacteriophage.

Whole genome sequencing of bacteriophages and bioinformatic data analysis

The total DNA isolation was performed using the standard phenol-chloroform extraction protocol as described previously [23]. Sequencing was carried out with the use of the MiSeq



Fig. 1. Plaque morphology for the vB_KpnP_NER40, vB_KpnM_VIK251 and vB_KpnM_FRZ284 bacteriophages

tool and the MiSeq Reagent Nano Kit v2 (500 cycle) (Illumina; USA) following the manufacturer's instructions.

Genomes were assembled with the SPAdes software (v.3.14.0). Open reading frames (ORFs) were predicted using GeneMarkS (version 4.32), Phast and VGAS. The tRNAScan-SE (University of California Santa Cruz, USA) and the ARAGORN (Murdoch University, Australia) software tools were used to predict the presence of transfer RNA (tRNA) in the genome. The expected functions of proteins, encoded by distinct ORFs, were predicted in the manual mode with the use of BLASTp, HHPred, Phast and InterPro. The search for genes encoding toxins and other factors in the bacteriophage genomes was performed using the pathogenic bacteria virulence factor databases [24]. Matching with the Antibiotic Resistance Gene Database was carried out in order to identify the antibiotic resistance determinants [25]. Phylogenetic analysis was performed using the amino acid sequences of RNA polymerase (for phages of *Autographiviridae* family) and terminase large subunit (for phages of *Myoviridae* family) following the guidelines issued by the International Committee on Taxonomy of Viruses (ICTV) (<https://talk.ictvonline.org/taxonomy>). Phylogenetic tree was constructed by the Genome-BLAST distance phylogeny method on the VICTOR web-server.

RESULTS

Isolation and phenotypic characteristics of three new *Klebsiella pneumoniae* phages

The Kp40 strain of *K. pneumoniae*, belonging to the sequence type (ST) 395 and capsular type K2, was used as a host strain for the vB_KpnP_NER40 phage. The Kp25-1 strain of *K. pneumoniae*, belonging to the ST268 and capsular type K20, was used as a host for isolation of vB_KpnM_VIK251 bacteriophage. The third strain of *K. pneumoniae*, Kp284, of the rare sequence type ST1655 and the undefined capsular type, was selected as a host strain for the vB_KpnM_FRZ284 phage. *K. pneumoniae* strains used as the host strains were resistant to three or more than three classes of antibiotics, including meropenem.

Bacteriophage vB_KpnP_NER40 formed large (3–5 mm) phage plaques, surrounded by wide halos. Plaques formed by the vB_KpnM_VIK251 phage were smaller (2–3 mm), and were surrounded by small (1–2 mm) halo. Phage vB_KpnM_FRZ284 formed small (1–2 mm) plaques with no halo (Fig. 1). According to literary sources, hazy halo surrounding the phage plaque is associated with the supposed bacteriophage-encoded depolymerase activity [26].

Table 1. Lytic spectrum of phages vB_KpnP_NER40, vB_KpnM_VIK251 and vB_KpnM_FRZ284

Capsular type	Total number of strains	Number of strains lysed by vB_KpnP_NER40 (% of the total number)	Number of strains lysed by vB_KpnM_VIK251 (% of the total number)	Number of strains lysed by vB_KpnM_FRZ284 (% of the total number)
K1	3	0	0	1 (33,3%)
K2	25	23 (92%)	0	4 (16%)
K7	1	0	0	1 (100%)
K19	4	0	0	2 (50%)
K20	17	0	12 (70,6 %)	2 (11,8%)
K23	6	0	0	3 (50%)
KL24	3	0	0	3 (100%)
KL25	2	0	0	0
KL38	1	0	0	0
KL39	14	0	0	8 (57,1%)
KL45	5	0	0	4 (80%)
K47	2	0	0	0
K57	6	0	0	3 (50%)
K60	1	0	0	0
KL62	1	0	0	1 (100%)
KL63	2	0	0	0
KL64	9	0	0	5 (55,6%)
KL107	1	0	0	1 (100%)
KL108	1	0	0	0
wzi475	1	0	0	1 (100%)

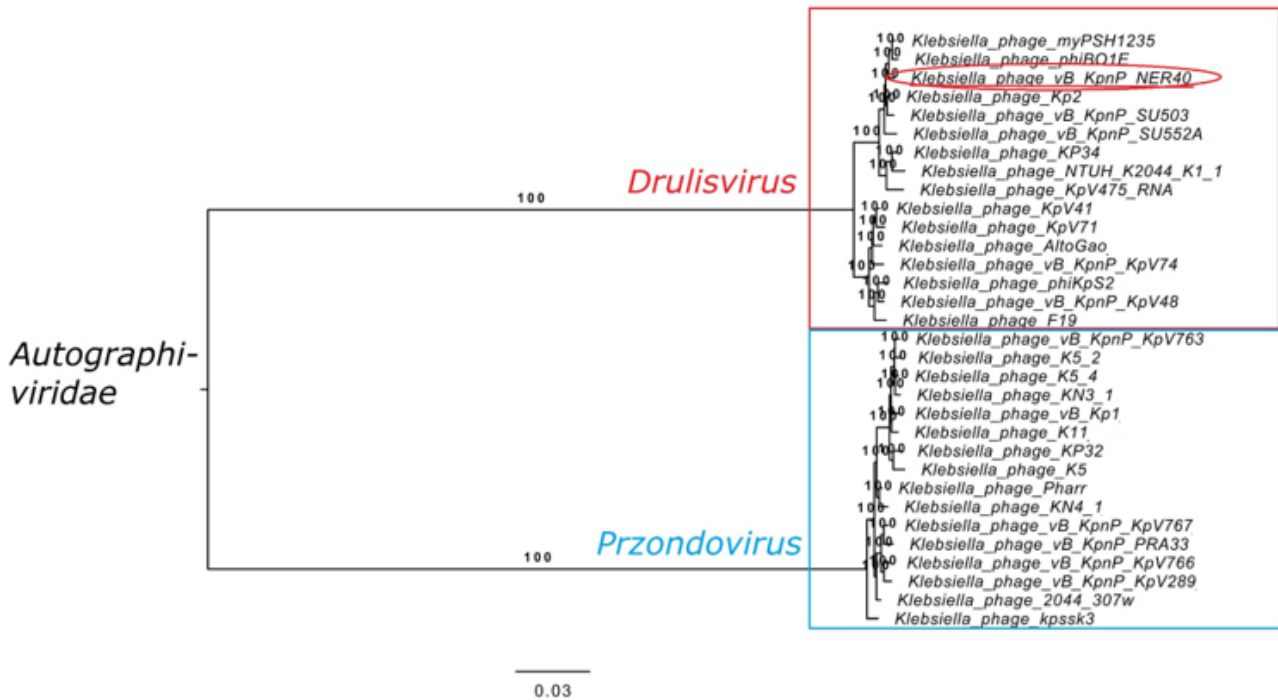


Fig. 2. Phylogeny of the *Autographiviridae* phage RNA polymerase amino acid sequences

Lytic spectrum of bacteriophages

The lytic spectrum of the studied phages was defined using the collection of 105 *K. pneumoniae* strains. According to the results of the *wzi* gene sequencing, *K. pneumoniae* strains had a total of 20 unique capsular types. The most common capsular types were as follows: K2 ($n = 25$; 23.8%), K20 ($n = 17$; 16.2%), KL39 ($n = 14$; 13.3%) and KL64 ($n = 9$; 8.6%).

Bacteriophages vB_KpnP_NER40 and vB_KpnM_VIK251 had a narrow lytic spectrum, which was limited to strains having one capsular type (Table 1). Phage vB_KpnP_NER40 lysed 23 out of 25 strains of the capsular type K2, whereas phage vB_KpnM_VIK251 lysed 12 out of 17 strains with the capsular type K20. By contrast, phage vB_KpnM_FRZ284 showed lytic activity, not limited to a single capsular type. The phage lysed 39 strains from the collections having 14 different capsular types (Table 1).

Analysis of bacteriophage whole-genome sequencing results

The whole-genome sequencing with subsequent data analysis was performed for bacteriophages vB_KpnP_NER40, vB_KpnM_VIK251 and vB_KpnM_FRZ284. Annotated genome sequences were deposited into the NCBI GenBank database under the numbers MZ602146 (vB_KpnP_NER40), MZ602147 (vB_KpnM_VIK251) and MZ602148 (vB_KpnM_FRZ284).

Genome of vB_KpnP_NER40 phage was represented by double-stranded DNA and had the size of 42,674 bp. The G + C content was 54.3%. Bioinformatic analysis revealed 53 ORFs with a total length of 39,659 bp (Table 2). Analysis of the genome nucleotide sequence using the BLASTn algorithm has shown that phage vB_KpnP_NER40 belongs to the *Autographiviridae* family. In order to verify the phylogenetic position of the phage, a phylogenetic tree was constructed based on the RNA polymerase amino acid sequences of the phages belonging to the *Autographiviridae* family, recommended by ICTV. Based on the phylogenetic analysis, phage vB_KpnP_NER40 belongs to the *Drulisvirus* genus of the *Autographiviridae* family, and seems

the most closely related with the phage phiBO1E (GenBank KM576124.1; 87% query cover and 92.05% sequence identity according to BLASTn) (Fig. 2).

The vB_KpnM_VIK251 phage genome was a linear dsDNA molecule with a length of 141,994 bp and the G + C content of 44.6%. A total of 242 open reading frames and 23 sequences encoding tRNAs were identified. According to BLASTn, the phage matched the *Myoviridae* family and seemed similar to the *Mydovirus* genus members.

The vB_KpnM_FRZ284 phage genome was also represented by dsDNA. According to BLASTn, it belonged to the *Myoviridae* family. However, it seemed much more similar to the phages of the *Jiaodavirus* genus. The phage had a length of 166,376 bp and the G + C content of 39.6%, it encoded 274 open reading frames and 16 tRNAs (see Table 2).

To clarify the phylogenetic position of the *Myoviridae* phages, the tree was constructed based on the amino acid sequences of the terminase large subunit of phages vB_KpnM_VIK251 and vB_KpnM_FRZ284, and phages, recommended by ICTV (Fig. 3). According to phylogenetic analysis, phage vB_KpnM_VIK251 belonged to the *Mydovirus* genus and was most closely related with the phage vB_KpnM_KB57 (GenBank KT934943.1; 87% query cover and 96.71% sequence identity according to BLASTn). Phage vB_KpnM_FRZ284 matched the phages of the *Myoviridae* family, genus *Jiaodavirus*, and seemed closely related with KPN5 (GenBank MN101229.1, 93% query cover and 97.23% sequence identity according to BLASTn) (see Fig. 3).

Functional annotation of *K. pneumoniae* phages

When performing annotation of the phage vB_KpnP_NER40, we managed to predict the functions of 25 proteins encoded by the genome. The vB_KpnP_NER40 phage structural organization was typical for T7-like phages and was characterized by the presence of phage DNA and RNA polymerases, as well as of the lysis cassette composed by spanin-, holin- and endolysin-encoding genes located next to each other [27]. No genes encoding tRNAs, known determinants of antibiotic

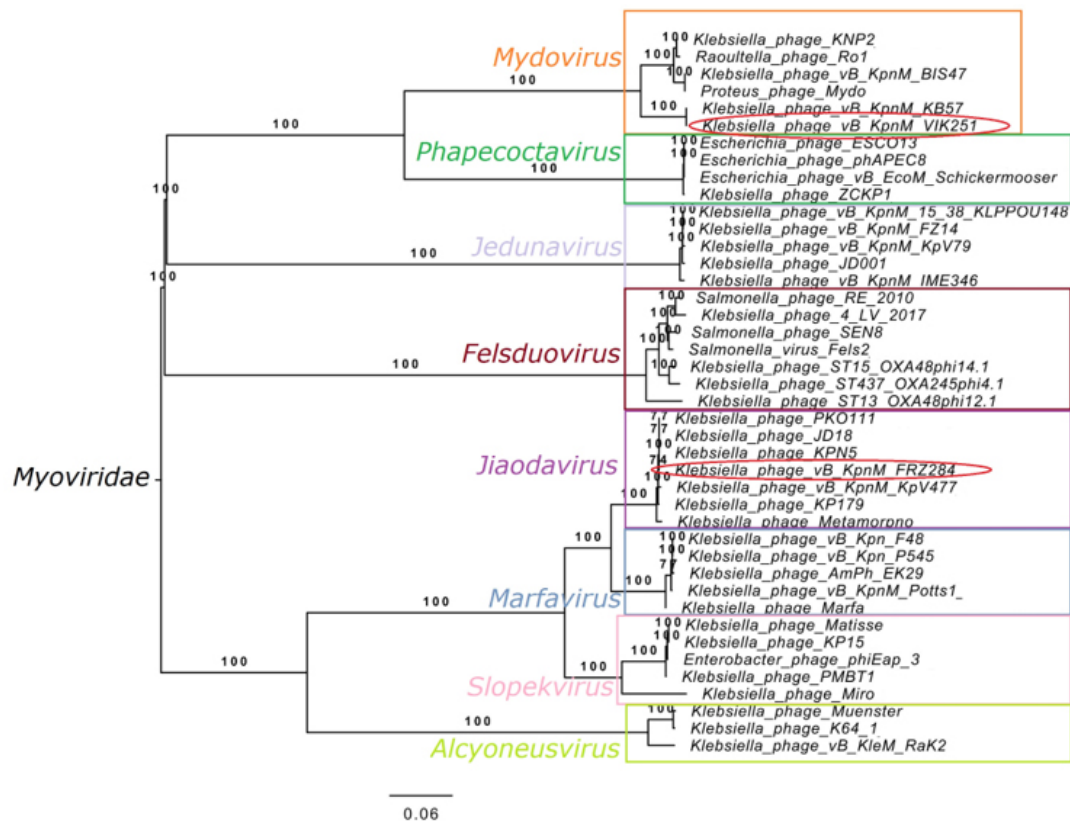


Fig. 3. Phylogeny of the *Myoviridae* family bacteriophage terminase large subunit amino acid sequences

susceptibility, integrases or toxins were found in the genome.

The vB_KpnP_NER40 phage genome encoded two proteins determining the host specificity: NER40_00045 and NER40_00053. The first protein, NER40_00045, has the length of 318 amino acids. It is the highly conserved protein for phages of the *Drulisvirus* genus. The second protein, NER40_00053, shows a high degree of homology with the tail fibers of six *K. pneumoniae* phages (QE50388.1, CAD5239035.1, QJ52632.1, YP_009789295.1, YP_009792408.1, YP_009006074.1; 96% query cover and 98.42–97.52% sequence identity according to BLASTp). Moreover, this protein encodes the potential pectate lyase domain possessing a beta helical structure, typical for the phage-derived depolymerases.

For the vB_KpnM_VIK251 phage, the expected function (structural proteins, enzymes involved in DNA replication, regulation, transcription and translation, lysis of the host) could be attributed to the products of 145 open reading frames. No genes were found, the function of which was somehow associated with the phage lysogenic cycle. At least two genes encoding proteins homologous to the phage fibers (VIK251_00041 and VIK251_00046) were found in the genome of this phage.

The vB_KpnM_FRZ284 bacteriophage encodes 126 proteins, which could be assigned the expected function. No genes encoding integrases, toxins or any other pathogenicity factors, ruling out the therapeutic use of the phage, were found in the genome. The receptor binding proteins of this phage are represented by four proteins (FRZ284_00009, FRZ284_00012, FRZ284_00098 and FRZ284_00101) homologous to the well known proteins of the *Jiaodavirus* phage fibrils.

DISCUSSION

Multidrug-resistant strains of *K. pneumoniae* of the sequence types 395 and 268 and the capsular types K2 and K20

were used as the host strains for bacteriophage isolation. Such isolates are widespread, and are often associated with nosocomial outbreaks, caused by carbapenem-resistant and hypervirulent strains in Asia and Europe [28, 29].

Three new lytic phages of *K. pneumoniae* were isolated within the framework of searching for possible alternative antimicrobial therapeutic agents. Phages vB_KpnM_VIK251 and vB_KpnM_FRZ284 belonged to different genera of the *Myoviridae* family. Phage vB_KpnP_NER40 belonged to the *Autographiviridae* family. Phages vB_KpnP_NER40 and vB_KpnM_VIK251 were markedly capsule-specific (K2- and K20-specific respectively) and lysed 70–90% strains of appropriate capsular type. In turn, vB_KpnM_FRZ284 lysed 36% strains of the collection regardless of the capsular type.

Bacteriophage vB_KpnP_NER40 encoded depolymerase comprised in the receptor binding protein, which determined host specificity. Depolymerase of phage vB_KpnP_NER40 was homologous to several phage receptor binding proteins, including the described above K2-specific depolymerase of phage KpV74 (NC_047811.1, 96% query cover and 98.2% sequence identity according to BLASTp) [14].

Looking at the vB_KpnM_VIK251 bacteriophage genome more closely, one finds out that VIK251_00052 gene encodes a protein with unknown function, however, the N-terminal region of this protein shows a high degree of homology with the tail fibril of the phage vB_KpnM_Seu621 (QO168629.1), carrying the receptor binding depolymerase domain. Other regions of this protein encode the pectate lyase domain possessing a beta helical structure, which could be the proof of this hypothetical protein belonging to the tail fibril machinery, responsible for recognition of host receptors and depolymerase activity of this phage. The putative vB_KpnM_VIK251 phage depolymerase has no homologous proteins deposited in the NCBI database, which is a matter of great interest due to the potential of depolymerases as possible therapeutic agents targeting *Klebsiella* infections [15].

Table 2. General characteristics of vB_KpnP_NER40, vB_KpnM_VIK251 and vB_KpnM_FRZ284 phage genomes

Bacteriophage	Genome, bp	G + C, %	ORF	Family	Genus
vB_KpnP_NER40	42 674	54,3	53	<i>Autographiviridae</i>	<i>Drulisvirus</i>
vB_KpnM_VIK251	14 1994	44,6	242	<i>Myoviridae</i>	<i>Mydovirus</i>
vB_KpnM_FRZ284	16 6376	39,6	274	<i>Myoviridae</i>	<i>Jiaodavirus</i>

To date, the mechanism of adsorption of the third phage, vB_KpnM_FRZ284, is unknown. However, broad lytic spectrum makes this phage promising for the further investigation aimed at potential expansion of the lytic spectra of other phages using the engineering approach.

When discussing the possibilities for treatment of infectious diseases caused by *K. pneumoniae*, it should be pointed out that the cocktail of the studied phages lyses 65% of the strain collection, which makes them comparable with the commercial phage-based products comprising several dozen bacteriophages in terms of efficiency [30].

CONCLUSIONS

Bacteriophages vB_KpnP_NER40, vB_KpnM_VIK251 and vB_KpnM_FRZ284, isolated from environmental sources, have a great potential as the alternative antibacterial agents targeting the antibiotic resistant *K. pneumoniae*. Strict host specificity of phages vB_KpnM_VIK251 and vB_KpnP_NER40, as well as the capability of breaking down capsular polysaccharides and the broad lytic spectrum of phage vB_KpnM_FRZ284 make the studied phages the prospective candidates for developing highly efficient phage cocktails.

References

- Paczosa MK, Meccas J. *Klebsiella pneumoniae*: going on the offense with a strong defense. *Microbiology and Molecular Biology Reviews*. 2016; 80 (3): 629–61.
- Podschun R, Ullmann U. *Klebsiella* spp. as nosocomial pathogens: Epidemiology, taxonomy, typing methods, and pathogenicity factors. *Clin Microbiol Rev*. 1998; 11 (4): 589–603.
- Lee CR, et al. Global dissemination of carbapenemase-producing *Klebsiella pneumoniae*: epidemiology, genetic context, treatment options, and detection methods. *Frontiers in microbiology*. 2016; 7: 895.
- Kuzmenkov AY, et al. AMRmap: an interactive web platform for analysis of antimicrobial resistance surveillance data in Russia. *Front Microbiol*. 2021; 12: 377.
- Górski A, et al. Phage therapy: current status and perspectives. *Med Res Rev*. 2020; 40 (1): 459–63.
- Payne RJH, Jansen VAA. Phage therapy: the peculiar kinetics of self-replicating pharmaceuticals. *Clin Pharmacol Ther*. 2000; 68 (3): 225–230.
- Schooley RT, et al. Development and use of personalized bacteriophage-based therapeutic cocktails to treat a patient with a disseminated resistant *Acinetobacter baumannii* infection. *Antimicrob Agents Chemother*. 2017; 61 (10): e00954–17.
- Dedrick RM, et al. Engineered bacteriophages for treatment of a patient with a disseminated drug-resistant *Mycobacterium abscessus*. *Nat Med*. 2019; 25 (5): 730–3.
- Clark JR, March JB. Bacteriophages and biotechnology: vaccines, gene therapy and antibacterials. *Trends Biotechnol*. 2006; 24 (5): 212–8.
- Pires DP, et al. Bacteriophage-encoded depolymerases: their diversity and biotechnological applications. *Appl Microbiol Biotechnol*. 2016; 100 (5): 2141–51.
- Wyres KL, et al. Identification of *Klebsiella* capsule synthesis loci from whole genome data. *Microb genomics*. 2016; 2 (12).
- Sobirk SK, Struve C, Jacobsson SG. Primary *Klebsiella pneumoniae* liver abscess with metastatic spread to lung and eye, a North-European Case Report of an emerging syndrome. *Open Microbiol*. 2010; 4 (1): 5–7.
- Knecht LE, Veljkovic M, Fieseler L. Diversity and function of phage encoded depolymerases. *Front Microbiol*. 2020; 10: 2949.
- Solovieva EV, et al. Comparative genome analysis of novel Podoviruses lytic for hypermucoviscous *Klebsiella pneumoniae* of K1, K2, and K57 capsular types. *Virus Res*. 2018; 243: 10–18.
- Volozhantsev N, et al. Characterization and therapeutic potential of Bacteriophage-encoded polysaccharide depolymerases with — galactosidase activity against *Klebsiella pneumoniae* K57 capsular type. *Antibiot*. 2020; 9 (11): 1–16.
- Scorpio A, et al. Treatment of experimental anthrax with recombinant capsule depolymerase. *Antimicrob Agents Chemother*. 2008; 52 (3): 1014.
- Kornienko M, et al. Analysis of nosocomial *Staphylococcus haemolyticus* by MLST and MALDI-TOF mass spectrometry. *Infect Genet Evol*. 2016; 39: 99–105.
- M100 Performance Standards for Antimicrobial Susceptibility Testing An informational supplement for global application developed through the Clinical and Laboratory Standards Institute consensus process. 29th ed. Clinical and Laboratory Standards Institute, Wayne, Pennsylvania, 2019. Available from: https://clsi.org/media/2663/m100ed29_sample.pdf.
- Diancourt L, et al. Multilocus sequence typing of *Klebsiella pneumoniae* nosocomial isolates. *J Clin Microbiol*. 2005; 43 (8): 4178–82.
- Brisse S, et al. Wzi gene sequencing, a rapid method for determination of capsular type for *Klebsiella* strains. *J Clin Microbiol*. 2013; 51 (12): 4073–8.
- Van Twest R, Kropinski AM. Bacteriophage enrichment from water and soil. *Methods Mol Biol*. 2009; 501: 15–21.
- Mazzocco A, et al. Enumeration of bacteriophages using the small drop plaque assay system. *Methods Mol Biol*. 2009; 501: 81–85.
- Sambrook J, Fritsch EF, Maniatis T. *Molecular cloning: a laboratory manual*. 1989; 2.
- Liu B, et al. VFDB 2019: a comparative pathogenomic platform with an interactive web interface. *Nucleic Acids Res*. 2019; 47 (D1): D687–D692.
- Liu B, Pop M. ARDB — Antibiotic Resistance Genes Database. *Nucleic Acids Res*. 2009; 37.
- Wang C, et al. Protective and therapeutic application of the depolymerase derived from a novel KN1 genotype of *Klebsiella pneumoniae* bacteriophage in mice. *Res Microbiol*. 2019; 170 (3): 156–64.
- D'Andrea MM, et al. ϕ bO1E, a newly discovered lytic bacteriophage targeting carbapenemase-producing *Klebsiella pneumoniae* of the pandemic Clonal Group 258 clade II lineage. *Sci Rep*. 2017; 7 (1): 1–8.
- Yang J, et al. A nosocomial outbreak of KPC-2-producing *Klebsiella pneumoniae* in a Chinese hospital: dissemination of ST11 and emergence of ST37, ST392 and ST395. *Clin Microbiol Infect*. 2013; 19 (11): E509–E515.
- Muggeo A, et al. Spread of *Klebsiella pneumoniae* ST395 non-susceptible to carbapenems and resistant to fluoroquinolones in North-Eastern France. *J Glob*. 2018; 13: 98–103.
- Kuptsov NS, Kornienko MA, Gorodnichev RB, Danilov DI, Malakhova MV, Parfenova TV, et al. Efficacy of commercial bacteriophage products against ESKAPE pathogens. *Bulletin of RSMU*. 2020; (3): 18–24.

Литература

- Paczosa MK, Mecsas J. *Klebsiella pneumoniae*: going on the offense with a strong defense. *Microbiology and Molecular Biology Reviews*. 2016; 80 (3): 629–61.
- Podschun R, Ullmann U. *Klebsiella* spp. as nosocomial pathogens: Epidemiology, taxonomy, typing methods, and pathogenicity factors. *Clin Microbiol Rev*. 1998; 11 (4): 589–603.
- Lee CR, et al. Global dissemination of carbapenemase-producing *Klebsiella pneumoniae*: epidemiology, genetic context, treatment options, and detection methods. *Frontiers in microbiology*. 2016; 7: 895.
- Kuzmenkov AY, et al. AMRmap: an interactive web platform for analysis of antimicrobial resistance surveillance data in Russia. *Front Microbiol*. 2021; 12: 377.
- Górski A, et al. Phage therapy: current status and perspectives. *Med Res Rev*. 2020; 40 (1): 459–63.
- Payne R, JH, Jansen VAA. Phage therapy: the peculiar kinetics of self-replicating pharmaceuticals. *Clin Pharmacol Ther*. 2000; 68 (3): 225–230.
- Schooley RT, et al. Development and use of personalized bacteriophage-based therapeutic cocktails to treat a patient with a disseminated resistant *Acinetobacter baumannii* infection. *Antimicrob Agents Chemother*. 2017; 61 (10): e00954–17.
- Dedrick RM, et al. Engineered bacteriophages for treatment of a patient with a disseminated drug-resistant *Mycobacterium abscessus*. *Nat Med*. 2019; 25 (5): 730–3.
- Clark JR, March JB. Bacteriophages and biotechnology: vaccines, gene therapy and antibacterials. *Trends Biotechnol*. 2006; 24 (5): 212–8.
- Pires DP, et al. Bacteriophage-encoded depolymerases: their diversity and biotechnological applications. *Appl Microbiol Biotechnol*. 2016; 100 (5): 2141–51.
- Wyres KL, et al. Identification of *Klebsiella* capsule synthesis loci from whole genome data. *Microb genomics*. 2016; 2 (12).
- Sobirk SK, Struve C, Jacobsson SG. Primary *Klebsiella pneumoniae* liver abscess with metastatic spread to lung and eye, a North-European Case Report of an emerging syndrome. *Open Microbiol*. 2010; 4 (1): 5–7.
- Knecht LE, Veljkovic M, Fieseler L. Diversity and function of phage encoded depolymerases. *Front Microbiol*. 2020; 10: 2949.
- Solovieva EV, et al. Comparative genome analysis of novel Podoviruses lytic for hypermucoviscous *Klebsiella pneumoniae* of K1, K2, and K57 capsular types. *Virus Res*. 2018; 243: 10–18.
- Volozhantsev N, et al. Characterization and therapeutic potential of Bacteriophage-encoded polysaccharide depolymerases with — galactosidase activity against *Klebsiella pneumoniae* K57 capsular type. *Antibiot*. 2020; 9 (11): 1–16.
- Scorpio A, et al. Treatment of experimental anthrax with recombinant capsule depolymerase. *Antimicrob Agents Chemother*. 2008; 52 (3): 1014.
- Kornienko M, et al. Analysis of nosocomial *Staphylococcus haemolyticus* by MLST and MALDI-TOF mass spectrometry. *Infect Genet Evol*. 2016; 39: 99–105.
- M100 Performance Standards for Antimicrobial Susceptibility Testing An informational supplement for global application developed through the Clinical and Laboratory Standards Institute consensus process. 29th ed. Clinical and Laboratory Standards Institute, Wayne, Pennsylvania, 2019. Available from: https://clsi.org/media/2663/m100ed29_sample.pdf.
- Diancourt L, et al. Multilocus sequence typing of *Klebsiella pneumoniae* nosocomial isolates. *J Clin Microbiol*. 2005; 43 (8): 4178–82.
- Brisse S, et al. Wzi gene sequencing, a rapid method for determination of capsular type for *Klebsiella* strains. *J Clin Microbiol*. 2013; 51 (12): 4073–8.
- Van Twest R, Kropinski AM. Bacteriophage enrichment from water and soil. *Methods Mol Biol*. 2009; 501: 15–21.
- Mazzocco A, et al. Enumeration of bacteriophages using the small drop plaque assay system. *Methods Mol Biol*. 2009; 501: 81–85.
- Sambrook J, Fritsch EF, Maniatis T. *Molecular cloning: a laboratory manual*. 1989; 2.
- Liu B, et al. VFDB 2019: a comparative pathogenomic platform with an interactive web interface. *Nucleic Acids Res*. 2019; 47 (D1): D687–D692.
- Liu B, Pop M. ARDB — Antibiotic Resistance Genes Database. *Nucleic Acids Res*. 2009; 37.
- Wang C, et al. Protective and therapeutic application of the depolymerase derived from a novel KN1 genotype of *Klebsiella pneumoniae* bacteriophage in mice. *Res Microbiol*. 2019; 170 (3): 156–64.
- D'Andrea MM, et al. ϕ B01E, a newly discovered lytic bacteriophage targeting carbapenemase-producing *Klebsiella pneumoniae* of the pandemic Clonal Group 258 clade II lineage. *Sci Rep*. 2017; 7 (1): 1–8.
- Yang J, et al. A nosocomial outbreak of KPC-2-producing *Klebsiella pneumoniae* in a Chinese hospital: dissemination of ST11 and emergence of ST37, ST392 and ST395. *Clin Microbiol Infect*. 2013; 19 (11): E509–E515.
- Muggeo A, et al. Spread of *Klebsiella pneumoniae* ST395 non-susceptible to carbapenems and resistant to fluoroquinolones in North-Eastern France. *J Glob*. 2018; 13: 98–103.
- Купцов Н. С., Корниенко М. А., Горюничев Р. Б., Данилов Д. И., Малахова М. В., Парфенова Т. В. и др. Эффективность препаратов бактериофагов против патогенов группы ESKAPE. *Вестник РГМУ*. 2020; (3): 19–26.

ANTENATAL AND EARLY POSTNATAL ETIOLOGICAL VERIFICATION OF RELEVANT CONGENITAL VIRAL INFECTIOUS DISEASES

Vasilyev VV^{1,4}, Grineva AA¹ ✉, Rogozina NV^{1,3}, Ivanova RA^{1,2}, Ushakova GM¹

¹ Pediatric Research and Clinical Center for Infectious Diseases, Saint-Petersburg, Russia

² Pavlov First Saint Petersburg State Medical University, Saint-Petersburg, Russia

³ St. Petersburg State Pediatric Medical University, Saint-Petersburg, Russia

⁴ Mechnikov North-Western State Medical University, Saint-Petersburg, Russia

Nonspecificity of clinical, laboratory and instrumental manifestations of congenital infectious diseases, including viral infections, and the diversity of methods for etiological verification of pathogens define both the need to choose the optimal approaches to the diagnosis of this pathology, and the feasibility of testing for a broad range of etiologic agents in case of suspected congenital viral infection. The analysis of current guidelines, international consensus documents issued by specialists, and published results of some studies has shown that identification of the genetic material of the pathogen with the use of amniocentesis/cordocentesis (for cytomegalovirus and parvovirus infections) or in the birth canal (for herpes simplex infection) is the key method for antenatal etiological verification of the widespread viral infections. During the postnatal period, molecular genetic testing is combined with serological diagnosis involving determining specific immunoglobulins M and G, as well as their avidity index.

Keywords: infections, children, pregnancy, cytomegalovirus, parvovirus, herpes viruses

Author contribution: Vasilyev VV — concept, final editing; Grineva AA, Vasilyev VV, Rogozina NV, Ivanova RA, Ushakova GM — raw data analysis, manuscript writing; Grineva AA — manuscript editing.

✉ **Correspondence should be addressed:** Alexandra A. Grineva
Professora Popova, 9, St. Petersburg, 197022; a.a.grineva@gmail.com

Received: 26.08.2021 **Accepted:** 12.09.2021 **Published online:** 25.09.2021

DOI: 10.47183/mes.2021.031

АНТЕНАТАЛЬНАЯ И РАННЯЯ ПОСТНАТАЛЬНАЯ ЭТИОЛОГИЧЕСКАЯ ВЕРИФИКАЦИЯ АКТУАЛЬНЫХ ВРОЖДЕННЫХ ВИРУСНЫХ ИНФЕКЦИЙ

В. В. Васильев^{1,4}, А. А. Гринева¹ ✉, Н. В. Рогозина^{1,3}, Р. А. Иванова^{1,2}, Г. М. Ушакова¹

¹ Детский научно-клинический центр инфекционных болезней Федерального медико-биологического агентства, Санкт-Петербург, Россия

² Первый Санкт-Петербургский государственный медицинский университет имени И. П. Павлова, Санкт-Петербург, Россия

³ Санкт-Петербургский государственный педиатрический медицинский университет, Санкт-Петербург, Россия

⁴ Северо-западный государственный медицинский университет имени И. И. Мечникова, Санкт-Петербург, Россия

Неспецифичность клинико-лабораторных и инструментальных проявлений врожденных инфекционных заболеваний, в том числе вирусной природы, многообразие методов этиологической верификации возбудителей определяют как необходимость выбора оптимальных подходов к диагностике этой патологии, так и целесообразность обследования на широкий спектр этиологических агентов при подозрении на врожденные вирусные инфекции. На основании анализа действующих рекомендаций профессиональных сообществ, международных консенсусов специалистов, результатов отдельных опубликованных исследований показано, что ключевым способом этиологической верификации широко распространенных вирусных инфекций в антенатальном периоде является выявление генетического материала возбудителей при амнио-, кордоцентезе (для цитомегаловирусной и парвовирусной инфекций), в родовых путях (для герпетической инфекции). В постнатальном периоде наряду с молекулярно-генетическим исследованием проводят серологическую диагностику с определением специфических иммуноглобулинов классов М и G и индекса их avidности.

Ключевые слова: инфекции, дети, беременность, цитомегаловирус, парвовирус, герпесвирусы

Вклад авторов: В. В. Васильев — концепция, окончательное редактирование; А. А. Гринева, В. В. Васильев, Р. А. Иванова, Г. М. Ушакова — анализ исходных материалов, написание текста; А. А. Гринева — редактирование статьи.

✉ **Для корреспонденции:** Александра Александровна Гринева
ул. Профессора Попова, д. 9. г. Санкт-Петербург, 197022; a.a.grineva@gmail.com

Статья получена: 26.08.2021 **Статья принята к печати:** 12.09.2021 **Опубликована онлайн:** 25.09.2021

DOI: 10.47183/mes.2021.031

Congenital viral diseases (CVDs) are the disorders associated with high mortality and often with disability, which cause substantial socio-economic damage to society [1–4].

According to ICD-10, CVDs belong to class XVI, "Certain conditions originating in the perinatal period", P35 [5].

Historically, among CVDs, rubella is the best known, the classical manifestations of which have been described by N. Gregg, the Australian ophthalmologist [6]. The development of the effective vaccine, and making it accessible have led to the diagnosis of congenital rubella (congenital rubella syndrome) currently being extremely rare and practically unknown in the developed countries. According to the State reports "On the state of sanitary and epidemiological well-being of the population in the Russian Federation", a total of seven congenital rubella

syndrome cases were registered in the Russian Federation in 2008–2020 [7].

Over the past decades, CVDs caused by other viruses, especially by the viruses of the herpesvirus family, have been playing an increasingly important role. It is known that representatives of almost all types can be transmitted from mother to fetus. However, the rate of such transmission and the impact on the fetus are quite different, and, with respect to a number of types, poorly understood. It is now believed that among CVDs, cytomegalovirus infection is the most common [8]. The existing data on the rate of fetal damage, caused by other viruses of this family, often vary considerably, which is probably due to the use of different research methods and heterogeneous groups of the examined individuals [9–15].

Implementation of modern methods for the diagnosis of infections (enzyme immunoassay, chemiluminescence immunoassay, immunocytochemistry, immunohistochemistry, and molecular genetic methods) had naturally led to the conclusion that, in addition to viral infections included in the original TORCH complex (rubella, cytomegalovirus, herpes simplex virus types 1 and 2), fetal damage may be caused by other viruses, such as parvovirus B19, enteroviruses, etc. [16].

It should be noted that available official data on the incidence of infectious diseases in the Russian Federation [7] contain no records of neonatal varicella, as well as of congenital parvovirus and enterovirus infection.

Regarding the congenital infections, the timely etiological diagnosis is crucial, since it defines both the pregnancy management tactics and the possibilities of etiotropic therapy. Meanwhile, antenatal diagnosis is the most topical, since neonatal diagnosis results in the uncontrolled infectious process development in the fetus, and worsens the outcome of congenital disease [15–18].

The Federal Law No. 323-FZ of November 21, 2011 “On the Basics of Health Protection of the Citizens in the Russian Federation” [19] stipulates that from January 1, 2022 the guidelines, developed and approved in accordance with the normative document of the Ministry of Health [20], become the documents, which largely determine the range and the procedure for diagnosis and treatment interventions in Russia. In the light of the current intensive work on preparation and approval of the guidelines for a significant number of nosological forms of the diseases, including some congenital infections, the authors have considered it necessary to provide the review of the modern approaches to antenatal and neonatal etiological verification of some relevant CVDs (herpes simplex types 1 and 2, cytomegalovirus infection, parvovirus B19V infection).

METHODS

The review includes the current foreign guidelines and the international consensus documents issued by professional communities, as well as the basic (according to the authors) review papers, systematic reviews and meta-analyses. The search for information was performed in the databases in English and Russian (MEDLINE, PubMed, Scopus, Web of science, Cochrane Library, eLIBRARY, etc.), the search depth was 15 years (the references to older studies of fundamental importance are provided).

The review does not include any guidelines and consensus documents, related to perinatal aspects of HIV infection, viral hepatitis, and other viral infections, the diagnostic approach to which is reported in the SanPin Sanitary Rules and Regulations 3.3686-21 “Sanitary and Epidemiological Requirements for Communicable Diseases Prevention” [20]; the papers, related to perinatal aspects of CVDs, the guidelines on which are temporary or non-legislative (COVID-19 and Zika virus disease), and the papers, substantiating the choice of the methods and instruments, included in the guidelines (this has been done by the developers of the guidelines and consensus documents).

Common approaches to antenatal etiological diagnosis of CVDs

Antenatal etiological diagnosis can be roughly divided into two stages. The first stage (“screening” stage) involves identifying the signs of probable congenital infection by non-invasive methods (in this context, by methods, preserving the integrity of the amniotic membrane). At this stage, laboratory testing of

body fluids (mostly blood, urine, saliva) of the pregnant woman is used in order to detect the genetic material or the antigens of microorganisms, or to reveal the markers of immune response (specific antibodies, antibody avidity determination), together with the imaging methods (most frequently various modifications of fetal ultrasound). Virological method (culturing viruses in a cell culture with subsequent identification) is seldom applied in practice due to its labour-intensity and time-consuming nature [21]. At this stage, one can form a well-informed opinion whether mother has some infectious disease, and assess the condition of the fetus, but he/she is unable to answer the question concerning the presence of congenital infectious disease in the fetus.

The second stage of the antenatal diagnosis (“expert” stage) is to prove or disprove the presence of certain infectious disease in the fetus, i.e. to establish a nosological diagnosis, specifying the etiology, which is decisive for the further pregnancy and childbirth management tactics. At this stage, the invasive procedures are performed aimed at obtaining the fetal biological samples (amniocentesis, cordocentesis) and assessing the samples in order to detect the genetic material of the microorganisms, isolate the pathogen, etc. (this paper does not address the issue of the chorionic villus sampling value for the diagnosis of CVDs).

Cordocentesis and amniocentesis are limited not only by the gestational age, but also by the age of infectious process in the pregnant woman, which reduces their diagnostic value in terms of the fetal disease duration (in case the pathogen has been transmitted). Therefore, in the modern antenatal diagnosis, great importance is attached to the screening stage and to the continuous improvement of screening.

Diagnosis of congenital infection caused by herpes simplex virus types 1 and 2

Genital herpes is one of the most common sexually transmitted infections, most often caused by the herpes simplex virus type 2 (up to 85%) [9, 11, 22]. Fetal infection occurs mainly after the neonate contacts with the virus when passing through the birth canal [23–30].

Herpes simplex virus type 2 (HSV-2) is mainly transmitted through sexual intercourse, the infection is most often acquired at the age of 20–30 years. WHO estimates that 13% of the global population aged 15–49 have this infection [9]. Various studies and reviews estimate that the prevalence of HSV-2 among pregnant women is 20–30%. Furthermore, about 10% of women seronegative for HSV-2 live with seropositive partners and therefore are at risk of being infected with genital herpes during pregnancy [23, 24, 30, 31]. Among serodiscordant couples, women seronegative (having no antibodies) for herpes simplex virus type 1 (HSV-1) antigens have the probability of seroconversion of 3.7%; in women seropositive for antibodies to HSV-1 antigens, the risk of seroconversion for HSV-2 is estimated at 1.7% [23, 24, 30, 31].

The risk of congenital infection is defined by the time of primary maternal infection in relation to the conception, as well as by the fact of the infection reactivation during pregnancy. It is generally accepted that the risk of transmission in case of primary maternal infection in pregnancy is up to 50%, and in case of reactivation the risk is about 4% [9].

HSV transmission occurs in utero, intrapartum and postpartum. It is believed that in 75–85% of cases, fetal infection occurs just before labour after the rupture of membranes, or intrapartum when passing through the infected birth canal. The proportion of intrauterine infection is 5–8% of neonatal

Table. Ultrasound signs of congenital CMVI in the antenatal period [39, 40]

Signs	Rate, %
Intracranial calcification	0.6–17.4
Microcephaly	14.5
Hyperechoic bowel	4.5–13
Intrauterine growth restriction	1.9–13
Subependymal cysts	11.6
Ventriculomegaly	4.5–1.5
Ascites	8.7
Pericardial effusion	7.2
Hyperechoic kidneys	4.3
Enlarged liver	4.3
Thick placenta or placental calcification	4.3
Hepatic calcification	1.4
Hydrops fetalis	0.6

herpes cases [24–28, 30, 31]. The risk of neonatal infection varies between 30–50% for HSV infection occurring during late pregnancy (last trimester); infection in early pregnancy poses a risk of about 1% [11, 24, 25, 29].

Antenatal diagnosis of congenital infection caused by HSV type 1 and 2

Screening in pregnancy aimed to define antibodies to herpes simplex virus in the blood is not recommended, regardless of the history of HSV infection symptoms [25–28, 30].

Assessment of pregnant women is recommended in case of the primary HSV-2 infection acquired during the first two trimesters of pregnancy. In this case, it is necessary to assess the dynamic changes in the levels of IgM, IgG to HSV-2 with an interval of 2–4 weeks in order to reveal seroconversion, as well as to perform a series of molecular genetic tests (polymerase chain reaction, PCR) in order to detect HSV-2 DNA in the vaginal discharge of the pregnant woman, starting from the 32nd week of gestation, to define the tactics for delivery and to find the solution to the question of prescribing antiviral therapy. In case of primary HSV-2 infection development during the last 4–6 weeks of gestation, the risk of vertical transmission and infected neonate is high (41%). In such a case, it is recommended to consider the possibility of cesarean delivery and prescribing etiotropic therapy to both mother and neonate [26, 28, 29].

According to the authors of this article, obligatory etiotropic treatment with direct-acting antiviral agents (acyclovir) in patients with herpes simplex in late pregnancy makes it possible to avoid transabdominal invasive procedures aimed at diagnosis/exclusion of fetal damage, recommended in patients with some other infectious diseases (see below).

Neonatal diagnosis of congenital infection caused by HSV type 1 and 2

Clinical features of neonatal herpes are diverse and non-pathognomonic, which in a number of cases makes the diagnosis difficult. The main manifestations, suggesting the presence of herpes simplex in children below the age of 6 weeks are as follows: rashes in the form of mucocutaneous vesicles, sepsis-like illness, cerebrospinal fluid pleocytosis, seizures, focal neurologic signs, respiratory distress syndrome, episodes of apnea, progressive pneumonitis, thrombocytopenia, conjunctivitis, signs of hepatitis or liver failure, elevated transaminase levels, radiographic signs of brain damage [28, 29].

In the current context, the main method of etiological verification used in such situations involves detecting the viral genetic material by PCR. Swab specimens from the mouth, nasopharynx, conjunctivae, and anus (“surface cultures”), cerebrospinal fluid samples in case of CNS involvement, additional blood samples in case of generalized forms of the disease, and print smears of the contents of vesicles should be obtained. Although the cytopathic effect of the herpes simplex virus becomes obvious during the first five days of culturing, and virological method enables typing of virus strains, such assessment is time-consuming, expensive and lacks practical applicability [29–32].

Diagnosis of congenital cytomegalovirus infection

The highest risk of fetal cytomegalovirus (CMV) infection and the development of severe forms of the disease are observed when the pregnant woman acquires primary cytomegalovirus infection (CMVI) (up to 30% of pregnant women are seronegative). The prevalence of primary CMVI in pregnant women reaches 1% [33, 34].

Antenatal diagnosis of cytomegalovirus infection

Primary maternal CMVI in pregnancy is difficult to suspect due to scarcity of symptomatic forms and nonspecific symptoms (acute respiratory illness with mildest catarrhal symptoms, multifocal lymphadenitis, hepatomegaly and splenomegaly). Ultrasound signs of possible fetal damage are also nonspecific (Table).

Currently, the routine testing of the specific IgM and IgG, the avidity of the latter (quantification in the blood serum), and the viral load (PCR) is not recommended [35–38]. These methods are feasible only in women from the risk groups: under 25 years of age, with signs of acute respiratory illness before week 20 of gestation, multiparous women having organized children, working in children's educational institutions (i.e., being at high risk of infection) [35–38].

Whenever the laboratory, clinical and instrumental signs of primary CMVI (latent viral reactivation, superinfection) are found, assessing the amniotic fluid obtained using amniocentesis (performed on or after the 6th week since the estimated time of the disease onset and not earlier than on the 20th week of gestation) by PCR is indicated. Cordocentesis is not recommended, because, according to the authors of the guidelines and consensus documents, this procedure has no

advantage over amniocentesis in the diagnosis of congenital CMVI [36–38, 41].

In the case that amniocentesis is impossible (or the informed refusal is obtained from the pregnant woman), or in the case of no signs of congenital CMVI detected during the first fetal ultrasound, the repeated screening fetal ultrasounds shall be performed every 2–3 weeks [36–38, 41].

The signs of congenital CMVI progression identified by fetal ultrasound can be considered the indication for terminating a pregnancy for medical reasons [35, 36, 38].

Postnatal diagnosis of cytomegalovirus infection

The indications for laboratory and instrumental examination, aimed to exclude/verify congenital CMVI in the newborn, are as follows: the baby showing clinical signs of congenital infection regardless of their possible etiology (including leukopenia, thrombocytopenia, elevated of hepatic transaminases and direct bilirubin); failure to pass the hearing screen; the documented primary maternal CMVI during pregnancy regardless of the presence or absence of clinical manifestations in the baby; subfebrile temperature, maternal influenza-like illness during the first 20 weeks of gestation; threatened preterm labour; preterm birth, intrauterine growth restriction; genetic material of the pathogen identified in the afterbirth by PCR; signs of intrauterine infection detected during the radiological examination [36, 38, 39].

Identification of the CMV DNA in saliva, urine, and blood during the first three weeks of life is the method of choice for etiological verification of the disease in case of suspected congenital CMVI in the neonate. Saliva (buccal swab can be collected) and urine testing are optimal, and blood testing is less optimal [36, 38, 41–44]. Cerebrospinal fluid is assessed only in case of CNS involvement and lumbar puncture performed with the use of molecular genetic method, involving identification of the CMV DNA. Simultaneous quantification of the CMV IgM and IgG levels in the blood serum, obtained from neonates, is a more affordable, but a less informative method: specific IgM in the first days of life should indicate the primary infection. However, these are not always found in babies with congenital CMVI; false positive results also occur [45]. The high-titer specific IgG antibodies are often found in neonates, however, the concentration of antibodies transferred across the placenta is reduced during the first three weeks of life [36, 38, 45, 46].

Diagnosis of congenital infection caused by human parvovirus B19

Human parvovirus B19 infection (HPV) in pregnancy increases the risk of fetal loss, spontaneous abortion and stillbirth. The risk of adverse pregnancy outcomes reaches 10%. The maternal infection acquired during pregnancy leads to fetal infection in 24–51% of cases [49, 50].

In the majority of cases, when parvovirus infection occurs during pregnancy, the fetus is not affected. However, infection may result in non-immune fetal hydrops due to severe anemia, congestive heart failure and myocarditis, which, with delayed diagnosis and treatment, leads to perinatal loss. The most sensitive period in terms of fetal exposure to human parvovirus B19 (B19V) is the period between 11 and 23 weeks of gestation. The fetal mortality rate in case of infection acquired before 20 weeks of gestation is about 17%, and in case of infection during the later stages this value is about 6%. However, infection acquired during the 3rd trimester can result in intrauterine fetal death without any signs of non-immune hydrops and anemia in 7.5% of cases [51–54].

Antenatal diagnosis of parvovirus B19 infection

About 40% women of childbearing age are seronegative for parvovirus and are therefore susceptible to infection. Approximately 50% of the infected pregnant women are asymptomatic, they develop no classic rash of erythema infectiosum, which is found in children. Atypical symptoms, such as arthralgia, are more frequent in adults than in children.

Testing for HPV is not regulated anywhere in the world and is merely advisory. It is worth noting that screening each and every pregnant woman both for HPV and CMVI is not recommended by professional communities. Identification of non-immune hydrops fetalis or fetal death is the only indication for testing the pregnant woman for parvovirus B19 [49, 51].

Enzyme-linked immunosorbent assay for assessment of specific IgM, IgG antibodies in blood serum of pregnant women is used as a screening laboratory test. While the existence of IgG confirms the past infection, any non-negative response to immunoglobulin M (positive or equivocal IgM test result) would require mandatory molecular genetic testing, involving identification of parvovirus B19 DNA in woman's blood, and the infectious diseases specialist consultation in the future [51–54].

In case of acute maternal HPV infection confirmed by laboratory tests (positive IgM antibody to parvovirus B19V, presence of parvovirus B19 DNA in blood), the constant fetal monitoring with the use of Doppler ultrasonographic assessment of the peak velocity of systolic blood flow in the middle cerebral artery for the diagnosis of fetal anemia and hydrops fetalis performed every 1–2 weeks for 12 weeks is indicated [55]. If ultrasound signs of non-immune hydrops fetalis are detected, the pregnant woman should be hospitalized at the specialized obstetric unit in order to perform amniocentesis or cordocentesis (after 18–20 weeks). If severe fetal anemia is suspected based on the Doppler ultrasound data, cordocentesis is preferred [51, 56].

Postnatal diagnosis of parvovirus B19 infection

The indications for laboratory and instrumental examination required to exclude/verify the congenital HPV infection in the neonate are almost the same as indications for testing for other CVDs (for example, CMVI). Diagnostic approaches are also similar: molecular genetic method (PCR) is the main method of etiological verification, the whole blood and its derivatives are used as a substrate [51, 56, 57]. Other clinical and laboratory tests are performed when clinically indicated.

CONCLUSION

The list of congenital infections goes well beyond the components of TORCH-complex. Currently, there are more than 50 microorganisms capable of causing fetal damage.

Antenatal etiological verification of infections (combined with neonatal verification) is the most important instrument to define the pregnancy and childbirth management tactics, and to assess the prospects for development of the fetus and the neonate. Today, the accurate verification of the pathogen in the fetus involves invasive interventions, which limits the feasibility of those to a certain extent.

Scientific research in the field of congenital infections is, among other things, following the path of studying the

potential of using both qualitative and quantitative methods for assessment of various infectious process markers, which is, for example, reflected in proposals to optimize testing the HIV-

positive pregnant women for CMVI [58, 59]. Perhaps in the near future such approaches would become more extensively used, especially in the situations related to mixed infections.

References

- Grosse SD, Leung J, Lanzieri TM. Identification of congenital CMV cases in administrative databases and implications for monitoring prevalence, healthcare utilization, and costs. *Curr Med Res Opin.* 2021 May; 37 (5): 769–79. PubMed PMID: 33591223.
- Grosse SD, Dollard SC, Ortega-Sanchez IR. Economic assessments of the burden of congenital cytomegalovirus infection and the cost-effectiveness of prevention strategies. *Semin Perinatol.* 2021; 45 (3): 151393. PubMed PMID: 33551180.
- Lieu JEC, Kenna M, Anne S, Davidson L. Hearing Loss in Children: a review. *JAMA.* 2020; 324 (21): 2195–205. PubMed PMID: 33258894.
- Velasco-Velásquez S, Celis-Giraldo D, Botero Hincapié A, Alejandro Hincapié Erira D, Sofía Cordero López S, Marulanda Orozco N, et al. Clinical, Socio-economic and Environmental Factors Related with Recurrences in Ocular Toxoplasmosis in Quindío, Colombia. *Ophthalmic Epidemiol.* 2021; 28 (3): 258–64. PubMed PMID: 33115293.
- MKB 10 — Mezhdunarodnaja klassifikacija boleznej 10-go peresmotra versija: 2019. Dostupno po sсыlke: <https://mkb-10.com/index.php?pid=15190> (08.09.2021). Russian.
- Gregg, NM. Congenital Cataract Following German Measles in the Mother. *Epidemiol Infect.* 1991; 107 (1): iii–xiv.
- Federal'naja sluzhba po nadzoru v sfere zashhity prav potrebitelej i blagopoluchija cheloveka. Razdel «Dokumenty». Dostupno po sсыlke: <https://www.rospotrebnadzor.ru/documents/documents.php> (08.09.2021). Russian.
- Moodley A, Payton KSE. The Term Newborn: Congenital Infections. *Clin Perinatol.* 2021; 48 (3): 485–511. PubMed PMID: 34353577.
- World Health Organization. 2017. [2019-05-07]. Herpes simplex virus. Available from: <https://www.who.int/news-room/fact-sheets/detail/herpes-simplex-virus>.
- Van Der Pol B. Type-specific detection of herpes simplex virus type 1 and type 2 using the cobas® HSV 1 and 2 test on the cobas® 4800 platform. *Expert Rev Mol Diagn.* 2016 ; 16 (11): 1145–54. PubMed PMID: 27687862.
- James SH, Kimberlin DW. Neonatal herpes simplex virus infection: epidemiology and treatment. *Clin Perinatol.* 2015; 42 (1): 47–59. PubMed PMID: 25677996.
- Tan MP, Koren G. Chickenpox in pregnancy: revisited. *Reprod Toxicol.* 2006 ; 21 (4): 410–20. PubMed PMID: 15979274.
- Smith CK, Arvin AM. Varicella in the fetus and newborn. *Semin Fetal Neonatal Med.* 2009; 14 (4): 209–17. PubMed PMID: 19097954.
- Sauerbrei A, Wutzler P. Neonatal varicella. *J Perinatol.* 2001 Dec; 21 (8): 545–9. PubMed PMID: 11774017.
- Trotta M, Borchi B, Niccolai A, Venturini E, Giaché S, Sterrantino G, et al. Epidemiology, management and outcome of varicella in pregnancy: a 20-year experience at the Tuscany Reference Centre for Infectious Diseases in Pregnancy. *Infection.* 2018 Oct; 46 (5): 693–9. PubMed PMID: 29766472.
- Auriti C, De Rose DU, Santisi A, Martini L, Piersigilli F, Bersani I, et al. Pregnancy and viral infections: Mechanisms of fetal damage, diagnosis and prevention of neonatal adverse outcomes from cytomegalovirus to SARS-CoV-2 and Zika virus. *Biochim Biophys Acta Mol Basis Dis.* 2021 Oct 1; 1867 (10): 166198. PubMed PMID: 34118406.
- Peyron F, McLeod R, Ajzenberg D, Contopoulos-Ioannidis D, Kieffer F, Mandelbrot L, et al. Congenital Toxoplasmosis in France and the United States: One Parasite, Two Diverging Approaches. *PLoS Negl Trop Dis.* 2017 Feb 16; 11 (2): e0005222. PubMed PMID: 28207736.
- Albright CM, Werner EF, Hughes BL. Cytomegalovirus Screening in Pregnancy: A Cost-Effectiveness and Threshold Analysis. *Am J Perinatol.* 2019 Jun; 36 (7): 678–87. PubMed PMID: 30567003.
- Federal'nyj zakon ot 21 nojabrja 2011 g. N 323-FZ «Ob osnovah ohrany zdorov'ja grazhdan v Rossijskoj Federacii» s izmenenijami i dopolnenijami. <https://base.garant.ru/12191967/> (Dostup 26.03.2021 g.). Russian.
- Prikaz Ministerstva zdavoohranenija Rossijskoj Federacii ot 28.02.2019 # 104n «Ob utverzhdenii porjadka i srokov odobrenija i utverzhdenija klinicheskikh rekomendacij, kriteriev prinjatija nauchno-prakticheskim sovetom reshenija ob odobrenii, otklonenii ili napravlenii na dorabotku klinicheskikh rekomendacij libo reshenija ob ih peresmotre». Dostupno po sсыlke: <https://www.garant.ru/products/ipo/prime/doc/72599420/>. (Data obrashhenija: 12.03.2020). Russian.
- Postanovlenie Glavnogo gosudarstvennogo sanitarnogo vracha Rossijskoj Federacii ot 28 janvarja 2021 goda # 4 ««Ob utverzhdenii sanitarnyh pravil i norm SanPIN 3.3686-21 «Sanitarno-jepidemiologicheskie trebovanija po profilaktike infekcionnyh boleznej»». Dostupno po sсыlke: <https://docs.cntd.ru/document/573660140> (07.09.2021). Russian.
- LeGoff J, Péré H, Bélec L. Diagnosis of genital herpes simplex virus infection in the clinical laboratory. *Virology.* 2014; 11: 83. PubMed PMID: 24885431.
- Pinninti SG, Kimberlin DW. Preventing herpes simplex virus in the newborn. *Clin Perinatol.* 2014 41 (4): 945–55. PubMed PMID: 25459782.
- Brown ZA, Selke S, Zeh J, et al. The acquisition of herpes simplex virus during pregnancy. *N Engl J Med.* 1997; 337 (8): 509–15.
- Management of Genital Herpes in Pregnancy: ACOG Practice Bulletin/ACOG Practice Bulletin, Number 220. *Obstet Gynecol.* 2020 May; 135 (5): e193–e202. PubMed PMID: 32332414.
- Samies NL, James SH. Prevention and treatment of neonatal herpes simplex virus infection. *Antiviral Res.* 2020 Apr; 176: 104721. PubMed PMID: 32044154.
- Grupo de Trabajo de Infección Neonatal por virus herpes simplex de la Sociedad Española de InfectologíaPediátrica. Guía de la Sociedad Española de InfectologíaPediátrica sobre prevención, diagnóstico y tratamiento de la infección neonatal por virus herpes simplex [The Spanish Society of Paediatric Infectious Diseases guidelines on the prevention, diagnosis and treatment of neonatal herpes simplex infections]. *An Pediatr.* 2018 Jul; 89 (1): 64.e1–64.e10. PubMed PMID: 29453157.
- Sénat MV, Anselem O, Picone O, Renesme L, Sananès N, Vauloup-Fellous C, et al. Prevention and management of genital herpes simplex infection during pregnancy and delivery: Guidelines from the French College of Gynaecologists and Obstetricians (CNGOF). *Eur J Obstet Gynecol Reprod Biol.* 2018 May; 224: 93–101. PubMed PMID: 29571124.
- Ramgopal S, Wilson PM, Florin TA. Diagnosis and Management of Neonatal Herpes Simplex Infection in the Emergency Department. *Pediatr Emerg Care.* 2020 Apr; 36 (4): 196–202. PubMed PMID: 32265379.
- Fernandes ND, Arya K, Ward R. Congenital Herpes Simplex. In: *StatPearls Treasure Island (FL): Stat Pearls Publishing, 2021 Jan.* PubMed PMID: 29939674.
- Shangase N, Kharsany ABM, Ntombela NP, Pettifor A, McKinnon LR. A Systematic Review of Randomized Controlled Trials of School Based Interventions on Sexual Risk Behaviors and Sexually Transmitted Infections Among Young Adolescents in Sub-Saharan Africa. *AIDS Behav.* 2021 Mar 27. PubMed PMID: 33772695.
- Otto WR, Myers AL, LaRussa B, Kimberlin DW, Jackson MA. Clinical Markers and Outcomes of Neonates With Herpes Simplex Virus Deoxyribonucleic Acid Persistence in Cerebrospinal Fluid in Disseminated and Central Nervous System Infection. *J Pediatric Infect Dis Soc.* 2018 May 15; 7 (2): e30–e33. PubMed PMID: 28510722.

33. Davis NL, King CC, Kourtis AP. Cytomegalovirus infection in pregnancy. *Birth Defects Res* 2017; 109 (5): 336–464.
34. Mussi-Pinhata MM, Yamamoto AY, Aragon DC, et al. Seroconversion for Cytomegalovirus Infection During Pregnancy and Fetal Infection in a Highly Seropositive Population: "The BraCHS Study". *J Infect Dis*. 2018; 218: 1200.
35. Hughes BL, Gyamfi-Bannerman C. Society for Maternal-Fetal Medicine (SMFM). Diagnosis and antenatal management of congenital cytomegalovirus infection. *Am J Obstet Gynecol*. 2016; 214 (6): B5–B11.
36. Rawlinson WD, Boppana SB, Fowler KB, Kimberlin DW, et al. Congenital cytomegalovirus infection in pregnancy and the neonate: consensus recommendations for prevention, diagnosis, and therapy. *Lancet Infect Dis*. 2017; 17 (6): e177–e188.
37. Britt WJ. Congenital human cytomegalovirus infection and the enigma of maternal immunity. *J Virol* 2017; 91 (15).
38. Luck SE, Wieringa JW, Blázquez-Gamero D, Henneke P, Schuster K, Butler K, et al. Congenital Cytomegalovirus: A European Expert Consensus Statement on Diagnosis and Management. *Pediatr Infect Dis J*. 2017; 36 (12): 1205–13. PubMed PMID: 29140947.
39. Capretti MG, Lanari M, Tani G, Ancora G, Sciutti R, Marsico C, et al. Role of cerebral ultrasound and magnetic resonance imaging in newborns with congenital cytomegalovirus infection. *Brain Dev*. 2014; 36 (3): 203–11. PubMed PMID: 23647916.
40. de Vries LS, Gunardi H, Barth PG, Bok LA, Verboon-Macielek MA, Groenendaal F. The spectrum of cranial ultrasound and magnetic resonance imaging abnormalities in congenital cytomegalovirus infection. *Neuropediatrics*. 2004 Apr; 35 (2): 113–9. PubMed PMID: 15127310.
41. Desveaux C, Klein J, Leruez-Ville M, et al. Identification of symptomatic fetuses infected with cytomegalovirus using amniotic fluid peptide biomarkers. *PLoS Pathog*. 2016; 12: e1005395.
42. Boppana SB, Ross SA, Shimamura M, Palmer AL, Ahmed A, Michaels MG, et al. Saliva polymerase-chain-reaction assay for cytomegalovirus screening in newborns. *N Engl J Med*. 2011; 364 (22): 2111–8. PubMed PMID: 21631323.
43. Ross SA, Ahmed A, Palmer AL, Michaels MG, Sánchez PJ, Bernstein DI, et al. Detection of congenital cytomegalovirus infection by real-time polymerase chain reaction analysis of saliva or urine specimens. *J Infect Dis*. 2014; 210 (9): 1415–8. PubMed PMID: 24799600.
44. Eventov-Friedman S, Manor H, Bar-Oz B, Averbuch D, Caplan O, Lifshitz A, et al. Saliva Real-Time Polymerase Chain Reaction for Targeted Screening of Congenital Cytomegalovirus Infection. *J Infect Dis*. 2019; 220 (11): 1790–6. PubMed PMID: 31310307.
45. Bilavsky E, Watad S, Levy I, Linder N, Pardo J, Ben-Zvi H, et al. Positive IgM in Congenital CMV Infection. *Clin Pediatr (Phila)*. 2017; 56 (4): 371–75. PubMed PMID: 28006975.
46. Rogozina NV, Vasilev VV, Grineva AA, Mihajlov AV, Kashtanova TA, Romanovskij AN, i dr. Ante- i postnatal'naja diagnostika i kompleksnoe lechenie vrozhdennoj citomegalovirusnoj infekcii. *Ros vestn perinatol i pediatri* 2019; 64: (6): 89–93. DOI: 10.21508/1027–4065–2019–64–6–89–93. Russian.
47. Marsico C, Kimberlin D. W. Congenital Cytomegalovirus infection: advances and challenges in diagnosis, prevention and treatment. *Ital J Pediatr*. 2017; 43: 38. Published online 2017 Apr 17. DOI: 10.1186/s13052-017-0358-8.
48. Ross SA, Ahmed A, Palmer AL, Michaels MG, Sánchez PJ, Bernstein DI, et al. Detection of Congenital Cytomegalovirus Infection by Real-Time Polymerase Chain Reaction Analysis of Saliva or Urine Specimens. *The Journal of Infectious Diseases* 2014; 210: 1415–8. DOI: 10.1093/infdis/jiu263.
49. Xiong YQ, Tan J, Liu YM, He Q, Li L, Zou K, et al. The risk of maternal parvovirus B19 infection during pregnancy on fetal loss and fetal hydrops: A systematic review and meta-analysis. *J Clin Virol*. 2019; 114: 12–20. PubMed PMID: 30897374.
50. Shishko GA, Ermolovich MA, Samojlovich EO, Artyushevskaja MV, Leonova EYu, Ustinovich YuA. Rol' parvovirusnoj infekcii v perinatal'noj patologii. *Reproduktivnoe zdorov'e. Vostochnaja Evropa*. 2015; 5: 95–102. Russian.
51. Attwood LO, Holmes NE, Hui L. Identification and management of congenital parvovirus B19 infection. *Prenat Diagn*. 2020 Dec; 40 (13): 1722–31. PubMed PMID: 32860469.
52. Salbetti MB, Pedranti MS, Barbero P, Molisani P, Lazzari M, Olivera N, et al. Molecular screening of the human parvoviruses B19 and bocavirus 1 in the study of congenital diseases as applied to symptomatic pregnant women and children. *Access Microbiol*. 2019; 1 (5): e000037. PubMed PMID: 32974527.
53. Hunter LA, Ayala NK. Parvovirus B19 in Pregnancy: A Case Review. *J Midwifery Womens Health*. 2021; 66 (3): 385–90. PubMed PMID: 34101977.
54. Gallinella G. The clinical use of parvovirus B19 assays: recent advances. *Expert Rev Mol Diagn*. 2018; 18 (9): 821–32. PubMed PMID: 30028234.
55. Prefumo F, Fichera A, Fratelli N, Sartori E. Fetal anemia: Diagnosis and management. *Best Pract Res Clin Obstet Gynaecol*. 2019; 58: 2–14. PubMed PMID: 30718211.
56. Voordouw B, Rockx B, Jaenisch T, Fraaij P, Mayaud P, Vossen A, et al. Performance of Zika Assays in the Context of Toxoplasma gondii, Parvovirus B19, Rubella Virus, and Cytomegalovirus (TORCH) Diagnostic Assays. *Clin Microbiol Rev*. 2019; 33 (1): e00130-18. PubMed PMID: 31826871.
57. Bascietto F, Liberati M, Murgano D, Buca D, Iacovelli A, Flacco ME, et al. Outcome of fetuses with congenital parvovirus B19 infection: systematic review and meta-analysis. *Ultrasound Obstet Gynecol*. 2018; 52 (5): 569–76. PubMed PMID: 29785793.
58. Shahgildjan VI, Aleksandrova EP, Kozyrina NV, Shipulina OYu, Dodonova YeA, Shahgildjan NV. Citomegalovirusnaja infekcija u beremennyh i novorozhdennyh: jepidemiologicheskij analiz, novye podhody k diagnostike i lecheniju. *Akusherstvo i ginekologija: novosti, mnenija, obuchenie*. 2020; 8 (2): 80–94. DOI: 10.24411/2303-9698-2020-12008. Russian.
59. Shahgildjan VI. Vrozhden'naja citomegalovirusnaja infekcija: aktual'nye voprosy, vozmozhnye otvety. *Neonatologija: novosti, mnenija, obuchenie*. 2020; 8 (4): 61–72. DOI: <https://doi.org/10.33029/2308-2402-2020-8-4-61-72>. Russian.

Литература

1. Grosse SD, Leung J, Lanzieri TM. Identification of congenital CMV cases in administrative databases and implications for monitoring prevalence, healthcare utilization, and costs. *Curr Med Res Opin*. 2021 May; 37 (5): 769–79. PubMed PMID: 33591223.
2. Grosse SD, Dollard SC, Ortega-Sanchez IR. Economic assessments of the burden of congenital cytomegalovirus infection and the cost-effectiveness of prevention strategies. *Semin Perinatol*. 2021; 45 (3): 151393. PubMed PMID: 33551180.
3. Lieu JEC, Kenna M, Anne S, Davidson L. Hearing Loss in Children: a review. *JAMA*. 2020; 324 (21): 2195–205. PubMed PMID: 33258894.
4. Velasco-Velásquez S, Celis-Giraldo D, Botero Hincapié A, Alejandro Hincapié Erira D, Sofia Cordero López S, Marulanda Orozco N, et al. Clinical, Socio-economic and Environmental Factors Related with Recurrences in Ocular Toxoplasmosis in Quindío, Colombia. *Ophthalmic Epidemiol*. 2021; 28 (3): 258–64. PubMed PMID: 33115293.
5. МКБ 10 — Международная классификация болезней 10-го пересмотра версия: 2019. Доступно по ссылке: <https://mkb-10.com/index.php?pid=15190> (08.09.2021).
6. Gregg, NM. Congenital Cataract Following German Measles in the Mother. *Epidemiol Infect*. 1991; 107 (1): iii–xiv.
7. Федеральная служба по надзору в сфере защиты прав потребителей и благополучия человека. Раздел «Документы». Доступно по ссылке: <https://www.rosпотребнадзор.ru/documents/documents.php> (08.09.2021).
8. Moodley A, Payton KSE. The Term Newborn: Congenital Infections. *Clin Perinatol*. 2021; 48 (3): 485–511. PubMed PMID: 34353577.
9. World Health Organization. 2017. [2019-05-07]. Herpes simplex

- virus. Available from: <https://www.who.int/news-room/fact-sheets/detail/herpes-simplex-virus>.
10. Van Der Pol B. Type-specific detection of herpes simplex virus type 1 and type 2 using the cobas® HSV 1 and 2 test on the cobas® 4800 platform. *Expert Rev Mol Diagn.* 2016 ; 16 (11): 1145–54. PubMed PMID: 27687862.
 11. James SH, Kimberlin DW. Neonatal herpes simplex virus infection: epidemiology and treatment. *Clin Perinatol.* 2015; 42 (1): 47–59. PubMed PMID: 25677996.
 12. Tan MP, Koren G. Chickenpox in pregnancy: revisited. *Reprod Toxicol.* 2006 ; 21 (4): 410–20. PubMed PMID: 15979274.
 13. Smith CK, Arvin AM. Varicella in the fetus and newborn. *Semin Fetal Neonatal Med.* 2009; 14 (4): 209–17. PubMed PMID: 19097954.
 14. Sauerbrei A, Wutzler P. Neonatal varicella. *J Perinatol.* 2001 Dec; 21 (8): 545–9. PubMed PMID: 11774017.
 15. Trotta M, Borchi B, Niccolai A, Venturini E, Giaché S, Sterrantino G, et al. Epidemiology, management and outcome of varicella in pregnancy: a 20-year experience at the Tuscany Reference Centre for Infectious Diseases in Pregnancy. *Infection.* 2018 Oct; 46 (5): 693–9. PubMed PMID: 29766472.
 16. Auriti C, De Rose DU, Santisi A, Martini L, Piersigilli F, Bersani I, et al. Pregnancy and viral infections: Mechanisms of fetal damage, diagnosis and prevention of neonatal adverse outcomes from cytomegalovirus to SARS-CoV-2 and Zika virus. *Biochim Biophys Acta Mol Basis Dis.* 2021 Oct 1; 1867 (10): 166198. PubMed PMID: 34118406.
 17. Peyron F, Mc Leod R, Ajzenberg D, Contopoulos-Ioannidis D, Kieffer F, Mandelbrot L, et al. Congenital Toxoplasmosis in France and the United States: One Parasite, Two Diverging Approaches. *PLoS Negl Trop Dis.* 2017 Feb 16; 11 (2): e0005222. PubMed PMID: 28207736.
 18. Albright CM, Werner EF, Hughes BL. Cytomegalovirus Screening in Pregnancy: A Cost-Effectiveness and Threshold Analysis. *Am J Perinatol.* 2019 Jun; 36 (7): 678–87. PubMed PMID: 30567003.
 19. Федеральный закон от 21 ноября 2011 г. N 323-ФЗ «Об основах охраны здоровья граждан в Российской Федерации» с изменениями и дополнениями. <https://base.garant.ru/12191967/> (Доступ 26.03.2021 г.).
 20. Приказ Министерства здравоохранения Российской Федерации от 28.02.2019 № 104н «Об утверждении порядка и сроков одобрения и утверждения клинических рекомендаций, критериев принятия научно-практическим советом решения об одобрении, отклонении или направлении на доработку клинических рекомендаций либо решения об их пересмотре». Доступно по ссылке: <https://www.garant.ru/products/ipo/prime/doc/72599420/>. (Дата обращения: 12.03.2020).
 21. Постановление Главного государственного санитарного врача Российской Федерации от 28 января 2021 года № 4 «Об утверждении санитарных правил и норм СанПиН 3.3686-21 «Санитарно-эпидемиологические требования по профилактике инфекционных болезней»». Доступно по ссылке: <https://docs.cntd.ru/document/573660140> (07.09.2021).
 22. LeGoff J, Péré H, Bélec L. Diagnosis of genital herpes simplex virus infection in the clinical laboratory. *Virology.* 2014; 11: 83. PubMed PMID: 24885431.
 23. Pinninti SG, Kimberlin DW. Preventing herpes simplex virus in the newborn. *Clin Perinatol.* 2014 41 (4): 945–55. PubMed PMID: 25459782.
 24. Brown ZA, Selke S, Zeh J, et al. The acquisition of herpes simplex virus during pregnancy. *N Engl J Med.* 1997; 337 (8): 509–15.
 25. Management of Genital Herpes in Pregnancy: ACOG Practice Bulletin. *Obstet Gynecol.* 2020 May; 135 (5): e193–e202. PubMed PMID: 32332414.
 26. Samies NL, James SH. Prevention and treatment of neonatal herpes simplex virus infection. *Antiviral Res.* 2020 Apr; 176: 104721. PubMed PMID: 32044154.
 27. Grupo de Trabajo de Infección Neonatal por virus herpes simplex de la Sociedad Española de Infectología Pediátrica. Guía de la Sociedad Española de Infectología Pediátrica sobre prevención, diagnóstico y tratamiento de la infección neonatal por virus herpes simplex [The Spanish Society of Paediatric Infectious Diseases guidelines on the prevention, diagnosis and treatment of neonatal herpes simplex infections]. *An Pediatr.* 2018 Jul; 89 (1): 64.e1–64.e10. PubMed PMID: 29453157.
 28. Sénat MV, Anselem O, Picone O, Renesme L, Sananès N, Vauloup-Fellous C, et al. Prevention and management of genital herpes simplex infection during pregnancy and delivery: Guidelines from the French College of Gynaecologists and Obstetricians (CNGOF). *Eur J Obstet Gynecol Reprod Biol.* 2018 May; 224: 93–101. PubMed PMID: 29571124.
 29. Ramgopal S, Wilson PM, Florin TA. Diagnosis and Management of Neonatal Herpes Simplex Infection in the Emergency Department. *Pediatr Emerg Care.* 2020 Apr; 36 (4): 196–202. PubMed PMID: 32265379.
 30. Fernandes ND, Arya K, Ward R. Congenital Herpes Simplex. In: *StatPearls Treasure Island (FL): Stat Pearls Publishing, 2021 Jan.* PubMed PMID: 29939674.
 31. Shangase N, Kharsany ABM, Ntombela NP, Pettifor A, McKinnon LR. A Systematic Review of Randomized Controlled Trials of School Based Interventions on Sexual Risk Behaviors and Sexually Transmitted Infections Among Young Adolescents in Sub-Saharan Africa. *AIDS Behav.* 2021 Mar 27. PubMed PMID: 33772695.
 32. Otto WR, Myers AL, LaRussa B, Kimberlin DW, Jackson MA. Clinical Markers and Outcomes of Neonates With Herpes Simplex Virus Deoxyribonucleic Acid Persistence in Cerebrospinal Fluid in Disseminated and Central Nervous System Infection. *J Pediatric Infect Dis Soc.* 2018 May 15; 7 (2): e30–e33. PubMed PMID: 28510722.
 33. Davis NL, King CC, Kourtis AP. Cytomegalovirus infection in pregnancy. *Birth Defects Res* 2017; 109 (5): 336–464.
 34. Mussi-Pinhata MM, Yamamoto AY, Aragon DC, et al. Seroconversion for Cytomegalovirus Infection During Pregnancy and Fetal Infection in a Highly Seropositive Population: "The BraCHS Study". *J Infect Dis.* 2018; 218: 1200.
 35. Hughes BL, Gyamfi-Bannerman C. Society for Maternal-Fetal Medicine (SMFM). Diagnosis and antenatal management of congenital cytomegalovirus infection. *Am J Obstet Gynecol.* 2016; 214 (6): B5–B11.
 36. Rawlinson WD, Boppana SB, Fowler KB, Kimberlin DW, et al. Congenital cytomegalovirus infection in pregnancy and the neonate: consensus recommendations for prevention, diagnosis, and therapy. *Lancet Infect Dis.* 2017; 17 (6): e177–e188.
 37. Britt WJ. Congenital human cytomegalovirus infection and the enigma of maternal immunity. *J Virol* 2017; 91 (15).
 38. Luck SE, Wieringa JW, Blázquez-Gamero D, Henneke P, Schuster K, Butler K, et al. Congenital Cytomegalovirus: A European Expert Consensus Statement on Diagnosis and Management. *Pediatr Infect Dis J.* 2017; 36 (12): 1205–13. PubMed PMID: 29140947.
 39. Capretti MG, Lanari M, Tani G, Ancora G, Sciutti R, Marsico C, et al. Role of cerebral ultrasound and magnetic resonance imaging in newborns with congenital cytomegalovirus infection. *Brain Dev.* 2014; 36 (3): 203–11. PubMed PMID: 23647916.
 40. de Vries LS, Gunardi H, Barth PG, Bok LA, Verboon-Macielek MA, Groenendaal F. The spectrum of cranial ultrasound and magnetic resonance imaging abnormalities in congenital cytomegalovirus infection. *Neuropediatrics.* 2004 Apr; 35 (2): 113–9. PubMed PMID: 15127310.
 41. Desveaux C, Klein J, Leruez-Ville M, et al. Identification of symptomatic fetuses infected with cytomegalovirus using amniotic fluid peptide biomarkers. *PLoS Pathog.* 2016; 12: e1005395.
 42. Boppana SB, Ross SA, Shimamura M, Palmer AL, Ahmed A, Michaels MG, et al. Saliva polymerase-chain-reaction assay for cytomegalovirus screening in newborns. *N Engl J Med.* 2011; 364 (22): 2111–8. PubMed PMID: 21631323.
 43. Ross SA, Ahmed A, Palmer AL, Michaels MG, Sánchez PJ, Bernstein DI, et al. Detection of congenital cytomegalovirus infection by real-time polymerase chain reaction analysis of saliva or urine specimens. *J Infect Dis.* 2014; 210 (9): 1415–8. PubMed PMID: 24799600.
 44. Eventov-Friedman S, Manor H, Bar-Oz B, Averbuch D, Caplan O, Lifshitz A, et al. Saliva Real-Time Polymerase Chain Reaction for Targeted Screening of Congenital Cytomegalovirus Infection. *J Infect Dis.* 2019; 220 (11): 1790–6. PubMed PMID: 31310307.
 45. Bilavsky E, Watad S, Levy I, Linder N, Pardo J, Ben-Zvi H, et al.

- Positive IgM in Congenital CMV Infection. *Clin Pediatr (Phila)*. 2017; 56 (4): 371–75. PubMed PMID: 28006975.
46. Рогозина Н. В., Васильев В. В., Гринева А. А., Михайлов А. В., Каштанова Т. А., Романовский А. Н. и др. Анте- и постнатальная диагностика и комплексное лечение врожденной цитомегаловирусной инфекции. *Рос вестн перинатол и педиатр* 2019; 64: (6): 89–93. DOI: 10.21508/1027–4065–2019–64–6–89–93.
 47. Marsico C, Kimberlin D. W. Congenital Cytomegalovirus infection: advances and challenges in diagnosis, prevention and treatment. *Ital J Pediatr*. 2017; 43: 38. Published online 2017 Apr 17. DOI: 10.1186/s13052-017-0358-8.
 48. Ross SA, Ahmed A, Palmer AL, Michaels MG, Sánchez PJ, Bernstein DI, et al. Detection of Congenital Cytomegalovirus Infection by Real-Time Polymerase Chain Reaction Analysis of Saliva or Urine Specimens. *The Journal of Infectious Diseases* 2014; 210: 1415–8. DOI: 10.1093/infdis/jiu263.
 49. Xiong YQ, Tan J, Liu YM, He Q, Li L, Zou K, et al. The risk of maternal parvovirus B19 infection during pregnancy on fetal loss and fetal hydrops: A systematic review and meta-analysis. *J Clin Virol*. 2019; 114: 12–20. PubMed PMID: 30897374.
 50. Шишко Г. А., Ермолович М. А., Самойлович Е. О., Артюшевская М. В., Леонова Е. Ю., Устинович Ю. А. Роль парвовирусной инфекции в перинатальной патологии. *Репродуктивное здоровье. Восточная Европа*. 2015; 5: 95–102.
 51. Attwood LO, Holmes NE, Hui L. Identification and management of congenital parvovirus B19 infection. *Prenat Diagn*. 2020 Dec; 40 (13): 1722–31. PubMed PMID: 32860469.
 52. Salbetti MB, Pedranti MS, Barbero P, Molisani P, Lazzari M, Olivera N, et al. Molecular screening of the human parvoviruses B19 and bocavirus 1 in the study of congenital diseases as applied to symptomatic pregnant women and children. *Access Microbiol*. 2019; 1 (5): e000037. PubMed PMID: 32974527.
 53. Hunter LA, Ayala NK. Parvovirus B19 in Pregnancy: A Case Review. *J Midwifery Womens Health*. 2021; 66 (3): 385–90. PubMed PMID: 34101977.
 54. Gallinella G. The clinical use of parvovirus B19 assays: recent advances. *Expert Rev Mol Diagn*. 2018; 18 (9): 821–32. PubMed PMID: 30028234.
 55. Prefumo F, Fichera A, Fratelli N, Sartori E. Fetal anemia: Diagnosis and management. *Best Pract Res Clin Obstet Gynaecol*. 2019; 58: 2–14. PubMed PMID: 30718211.
 56. Voordouw B, Rockx B, Jaenisch T, Fraaij P, Mayaud P, Vossen A, et al. Performance of Zika Assays in the Context of Toxoplasma gondii, Parvovirus B19, Rubella Virus, and Cytomegalovirus (TORCH) Diagnostic Assays. *Clin Microbiol Rev*. 2019; 33 (1): e00130-18. PubMed PMID: 31826871.
 57. Bascietto F, Liberati M, Murgano D, Buca D, Iacovelli A, Flacco ME, et al. Outcome of fetuses with congenital parvovirus B19 infection: systematic review and meta-analysis. *Ultrasound Obstet Gynecol*. 2018; 52 (5): 569–76. PubMed PMID: 29785793.
 58. Шахгильдян В. И., Александрова Е. П., Козырина Н. В., Шипулина О. Ю., Додонова Э. А., Шахгильдян Н. В. Цитомегаловирусная инфекция у беременных и новорожденных: эпидемиологический анализ, новые подходы к диагностике и лечению. *Акушерство и гинекология: новости, мнения, обучение*. 2020; 8 (2): 80–94. DOI: 10.24411/2303-9698-2020-12008.
 59. Шахгильдян В. И. Врожденная цитомегаловирусная инфекция: актуальные вопросы, возможные ответы. *Неонатология: новости, мнения, обучение*. 2020; 8 (4): 61–72. DOI: <https://doi.org/10.33029/2308-2402-2020-8-4-61-72>.

MECHANISMS OF B LYMPHOCYTE INVOLVEMENT IN THE PATHOGENESIS OF MULTIPLE SCLEROSIS

Melnikov MV^{1,2,3} ✉, Rogovskii VS^{1,2}, Lopatina AV^{1,2}, Sviridova AA^{1,2}, Volkov AI¹, Boyko AN^{1,2}¹ Federal Center for Brain and Neurotechnology of Federal Medical-Biological Agency, Moscow, Russia² Pirogov Russian National Research Medical University, Moscow, Russia³ Institute of Immunology of Federal Medical-Biological Agency, Moscow, Russia

Multiple sclerosis (MS) is a chronic demyelinating disease of the central nervous system involving autoimmune mechanisms. MS has been treated as a disorder mediated mainly by T cells for a long time. However, recent findings demonstrate that B lymphocytes are of crucial pathogenetic significance in MS. In patients with MS, B cells can possess both pro-inflammatory and anti-inflammatory effects. The paper reports the main mechanisms of B lymphocyte involvement in the pathogenesis of MS. Diagnostic value of assessing humoral immune parameters in individuals with demyelinating diseases and modern possibility of B cell function modulation are discussed.

Keywords: B cells, neurodegeneration, neuroinflammation, multiple sclerosis

Author contribution: Melnikov MV — manuscript writing and editing; Rogovskii VS, Lopatina AV, Volkov AI — manuscript writing; Sviridova AA — manuscript writing and formatting; Boyko AN — study concept and design, manuscript editing

✉ **Correspondence should be addressed:** Mikhail V. Melnikov
Ostrovitianova, 1, Moscow, 117997; medikms@yandex.ru

Received: 17.07.2021 **Accepted:** 06.08.2021 **Published online:** 16.08.2021

DOI: 10.47183/mes.2021.020

МЕХАНИЗМЫ УЧАСТИЯ В-ЛИМФОЦИТОВ В ПАТОГЕНЕЗЕ РАССЕЯННОГО СКЛЕРОЗА

М. В. Мельников^{1,2,3} ✉, В. С. Роговский^{1,2}, А. В. Лопатина^{1,2}, А. А. Свиридова^{1,2}, А. И. Волков¹, А. Н. Бойко^{1,2}¹ Федеральный центр мозга и нейротехнологий Федерального медико-биологического агентства, Москва, Россия² Российский национальный исследовательский медицинский университет имени Н. И. Пирогова, Москва, Россия³ Институт иммунологии Федерального медико-биологического агентства, Москва, Россия

Рассеянный склероз (РС) — хроническое демиелинизирующее заболевание центральной нервной системы с аутоиммунным механизмом развития. Долгое время РС рассматривали как заболевание, опосредованное преимущественно Т-клетками. Однако исследования последних лет указывают на критическое патогенетическое значение В-лимфоцитов при РС. При РС В-клетки способны оказывать как про-, так и противовоспалительное действие. В статье рассмотрены основные механизмы участия В-клеток в патогенезе РС. Обсуждены диагностическая значимость оценки характеристик гуморального звена иммунной системы при демиелинизирующих заболеваниях, а также современные возможности модуляции функций В-клеток.

Ключевые слова: В-клетки, нейродегенерация, невровоспаление, рассеянный склероз.

Вклад авторов: М. В. Мельников — написание и редактирование рукописи; В. С. Роговский М, А. В. Лопатина, А. И. Волков — написание рукописи; А. А. Свиридова — написание и форматирование рукописи; А. Н. Бойко — концепция и дизайн исследования, редактирование рукописи

✉ **Для корреспонденции:** Михаил Валерьевич Мельников
ул. Островитянова, д. 1, г. Москва, 117997; medikms@yandex.ru

Статья получена: 17.07.2021 **Статья принята к печати:** 06.08.2021 **Опубликована онлайн:** 16.08.2021

DOI: 10.47183/mes.2021.020

Multiple sclerosis (MS) is a chronic demyelinating and neurodegenerative disease of the central nervous system (CNS) involving autoimmune mechanisms. MS is one of the most complex and socially significant issues of clinical neurology, as confirmed by high prevalence of the disease, constantly growing number of affected people, and severe disabilities in patients with MS, represented mainly by young people aged 18–45 [1].

MS had been treated as a disorder mediated mainly by T cell immune response for a long time. Th1 and Th17 cells (subpopulations of CD4⁺ T cells), producing interferon- γ (IFN γ) and interleukin-17 (IL17) pro-inflammatory cytokines, were considered of most pathogenetic significance [2].

However, recent findings have shown that B cells play a vital part in the pathogenesis of MS along with T cells. It is known that B cells are not only able to differentiate into plasma cells and produce antibodies, but also produce cytokines and present antigens. High diagnostic yield of determining the levels of oligoclonal immunoglobulins and free immunoglobulin κ - and λ -light chains in cerebrospinal fluid, as well as clinical efficacy of anti-B-cell therapy in patients with MS, support B cell involvement in the pathogenesis of MS [3, 4].

The review summarizes the main mechanisms of pro-inflammatory and anti-inflammatory effects of B lymphocytes involved in the pathogenesis of demyelinating diseases. Diagnostic and prognostic value of assessing humoral immune parameters in individuals with demyelinating disorders are discussed, together with new approaches to B cell functional modulation in individuals with MS.

B lymphocytes: development, differentiation and subpopulations*B lymphocyte differentiation*

B lymphocytes (B cells) develop from pluripotent hematopoietic stem cells (HSCs) of bone marrow. These cells are a self-maintaining population; they give rise to lymphoid and myeloid lineage cells. Lymphoid lineage cells give rise to T and B lymphocyte progenitors. IL7 is important for B cell differentiation [5].

The newly formed B cells with an intact B-cell receptor migrate from bone marrow into peripheral blood and secondary lymphoid organs [6]. It is worth noting that the data on B cell differentiation are often controversial, since a wealth of

information has been obtained during studies involving rodents. It is often difficult to match the populations of human and murine B cells.

In humans, CD10⁺CD38^{high}CD24^{high} are the earliest B cells, reconstituting the periphery after B-cell therapy. These B cells are further subdivided into type 1 (T1) and type 2 (T2), as well as CD10^{neg} T3 cells, based on incrementally lower expression of CD24 and CD38. These cells are capable of stepwise differentiation into mature- naïve-phenotype B cells in vitro. Mature naïve B cells have a CD10^{neg}CD38^{low/neg} phenotype [7].

Further differentiation of B cells takes place after antigenic stimulation. Stimulation of B cells is being promoted by interaction of antigen with B-cell receptor (BCR). In contrast to T-cell receptor, BCR recognizes an antigen without contact with the protein of the major histocompatibility complex (MHC). CD19, a co-receptor of BCR complex, is one of the earliest and most specific markers of B cells [8]. CD20 is also a common marker of B cells, expressed by the majority of B cells. However, CD20 is not expressed in terminally differentiating plasmablasts and plasma cells. Unlike CD19, the functional role of CD20 has been studied much less [9].

Antigenic stimulation is followed by a complex process of differentiation, which depends also on the antigen affinity for BCR. In particular, short-lived and long-lived plasma cells, which produce antibodies, as well as memory B cells, are formed during differentiation. It's interesting that, according to modern concept, memory B cells develop from B cells with lower affinity for antigen, which provides an opportunity of B-cell receptor fast adaptation to modified antigen (for example, resulting from mutation of the virus) [10].

B lymphocyte subpopulations

1. Memory B cells

Memory B cells are the long-lived resting cells, which are able to respond rapidly to antigen reappearance. In cases where the levels of circulating antibodies are insufficient for immediate neutralization and elimination of pathogens, the memory B cell expansion takes place. It is worth noting that memory B cells are localized to sites with maximum probability of contact with antigens. Moreover, macrophages (CD169⁺), which are able to present antigens to B cells, are represented this wide within these sites. Antigens are presented both to naïve B cells and memory B cells [10].

Thus, two types of B-cell memory can be distinguished. Realization of type 1 involves antibodies, produced by long-lived plasma cells. Human plasma cells are characterized by co-expression of CD138 and CD38, which makes it possible to identify plasma cells in bone marrow or single cell suspensions, isolated from tissues by multicolor flow cytometry. These terminally differentiated B cells lose the ability to express CD19 and CD20 (markers of B cells) on the cell surface, while retaining CD27 expression [8].

Type 2 B-cell memory is mediated by memory B cells, which are in the resting state and are recruited in case of insufficient immune response, generated by type 1 B-cell memory. Therefore, it is worth mentioning that the lack of specific antibodies in blood plasma should not be considered the lack of capability to generate the repeated immune response in memory B cells.

There are several types of memory B cells, which are classified based on their origin, differential expression of CD27, and expressed immunoglobulin isotype. There are three main characteristic sites, memory B cells originate from:

spleen, germinal centers (structures located in secondary lymphoid organs, especially in lymph nodes, where mature B cells proliferate and differentiate), and lamina propria of intestinal mucosa. Memory cells, originating from spleen, are characterized by production of markers CD27-IgG⁺. Memory B cells of germinal centers express CD27⁺IgM⁺IgD⁻. These cells are characterized by switching from expression of IgM to expression of CD27⁺IgG/IgA⁺. Intestinal memory B cells express CD27-IgA⁺ [11].

According to current understanding of the issue, human memory B cells in blood and bone marrow can be divided into three main populations: CD19⁺CD27⁺IgM⁺IgD⁺ (similar to marginal zone B cells), CD19⁺CD27⁺IgM⁺IgD⁻ (i.e., IgM positive only), and immunoglobulin class-switched cells CD19⁺CD27⁺IgM⁻(IgG⁺ or IgA⁺) [10].

After their activation and differentiation in germinal centers, B cells develop into high affinity B cells, which migrate to bone marrow, where they can persist for a long time without any antigenic stimulation, providing the basis for long-term humoral immunity [10].

Memory B cells can be also localized in the body areas being the gateways and predominant areas of infection dissemination; such cells are memory B cells, which reside in tissue [12]. After representation of the antigen, B cells begin to rapidly proliferate and differentiate into plasma cells. Furthermore, these cells can enter germinal centers again for further retraining, i.e. to increase their affinity and shift the class of immunoglobulins produced [10].

It is worth noting that follicular CD4⁺ T cells (follicular helper T cells or T_{fh} cells), which promote memory B cell differentiation into plasma cells through IL21 production, play a vital part in germinal centers. It is known that IL21 is an important cytokine involved in the pathogenesis of MS, which enables differentiation of Th17 cells. According to the latest data, T_{fh} cells play an important role in Th17-induced neuroinflammation and therefore are a potential target for MS [10, 13].

2. Regulatory B cells

The recently identified subpopulation of regulatory B cells (B_{reg}), which produce IL10 and are able to suppress immune response to foreign antigens and autoantigens, is of great interest [13, 14]. Types of B_{reg}, most frequently found in literature, are as follows: B cells CD24^{high}CD38^{high} and CD27^{int}CD38^{high}. Breg are able to stimulate differentiation of CD4⁺ T cells into regulatory T cells (T_{reg}), inhibit Th1 immune response and differentiation of Th17 cells. Breg can also suppress production of IFN- α by dendritic cells. Suppressor activity of B_{reg} decreases in individuals with autoimmune disorders [14].

Mechanisms of B cell involvement in the immunopathogenesis of MS (antibodies, cytokines, antigen presentation)

B cells are involved in the pathogenesis of MS through various mechanisms, such as antigen presentation to T cells, secretion of pro-inflammatory and anti-inflammatory cytokines, and production of autoantibodies [15].

B cells are professional antigen-presenting cells. They specifically recognize even low concentrations of antigens and constitutively express the major histocompatibility complex (MHC) class II molecules and co-stimulatory molecules, which enables B cells to prime T cells and, in turn, induce their own differentiation into memory cells and plasma cells that produce

antibodies [16, 17]. The increased activation of infiltrating T cells in the CNS, which then realize their damaging effects in brain and spinal cord, is possibly due to these processes [17].

Secretion of cytokines by B cells support neuroinflammation. B cells of patients with MS are characterized by pro-inflammatory cytokine profile. These cells produce increased amounts of IL6, lymphotoxin- α and tumor necrosis factor- α (TNF α), along with reduced production of anti-inflammatory IL10 [17]. It is found that anti-B-cell therapy suppresses autoimmune reactions via depletion of IL6-producing B lymphocytes [18].

MS is also characterized by increased intrathecal synthesis of IgG. Elevated IgG levels in cerebrospinal fluid are likely to be associated with elevated levels of circulating antibodies, particularly, with selective elevation of IgG1 and IgG3 subclass levels. Antibody production by circulating B cells contributes significantly to the pathogenesis of MS [19].

It is important that B lymphocyte involvement in the pathogenesis of MS is associated with B lymphocyte functioning both in the periphery and in the CNS. It is shown that ectopic lymphoid follicles, represented mainly by B lymphocytes, are formed in the meninges of patients with secondary progressive MS. It is believed that such B-cell structures are particularly likely to contribute to cortical demyelination and disease progression. Moreover, it has recently been found that meningeal B-cell follicles are formed from the earliest stages of demyelination, which may explain neurodegenerative changes at the disease onset [20, 21].

Diagnostic and prognostic value of assessing humoral immune parameters in individuals with demyelinating diseases

Regardless of the successes in understanding the pathogenesis of MS, no biomarkers, enabling early diagnosis of MS with high specificity and sensitivity, have been found. To date, among many immunological parameters assessed in individuals with MS, the humoral immune parameters (particularly, oligoclonal bands of immunoglobulins and IgG in cerebrospinal fluid) are of the greatest diagnostic and prognostic value [22–24].

Oligoclonal bands of immunoglobulins are determined in paired samples of blood serum and cerebrospinal fluid. The bands are formed by IgG and IgM, produced by plasma cells of the CNS. Simultaneous presence of such bands in cerebrospinal fluid and their absence in blood serum indicate the increased intrathecal antibody production and are associated with MS (oligoclonal bands of immunoglobulins present in cerebrospinal fluid and absent in blood serum are found in 95% of patients with MS). However, it is worth mentioning that oligoclonal bands of immunoglobulins are not specific for MS and can be found in individuals with different inflammatory disorders of the CNS [23]. Thus, this is an additional indicator to be used for diagnosis of MS; it is rather used to bear out the nature of the disorder when trying to exclude other inflammatory disorders of the CNS.

Assessment of free immunoglobulin κ -light chains in cerebrospinal fluid is highly sensitive and specific for MS [25].

Prognostic value of assessing oligoclonal bands of immunoglobulins and free immunoglobulin κ -light chains in cerebrospinal fluid in order to estimate the risk of conversion from clinically isolated syndrome (CIS) and radiologically isolated syndrome (RIS) (early forms of demyelination) is also discussed. Thus, several major studies have shown that the presence of oligoclonal bands of immunoglobulins in patients with CIS and RIS increases the risk of conversion in individuals with MS [25–27].

Humoral immune parameters are also studied in individuals with different disorders of the CNS. For example, antibodies to

aquaporin-4, as well as to myelin oligodendrocyte glycoprotein (MOG), are of high value for diagnosis of neuromyelitis optica spectrum disorder (NMOSD) and MOG-antibody associated diseases respectively [28].

Impact of anti-B-cell therapy on the course of MS

Understanding of the anti-B-cell therapy (especially based on monoclonal anti-CD20 antibody) clinical efficiency in individuals with MS has recently become one of the most important events in treatment of this disorder. Moreover, to date, anti-B-cell therapy with ocrelizumab is the only method for treatment of primary progressive MS with proven efficacy [29]. Ocrelizumab and ofatumumab (the latter has not yet been approved in Russian Federation) are being actively used in individuals with active relapsing MS and secondary progressive MS with exacerbations. The need to determine the criteria for such medication personalized prescription, i. e. identification of prognostic markers of optimal/suboptimal response to therapy, is one of the main issues related to anti-B-cell therapy prescription. Optimal drug dose and dosage frequency are the other issue.

From this perspective, determining the percentage of the immunological memory B cells (CD19⁺CD27⁺) attracts the greatest attention [30, 31]. Currently, this method is used (off-label) in the countries of the European Union and in the USA within the framework of personalized approach to treatment of patients, who receive rituximab and ocrelizumab for treatment of MS and neuromyelitis optica [30]. Control of memory B cell levels aimed at optimization of rituximab therapy in individuals with neuromyelitis optica spectrum disorders (NMOSD) is recommended by the French cohort on NMO and related disorders (NOMADMUS) [32]. Memory B cells in the peripheral blood mononuclear cell fraction were analyzed within the framework of several clinical trials in order to optimize treatment of neuromyelitis optica with rituximab [23–35]. In the course of one of these trials 100 patients with neuromyelitis optica were treated with rituximab during an average period of 67 months (achieving the levels of memory B cells of > 0.05% of the peripheral blood mononuclear cell number in two years and of > 0.1% in the following years) [34]. The annualized relapse rate was reduced from 2.4 to 0.1 upon treatment, and disability improved or stabilized in 96% of patients.

However, there are no known trials, during which the recording of individual clinical, brain imaging and immunological parameters has served as an occasion for modifying the protocol of MS treatment with alemtuzumab, cladribine, ocrelizumab, with the exception of adverse reactions, including lymphopenia.

When studying the mechanism of action of the listed above medications, it has been found, that selective apoptosis of the immunological memory B cell pool is a key aspect of these medications efficiency in treatment of MS and NMOSD. Thus, alemtuzumab, one of the highly effective medications for treatment of MS, induces T and B cell death followed by rapid recovery of the population of immature and mature B cells, along with the long-term decrease in the levels of the CD19⁺CD27⁺ memory B cells [36]. Analysis of lymphocyte subpopulations, performed within the framework of cladribine tablets clinical trial, showed that the decrease in the levels of CD4⁺ T cells was 40–45%, and the decrease in the levels of CD8⁺ cells was 15–20% throughout the year after using the medication. However, the decrease in the levels of CD19⁺ B cells was more sufficient [37, 38]. It should be noted that high clinical efficacy of cladribine cannot be explained by the

Table. Effects of medications, modifying the course of MS, on B cell functions in EAE and MS

Therapy	Disorder	Effects on B lymphocytes	Authors
Glatiramer acetate	EAE	Increased production of IL4, IL10 and IL13 along with reduced production of IL6, IL12 and TNF α by B cells	[44, 45]
	MS	Reduced expression of CXCR5 and ICAM-3 in B lymphocytes. Reduced production of IL6 and TNF α , increased production of IL10 by B cells	[44, 46]
IFN β	EAE	Increased number of IL10-producing B _{reg} cells	[47]
	MS	Suppressed expression of IL1 β , IL23 genes. Increased number of IL10-producing B _{reg} cells	[47, 48]
Dimethyl fumarate	EAE	Suppressed expression of MHC II in B cells B, reduced production of GM-CSF, TNF α and IL6 by B cells	[49, 50]
	MS	Reduced number of CD19 ⁺ CD27 ⁺ memory B cells. Reduced production of GM-CSF, IL6 and TNF α by B cells	[49, 51]
Teriflunomide	EAE	Reduced number of B cells migrating to CNS	[52]
	MS	Reduced total number of B cells	[53, 54]
Fingolimod	EAE	Prevention of B cell follicle formation in meninges	[50]
	MS	Reduced number of circulating B cells. Reduced production of TNF α and increased production of IL10 by B cells	[49, 50, 54]
Natalizumab	MS	Increased number of B _{reg} cells circulating in peripheral blood. Reduced number of B cells in cerebrospinal fluid	[50, 55]
Ocrelizumab	EAE	Reduced number of B cells in bone marrow, lymph nodes and spleen	[56]
	MS	Reduced number of CD20 ⁺ B cells	[53, 57]
Cladribine	MS	Reduced number of circulating memory B cells. Increased production of IL10 by B cells	[53]
Alemtuzumab	MS	Reduced number of circulating B cells	[49, 50]

decrease in CD4⁺ T cells only; studying monoclonal anti-CD4 antibodies showed that the decrease in the levels of CD4⁺ T cells resulted in slightly reduced MS relapse rate by 60–70% [39]. The cladribine tablets clinical trial revealed the dose-dependent effect (between the doses of 5.25 mg/kg and 3.5 mg/kg) on the CD4 and CD8 cell populations, but not on B cells [37]. Taking into account the same results of using both doses of cladribine, the effects of this medication were attributed to its effects exerted primarily on B cells [38]. In contrast, recovery of memory B cell population upon treatment with alemtuzumab was combined with recurrence of MS activity and the need for repeated courses of treatment [38, 40–42].

It has been shown that anti-B-cell therapy with monoclonal anti-CD20 antibody is highly effective in individuals with MS. The use of ocrelizumab results in significantly decreased levels of CD19⁺ B cells. That is why administration of the drug every 6 months may be too much for some patients. Thus, during phase II clinical trial of ocrelizumab in individuals with relapse MS, where the experimental groups, which received placebo and IFN β , were treated by ocrelizumab after 24 weeks, and then received

the medication after 24, 48, 72 weeks and were followed-up up to week 144, the relapse rate and disability progression were low within 18 months after the last administration of the drug [43].

It is important to mention that B cell functions are affected not only by anti-B-cell therapy, but also by other drugs, modifying the course of MS. This could explain these medications' clinical efficacy. Effects of other disease-modifying treatments of MS on B cell functions in animals with experimental autoimmune encephalomyelitis (EAE) and individuals with MS are presented in the Table.

CONCLUSIONS

The importance of humoral immunity in the pathogenesis and treatment of demyelinating diseases of the CNS is not subject to doubt. However, the mechanisms mediating the role of B cells in such disorders are poorly understood. Migration of B cells from the periphery into CNS through blood-brain barrier, importance of B cells at the early stages of demyelination, and effects of anti-B-cell therapy on B cells of the CNS are just some of many issues to be clarified.

References

- Boyko A, Melnikov M. Prevalence and incidence of multiple sclerosis in Russian Federation: 30 years of studies. *Brain Sci.* 2020 May 18; 10 (5): 305. DOI: 10.3390/brainsci10050305.
- Kamali AN, Noorbakhsh SM, Hamedifar H, Jadidi-Niaragh F, Yazdani R, Bautista JM, et al. A role for Th1-like Th17 cells in the pathogenesis of inflammatory and autoimmune disorders. *Mol Immunol.* 2019 Jan; 105: 107–15. DOI: 10.1016/j.molimm.2018.11.015.
- Ziemssen T, Akgün K, Brück W. Molecular biomarkers in multiple sclerosis. *J Neuroinflammation.* 2019 Dec 23; 16 (1): 272. DOI: 10.1186/s12974-019-1674-2.
- Milo R. Therapies for multiple sclerosis targeting B cells. *Croat Med J.* 2019 Apr 30; 60 (2): 87–98. DOI: 10.3325/cmj.2019.60.87.
- Corfe SA, Paige CJ. The many roles of IL7 in B cell development; mediator of survival, proliferation and differentiation. *Semin Immunol.* 2012; 24 (3), 198–208. DOI: 10.1016/j.smim.2012.02.001.
- Bemark M. Translating transitions — how to decipher peripheral human B cell development. *J Biomed Res.* 2015; 29 (4): 264–84. DOI: 10.7555/JBR.29.20150035.
- Kaminski DA, Wei C, Qian Y, Rosenberg AF, Sanz I. Advances in human B cell phenotypic profiling. *Front Immunol* 3. 2012; 302. DOI: 10.3389/fimmu.2012.00302.
- Khodadadi L, Cheng Q, Radbruch A, Hiepe F. The maintenance of memory plasma cells. *Front Immunol* 10. 2019; 721. DOI: 10.3389/fimmu.2019.00721.
- Pavlasova G, Mraz M. The regulation and function of CD20: an "enigma" of B-cell biology and targeted therapy. *Haematologica.* 2020; 105 (6): 1494–506. DOI: 10.3324/haematol.2019.243543.
- Palm AE, Henry C. Remembrance of things past: long-term B cell memory after infection and vaccination. *Front Immunol.* 2019; 10:

1787. DOI: 10.3389/fimmu.2019.01787.
11. Luz EC, Damaris EL. "Introduction to T and B lymphocytes," in autoimmunity: from bench to bedside. El Rosario University Press, 2013.
 12. Adachi Y, Onodera T, Yamada Y, Daio R, Tsuiji M, Inoue T, et al. Distinct germinal center selection at local sites shapes memory B cell response to viral escape. *J Exp Med*. 2015; 212 (10), 1709–23. DOI: 10.1084/jem.20142284.
 13. Quinn JL, Kumar G, Agasing A, Ko RM, Axtell RC. Role of TFH cells in promoting T helper 17-induced neuroinflammation. *Front Immunol*. 2018; 9: 382. DOI: 10.3389/fimmu.2018.00382.
 14. Atisha-Fregoso Y, Zou YR, Diamond B. "B cells and generation of antibodies". In: Dubois' Lupus Erythematosus and Related Syndromes. Elsevier, 2019; 101–15.
 15. Sospedra M. B cells in multiple sclerosis. *Curr Opin Neurol*. 2018; 31 (3): 256–262. DOI: 10.1097/WCO.0000000000000563.
 16. Adler LN, Jiang W, Bhamidipati K, Millican M, Macaubas C, et al. The other function: class II-restricted antigen presentation by B cells. *Front Immunol*. 2017; 8: 319. DOI: 10.3389/fimmu.2017.00319.
 17. Hausser-Kinzel S, Weber MS. The role of B cells and antibodies in multiple sclerosis, neuromyelitis optica, and related disorders. *Front Immunol*. 2019; 10: 201. DOI: 10.3389/fimmu.2019.00201.
 18. Barr TA, Shen P, Brown S, Lampropoulou V, Roch T, Lawrie S, et al. B cell depletion therapy ameliorates autoimmune disease through ablation of IL6-producing B cells. *J Exp Med*. 2012; 209 (5): 1001–10. DOI: 10.1084/jem.20111675.
 19. Yu X, Graner M, Kennedy PGE, Liu Y. The role of antibodies in the pathogenesis of multiple sclerosis. *Front Neurol*. 2020; 11: 533388. DOI: 10.3389/fneur.2020.533388.
 20. Negron A, Stüve O, Forsthuber TG. Ectopic lymphoid follicles in multiple sclerosis: Centers for Disease Control. *Front Neurol*. 2020 Dec 8; 11: 607766. DOI: 10.3389/fneur.2020.607766.
 21. Bell L, Lenhart A, Rosenwald A, Monoranu CM, Berberich-Siebelt F. Lymphoid aggregates in the CNS of progressive multiple sclerosis patients lack regulatory T cells. *Front Immunol*. 2020 Jan 15; 10: 3090. DOI: 10.3389/fimmu.2019.03090.
 22. Ziemssen T, Akgün K, Brück W. Molecular biomarkers in multiple sclerosis. *J Neuroinflammation*. 2019 Dec 23; 16 (1): 272. DOI: 10.1186/s12974-019-1674-2.
 23. Schwenkenbecher P, Konen FF, Wurster U, Jendretzky KF, Gingele S, Sühs KW, et al. The persisting significance of oligoclonal bands in the dawn era of kappa free light chains for the diagnosis of multiple sclerosis. *Int J Mol Sci*. 2018 Nov 29; 19 (12): 3796. DOI: 10.3390/ijms19123796.
 24. Lefvert A, Link H. IgG production within the central nervous system: a critical review of proposed formulae. *Ann Neurol*. 1985; 17: 13–20. DOI: 10.1002/ana.410170105.
 25. Tintore M, Rovira À, Río J, Otero-Romero S, Arrambide G, Tur C, et al. Defining high, medium and low impact prognostic factors for developing multiple sclerosis. *Brain*. 2015 Jul; 138 (Pt 7): 1863–74. DOI: 10.1093/brain/aww105.
 26. Kuhle J, Disanto G, Dobson R, et al. Conversion from clinically isolated syndrome to multiple sclerosis: A large multicentre study. *Mult Scler*. 2015; 21 (8): 1013–24.
 27. Lebrun-Frenay C, Kantarci O, Siva A, Sormani MP, Pelletier D, Okuda DT. 10-year RISC study group on behalf of SFSEP, OFSEP. Radiologically isolated syndrome: 10-year risk estimate of a clinical event. *Ann Neurol*. 2020 Aug; 88 (2): 407–17. DOI: 10.1002/ana.25799.
 28. Hor JY, Asgari N, Nakashima I, Broadley SA, Leite MI, Kissani N, et al. Epidemiology of neuromyelitis optica spectrum disorder and its prevalence and incidence worldwide. *Front Neurol*. 2020 Jun 26; 11: 501. DOI: 10.3389/fneur.2020.00501.
 29. Greenfield AL, Hauser SL. B-cell therapy for multiple sclerosis: entering an era. *Ann Neurol*. 2018 Jan; 83 (1): 13–26. DOI: 10.1002/ana.25119.
 30. Baker D, Marta M, Pryce G, Giovannoni G, Schmierer K. Memory B cells are major targets for effective immunotherapy in relapsing multiple sclerosis. *E Bio Medicine*. 2017; 16: 41–50.
 31. Bose T. Role of immunological memory cells as a therapeutic target in multiple sclerosis. *Brain Sci*. 2017; 7 (11): E148.
 32. Ciron J, Audoin B, Bourre B, Brassat D, Durand-Dubief F, Laplaud D, et al. NOMADMUS group, under the aegis of OFSEP, SFSEP. Recommendations for the use of Rituximab in neuromyelitis optica spectrum disorders *Rev Neurol (Paris)*. 2018; 174 (4): 255–64.
 33. Kim SH, Kim W, Li XF, Jung IJ, Kim HJ. Repeated treatment with rituximab based on the assessment of peripheral circulating memory B cells in patients with relapsing neuromyelitis optica over 2 years. *Arch Neurol*. 2011; 68, 1412–20.
 34. Kim SH, Jeong IH, Hyun JW, Joung A, Jo HJ, Hwang SH, et al. Treatment outcomes with rituximab in 100 patients with neuromyelitis optica: influence of FCGR3A polymorphisms on the therapeutic response to rituximab. *JAMA Neurol*. 72: 989–95.
 35. Kim SH, Huh SY, Lee SJ, Joung A, Kim HJ. A5-year follow-up of rituximab treatment in patients with neuromyelitis optica spectrum disorder. *JAMA Neurol*. 2013; 70: 1110–7.
 36. Thompson SA, Jones JL, Cox AL, et al. B-cell reconstitution and BAFF after alemtuzumab (CAMPATH-1H) treatment of multiple sclerosis. *J Clin Immunol*. 2010; 30: 99–105.
 37. Duddy M, Niino M, Adatia F, et al. Distinct effector cytokine profile of memory and naive human B cell subsets and implication in multiple sclerosis. *J Immunol*. 2007; 178: 6092–9.
 38. Giovannoni G, Cohen JA, Coles AJ, Hartung HP, Havrdova E, Selmaj KW, et al. CARE-MS II Investigators. Alemtuzumab improves preexisting disability in active relapsing-remitting MS patients. *Neurology*. 2016 Nov 8; 87 (19): 1985–92.
 39. Van Oosten BW, Lai M, Hodgkinson S, et al. Treatment of multiple sclerosis with the monoclonal anti-CD4 antibody cM-T412: results of a randomized, double-blind, placebo-controlled, MR-monitored phase II trial. *Neurology*. 1997; 49: 351–7.
 40. Ceronie B, Jacobs BM, Baker D, Dubuisson N, Mao Z, Ammoscato F, et al. Cladribine treatment of multiple sclerosis is associated with depletion of memory B cells. *J Neurol*. 2018 May; 265 (5): 1199–209.
 41. Giovannoni G, Cohen JA, Coles AJ, Hartung HP, Havrdova E, Selmaj KW, et al. CARE-MS II Investigators. Alemtuzumab improves preexisting disability in active relapsing-remitting MS patients. *Neurology*. 2016 Nov 8; 87 (19): 1985–92.
 42. Havrdova E, Arnold DL, Cohen JA, Hartung HP, Fox EJ, Giovannoni G, et al. CARE-MS I and CAMMS03409 Investigators. Alemtuzumab CARE-MS I 5-year follow-up: Durable efficacy in the absence of continuous MS therapy. *Neurology*. 2017 Sep 12; 89 (11): 1107–16. *Neurology*. 2018 Apr 17; 90 (16): 755.
 43. Genovese MC, Kaine JL, Lowenstein MB, et al. Ocrelizumab, a humanized antiCD20 monoclonal antibody, in the treatment of patients with rheumatoid arthritis: a phase I/II randomized, blinded, placebo-controlled, dose-ranging study. *Arthritis Rheum*. 2008; 58: 2652–61.
 44. Kuerten S, Jackson LJ, Kaye J, Vollmer TL. Impact of glatiramer acetate on B cell-mediated pathogenesis of multiple sclerosis. *CNS Drugs*. 2018; 32 (11): 1039–51.
 45. Begum-Haque S, Christy M, Ochoa-Reparaz J, Nowak EC, Mielcarz D, Haque A, et al. Augmentation of regulatory B cell activity in experimental allergic encephalomyelitis by glatiramer acetate. *J Neuroimmunol*. 2011 Mar; 232 (0): 136–44.
 46. Ireland SJ, Guzman AA, O'Brien DE, Hughes S, Greenberg B, Flores A, et al. The effect of glatiramer acetate therapy on functional properties of B cells from patients with relapsing-remitting multiple sclerosis. *JAMA Neurol*. 2014 Nov; 71 (11): 1421–8.
 47. Schubert RD, Hu Y, Kumar G, Szeto S, Abraham P, Winderl J, et al. Interferon- β treatment requires B cells for efficacy in neuro-autoimmunity. *J Immunol*. 2015 Mar 1; 194 (5): 2110–6.
 48. Ramgolam VS, Sha Y, Marcus KL, Choudhary N, Troiani L, Chopra M, et al. B cells as a therapeutic target for IFN- β in relapsing-remitting multiple sclerosis. *J Immunol*. 2011; 186 (7): 4518–26.
 49. Sabatino JJ, Zamvil SS, Hauser SL. B-cell therapies in multiple sclerosis. *Cold Spring Harb Perspect Med*. 2019 Feb; 9 (2): a032037.
 50. Lehmann-Horn K, Kinzel S, Weber MS. Deciphering the role of B cells in multiple sclerosis-towards specific targeting of pathogenic function. *Int J Mol Sci*. 2017 Oct; 18 (10): 2048.
 51. Gregson A, Thompson K, Tsirka SE, Selwood DL. Emerging small-molecule treatments for multiple sclerosis: focus on B cells. *F1000Res*. 2019; 8: F1000 Faculty Rev-245.
 52. Braley TJ, Segal BM. B-cell targeting agents in the treatment of multiple sclerosis. *Curr Treat Options Neurol*. 2013 Jun; 15 (3): 259–69.

53. Traub JW, Häusser-Kinzel S, Weber MS. Differential effects of MS therapeutics on B cells-implications for their use and failure in AQP4-positive NMOSD patients. *Int J Mol Sci.* 2020 Jul; 21 (14): 5021.
54. Claes N, Fraussen J, Stinissen P, Hupperts R, Somers V. B cells are multifunctional players in multiple sclerosis pathogenesis: insights from therapeutic interventions. *Front Immunol.* 2015; 6: 642.
55. Traub JW, Pellkofer HL, Grondey K, Seeger I, Rowold C, Brück W, et al. Natalizumab promotes activation and pro-inflammatory differentiation of peripheral B cells in multiple sclerosis patients. *J Neuroinflammation.* 2019; 16: 228.
56. Häusler D, Häusser-Kinzel S, Feldmann L, Torke S, Lepennetier G, Bernard CCA, et al. Functional characterization of reappearing B cells after anti-CD20 treatment of CNS autoimmune disease. *Proc Natl Acad Sci USA.* 2018 Sep 25; 115 (39): 9773–8.
57. Fernández-Velasco JI, Kuhle J, Monreal E, et al. Effect of ocrelizumab in blood leukocytes of patients with primary progressive MS. *Neurol Neuroimmunol Neuroinflamm.* 2021 Mar; 8 (2): e940.

Литература

1. Boyko A, Melnikov M. Prevalence and incidence of multiple sclerosis in Russian Federation: 30 years of studies. *Brain Sci.* 2020 May 18; 10 (5): 305. DOI: 10.3390/brainsci10050305.
2. Kamali AN, Noorbakhsh SM, Hamedifar H, Jadidi-Niaragh F, Yazdani R, Bautista JM, et al. A role for Th1-like Th17 cells in the pathogenesis of inflammatory and autoimmune disorders. *Mol Immunol.* 2019 Jan; 105: 107–15. DOI: 10.1016/j.molimm.2018.11.015.
3. Ziemssen T, Akgün K, Brück W. Molecular biomarkers in multiple sclerosis. *J Neuroinflammation.* 2019 Dec 23; 16 (1): 272. DOI: 10.1186/s12974-019-1674-2.
4. Milo R. Therapies for multiple sclerosis targeting B cells. *Croat Med J.* 2019 Apr 30; 60 (2): 87–98. DOI: 10.3325/cmj.2019.60.87.
5. Corfe SA, Paige CJ. The many roles of IL7 in B cell development; mediator of survival, proliferation and differentiation. *Semin Immunol.* 2012; 24 (3), 198–208. DOI: 10.1016/j.smim.2012.02.001.
6. Bemark M. Translating transitions — how to decipher peripheral human B cell development. *J Biomed Res.* 2015; 29 (4): 264–84. DOI: 10.7555/JBR.29.20150035.
7. Kaminski DA, Wei C, Qian Y, Rosenberg AF, Sanz I. Advances in human B cell phenotypic profiling. *Front Immunol.* 2012; 3: 302. DOI: 10.3389/fimmu.2012.00302.
8. Khodadadi L, Cheng Q, Radbruch A, Hiepe F. The maintenance of memory plasma cells. *Front Immunol.* 2019; 10: 2019. DOI: 10.3389/fimmu.2019.00721.
9. Pavlasova G, Mraz M. The regulation and function of CD20: an "enigma" of B-cell biology and targeted therapy. *Haematologica.* 2020; 105 (6): 1494–506. DOI: 10.3324/haematol.2019.243543.
10. Palm AE, Henry C. Remembrance of things past: long-term B cell memory after infection and vaccination. *Front Immunol.* 2019; 10: 1787. DOI: 10.3389/fimmu.2019.01787.
11. Luz EC, Damaris EL. "Introduction to T and B lymphocytes," in autoimmunity: from bench to bedside. El Rosario University Press, 2013.
12. Adachi Y, Onodera T, Yamada Y, Daio R, Tsujii M, Inoue T, et al. Distinct germinal center selection at local sites shapes memory B cell response to viral escape. *J Exp Med.* 2015; 212 (10), 1709–23. DOI: 10.1084/jem.20142284.
13. Quinn JL, Kumar G, Agasing A, Ko RM, Axtell RC. Role of TFH cells in promoting T helper 17-induced neuroinflammation. *Front Immunol.* 2018; 9: 382. DOI: 10.3389/fimmu.2018.00382.
14. Atisha-Fregoso Y, Zou YR, Diamond B. "B cells and generation of antibodies". In: Dubois' Lupus Erythematosus and Related Syndromes. Elsevier, 2019; 101–15.
15. Sospedra M. B cells in multiple sclerosis. *Curr Opin Neurol.* 2018; 31 (3): 256–262. DOI: 10.1097/WCO.0000000000000563.
16. Adler LN, Jiang W, Bhamidipati K, Millican M, Macaubas C, et al. The other function: class II-restricted antigen presentation by B cells. *Front Immunol.* 2017; 8: 319. DOI: 10.3389/fimmu.2017.00319.
17. Häusser-Kinzel S, Weber MS. The role of B cells and antibodies in multiple sclerosis, neuromyelitis optica, and related disorders. *Front Immunol.* 2019; 10: 201. DOI: 10.3389/fimmu.2019.00201.
18. Barr TA, Shen P, Brown S, Lampropoulou V, Roch T, Lawrie S, et al. B cell depletion therapy ameliorates autoimmune disease through ablation of IL6-producing B cells. *J Exp Med.* 2012; 209 (5): 1001–10. DOI: 10.1084/jem.20111675.
19. Yu X, Graner M, Kennedy PGE, Liu Y. The role of antibodies in the pathogenesis of multiple sclerosis. *Front Neurol.* 2020; 11: 533388. DOI: 10.3389/fneur.2020.533388.
20. Negron A, Stüve O, Forsthuber TG. Ectopic lymphoid follicles in multiple sclerosis: Centers for Disease Control. *Front Neurol.* 2020 Dec 8; 11: 607766. DOI: 10.3389/fneur.2020.607766.
21. Bell L, Lenhart A, Rosenwald A, Monoranu CM, Berberich-Siebelt F. Lymphoid aggregates in the CNS of progressive multiple sclerosis patients lack regulatory T cells. *Front Immunol.* 2020 Jan 15; 10: 3090. DOI: 10.3389/fimmu.2019.03090.
22. Ziemssen T, Akgün K, Brück W. Molecular biomarkers in multiple sclerosis. *J Neuroinflammation.* 2019 Dec 23; 16 (1): 272. DOI: 10.1186/s12974-019-1674-2.
23. Schwenkenbecher P, Konen FF, Wurster U, Jendretzky KF, Gingele S, Sühs KW, et al. The persisting significance of oligoclonal bands in the dawning era of kappa free light chains for the diagnosis of multiple sclerosis. *Int J Mol Sci.* 2018 Nov 29; 19 (12): 3796. DOI: 10.3390/ijms19123796.
24. Lefvert A, Link H. IgG production within the central nervous system: a critical review of proposed formulae. *Ann Neurol.* 1985; 17: 13–20. DOI: 10.1002/ana.410170105.
25. Tintore M, Rovira À, Río J, Otero-Romero S, Arrambide G, Tur C, et al. Defining high, medium and low impact prognostic factors for developing multiple sclerosis. *Brain.* 2015 Jul; 138 (Pt 7): 1863–74. DOI: 10.1093/brain/awv105.
26. Kuhle J, Disanto G, Dobson R, et al. Conversion from clinically isolated syndrome to multiple sclerosis: A large multicentre study. *Mult Scler.* 2015; 21 (8): 1013–24.
27. Lebrun-Frenay C, Kantarci O, Siva A, Sormani MP, Pelletier D, Okuda DT. 10-year RISC study group on behalf of SFSEP, OFSEP. Radiologically isolated syndrome: 10-year risk estimate of a clinical event. *Ann Neurol.* 2020 Aug; 88 (2): 407–17. DOI: 10.1002/ana.25799.
28. Hor JY, Asgari N, Nakashima I, Broadley SA, Leite MI, Kissani N, et al. Epidemiology of neuromyelitis optica spectrum disorder and its prevalence and incidence worldwide. *Front Neurol.* 2020 Jun 26; 11: 501. DOI: 10.3389/fneur.2020.00501.
29. Greenfield AL, Hauser SL. B-cell therapy for multiple sclerosis: entering an era. *Ann Neurol.* 2018 Jan; 83 (1): 13–26. DOI: 10.1002/ana.25119.
30. Baker D, Marta M, Pryce G, Giovannoni G, Schmierer K. Memory B cells are major targets for effective immunotherapy in relapsing multiple sclerosis. *E Bio Medicine.* 2017; 16: 41–50.
31. Bose T. Role of immunological memory cells as a therapeutic target in multiple sclerosis. *Brain Sci.* 2017; 7 (11): E148.
32. Ciron J, Audoin B, Bourre B, Brassat D, Durand-Dubief F, Laplaud D, et al. NOMADMUS group, under the aegis of OFSEP, SFSEP. Recommendations for the use of Rituximab in neuromyelitis optica spectrum disorders. *Rev Neurol (Paris).* 2018; 174 (4): 255–64.
33. Kim SH, Kim W, Li XF, Jung IJ, Kim HJ. Repeated treatment with rituximab based on the assessment of peripheral circulating memory B cells in patients with relapsing neuromyelitis optica over 2 years. *Arch Neurol.* 2011; 68, 1412–20.
34. Kim SH, Jeong IH, Hyun JW, Joung A, Jo HJ, Hwang SH, et al. Treatment outcomes with rituximab in 100 patients with neuromyelitis optica: influence of FCGR3A polymorphisms on the therapeutic response to rituximab. *JAMA Neurol.* 2013; 70: 989–95.
35. Kim SH, Huh SY, Lee SJ, Joung A, Kim HJ. A5-year follow-up of rituximab treatment in patients with neuromyelitis optica spectrum disorder. *JAMA Neurol.* 2013; 70: 1110–7.
36. Thompson SA, Jones JL, Cox AL, et al. B-cell reconstitution and BAFF after alemtuzumab (CAMPATH-1H) treatment of multiple

- sclerosis. *J Clin Immunol*. 2010; 30: 99–105.
37. Duddy M, Niino M, Adatia F, et al. Distinct effector cytokine profiles of memory and naive human B cell subsets and implication in multiple sclerosis. *J Immunol*. 2007; 178: 6092–9.
 38. Giovannoni G, Cohen JA, Coles AJ, Hartung HP, Havrdova E, Selmaj KW, et al. CARE-MS II Investigators. Alemtuzumab improves preexisting disability in active relapsing-remitting MS patients. *Neurology*. 2016 Nov 8; 87 (19): 1985–92.
 39. Van Oosten BW, Lai M, Hodgkinson S, et al. Treatment of multiple sclerosis with the monoclonal anti-CD4 antibody cM-T412: results of a randomized, double-blind, placebo-controlled, MR-monitored phase II trial. *Neurology*. 1997; 49: 351–7.
 40. Ceronie B, Jacobs BM, Baker D, Dubuisson N, Mao Z, Ammoscato F, et al. Cladribine treatment of multiple sclerosis is associated with depletion of memory B cells. *J Neurol*. 2018 May; 265 (5): 1199–209.
 41. Giovannoni G, Cohen JA, Coles AJ, Hartung HP, Havrdova E, Selmaj KW, et al. CARE-MS II Investigators. Alemtuzumab improves preexisting disability in active relapsing-remitting MS patients. *Neurology*. 2016 Nov 8; 87 (19): 1985–92.
 42. Havrdova E, Arnold DL, Cohen JA, Hartung HP, Fox EJ, Giovannoni G, et al. CARE-MS I and CAMMS03409 Investigators. Alemtuzumab CARE-MS I 5-year follow-up: Durable efficacy in the absence of continuous MS therapy. *Neurology*. 2017 Sep 12; 89 (11): 1107–16. *Neurology*. 2018 Apr 17; 90 (16): 755.
 43. Genovese MC, Kaine JL, Lowenstein MB, et al. Ocrelizumab, a humanized anti-CD20 monoclonal antibody, in the treatment of patients with rheumatoid arthritis: a phase I/II randomized, blinded, placebo-controlled, dose-ranging study. *Arthritis Rheum*. 2008; 58: 2652–61.
 44. Kuerten S, Jackson LJ, Kaye J, Vollmer TL. Impact of glatiramer acetate on B cell-mediated pathogenesis of multiple sclerosis. *CNS Drugs*. 2018; 32 (11): 1039–51.
 45. Begum-Haque S, Christy M, Ochoa-Reparaz J, Nowak EC, Mielcarz D, Haque A, et al. Augmentation of regulatory B cell activity in experimental allergic encephalomyelitis by glatiramer acetate. *J Neuroimmunol*. 2011 Mar; 232 (0): 136–44.
 46. Ireland SJ, Guzman AA, O'Brien DE, Hughes S, Greenberg B, Flores A, et al. The effect of glatiramer acetate therapy on functional properties of B cells from patients with relapsing-remitting multiple sclerosis. *JAMA Neurol*. 2014 Nov; 71 (11): 1421–8.
 47. Schubert RD, Hu Y, Kumar G, Szeto S, Abraham P, Winderl J, et al. Interferon- β treatment requires B cells for efficacy in neuro-autoimmunity. *J Immunol*. 2015 Mar 1; 194 (5): 2110–6.
 48. Ramgolam VS, Sha Y, Marcus KL, Choudhary N, Troiani L, Chopra M, et al. B cells as a therapeutic target for IFN- β in relapsing-remitting multiple sclerosis. *J Immunol*. 2011; 186 (7): 4518–26.
 49. Sabatino JJ, Zamvil SS, Hauser SL. B-cell therapies in multiple sclerosis. *Cold Spring Harb Perspect Med*. 2019 Feb; 9 (2): a032037.
 50. Lehmann-Horn K, Kinzel S, Weber MS. Deciphering the role of B cells in multiple sclerosis-towards specific targeting of pathogenic function. *Int J Mol Sci*. 2017 Oct; 18 (10): 2048.
 51. Gregson A, Thompson K, Tsirka SE, Selwood DL. Emerging small-molecule treatments for multiple sclerosis: focus on B cells. *F1000Res*. 2019; 8: F1000 Faculty Rev-245.
 52. Braley TJ, Segal BM. B-cell targeting agents in the treatment of multiple sclerosis. *Curr Treat Options Neurol*. 2013 Jun; 15 (3): 259–69.
 53. Traub JW, Häusser-Kinzel S, Weber MS. Differential effects of MS therapeutics on B cells-implications for their use and failure in AQP4-positive NMOSD patients. *Int J Mol Sci*. 2020 Jul; 21 (14): 5021.
 54. Claes N, Fraussen J, Stinissen P, Hupperts R, Somers V. B cells are multifunctional players in multiple sclerosis pathogenesis: insights from therapeutic interventions. *Front Immunol*. 2015; 6: 642.
 55. Traub JW, Pellkofer HL, Gröndey K, Seeger I, Rowold C, Brück W, et al. Natalizumab promotes activation and pro-inflammatory differentiation of peripheral B cells in multiple sclerosis patients. *J Neuroinflammation*. 2019; 16: 228.
 56. Häusler D, Häusser-Kinzel S, Feldmann L, Torke S, Lepennetier G, Bernard CCA, et al. Functional characterization of reappearing B cells after anti-CD20 treatment of CNS autoimmune disease. *Proc Natl Acad Sci USA*. 2018 Sep 25; 115 (39): 9773–8.
 57. Fernández-Velasco JI, Kuhle J, Monreal E, et al. Effect of ocrelizumab in blood leukocytes of patients with primary progressive MS. *Neurol Neuroimmunol Neuroinflamm*. 2021 Mar; 8 (2): e940.

DIABETES MELLITUS MANAGEMENT STRATEGIES IN ATHLETES

Dergacheva LI¹, Derevoyedov AA¹, Vykhodets IT², Pavlova AA¹ ✉, Parastayev SA^{1,3}¹ Federal Research and Clinical Center for Sports Medicine and Rehabilitation of the Federal Medical Biological Agency, Moscow, Russia² Office of the Sports Medicine organization and digitalization of the Federal Medical and Biological Agency, Moscow, Russia³ Pirogov Russian National Research Medical University, Moscow, Russia

Glycemic control is the biggest challenge for athletes with diabetes mellitus (DM) on insulin therapy. Done well, it can keep glycogen metabolism normal and allow performance improvement through adjustment of the insulin doses to the specifics of nutrition and exercising. In DM Type 1 and Type 2 patients, intense physical activity and resistance exercising, as well as interval training, enable optimal physiological adaptation during the training period and prove to be beneficial when the athlete does one-time exercise sets. But for athletes with DM on insulin therapy, keeping blood glucose at the optimal level is not the only important issue. It is also necessary to factor in the potential body temperature regulation disturbances that increase the risk of heat stress during training/competition, learn the effects the drugs used by athletes may have on the glycemic status, control electrolyte balance and dehydration, know how to execute the application for permission to use insulin for therapeutic purposes submitted to the anti-doping organization. The purpose of this review was to draw attention of sports medicine physicians and coaches to the above problems and to the need for wider use of the new DM control technology; help athletes with DM on insulin therapy continuously perform well and ensure their athletic longevity.

Keywords: athletes; diabetes mellitus; therapeutic use exemption; insulin; physiological adaptation, sports performance, physical loads/exercises

Funding: the study relied on the financial support released under the State Assignment No. 67.003.20.800 issued by the Federal Medical Biological Agency of Russia.

Author contribution: Dergacheva LI — significant contribution to the study conceptualization, data collection, content analysis, text authoring; Derevoyedov AA, Parastayev SA — critical review of the content, approval of the final version of the article; Vykhodets IT — approval of the final version of the article; Pavlova AA — text authoring, manuscript formalization.

✉ **Correspondence should be addressed:** Anna A. Pavlova
Bolshaya Dorogomilovskaya, 5, Moscow, 121059; dr_pavlova@hotmail.com

Received: 20.07.2021 **Accepted:** 27.08.2021 **Published online:** 28.09.2021

DOI: 10.47183/mes.2021.034

СТРАТЕГИИ УПРАВЛЕНИЯ САХАРНЫМ ДИАБЕТОМ У СПОРТСМЕНОВ

Л. И. Дергачева¹, А. А. Деревоедов¹, И. Т. Выходец², А. А. Павлова¹ ✉, С. А. Парастаев^{1,3}¹ Федеральный научно-клинический центр спортивной медицины и реабилитации Федерального медико-биологического агентства, Москва, Россия² Управление спортивной медицины и цифровизации Федерального медико-биологического агентства, Москва, Россия³ Российский национальный исследовательский медицинский университет имени Н. И. Пирогова, Москва, Россия

Контроль гликемии — самая сложная проблема для получающих инсулин спортсменов с сахарным диабетом (СД). При хорошем управлении гликемией обмен гликогена может быть нормальным, а работоспособность повышена коррекцией доз инсулина в соответствии с физической нагрузкой и питанием. Интенсивность физической нагрузки, упражнения с сопротивлением, интервальные тренировки при СД 1-го и 2-го типов обеспечивают оптимальную физиологическую адаптацию в период тренировок и демонстрируют хорошие гликемические преимущества при однократных нагрузочных сетах. Но для получающих инсулинотерапию спортсменов с СД важно не только поддержание оптимального уровня глюкозы во время тренировок и соревнований. Нужно учитывать и потенциальные нарушения терморегуляции, увеличивающие риск теплового стресса во время тренировок/соревнований, знать возможное влияние применяемых спортсменами лекарств на гликемию, электролитный баланс и гидратацию, знать порядок оформления направляемых в антидопинговую организацию документов для запроса на терапевтическое использование инсулина. Целью обзора было попытаться привлечь внимание спортивных врачей и тренеров к вышеописанным проблемам и к необходимости более широкого использования новых технологий по контролю СД; помочь применяющим инсулин спортсменам с СД сохранять высокую работоспособность и спортивное долголетие.

Ключевые слова: спортсмены, сахарный диабет, разрешение на терапевтическое использование, инсулин, физиологическая адаптация, физические нагрузки/упражнения, спортивная результативность

Финансирование: исследование выполнено при финансовой поддержке Государственного задания Федерального медико-биологического агентства России № 67.003.20.800.

Вклад авторов: Л. И. Дергачева — существенный вклад в концепцию работы, сбор данных, анализ содержания, написание текста; А. А. Деревоедов, С. А. Парастаев — критический пересмотр содержания, утверждение окончательного варианта статьи; И. Т. Выходец — утверждение окончательного варианта статьи; А. А. Павлова — написание текста, оформление рукописи.

✉ **Для корреспонденции:** Анна Александровна Павлова
ул. Большая Дорогомиловская, д. 5, г. Москва, 121059; dr_pavlova@hotmail.com

Статья получена: 20.07.2021 **Статья принята к печати:** 27.08.2021 **Опубликована онлайн:** 28.09.2021

DOI: 10.47183/mes.2021.034

One of the problems faced by athletes with type 1 or type 2 DM (T1DM, T2DM) is reaching the maximum performance level when their blood glucose level deviates from the optimal value even minimally. Exercising is often more challenging for insulin users because their contracting muscles can stimulate absorption of the blood glucose regardless of the current insulin level, which leads to hypoglycemia. Moreover, even T2DM

patients that do not use insulin on a daily basis need to balance many factors to ensure acceptable exercise tolerance. There is an extensive list of conditions that need to be observed in order to maintain the glycemic status optimal for sports (Fig. 1).

Thus, modifiable factors associated with exercising can cause significant fluctuations in the blood glucose level. In addition, insulin doses and nutrition should be adjusted

to prevent hypo- or hyperglycemia both during and after the exercise session. Water and electrolyte balance, which can be disturbed by hyperglycemia and medications commonly prescribed to DM patients, is another factor potentially altering athletic performance.

Blood glucose control

Strong athletic performance requires keeping the blood glucose level within the safe range. Therefore, it is important to understand what factors can affect the blood glucose level and how deviations from the said range may change the athlete's current ability.

Hypoglycemia

When an athlete's blood glucose level drops below 4.0 mmol/l during a training session, he/she runs health deterioration risks, and if the level drops below 3.6 mmol/l, his/her training effectiveness goes down by approximately 20% [2]. Hypoglycemia is usually associated with the use of exogenous insulin; it often leads to peripheral hyperinsulinemia that develops during exercising. In addition to persistent hypoglycemia, which usually develops within 15 hours after the exercise session [3], there is an issue of the potassium level that may drop and remain low for several hours after blood glucose returns to the normal level [4]. The severity of hypokalemia can contribute to the development of a cardiac beat disorder and skeletal muscle contractility, which adversely affect athletic performance. Nocturnal hypoglycemia caused by training activities is another significant problem.

Hyperglycemia

Maintaining higher blood glucose level is an anti-hyperglycemia tactic often considered appropriate by athletes with DM on insulin therapy and sports medicine physicians. However, such tactic can make training less effective. When the blood glucose concentration is between 8.9 and 10 mmol/l, kidneys fail to completely reabsorb it from primary urine. When the

above "renal threshold", which is unique to every person, is reached, glucose concentration in urine goes up, which results in a significant loss of fluid through osmotic diuresis. Besides, hyperglycemia bring down concentration of sodium, chloride and calcium in the blood plasma while increasing that of potassium [4], which weakens muscle function. In addition to the above, athletes with T1DM who have unexplained hyperglycemia (≥ 13.0 mmol/l) should mandatorily take a blood ketone test. If the test shows increased values thereof (≥ 1.5 mmol/l), training should be stopped because the level of both glucose and ketones can continue to rise even with moderately intense exercising in the background [5].

Types of exercise type and exercising time

Recently, strength training and high-intensity interval training (HIIT) have been attracting attention of the researchers as an alternative to long aerobic exercise sessions. Compared to such long aerobic exercise training sessions, intense physical loads, even in short sets, may be more beneficial from the points of view of general fitness and reduction of the cardiovascular disease risks, serum lipoprotein levels, endothelial dysfunction suppression [6]. Even in people with sedentary lifestyles and in elderly T2DM patients HIIT improves liver and muscle insulin sensitivity and their oxidative capacity better than long moderate-intensity exercising [6]. A study of physically active adults with T2DM showed that a single high-intensity interval training improves night and morning blood glucose within 24 hours after the training session [7]. T1DM patients may benefit from adding short HIIT sessions to their training schedules because they help decrease the risk of hypoglycemia during exercising. However, the question of whether HIIT sessions in the afternoon translate into greater risk of nocturnal hypoglycemia compared to aerobic exercise alone is still a matter of debate [8].

It should be noted that high-intensity exercise during training or competitions affect the release of catecholamines (adrenalin/noradrenalin) and can trigger significantly greater release of glucose from the liver, which, with exercising or competing in the background, potentially leads to hyperglycemia. In fact, the

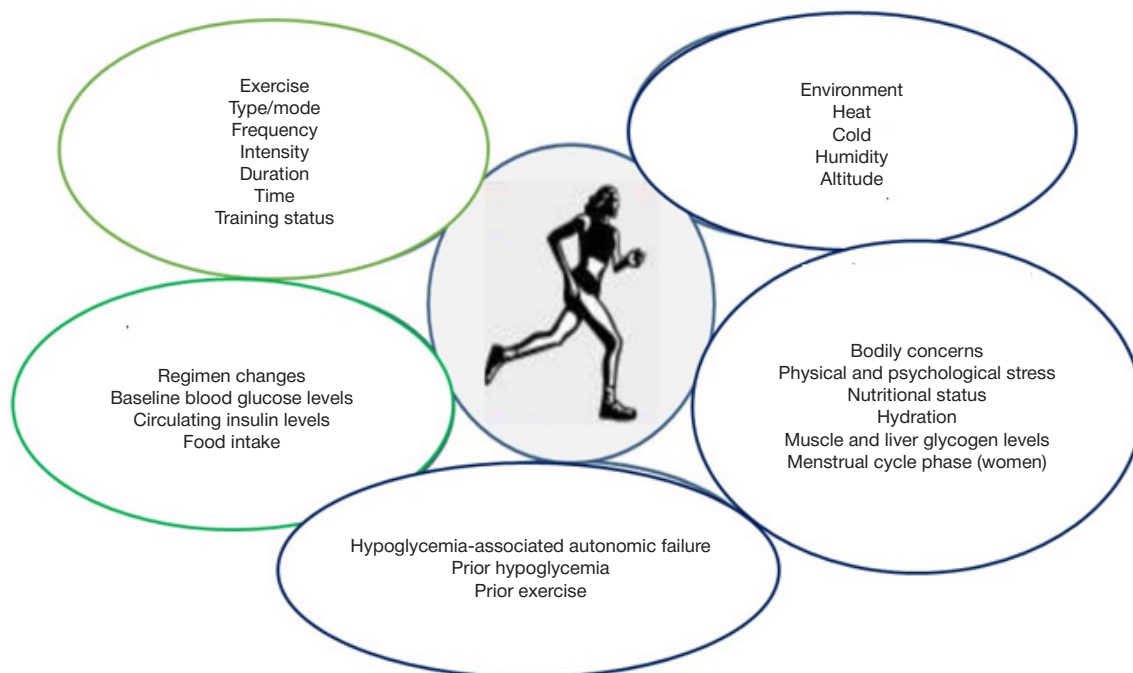


Fig. 1. Factors that can change blood glucose levels in T1DM patients during exercising [1]

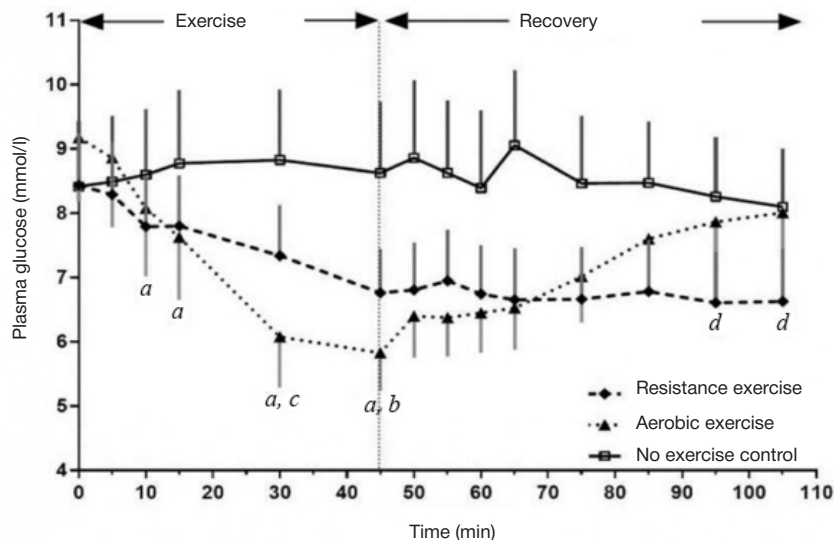


Fig. 2. Effect of different types of exercises on blood glucose stability in T1DM patients (HbA1c 7.1 ± 1.0%) [9]. Mean (± SE) plasma glucose level during exercising and over 60 minutes of recovery (n = 12). ◆ — no training (control); ♦ — resistance exercise (three sets of seven exercises, eight repetitions maximum, in 45 minutes); ▲ — aerobic exercise (running at 60% of the maximum calculated heart rate for 45 minutes); a — significant deviation from baseline for aerobic exercise; b — significant deviation from baseline for resistance exercise; c — significant difference between control and aerobic session; d — significant changes during recovery from aerobic exercise; the differences were considered significant only if they remained significant after Bonferroni adjustments

condition may develop even before the actual physical stress, since the anticipation of the event is a reason enough to force the catecholamine levels and blood glucose to go up [9].

Strength training exercises are also beneficial in many ways; it is advisable to include them in the training schedule of athletes with diabetes. In addition to boosting muscle performance by increasing intensity and rate of contraction, resistance exercises have other positive effects, including higher resting energy expenditure (faster basal metabolic rate), increased bone mineral density and improved body composition [10]. In adult T1DM patients, such exercises prevent blood glucose from excessive dropping better than aerobic training (Fig. 2) [11], and may even provide protection from such a drop if performed before aerobic exercises [12].

In a recent study, fasting exercise in people with T2DM resulted in a more significant improvement of postprandial glycemic profiles over the next 24 hours than exercising after breakfast [7].

In one study, 35 T1DM patients using insulin pumps exercised before breakfast on some days and in the afternoon on other; when they had fasting training sessions, they suffered less hypoglycemia events, and continuous glucose monitoring (CGM) readings were more likely to remain in the range close to the euglycemic state [3]. Other studies have shown that when T1DM patients do resistance exercises before breakfast their blood glucose level may grow up [8], and, on the contrary, when they exercised in the daytime, the blood glucose level went down [11]. Morning exercising can make blood glucose go up, which, to control hyperglycemia, is countered with an appropriate dose of rapid-acting insulin administered 2 hours after the session; this dose of rapid-acting insulin does not cause hypoglycemia [13]. Although the studies cited were

small, their results, as limited in application as they are, suggest that athletes with T1DM who frequently suffer hypoglycemia may want to exercise in the morning, and those struggling with hyperglycemia may go for daytime sessions every now and then. The type and time of the forthcoming competition should be factored into the recommendations given to athletes with DM: anaerobic exercising in the daytime may yield better results in the short term, while regular training sessions in the morning may improve the performance when it is generally reduced [14].

Carbohydrate intake and insulin dose adjustments as basis for the athletic training optimization

Athletic competition requires prevention of both hypo- and hyperglycemia. In particular, non-prevented hypoglycemia will certainly reduce physical performance in training and in competitions [15], but glycemic balance can be achieved with the help of a strategy of correct carbohydrate intake, adjustment of insulin doses and time of their administration. Usually, hypoglycemia prevention when a training session lasts 30 minutes requires no additional carbohydrates or insulin dose reduction. Aerobic exercise lasting 30–60 minutes with low/normal insulin levels may call for 10–15 g of carbohydrates to prevent hypoglycemia [16]; if there is relative hyperinsulinemia in the background (after administration of bolus insulin, i.e., short (ultra-short) action insulin to maintain target blood glucose level after food intake and to control hyperglycemia), 30–60 g of carbohydrates per hour of exercise may be required [17]. For long training sessions or competition events (such as a marathon), this additional carbohydrate intake is beneficial regardless of the type of diabetes [18].

Table. Pre-meal insulin bolus injection reduction recommendations, applicable if training session starts within 90 minutes after bolus administration*

Type of activity	Duration of activity about 30 minutes	Duration of activity about 60 minutes
Light aerobic exercise (30–39% PR**)	–25%	–50%
Moderate intensity aerobic exercise (40–59% PR)	–50%	–75%
Intensive aerobic exercises (60–89% PR)	–75%	Not rated

Note: * — compiled from sources [29, 30, 31, 32]; **PR — pulse reserve.

After exercising, the level of muscle glycogen restores rather slowly, at a rate of 5–7% per hour. The rate of recovery increases when the glycogen depot is depleted and slows down as it fills up. At the same time, as muscle glycogen level reaches the usual value, the effect of insulin begins to weaken [19]. On the positive side, the earlier glycogen level is restored, the lower the likelihood of an athlete with T1DM developing late-onset hypoglycemia, which occurs a day or two after training. Insufficient carbohydrate intake after exercising or taking carbohydrates when blood insulin is low can also reduce or delay glycogen recovery in the body. Therefore, to maintain and restore liver/muscle glycogen and blood glucose levels, athletes in training are advised to take a sufficient amount of carbohydrates before, during and after long exercising sessions (moderate or high intensity) appropriate to the adequate doses of insulin, especially during the "window of opportunity" (30 minutes to 2 hours after exercising).

Adjusting insulin doses to prevent hypoglycemia

As a substitute for, or in addition to, taking carbohydrates with the aim to mitigate the risk of exercise-induced hypoglycemia, both basal and/or bolus insulin can be reduced. People using multiple daily injections of insulin (intensified basal insulin therapy) can have the basal insulin doses administered both before and after the training session reduced by 20%. To optimize blood glucose levels during exercising, athletes can also adjust administration timing and size of the bolus [20] of rapid-acting insulin taken with meals and pre-session snacks. Such adjustments, not changing the blood ketone level significantly, are feasible when an exercising session lasts for up to 45 minutes continuously [21]. Athletes using an insulin pump, which enables continuous subcutaneous insulin infusion, can make the decrease of the blood glucose level less abrupt by reducing or pausing basal insulin infusion at the beginning of a training session or even 30–60 minutes before it [22]. If the session takes place within 2–3 hours after a bolus injection (done with pen or pump), the 25–75% drop of the insulin level (before meals) may diminish the likelihood of hypoglycemia [23] (Table). Regardless of whether insulin dosage has been altered or not, frequent blood glucose checks and possibly intake of additional carbohydrates may be required to ensure safety of an exercising athlete.

For those receiving injectable insulin (pens), the risk of nocturnal hypoglycemia can be minimized by reducing the daily basal insulin dose by approximately 20% and reducing the prandial bolus insulin and intake of low-glycemic carbohydrate food after evening training sessions [24]. Patients with an insulin pump can avoid nocturnal hypoglycemia by reducing the basal injection rate by 20% for sleep time and for the period of 6 hours after daytime exercising [25]. For T1DM and T2DM patients on insulin therapy, it may make sense to have an additional snack before bedtime (2 bread units, 20–24 g of carbohydrates), check the glucose level at night and/or use a signaling CGM system [26].

It is also important to note that the rate of absorption of insulin can be improved by heating the injection point or massaging it or the area around it, with such improved absorption translating into shorter injection-to-action time [27].

There are other ways, alternative to insulin dose and carbohydrate intake adjustment, to prevent hypoglycemia, at least in the short term, like a short maximum effort sprint before or after a session of moderate intensity exercise [28].

Insulin therapeutic use exemption

The athlete taking insulin and the doctor prescribing the drug must comply with the requirements of the Russian national anti-doping rules and those by international anti-doping organizations, since insulin is included in the S4 class "Hormones and metabolic modulators" of the Prohibited List. Athletes requiring insulin must apply to the anti-doping organization and obtain the appropriate therapeutic use exemption. Medical documents attached to the application should be prepared by the physician prescribing the insulin. These documents, under the requirements of the WADA International Standard for Therapeutic Use Exemptions [33], must specify that:

1) the prohibited substance or prohibited method in question is needed to treat a diagnosed medical condition supported by relevant clinical evidence;

2) the therapeutic use of the prohibited substance or prohibited method will not, on the balance of probabilities, produce any additional enhancement of performance beyond what might be anticipated by a return to the athlete's normal state of health following the treatment of the medical condition;

3) the prohibited substance or prohibited method is an indicated treatment for the medical condition, and there is no reasonable permitted therapeutic alternative.

Requirements for the preparation of medical documents for therapeutic insulin use exemption application are set out in the Therapeutic Use Exemptions Physician Guidelines: Diabetes Mellitus published to the Therapeutic Use Exemption section of the World Anti-Doping Agency's website and, in Russian, to the RUSADA Russian Anti-Doping Agency's website [34].

Oral hypoglycemic agents are not prohibited; they can be used without applying for a therapeutic use exemption (TUE).

Use of the new technologies

A breakthrough in DM control occurred in 1998, when continuous glycemic monitoring (CGM) system became widely and routinely used. Such systems measure glucose in the interstitial fluid continuously, every 5–15 minutes, relying on subcutaneous sensors, and transmit data to a smartphone/computer of the athlete, coach, sports medicine physician. However, there is a difference between the displayed interstitial glucose and its real level in capillary blood: on average, the data from the sensors arrives with a 8–10 minute delay (maximum — 20 minute delay). Thus, if the blood glucose level is stable, the readings will be close to the capillary glucose level, but during rapid glycemic changes the displayed value will be either lower or higher than the current real level.

Use of CGM systems by athletes is still a matter of debate. One study showed that such systems help detect asymptomatic hypoglycemia and hyperglycemia after exercise sessions (other studies identified accuracy limitations peculiar to the current systems and its dependency on the length of use of the sensor, irritation of the skin and problems with the contact therewith) [35]. Several studies have confirmed that CGM systems are accurate enough to be used in training session situations [36]; other researchers, however, reported insufficient accuracy and problems related to broken sensory filaments, inability to calibrate the systems and time from the moment the capillary blood glucose level changes to the moment it is reported by the sensor [37]. Although continuous monitoring is a very useful tool for tracking blood glucose trends during exercising and preventing hypoglycemia after the sessions, so far CGM systems cannot completely replace capillary blood glucose testing with individual glucometers.

Insulin pumps enable continuous subcutaneous infusion of insulin with continuous glucose monitoring in real time. Compared to daily basal-bolus injections, such pumps allow changing the basal insulin delivered subcutaneously during training, which makes stress response more physiological. Bodies of people using a pen once or twice a day to administer basal insulin are less quick to respond to the changing demand therefor during and after exercising [38]. However, athletes must be able to control the pump if it remains on during physical activity, and this can be difficult in contact sports, team games etc. Besides, environmental factors (such as heat) can adversely affect the quality of insulin in the pump.

Automated insulin delivery systems (closed loop type), called "artificial pancreas", are the state-of-the-art technology designed to treat insulin-dependent diabetes mellitus. Such systems include a CGM module, an insulin pump and control algorithms (some of which may be smartphone-based). It is a closed-loop system that, unlike a single CGM sensor, does not require the user to enter his/her data in response to the readings; the monitoring and insulin pump system automatically delivers the correct amount of insulin based on the values transmitted. Thus, the insulin infusion adjustment can be as accurate as the measuring device the whole system relies on [39]. Studies that involved T1DM patients showed that adding an alarm to the closed-loop system that is triggered when the glucose level falls below a predetermined critical level (4–4.5 mmol/l) reduces the risk of hypoglycemia during and immediately after exercising even further [40].

Other factors affecting the performance of an athlete with diabetes

Studies have shown that T1DM and T2DM patients often have thermoregulation disorders [41]. In particular, type 1 diabetes impairs perspiration, especially with higher level exercising in the background. Where dehydration can lead to further deterioration of sweating, it is very important to closely monitor blood glucose levels during competition in hot weather to avoid further exacerbation of the existing disorders body cooling mechanisms [42].

Studies that involved people with T2DM showed that increased sitting time is associated with poor glycemic control and metabolic risks, and that there is no dependency on the intermittent moderate to high-level vigorous activity [43]. Another study found that as little as 3 minutes of light walking combined with simple resistance exercises every 30 minutes of a period a person needs to remain seated for a long time enabled adequate glycemic management throughout the day [44].

The effect of drugs should also be factored in. In addition to insulin, all athletes with diabetes can take a variety of prescription or over-the-counter medications to treat a variety of diseases (conditions). Their potential impact on athletic performance will be largely mediated by the changes in blood glucose levels and fluid and electrolyte balance, which can impair hydration status and muscle contractility. Such medications are some antihypertensive, diuretic, steroid and non-steroidal anti-inflammatory drugs, symptomatic cold medications and some other substances.

Corticosteroids, which can be prescribed for some common conditions (e.g., asthma, arthritis, and allergic rhinitis), can cause hyperglycemia in people with diabetes [45]; these drugs also require a TUE. Antipsychotic drugs can reduce insulin sensitivity and thus increase the risk of hyperglycemia and dehydration in athletes with diabetes [46]. Medicines with

phenylephrine or pseudoephedrine as active ingredients (e.g., cold/flu and allergy drugs) tend to increase glycogenolysis in the liver, same as catecholamines, which often leads to hyperglycemia in people with diabetes [47]. Of course, it is unlikely that athletes will use such drugs during competition: pseudoephedrine and adrenaline are on the WADA Prohibited List, and phenylephrine is in the Monitoring Program, but it is possible that younger and/or less experienced athletes can use them out of competition, not knowing the impact of these substances on athletic performance and blood glucose levels.

Athletes with T2DM can receive a therapy that combines insulin administration (basal insulin/mixed insulin/basal-bolus therapy) and oral glucose-lowering drugs. In these cases, special attention should be paid to the possible side effects of the patten that can disturb the electrolyte balance and influence athletic performance.

Metformin, one of the most well-known biguanide oral antidiabetic drugs, can cause indigestion and diarrhea. Another hypoglycemic agent, acarbose (an alpha-glucosidase inhibitor), produces a similar effect: it inhibits digestion and absorption of carbohydrates in the small intestine. Diarrhea can decrease the blood potassium level, therefore, athletes taking the above drugs should monitor their electrolyte levels more often, especially during the competition period.

Modern antidiabetic drugs such as glucagon-like peptide-1 receptor agonists (GLP-1 receptor agonists, or incretin mimetics), dipeptidyl peptidase 4 inhibitors (DPP-4 inhibitors, or gliptins), activate incretin response, reduce the level of postprandial glycemia by stimulating glucose-dependent secretion of insulin and inhibiting release of glucagon. The more common side effects thereof are diarrhea and vomiting, while dehydration is infrequent, which requires closer monitoring of the level of blood electrolytes in athletes. The use of GLP-1 receptor agonists was associated with the risk of acute pancreatitis, and a combination with insulin translated into an increased risk of hypoglycemia. Inhibitors of the sodium-dependent glucose cotransporter type 2 (SGLT2 inhibitors, or gdflozins), as well as type 2 and 1 (SGLT1 and SGLT2) reduce renal glucose reabsorption and thus bring down blood glucose and glycated hemoglobin (HbA1c). Their positive side effects are the decreased body weight, systolic blood pressure and blood uric acid level. These drugs, increasing the volume of excreted urine (especially with initial hyperglycemia in the background), may lead to dehydration and side reactions associated with decreased volume of intercellular fluid: hypotension, postural dizziness, orthostatic hypotension. With some drugs of this class (canagliflozin), there was a slight but significant decrease in the total BMD of the hip joint, an increase in biomarkers of bone formation and resorption and a higher risk of bone fracture identifiable as early as 12 weeks into the therapy [48]. A medicine from this class, sotagliflozin (SGLT1 and SGLT2 inhibitor), has been approved for treatment of type 1 diabetes.

Since hypertension is a common complication of diabetes, it is possible that athletes with diabetes, depending on their age and history, may be prescribed angiotensin converting enzyme (ACE) inhibitors, angiotensin II receptor antagonists (ARA) or some diuretic drugs. ACE and ARA can cause hyperkalemia [49], and high blood potassium levels can impair athletic performance by making muscles weaker or cause cardiac arrhythmias that can even be fatal. Diuretics prescribed to control blood pressure lead to polyuria and increase the risk of dehydration and electrolyte imbalance. In particular, thiazide diuretics are associated with a greater risk of hyponatremia, which increases with age, is higher in women, and tends to

affect people with lower weight more than those with higher weight. Thiazides can also increase urinary potassium loss, sometimes increasing the risk of hypokalemia [50]. In addition, the use of diuretics is regulated by the WADA standards.

CONCLUSION

Although glycemic management in athletes with diabetes can be quite challenging due to the intensity of exercising and hectic training and competition schedules, such athletes have the potential to be as successful as athletes without diabetes. The

intensity, type and timing of exercising, as well as insulin and food dosage and timing, affect the athlete's blood glucose level and performance, but they can be effectively controlled with appropriate changes in the regimen. Athletes, sports medicine physicians and coaches need to be aware of the effects of blood glucose and medications on hydration and electrolyte balance in order to make the necessary adjustments seeking to achieve the optimal results. The latest technologies for diabetes monitoring and control, although somewhat limited in accuracy and use at present, can help athletes to better control glycemia and achieve peak athletic performance.

References

- Solberg SR, Land R, Desay E, Ker D. Physical activity and type 1 diabetes: time for a rewiring? *J Diabetes Sci Technol.* 2015; 9: 609–18.
- Kelly D, Hamilton JK, Riddell MC. Blood glucose levels and performance in a sports cAMP for adolescents with type 1 diabetes mellitus: a field study. *Int J Pediatr.* 2010.
- Gomez AM, Gomez C, Aschner P, et al. Effects of performing morning versus afternoon exercise on glycemic control and hypoglycemia frequency in type 1 diabetes patients on sensor-augmented insulin pump therapy. *J Diabetes Sci Technol.* 2015; 9: 619–24.
- Caduff A, Lutz HU, Heinemann L, et al. Dynamics of blood electrolytes in repeated hyper- and/or hypoglycaemic events in patients with type 1 diabetes. *Diabetologia.* 2011; 54: 2678–89.
- Colberg SR, Yardley JE, Riddell MC, et al. Physical activity/exercise and diabetes: a position statement of the American Diabetes Association. *Diabetes Care.* 2016; 39 (11): 2065–79.
- Gibala MJ, Little JP, Macdonald MJ, Hawley JA. Physiological adaptations to low-volume, high-intensity interval training in health and disease. *J Physiol.* 2012; 590: 1077–84.
- Terada T, Wilson BJ, Myette-Co'te'E, et al. Targeting specific interstitial glycemic parameters with high-intensity interval exercise and fasted-state exercise in type 2 diabetes. *Metabolism.* 2016; 65: 599–608.
- Iscoe KE, Riddell MC. Continuous moderate-intensity exercise with or without intermittent high-intensity work: effects on acute and late glycaemia in athletes with Type 1 diabetes mellitus. *Diabet Med.* 2011; 28: 824–32.
- Yardley JE, Kenny GP, Perkins BA, et al. Resistance versus aerobic exercise: acute effects on glycemia in type 1 diabetes. *Diabetes Care.* 2013; 36 (3): 537–42.
- Westcott WL. Resistance training is medicine: effects of strength training on health. *Curr Sports Med Rep.* 2012; 11: 209–16.
- Turner D, Luzio S, Gray BJ, et al. Impact of single and multiple sets of resistance exercise in type 1 diabetes. *Scand. J Med Sci Sports.* 2015; 25: 99–109.
- Yardley JE, Kenny GP, Perkins BA, et al. Effects of performing resistance exercise before versus after aerobic exercise on glycemia in type 1 diabetes. *Diabetes Care.* 2012; 35: 669–75.
- Turner D, Luzio S, Gray BJ, et al. Algorithm that delivers an individualized rapid-acting insulin dose after morning resistance exercise counters postexercise hyperglycemia in people with Type 1 diabetes. *Diabet. Med.* 2016; 33: 506–10.
- Chtourou H, Souissi N. The effect of training at a specific time of day: a review. *J Strength Cond Res.* 2012; 26: 1984–2005.
- Murillo S, Brugnara L, Novials A. One year follow-up in a group of halfmarathon runners with type-1 diabetes treated with insulin analogues. *J Sports Med Phys Fitness.* 2010; 50: 506–10.
- Riddell MC, Milliken J. Preventing exercise-induced hypoglycemia in type 1 diabetes using real-time continuous glucose monitoring and a new carbohydrate intake algorithm: an observational field study. *Diabetes Technol Ther.* 2011; 13: 819–25.
- Francescato MP, Stel G, Stenner E, Geat M. Prolonged exercise in type 1 diabetes: performance of a customizable algorithm to estimate the carbohydrate supplements to minimize glycemic imbalances. *PLoS One.* 2015; 10: e0125220.
- Adolfsson P, Mattsson S, Jendle J. Evaluation of glucose control when a new strategy of increased carbohydrate supply is implemented during prolonged physical exercise in type 1 diabetes. *Eur J Appl Physiol.* 2015; 115: 2599–607.
- Jensen TE, Richter EA. Regulation of glucose and glycogen metabolism during and after exercise. *J Physiol.* 2012; 590: 1069–76.
- West DJ, Stephens JW, Bain SC, et al. A combined insulin reduction and carbohydrate feeding strategy 30 min before running best preserves blood glucose concentration after exercise through improved fuel oxidation in type 1 diabetes mellitus. *J Sports Sci.* 2011; 29: 279–89.
- Bracken RM, West DJ, Stephens JW, et al. Impact of pre-exercise rapid-acting insulin reductions on ketogenesis following running in type 1 diabetes. *Diabet Med.* 2011; 28: 218–22.
- Franc S, Daoudi A, Pochat A, et al. Insulin-based strategies to prevent hypoglycaemia during and after exercise in adult patients with type 1 diabetes on pump therapy: the DIABRASPORT randomized study. *Diabetes Obes. Metab.* 2015; 17: 1150–57.
- West DJ, Morton RD, Bain SC, et al. Blood glucose responses to reductions in pre-exercise rapid-acting insulin for 24 h after running in individuals with type 1 diabetes. *J Sports Sci.* 2010; 28: 781–88.
- Campbell MD, Walker M, Bracken RM, et al. Insulin therapy and dietary adjustments to normalize glycemia and prevent nocturnal hypoglycemia after evening exercise in type 1 diabetes: a randomized controlled trial. *BMJ Open Diabetes Res Care.* 2015; 3: e000085.
- Taplin CE, Cobry E, Messer L, et al. Preventing post-exercise nocturnal hypoglycemia in children with type 1 diabetes. *J Pediatr.* 2010; 157: 784–88. e781.
- Garg SK, Brazg RL, Bailey TS, et al. Hypoglycemia begets hypoglycemia: the order effect in the ASPIRE in-clinic study. *Diabetes Technol Ther.* 2014; 16: 125–30.
- Freckmann G, Pleus S, Haug C, et al. Increasing local blood flow by warming the application site: beneficial effects on postprandial glycemic excursions. *J Diabetes Sci Technol.* 2012; 6: 780–5.
- Yardley J, Mollard R, Macintosh A, et al. Vigorous intensity exercise for glycemic control in patients with type 1 diabetes. *Can J Diab.* 2013; 37: 427–32.
- Campbell MD, Walker M, Trenell MI, et al. Metabolic implications when employing heavy pre- and post-exercise rapid-acting insulin reductions to prevent hypoglycaemia in type 1 diabetes patients: a randomised clinical trial. *PLoS One.* 2014; 9 (5): e97143.
- Moser O, et al. Effects of high-intensity interval exercise versus moderate continuous exercise on glucose homeostasis and hormone response in patients with type 1 diabetes mellitus using novel ultra-long-acting insulin. *PLoS One.* 2015; 10 (8): e0136489.
- Shetty VB, Fournier PA, Davey RJ, et al. Effect of exercise intensity on glucose requirements to maintain euglycaemia during exercise in type 1 diabetes. *J Clin Endocrinol Metab.* 2016; 101 (3): 972–80.
- Dedov II, Shestakova MV, Majorov AY. Algoritmy specializirovannoj medicinskoj pomoshti bol'nym sahar'nym diabetom: klinicheskie

- rekomenadii. 2019; 22 (1S1): 1–144.
33. World Anti-Doping Agency. International standard for therapeutic use exemptions (ISTUE) [cited 2021 Jul 14]. Available from: <https://www.wada-ama.org/en/resources/therapeutic-use-exemption-tue/international-standard-for-therapeutic-use-exemptions-istue>.
 34. Meditsinskaya informatsiya dlya podderzhki resheniy Komitetov po TI. Sakharomy diabet [cited 2021 Jul 14] Available from: <https://rusada.ru/upload/iblock/688/Диабет%20версия%204.2%20февраль%202020.pdf>.
 35. P'jankova EYu, Anshakova LA, P'jankov IA, i dr. Sovremennye tehnologii v upravlenii saharnym diabetom — nepreryvnoe monitorirovanie gljukozy i pomprovaja insulinoterapija. Zdravoohranenie Dal'nego Vostoka. 2021; 1: 50–55.
 36. Hásková A, Radovnická L, Petruželková L, Parkin CG, Grunberger G, Horová E, et al. Is superior to flash glucose monitoring for glucose control in type 1 diabetes: the CORRIDA randomized controlled trial. *Diabetes Care*. 2020 Nov; 43 (11): 2744–50.
 37. Dreval AV, Shestakova TP, Manukjan AA, Brezhneva OG. Individualizirovannyj statisticheskij analiz massiva dannyh nepreryvnogo monitorirovanija gljukozy. Al'manah klinicheskoy mediciny. 2021; 48 (7): 459–68.
 38. Nimri R, Nir J, Phillip M. Insulin pump therapy. *American journal of therapeutics*. 2020; 27 (1): e30–e41.
 39. The Food and Drug Administration. What is the pancreas? What is an artificial pancreas device system? [fda.gov](http://www.fda.gov) [cited 2021 Jul 14]. Available from: <https://www.fda.gov/medical-devices/artificial-pancreas-device-system/what-pancreas-what-artificial-pancreas-device-system>.
 40. Sorokin DYU, Laptev DN. Nekommercheskie sistemy vvedenija insulina v zamknutom konture. *Consilium Medicum*. 2020; 22 (4): 27–30.
 41. Kenny GP, Stapleton JM, Yardley JE, et al. Older adults with type 2 diabetes store more heat during exercise. *Med Sci Sports Exerc*. 2013; 45: 1906–14.
 42. Carter MR, McGinn R, Barrera-Ramirez J, et al. Impairments in local heat loss in type 1 diabetes during exercise in the heat. *Med Sci Sports Exerc*. 2014; 46: 2224–33.
 43. Fritschi C, Park H, Richardson A, et al. Association between daily time spent in sedentary behavior and duration of hyperglycemia in type 2 diabetes. *Biol Res Nurs*. 2015.
 44. Dempsey PC, Larsen RN, Sethi P, et al. Benefits for type 2 diabetes of interrupting prolonged sitting with brief bouts of light walking or simple resistance activities. *Diabetes Care*. 2016; 39: 964–72.
 45. Abdiramasheva KS. Gljukokortikoidy i razvitie saharnogo diabeta. *Theoretical Applied Science*. 2019; 4: 15–19.
 46. Buhtin OV, Rjabcev AS. Ocenka vijianija psihotropnyh preparatov na razvitie jendokrinnoj patologii. Vozmozhnosti ee profilaktiki. V sbornike: *Sovremennye voprosy morfologii jendokrinnoj sistemy. Materialy IV mezhtsebnogo nauchno-prakticheskogo konferencii studentov, aspirantov i molodyh uchenyh. Pod redakciej O.Ju. Patjuchenko, A.A. Sozykina, M.A. Zatolokinoj, G.N. Suvorovoj, M.N. Dmitrieva. Kazan': Buk, 2020; s. 23–29.*
 47. Maklakova AS, Maslova MV, Graf AV, Sokolova NA. Vegetativnaja nervnaja sistema v norme i pri patologii. Mediatory i kotransmitter. M.: Tovarishhestvo nauchnyh izdanij KMK, 2020; 147 s.
 48. FDA revises label of diabetes drug canagliflozin (Invokana, Invokamet) to include updates on bone fracture risk and new information on decreased bone mineral density. 2015 [3/1/16]. Data summary. Available from: <http://www.fda.gov/Drugs/DrugSafety/ucm461449.htm>.
 49. Stolov SV. Inaktivacija renin-angiotenzin-al'dosteronovoj sistemy. Kakoj klass preparatov predpochest'? *Evrzjskij kardiologicheskij zhurnal*. 2020; 4: 64–78.
 50. Nedogoda SV. Diuretiki pri arterial'noj gipertenzii v svete novyh klinicheskikh rekomendacij i metaanalizov. *Rossijskij kardiologicheskij zhurnal*. 2021; 3: 91–94.

Литература

1. Solberg SR, Land R, Desay E, Ker D. Physical activity and type 1 diabetes: time for a rewiring? *J Diabetes Sci Technol*. 2015; 9: 609–18.
2. Kelly D, Hamilton JK, Riddell MC. Blood glucose levels and performance in a sports cAMP for adolescents with type 1 diabetes mellitus: a field study. *Int J Pediatr*. 2010.
3. Gomez AM, Gomez C, Aschner P, et al. Effects of performing morning versus afternoon exercise on glycemic control and hypoglycemia frequency in type 1 diabetes patients on sensor-augmented insulin pump therapy. *J Diabetes Sci Technol*. 2015; 9: 619–24.
4. Caduff A, Lutz HU, Heinemann L, et al. Dynamics of blood electrolytes in repeated hyper- and/or hypoglycaemic events in patients with type 1 diabetes. *Diabetologia*. 2011; 54: 2678–89.
5. Colberg SR, Yardley JE, Riddell MC, et al. Physical activity/exercise and diabetes: a position statement of the American Diabetes Association. *Diabetes Care*. 2016; 39 (11): 2065–79.
6. Gibala MJ, Little JP, Macdonald MJ, Hawley JA. Physiological adaptations to low-volume, high-intensity interval training in health and disease. *J Physiol*. 2012; 590: 1077–84.
7. Terada T, Wilson BJ, Myette-Co'te'E, et al. Targeting specific interstitial glycemic parameters with high-intensity interval exercise and fasted-state exercise in type 2 diabetes. *Metabolism*. 2016; 65: 599–608.
8. Iscoe KE, Riddell MC. Continuous moderate-intensity exercise with or without intermittent high-intensity work: effects on acute and late glycaemia in athletes with Type 1 diabetes mellitus. *Diabet Med*. 2011; 28: 824–32.
9. Yardley JE, Kenny GP, Perkins BA, et al. Resistance versus aerobic exercise: acute effects on glycemia in type 1 diabetes. *Diabetes Care*. 2013; 36 (3): 537–42.
10. Westcott WL. Resistance training is medicine: effects of strength training on health. *Curr Sports Med Rep*. 2012; 11: 209–16.
11. Turner D, Luzio S, Gray BJ, et al. Impact of single and multiple sets of resistance exercise in type 1 diabetes. *Scand. J Med Sci Sports*. 2015; 25: 99–109.
12. Yardley JE, Kenny GP, Perkins BA, et al. Effects of performing resistance exercise before versus after aerobic exercise on glycemia in type 1 diabetes. *Diabetes Care*. 2012; 35: 669–75.
13. Turner D, Luzio S, Gray BJ, et al. Algorithm that delivers an individualized rapid-acting insulin dose after morning resistance exercise counters postexercise hyperglycemia in people with Type 1 diabetes. *Diabet. Med*. 2016; 33: 506–10.
14. Chtourou H, Souissi N. The effect of training at a specific time of day: a review. *J Strength Cond Res*. 2012; 26: 1984–2005.
15. Murillo S, Brugnara L, Novias A. One year follow-up in a group of halfmarathon runners with type-1 diabetes treated with insulin analogues. *J Sports Med Phys Fitness*. 2010; 50: 506–10.
16. Riddell MC, Milliken J. Preventing exercise-induced hypoglycemia in type 1 diabetes using real-time continuous glucose monitoring and a new carbohydrate intake algorithm: an observational field study. *Diabetes Technol Ther*. 2011; 13: 819–25.
17. Francescato MP, Stel G, Stenner E, Geat M. Prolonged exercise in type 1 diabetes: performance of a customizable algorithm to estimate the carbohydrate supplements to minimize glycemic imbalances. *PLoS One*. 2015; 10: e0125220.
18. Adolfsson P, Mattsson S, Jendle J. Evaluation of glucose control when a new strategy of increased carbohydrate supply is implemented during prolonged physical exercise in type 1 diabetes. *Eur J Appl Physiol*. 2015; 115: 2599–607.
19. Jensen TE, Richter EA. Regulation of glucose and glycogen metabolism during and after exercise. *J Physiol*. 2012; 590: 1069–76.
20. West DJ, Stephens JW, Bain SC, et al. A combined insulin reduction and carbohydrate feeding strategy 30 min before running best preserves blood glucose concentration after exercise through improved fuel oxidation in type 1 diabetes mellitus. *J Sports Sci*. 2011; 29: 279–89.

21. Bracken RM, West DJ, Stephens JW, et al. Impact of pre-exercise rapidacting insulin reductions on ketogenesis following running in type 1 diabetes. *Diabet Med*. 2011; 28: 218–22.
22. Franc S, Daoudi A, Pochat A, et al. Insulin-based strategies to prevent hypoglycaemia during and after exercise in adult patients with type 1 diabetes on pump therapy: the DIABRASPORT randomized study. *Diabetes Obes. Metab*. 2015; 17: 1150–57.
23. West DJ, Morton RD, Bain SC, et al. Blood glucose responses to reductions in pre-exercise rapid-acting insulin for 24 h after running in individuals with type 1 diabetes. *J Sports Sci*. 2010; 28: 781–88.
24. Campbell MD, Walker M, Bracken RM, et al. Insulin therapy and dietary adjustments to normalize glycemia and prevent nocturnal hypoglycemia after evening exercise in type 1 diabetes: a randomized controlled trial. *BMJ Open Diabetes Res Care*. 2015; 3: e000085.
25. Taplin CE, Cobry E, Messer L, et al. Preventing post-exercise nocturnal hypoglycemia in children with type 1 diabetes. *J Pediatr*. 2010; 157: 784–88. e781.
26. Garg SK, Brazg RL, Bailey TS, et al. Hypoglycemia begets hypoglycemia: the order effect in the ASPIRE in-clinic study. *Diabetes Technol Ther*. 2014; 16: 125–30.
27. Freckmann G, Pleus S, Haug C, et al. Increasing local blood flow by warming the application site: beneficial effects on postprandial glycemic excursions. *J Diabetes Sci Technol*. 2012; 6: 780–5.
28. Yardley J, Mollard R, Macintosh A, et al. Vigorous intensity exercise for glycemic control in patients with type 1 diabetes. *Can J Diab*. 2013; 37: 427–32.
29. Campbell MD, Walker M, Trenell MI, et al. Metabolic implications when employing heavy pre- and post-exercise rapid-acting insulin reductions to prevent hypoglycaemia in type 1 diabetes patients: a randomised clinical trial. *PLoS One*. 2014; 9 (5); e97143.
30. Moser O, et al. Effects of high-intensity interval exercise versus moderate continuous exercise on glucose homeostasis and hormone response in patients with type 1 diabetes mellitus using novel ultra-long-acting insulin. *PLoS One*. 2015; 10 (8): e0136489.
31. Shetty VB, Fournier PA, Davey RJ, et al. Effect of exercise intensity on glucose requirements to maintain euglycaemia during exercise in type 1 diabetes. *J Clin Endocrinol Metab*. 2016; 101 (3): 972–80.
32. Дедов И. И., Шестакова М. В., Майоров А. Ю. Алгоритмы специализированной медицинской помощи больным сахарным диабетом: клинические рекомендации. 2019; 22 (1S1): 1–144.
33. World Anti-Doping Agency. International standard for therapeutic use exemptions (ISTUE) [cited 2021 Jul 14]. Available from: <https://www.wada-ama.org/en/resources/therapeutic-use-exemption-tue/international-standard-for-therapeutic-use-exemptions-istue>.
34. Медицинская информация для поддержки решений Комитетов по ТИ. Сахарный диабет [cited 2021 Jul 14]. Доступно по ссылке: [//rusada.ru/upload/iblock/688/Диабет%20версия%204.2%20февраль%202020.pdf](http://rusada.ru/upload/iblock/688/Диабет%20версия%204.2%20февраль%202020.pdf).
35. Пьянкова Е. Ю., Аншакова Л. А., Пьянков И.А. и др. Современные технологии в управлении сахарным диабетом — непрерывное мониторирование глюкозы и помповая инсулинотерапия. *Здравоохранение Дальнего Востока*. 2021; 1: 50–55.
36. Hásková A, Radovnická L, Petruželková L, Parkin CG, Grunberger G, Horová E, et al. Is superior to flash glucose monitoring for glucose control in type 1 diabetes: the CORRIDA randomized controlled trial. *Diabetes Care*. 2020 Nov; 43 (11): 2744–50.
37. Древаль А. В., Шестакова Т. П., Манукян А. А., Брежнева О. Г. Индивидуализированный статистический анализ массива данных непрерывного мониторирования глюкозы. *Альманах клинической медицины*. 2021; 48 (7): 459–68.
38. Nimri R, Nir J, Phillip M. Insulin pump therapy. *American journal of therapeutics*. 2020; 27 (1): e30–e41.
39. The Food and Drug Administration. What is the pancreas? What is an artificial pancreas device system? [fda.gov](https://www.fda.gov/medical-devices/artificial-pancreas-device-system/what-pancreas-what-artificial-pancreas-device-system) [cited 2021 Jul 14]. Available from: <https://www.fda.gov/medical-devices/artificial-pancreas-device-system/what-pancreas-what-artificial-pancreas-device-system>.
40. Сорокин Д. Ю., Лаптев Д. Н. Некоммерческие системы введения инсулина в замкнутом контуре. *Consilium Medicum*. 2020; 22 (4): 27–30.
41. Kenny GP, Stapleton JM, Yardley JE, et al. Older adults with type 2 diabetes store more heat during exercise. *Med Sci Sports Exerc*. 2013; 45: 1906–14.
42. Carter MR, McGinn R, Barrera-Ramirez J, et al. Impairments in local heat loss in type 1 diabetes during exercise in the heat. *Med Sci Sports Exerc*. 2014; 46: 2224–33.
43. Fritschi C, Park H, Richardson A, et al. Association between daily time spent in sedentary behavior and duration of hyperglycemia in type 2 diabetes. *Biol Res Nurs*. 2015.
44. Dempsey PC, Larsen RN, Sethi P, et al. Benefits for type 2 diabetes of interrupting prolonged sitting with brief bouts of light walking or simple resistance activities. *Diabetes Care*. 2016; 39: 964–72.
45. Абдирамашева К. С. Глюкокортикоиды и развитие сахарного диабета. *Theoretical Applied Science*. 2019; 4: 15–19.
46. Бухтин О. В., Рябцев А. С. Оценка влияния психотропных препаратов на развитие эндокринной патологии. Возможности ее профилактики. В сборнике: *Современные вопросы морфологии эндокринной системы. Материалы IV межрегиональной научно-практической конференции студентов, аспирантов и молодых ученых*. Под редакцией О.Ю. Патюченко, А.А. Созыкина, М.А. Затолокиной, Г.Н. Суворовой, М.Н. Дмитриева. Казань: Бук, 2020; с. 23–29.
47. Маклакова А. С., Маслова М. В., Граф А. В., Соколова Н. А. Вегетативная нервная система в норме и при патологии. Медиаторы и котрансмиттер. М.: Товарищество научных изданий КМК, 2020; 147 с.
48. FDA revises label of diabetes drug canagliflozin (Invokana, Invokamet) to include updates on bone fracture risk and new information on decreased bone mineral density. 2015 [3/1/16]. Data summary. Available from: <http://www.fda.gov/Drugs/DrugSafety/ucm461449.htm>.
49. Столов С. В. Инактивация ренин-ангиотензин-альдостероновой системы. Какой класс препаратов предпочесть? *Евразийский кардиологический журнал*. 2020; 4: 64–78.
50. Недогода С. В. Диуретики при артериальной гипертензии в свете новых клинических рекомендаций и метаанализов. *Российский кардиологический журнал*. 2021; 3: 91–94.

BRAIN CONCUSSION IN YOUNG ATHLETES: MAJOR PAIN POINTS

Klyuchnikov SO¹, Feshchenko VS^{1,2}, Zholinsky AV¹, Tarasova MS¹✉, Slivin AV², Efimov PV²¹ Federal Research and Clinical Center of Sports Medicine and Rehabilitation of FMBA, Moscow, Russia² Pirogov Russian National Research Medical University, Moscow, Russia

Numerous studies conducted in recent decades have generated vast amounts of knowledge on sport-related concussions. This review analyzes international data on pediatric and adolescent sport-related concussions. Drawing on the most recent research into the pathophysiology of brain concussions, the authors identify and discuss "pain points" associated with SRC, i.e. unsolved problems of diagnostic criteria, the use of modern neuroimaging modalities and promising biomarkers. Special attention is paid to the physiology of children and adolescents and predisposing factors important for developing adequate diagnostic and management strategies. The authors formulate problems that need to be solved in order to improve care for young athletes with brain concussions.

Keywords: elite athletes, brain concussion, youth sports

Funding: this review is part of the applied research study on the *Clinical and prognostic significance of neurometabolic cascade for the development of delayed complications of hypoxic and traumatic brain injuries in athletes* (Neurocascade-20, ID 76.35.41) conducted by the Federal Research and Clinical Center of Sports Medicine and Rehabilitation of FMBA under the State Assignment for years 2020–2021.

Author contribution: Klyuchnikov SO searched and analyzed the literature and contributed to writing the manuscript; Feshchenko VS contributed to writing the manuscript and edited the final version; Zholinsky AV edited the final version of the manuscript; Tarasova MS, Slivin AV, Efimov PV searched and analyzed the literature.

✉ **Correspondence should be addressed:** Maria S. Tarasova
Raevskogo, 4, 121151, Moscow; tarasovams@sportfmba.ru

Received: 20.07.2021 **Accepted:** 12.08.2021 **Published online:** 17.09.2021

DOI: 10.47183/mes.2021.026

«БОЛЕВЫЕ ТОЧКИ» СОТРЯСЕНИЯ ГОЛОВНОГО МОЗГА У ЮНЫХ СПОРТСМЕНОВ

С. О. Ключников¹, В. С. Фещенко^{1,2}, А. В. Жолинский¹, М. С. Тарасова¹✉, А. В. Сливин², П. В. Ефимов²¹ Федеральное научно-клиническое учреждение спортивной медицины и реабилитации Федерального медико-биологического агентства, Москва, Россия² Российский национальный исследовательский медицинский университет имени Н. И. Пирогова, Москва, Россия

Проведенные в последние десятилетия многочисленные исследования позволили получить большой объем научной информации по проблемам, связанным со спорт-ассоциированными сотрясениями головного мозга. В обзоре сделан анализ мировых данных о сотрясении головного мозга при занятиях спортом детей и юных спортсменов. Обсуждены «болевые точки» проблемы, к которым авторы относят сложные и нерешенные вопросы по критериям диагностики, применению современных методов нейровизуализации и перспективных биомаркеров с учетом новых научных данных о патофизиологических механизмах сотрясений головного мозга. Большое внимание уделено описанию физиологических особенностей детей и подростков и предрасполагающих факторов, значимых как для диагностики, так и для тактики ведения при возникновении этого состояния. Сформулированы актуальные задачи, решение которых необходимо для совершенствования практики спортивной медицины при сотрясении головного мозга у спортсменов детско-юношеского возраста.

Ключевые слова: спорт высших достижений, сотрясение головного мозга, детско-юношеский спорт

Финансирование: статья подготовлена в рамках прикладной научно-исследовательской работы «Клинико-прогностическое значение особенностей нейрометаболического каскада для развития отсроченных осложнений гипоксических и травматических повреждений мозга у спортсменов» (шифр темы: «Нейрокаскад-20», код темы: 76.35.41), выполненной ФГБУ ФНКЦСМ ФМБА России по государственному заданию на 2020–2021 год.

Вклад авторов: С. О. Ключников — поиск и анализ источников, написание текста; В. С. Фещенко — написание текста, общее редактирование; А. В. Жолинский — общее редактирование; М. С. Тарасова, А. В. Сливин, П. В. Ефимов — поиск и анализ источников.

✉ **Для корреспонденции:** Мария Сергеевна Тарасова
ул. Раевского, д. 4, 121151, г. Москва; tarasovams@sportfmba.ru

Статья получена: 20.07.2021 **Статья принята к печати:** 12.08.2021 **Опубликована онлайн:** 17.09.2021

DOI: 10.47183/mes.2021.026

Numerous studies conducted in recent decades and the debate they sparked in top-tier scientific journals and at international forums have generated vast amounts of data on sport-related concussions (SRCs). A series of systematic reviews and meta-analyses have described how SRC characteristics vary depending on the type of sport, duration of training activities and sex. A wealth of diagnostic modalities, protocols, policies and laws have been elaborated to manage SRCs in a clinical setting [1, 2]. One would think that the amount of knowledge accrued to date and the advances in medical and biological technology would be enough to solve SRC-associated diagnostic and therapeutic challenges. Yet many of the complex aspects of SRCs remain unresolved. Paradoxically, there is no clear-cut definition for this injury type, no objective diagnostic criteria and consensus management strategies that would account for the young athlete's age.

Very mild symptoms, the lack of specific presenting complaints and a relatively short recovery period in the absence of medication therapy foster a misconception about the insignificant impact of brain concussion on the young athlete's health. There is convincing evidence accumulated to date that even a single SRC may adversely affect academic achievement; repeated SRCs dramatically increase the risk of academic performance decline [3]. Children are at particularly high risk for long-term sequelae after SRC, especially if another episode of brain concussion occurs during the recovery period. [4; 5]. Sports medicine physicians are faced with a multitude of SRC-related questions that need to be addressed.

One of them is the incidence of brain concussions. SRC statistics cited in the literature traditionally refers to the American population of young athletes, largely due to the abundance of

data generated from large sample sizes; in the USA, there are 1.1 to 1.9 million SRC reported cases among children annually [6]. According to other sources, the annual incidence of SRC among athletes varies from 1.6 to 3.8 million a year, being the second common cause of head injury after car accidents [7]. These statistics include college and school athletes and recreational injuries sustained during recreational activities (as opposed to practice and competition). Recent epidemiology studies have reported a surge in SRC incidence. In 2006, there were 569.4 SRCs per 100,000 injuries; in 2012 their number increased to 807.9 per 100,000 injuries [8]. This increase may be explained by but is not limited to the growing attention to SRC from doctors, coaches and parents [9]. Some amendments to legislation and socioeconomic factors discussed in [10; 11] may, too, have contributed to the active reporting of SRCs.

Although it is well known that about 70% of injuries are sustained by children under 19 years [12], until recently pediatric and adolescent SRCs were considered a minor injury. It was argued that SRCs are well compensated by physiological and adaptive resources, and their long-term effects are rare and/or mild [13]. The argumentation was based on multiple clinical studies which reported obvious clinical symptoms or signs of neuropsychological disturbance after SRC in only a small proportion of the affected children [14].

Innovative diagnostic approaches, experimental, clinical, functional and neurophysiological studies of the brain increasingly suggest that conventional methods of clinical assessment are insufficient to detect and differentiate between subtle and heterogeneous pathologies associated with SRC, especially in children. There is mounting evidence that SRC may have long-term effects on pediatric and adolescent health that persist past recovery. Most clinicians use commercial tests like ImPACT or SCAT for the clinical evaluation of SRC. Indeed, these pediatric tests have a number of indisputable advantages over baseline concussion tests, but studies have demonstrated their insufficient reliability and sensitivity for detecting SRC and predicting its sequelae that develop after the acute phase of the injury [1; 15; 16].

Many researchers have convincingly demonstrated that most SRCs sustained by athletes of any age are not reported to healthcare providers. There are a few major reasons for that. Coaches do not always pay careful attention to the symptoms experienced by players; athletes do not know much about this type of injury or tend to underreport any health-related issues out of fear of being suspended from practice or competitions, etc. According to [17], 40 to 76% of young athletes attempt to conceal their injuries. According to [18], up to 80% of adolescent rugby players do not report their injuries or return to active training before making a complete recovery.

The incidence of SRC depends on the type of sports. The most injurious sport is American football. Lacrosse, ice hockey, martial arts, snowboarding and some other kinds of sports, including contact sports, are associated with high risk of SRC [5].

Pathophysiologically, SRCs is characterized by temporary neuronal and axonal dysfunction and impairments of the vascular network of the brain due to a cerebrospinal fluid shock wave and rotational mechanism; this impacts neurotransmission and neurometabolism. Besides, SRC can provoke a petechial hemorrhage around the Sylvian aqueduct [19]. Recent studies conducted in different parts of the world have paved the way to understanding fundamental SRC-inducing biokinetic mechanisms. The most crucial of them are head accelerations and decelerations, which usually alternate rapidly during the impact, and head rotation [20]. SRCs are thought to occur due to a direct blow/impact to the head. Importantly, SRCs can be

caused by blows to other parts of the body if the applied force is transmitted to the head [1]. Weak neck muscles typically seen in women and children might be critical for a concussion. Some authors think that children are at greater risk for SRC because of weak neck muscles as they cannot dampen the impact to the head [21].

Pediatricians have long known that vigorous acceleration-deceleration of the head in children under 5 years often has dramatic consequences and provokes the so-called shaken baby syndrome. The term *whiplash shaken infant syndrome* (WSIS) was coined to describe a diagnostically important combination of symptoms, including retinal hemorrhage, subdural and/or subarachnoid hemorrhage with or without mild injury to the skull [22].

Unlike older children, the brain of younger children has a number of physiological characteristics predisposing to a dramatic clinical picture after SRC. A big head and weak neck muscles render a child vulnerable to the impact of acceleration and deceleration forces during SRC. Incomplete myelination and highly hydrophilic brain tissue typical for young age also significantly increase the risk of SRC during rapid or sudden head acceleration, deceleration and rotation [23].

Damage to the myelin sheath impairs transmission of nerve impulses and makes the brain more susceptible to injury during repeated impacts. This fact has been proved for hypoxic-ischemic brain injury and, more specifically, stroke in adult patients. There are ample reports that a past history of brain concussion increases the risk of a repeated concussion 2-5.8-fold [24; 25]. According to experts, repeated SRCs significantly contribute to the development of delayed complications and shape the pattern of recovery [5].

Being a highly heterogeneous group of pathologies, brain concussions are considered minor traumatic brain injuries. The underlying pathophysiology and clinical manifestations suggest that every SRC is unique and is characterized by a wide palette of symptoms ranging in severity. The diversity of SRC manifestations, which often overlap with the symptoms of other conditions, poses a diagnostic difficulty. Neuroimaging techniques (MRI, CT) used in clinical practice do not detect any pathological transformations in the brain after a concussion. However, these techniques help to differentiate SRC from other conditions with similar presentations.

Recent decades have witnessed multiple attempts to create a detailed description and a classification of SRC symptoms in different age groups of athletes involved in various sports. All SRC symptoms can be categorized into somatic, behavioral and cognitive.

The list of somatic SRC symptoms includes headache, nausea, vomiting, blurred vision, eye floaters, balance problems, increased sensitivity to light or noise, and tinnitus.

Among the behavioral and emotional effects of SRC are sleep disturbances, sleepiness, fatigue, irritability, anxiety, and depression.

The group of cognitive symptoms comprises difficulty concentrating or remembering things, slow reaction time, etc. [26].

A systematic review has analyzed the typical signs of SRC described in the literature [2]. The following manifestations were identified as common for athletes:

- observed and documented disorientation/confusion immediately after injury;
- inability to maintain balance within 24 h after injury;
- slow reaction time within 2 days after injury and/or
- impaired verbal learning and memory within 2 days after injury.

Owing to the technological advancements in neuroimaging, it is now possible to objectively assess the effects of injury on

the brain. According to the currently held view, the definition of brain concussion should be limited to conditions caused by biomechanical exposure and not accompanied by structural changes in the brain. However, there are published diffusion tensor imaging data demonstrating the presence of microstructural brain pathology (slightly disrupted integrity of long white matter tracts, diapedesis hemorrhage) even after minor TBI and suspected SRC. It is hypothesized that such microchanges may be a sign of minimal TBI, but their clinical significance remains unclear.

Nevertheless, research into functional connectivity of the brain suggests that SRC and subconcussive impacts exert a negative effect on neuronal communication in young athletes. For example, a diffusion tensor imaging study [27] revealed that whole-brain fractional anisotropy was significantly increased in adolescent athletes 6 months after brain concussion, suggesting changes to myelination and fiber density [28]. At the same time, despite the disrupted integrity of the white matter inferred from the level of fractional anisotropy in the acute injury phase, children were able to recover the normal values of the measured parameters 6 months after injury [29]. This discrepancy complicates clinical interpretation, dictating the need for further research.

Some valuable data have been generated by neurometabolic studies. Adult athletes with SRC are reported to have elevated glutamate [30], choline [31], creatinine [32] and low N-acetylaspartate [32]. These compounds are important participants of brain metabolism; the levels of their expression correlate with neuropsychological performance [33] and results of experimental tests conducted among athletes [31]. Studies looking into the neurometabolism of children with SRC are scarce. One of them describes age-dependent changes in the metabolic profiles of children [34]. PET studies have confirmed considerable functional shifts in brain metabolism among children with sustained SRC. For example, initially excessive consumption of glucose after injury is followed by an “energy crisis” [35].

The growing interest in brain metabolism is predicated on the idea of using biomarkers in the diagnostics of brain disorders. This idea is supported by compelling scientific evidence and the potential of diagnostic agents demonstrated by stroke studies. There are promising data on the role of neuromarkers in TBI. For example, it has been established that impulse transmission between neurons is driven by changes in the transmembrane potential regulated by ion channels and glutamate receptors. The latter participate in most excitation pathways of the brain and play the key role in neuron plasticity, adaptation, learning, and memory [36].

During the acute TBI phase or axonal injury, massive amounts of glutamate are released into the synaptic cleft, initiating the activation of AMPA receptors that mediate excitation. The N-terminal domain of AMPAR gets cleaved by extracellular proteases, permeates the disrupted blood-brain barrier and enters the bloodstream. The product of AMPAR degradation, the AMPA-peptide, can be detected in the blood. Blood levels of AMPA-peptide were measured in 84 American football athletes as part of a complex diagnostic procedure which included neurocognitive testing and neuroimaging. This study conducted in the USA demonstrated that subjects with SRC had reduced visual memory, low ImPACT scores and elevated levels of the AMPA-peptide. During a 1.5-year-long follow-up, only 18 of 33 athletes recovered normal levels of the peptide and were able to resume active training [37].

In addition to glutamate-associated markers, some other compounds have been proposed for the assessment of brain concussions: S100, glial fibrillary acidic protein, neurotrophic

factors, creatinine kinases, etc. However, their practical value as diagnostic markers of SRC in young athletes has not been confirmed. Objective diagnostic criteria for concussions and health assessment criteria for athletes undergoing rehabilitation are yet to be found.

One of the hypothesized pathophysiological mechanisms of SRC is a cerebrovascular reactivity disturbance. It is reported that 16 to 22-year-old athletes with SRC recover from hypo- and hyperventilation more slowly than their healthy peers [38]. SRC may cause chronic cerebrovascular dysfunction. A study describes a significant reduction in cerebral blood flow a month after injury in 11 to 15-year-old children [39]. Their behavioral symptoms completely resolved 2 weeks after injury, but cerebral blood flow disturbances persisted in 64% of the participants. Thirty days after injury, all of the examined children performed well in neuropsychological tests, but 36% of them still had cerebrovascular dysfunction. Pronounced cerebrovascular dysfunction can persist for up to 12 months after injury in athletes who show no clinical symptoms of concussion and perform well in the offered tests [40]. This suggests formation of a long physiologically vulnerable period after SRC when a recurrent event, which does not have to be a biomechanical impact, can increase the risk of developing long-term adverse effects [1].

Research into neuroelectric function of the brain holds promise for shedding light on SRC-induced neurophysiological changes. The highest specificity and sensitivity are demonstrated by the event-related potentials technique. Children with brain concussion exhibit deficits in attention and executive control and are less aware of mistakes they make [41]. Even a single concussion can provoke profound changes in neuroelectric brain function, causing attention deficit, especially in cognitively demanding circumstances [42].

Summing up the above facts, SRC can provoke serious neurophysiological changes in children that can be detected by modern diagnostic tools; however, the neuroanatomic consequences of SRC remain unstudied. Despite some morphological and functional differences, the pathophysiological picture of SRC in young as well as adult athletes is quite distinct and manifests as persistent changes to functional connectivity, cerebral blood flow and neuroelectric function of the brain.

Age is a significant factor for SRC outcomes. A series of studies have shown that children recover at slower pace than adults [43; 44]. Longitudinal clinical studies of SRC, which generally report optimistic outcomes, suggest that children under 10 years of age are at significantly greater risk of delayed SRC complications [14; 45]. Extensive research emphasizes the importance of recognizing prepubertal children (under 10 years) as a separate age group that is at high risk of persistent neuropsychological and neuropsychiatric impairments. But careful attention should be paid to young athletes' health throughout puberty because adolescent athletes recover at slower pace than adults [46; 47].

There is an opinion that this vulnerability of young athletes is largely determined by some age-related aspects of myelination and development of functional connectivity in maturing and developing frontal regions of the young brain [48; 49]. However, it is not shared by everyone in the scientific community. A team of 11 experts led by F. P. Rivara has analyzed a vast array of publications released in 1980–2018 and concluded that there is no convincing evidence that young athletes are more susceptible to SRC than adults [5]. At the same time, the experts are unanimous in stating that the quality of research studies has changed significantly over the past years, which complicates comparison and interpretation of data yielded by of research studies from different time periods.

Traditionally, the contribution of sex differences to SRC outcomes remains the subject of heated debate. Some authors point to the higher incidence of SRC in young female students [50; 51]; these findings are supported by the conclusion of the expert panel [5]. According to the literature, the frequency and intensity of clinical symptoms and the rate of unfavorable outcomes are generally higher for female underage athletes than for young male athletes [52; 53]. This could be explained by the well-established fact that females have weaker neck muscles rendering them more susceptible to biomechanical injury [54]. At the same time, young females pay more attention to their health and promptly report their symptoms to coaches or medical personnel [55]. It is only fair to say that weakness of neck muscles is typical for children, and some specialists believe that sports training programs should include special exercise for neck strengthening that can protect against traumatic injury. However, we found no studies comparing the incidence and severity of SRC consequences between athletes and non-athletes that would factor in age.

CONCLUSION

Pediatric and adolescent sport-related brain concussions pose a challenge to contemporary science in general and sports

medicine in particular. Recent research suggests that SRCs lead to profound changes in the body and require improved diagnostic approaches, as well as refined preventive and treatment strategies. The following problems remain unsolved to this day and demand special attention:

- new methods are needed for SRC diagnostics and the dynamic assessment of the brain's functional state that would account for the age-related characteristics of young athletes; such methods could be based on neuroimaging techniques like functional magnetic resonance imaging, magnetic resonance spectroscopy, diffusion tensor imaging, functional magnetoencephalography, transcranial magnetic stimulation, etc.

- it is important to continue the search for and the development of special approaches to medication therapy and metabolic correction of typical delayed complications of SRC in young athletes, such as functional connectivity disorders, neurometabolic and circulatory changes, cognitive and sensor impairments;

- there is a need for training programs, protocols for SRC rehabilitation and medical surveillance to regulate return to active practice after injury;

- information leaflets for coaches should be prepared explaining what measures need to be taken if a young athlete sustains SRC and how SRC can be prevented.

References

1. McCrory P, Meeuwisse W, Dvorak J, et al. Consensus statement on concussion in sport—the 5th international conference on concussion in sport held in Berlin. *Br J Sports Med.* 2016; 51 (11): 838–47.
2. Giza CC, Hovda DA. The new neurometabolic cascade of concussion. *Neurosurgery.* 2014; 75 (suppl 4): S24–S33.
3. Neelakantan M, Ryali B, Cabral MD, Harris A, McCarroll J, Patel DR. Academic Performance Following Sport-Related Concussions in Children and Adolescents: A Scoping Review. *Int J Environ Res Public Health.* 2020; 17: 7602.
4. Davis GA, Anderson V, Babl FE, Gioia GA, Giza CC, Meehan W, et al. What is the difference in concussion management in children as compared with adults? A systematic review. *Br J Sports Med.* 2017; 51: 949–57.
5. Rivara FP, Tennyson R, Mills B, Brownd SR, Emery CA, Gioia G, et al. Consensus Statement on Sports-Related Concussions in Youth Sports. *JAMA Pediatr.* 2020; 174 (1): 79–85.
6. Bryan MA, Rowhani-Rahbar A, Comstock RD, Rivara F. Sports- and recreation-related concussions in US youth. *Pediatrics.* 2016; 138: e20154635.
7. Zuckerman SL, Kerr ZY, Yengo-Kahn A, Wasserman E, Covassin T, Solomon GS. Epidemiology of sports-related concussion in NCAA athletes from 2009–2010 to 2013–2014: incidence, recurrence, and mechanisms. *Am J Sports Med.* 2015; 43: 2654–62.
8. Cancelliere C, Coronado VG, Taylor CA, Xu L. Epidemiology of isolated versus nonisolated mild traumatic brain injury treated in emergency departments in the United States, 2006–2012: sociodemographic characteristics. *J Head Trauma Rehabil.* 2017; 32 (4): E37–E46.
9. Kerr ZY, Yeargin S, Valovich McLeod TC, Nittoli VC, Mensch J, Dodge T, et al. Comprehensive coach education and practice contact restriction guidelines result in lower injury rates in youth American football. *Orthopaedic Journal of Sports Medicine.* 2015; 3 (7): 2325967115594578. DOI: 10.1177/2325967115594578. PMID: 26674011; PMCID: PMC4622331.
10. Bompadre V, Jinguji TM, Yanez ND, Satchell EK, Gilbert K, Burton M, et al. Washington State's Lystedt law in concussion documentation in Seattle public high schools. *Journal of Athletic Training.* 2014; 49 (4): 486–92.
11. Yang J, Comstock RD, Yi H, Harvey HH, Xun P. New and recurrent concussions in high-school athletes before and after traumatic brain injury laws, 2005–2016. *American Journal of Public Health.* 2017; e1–e7.
12. Coronado VG, Haileyesus T, Cheng TA, Bell JM, Haarbauer-Krupa J, Lionbarger MR, et al. Trends in sports- and recreation-related traumatic brain injuries treated in US emergency departments: the National Electronic Injury Surveillance System-All Injury Program (NEISS-AIP) 2001–2012. *J Head Trauma Rehabil.* 2015; 30 (3): 185–97.
13. Carroll LJ, Cassidy JD, Holm L, Kraus J, Coronado VG. Methodological issues and research recommendations for mild traumatic brain injury: the WHO collaborating centre task force on mild traumatic brain injury. *J Rehabil Med.* 2004; S (43): 113–25.
14. Babikian T, Satz P, Zaucha K, Light R, Lewis RS, Asarnow RF. The UCLA longitudinal study of neurocognitive outcomes following mild pediatric traumatic brain injury. *J Int Neuropsychol Soc.* 2011; 17 (5): 886–95.
15. Resch J, Driscoll A, McCaffrey N, Brown C, Ferrara MS, Macciocchi S, et al. ImPact test-retest reliability: reliably unreliable? *J Athl Train.* 2013; 48 (4): 506–11.
16. Bruce J, Echemendia R, Meeuwisse W, Comper P, Sisco A. 1 year test-retest reliability of ImPACT in professional ice hockey players. *Clin Neuropsychol.* 2014; 28 (1): 14–25.
17. Prasad MR, Swank PR, Ewing-Cobbs L. Long-term school outcomes of children and adolescents with traumatic brain injury. *J Head Trauma Rehabil.* 2017; 32: E24–E32.
18. Alexander DG, Shuttleworth-Edwards AB, Kidd M, Malcolm CM. Mild traumatic brain injuries in early adolescent rugby players: Long-term neurocognitive and academic outcomes. *Brain Injury.* 2015; 29: 1113–25.
19. Gusev EI, Skvorcova VI. Ishemija golovnogo mozga. M.: Medicina, 2001; 328 c. Russian.
20. Ommaya AK, Gennarelli TA. Cerebral concussion and traumatic unconsciousness. Correlation of experimental and clinical observations of blunt head injuries. *Brain.* 1974; 97 (4): 633–54.
21. Buzzini SR, Guskiewicz KM. Sport-related concussion in the young athlete. *Curr Opin Pediatr.* 2006; 18 (4): 376–82.
22. Rumjancev AG, Dreval ON, Feniksov VM. Sindrom «Shaken Baby»: diagnostika, lechenie, profilaktika. *Voprosy prakticheskoy pediatrii.* 2007; 2 (2): 23–29. Russian.

23. Adam JO, Jai S, Kshitij M. Parenchymal brain injuries in abusive head trauma. *Pediatr Radiol*. 2021; Feb 27.
24. Emery C, Kang J, Shrier I, Goulet C, Hagel B, Benson B, et al. Risk of injury associated with bodychecking experience among youth hockey players. *Can Med Assoc J*. 2011; 183: 1249–56.
25. Hollis SJ, Stevenson MR, McIntosh AS. Incidence, Risk, and Protective Factors of Mild Traumatic Brain Injury in a Cohort of Australian Nonprofessional Male Rugby Players. *Am J Sports Med*. 2009; Dec; 37 (12): 2328–33.
26. Halstead ME, Walter KD, Moffatt K, Council on sports medicine and fitness. Sport-Related Concussion in Children and Adolescents. *Pediatrics* December. 2018; 142 (6): e20183074.
27. Virji-Babul N, Borich MR, Mankan N, Moore T, Frew K, Emery CA, et al. Diffusion tensor imaging of sports-related concussion in adolescents. *Pediatr Neurol*. 2013; 48 (1): 24–29.
28. Feldman HM, Yeatman JD, Lee ES, Barde LH, Gaman-Bean S. Diffusion tensor imaging: a review for pediatric researchers and clinicians. *J Dev Behav Pediatr*. 2010; 31 (4): 346–56.
29. Van BL, Ghesquière P, Lagae L, De SB. Arithmetic difficulties in children with mild traumatic brain injury at the subacute stage of recovery. *Dev Med Child Neurol*. 2015; 57 (11): 1042–8.
30. Gasparovic C, Yeo R, Mannell M, Ling J, Elgie R, Phillips J, et al. Neurometabolite concentrations in gray and white matter in mild traumatic brain injury: an 1H-magnetic resonance spectroscopy study. *J Neurotrauma*. 2009; 26 (10): 1635–43.
31. Yeo RA, Phillips JP, Jung RE, Brown AJ, Campbell RC, Brooks WM. Magnetic resonance spectroscopy detects brain injury and predicts cognitive functioning in children with brain injuries. *J Neurotrauma*. 2006; 23 (10): 1427–35.
32. Vagnozzi R, Signoretti S, Floris R, Marziali S, Manara M, Amorini AM, et al. Decrease in N-acetylaspartate following concussion may be coupled to decrease in creatine. *J Head Trauma Rehabil*. 2013; 28 (4): 284–92.
33. Babikian T, Freier MC, Ashwal S, Riggs ML, Burley T, Holshouser BA. MR spectroscopy: predicting long-term neuropsychological outcome following pediatric TBI. *J Magn Reson Imaging*. 2006; 2 (4): 801–11.
34. McCrear M, Meier T, Huber D, Pfitz A, Bigler E, Debert CT, et al. Role of advanced neuroimaging, fluid biomarkers and genetic testing in the assessment of sport-related concussion: a systematic review. *Br J Sports Med*. 2017; 51 (12): 919–29.
35. Halstead ME, Walter KD. Clinical report—sport-related concussion in children and adolescents. *Pediatrics*. 2010; 126 (3): 597–615.
36. Dambinova SA, Shikuev AV, Weissman JD, Mullins CD. AMPAR Peptide Values in Blood of Nonathletes and Club Sport Athletes With Concussions. *Military Medicine*. 2013; 178 (3): 285–90.
37. Dambinova KT, Aliev EV, Bondarenko GV, Ponomarev AA, Skoromec AP, Skoromec TA, et al. Biomarkery ishemii golovnogo mozga kak novyj metod dokazatel'stva jeffektivnosti nejrocitoprotektorov. *Zhurnal nevrologii i psihiatrii im. S. S. Korsakova*. 2017; 117 (5): 62–67. Russian.
38. Len TK, Neary JP, Asmundson GJG, Goodman DG, Bjornson B, Bhambhani YN. Cerebrovascular reactivity impairment after sport-induced concussion. *Med Sci Sports Exerc*. 2011; 43 (12): 2241–8.
39. Maugans TA, Farley C, Altave M, Leach J, Cecil KM. Pediatric sports-related concussion produces cerebral blood flow alterations. *Pediatrics*. 2012; 129 (1): 28–37.
40. Wang Y, West JD, Bailey JN, Westfall DR, Xiao H, Arnold TW, et al. Decreased cerebral blood flow in chronic pediatric mild TBI: an MRI perfusion study. *Dev Neuropsychol*. 2015; 40 (1): 40–44.
41. Moore DR, Pindus DM, Raine LB, Drollette ES, Scudder MR, Ellemberg D, et al. The persistent influence of concussion on attention, executive control, and neuroelectric function in preadolescent children. *Int J Psychophysiol*. 2016; 99: 85–95.
42. Moor RD, Jacob JK, Ellemberg D. The long-term outcomes of sport-related concussion in pediatric populations. *Int J Psychophysiol*. 2018; 132 (Pt A): 14–24.
43. Baillargeon A, Lassonde M, Leclerc S, Ellemberg D. Neuropsychological and neurophysiological assessment of sport concussion in children, adolescents and adults. *Brain Inj*. 2012; 26 (3): 211–20.
44. Nelson LD, Guskiewicz KM, Barr WB, Hammeke TA, Randolph C, Ahn KW, et al. Age differences in recovery after sport-related concussion: a comparison of high school and collegiate athletes. *J Athl Train*. 2016; 51 (2): 142–52.
45. Hessen E, Nestvold K, Anderson V. Neuropsychological function 23 years after mild traumatic brain injury: a comparison of outcome after pediatric and adult head injuries. *Brain Inj*. 2007; 21 (9): 963–79.
46. Babcock L, Byczkowski T, Wade SL, Ho M, Mookerjee S, Bazarian JJ. Predicting postconcussion syndrome after mild traumatic brain injury in children and adolescents who present to the emergency department. *JAMA Pediatr*. 2013; 167 (2): 156–61.
47. Baillargeon A, Lassonde M, Leclerc S, Ellemberg D. Neuropsychological and neurophysiological assessment of sport concussion in children, adolescents and adults. *Brain Inj*. 2012; 26 (3): 211–20.
48. Prins ML, Giza CC. Repeat traumatic brain injury in the developing brain. *Int J Dev Neurosci*. 2012; 30 (3): 185–90.
49. Moore DR, Pindus DM, Drollette ES, Scudder MR, Raine LB, Hillman CH. The persistent influence of pediatric concussion on attention and cognitive control during flanker performance. *Biol Psychol*. 2015; 109: 93–102.
50. Gessel LM, Fields SK, Collins CL, Dick RW, Comstock RD. Concussions among United States high school and collegiate athletes. *J Athl Train*. 2007; 42 (4): 495–503.
51. Covassin T, Moran R, Elbin RJ. Sex differences in reported concussion injury rates and time loss from participation: an update of the National Collegiate Athletic Association Injury Surveillance Program from 2004–2005 through 2008–2009. *J Athl Train*. Large study summarizing sex differences in concussion rates and recovery after SRC in collegiate athletes. 2016; 51: 189–94.
52. Ono KE, Burns TG, Bearden DJ, McManus SM, King H, Reisner A. Sex-based differences as a predictor of recovery trajectories in young athletes after a sports-related concussion. *Am J Sports Med*. 2016; 44 (3): 748–52.
53. Tanveer SR, Zecavati N, Delasobera EB, Oyegbile TO. Gender differences in concussion and post-injury cognitive findings in an older and younger pediatric population. *Pediatr Neurol*. 2017; 70: 40–49.
54. Caccese JB, Kaminski TW. Minimizing head acceleration in soccer: a review of the literature. *Sports Medicine*. 2016; 46 (11): 1591–604.
55. Wallace J, Covassin T, Beidler E. Sex differences in high school athletes' knowledge of sport-related concussion symptoms and reporting behaviors. *J Athl Train*. 2017; 52: 682–8.

Литература

1. McCrory P, Meeuwisse W, Dvorak J, et al. Consensus statement on concussion in sport—the 5th international conference on concussion in sport held in Berlin. *Br J Sports Med*. 2016; 51 (11): 838–47.
2. Giza CC, Hovda DA. The new neurometabolic cascade of concussion. *Neurosurgery*. 2014; 75 (suppl 4): S24–S33.
3. Neelakantan M, Ryali B, Cabral MD, Harris A, McCarroll J, Patel DR. Academic Performance Following Sport-Related Concussions in Children and Adolescents: A Scoping Review. *Int J Environ Res Public Health*. 2020; 17: 7602.
4. Davis GA, Anderson V, Babi FE, Gioia, GA, Giza CC, Meehan W, et al. What is the difference in concussion management in children as compared with adults? A systematic review. *Br J Sports Med*. 2017; 51: 949–57.
5. Rivara FP, Tennyson R, Mills B, Browd SR, Emery CA, Gioia G, et al. Consensus Statement on Sports-Related Concussions in Youth Sports. *JAMA Pediatr*. 2020; 174 (1): 79–85.
6. Bryan MA, Rowhani-Rahbar A, Comstock RD, Rivara F. Sports- and recreation-related concussions in US youth. *Pediatrics*. 2016; 138: e20154635.

7. Zuckerman SL, Kerr ZY, Yengo-Kahn A, Wasserman E, Covassin T, Solomon GS. Epidemiology of sports-related concussion in NCAA athletes from 2009-2010 to 2013-2014: incidence, recurrence, and mechanisms. *Am J Sports Med.* 2015; 43: 2654–62.
8. Cancelliere C, Coronado VG, Taylor CA, Xu L. Epidemiology of isolated versus nonisolated mild traumatic brain injury treated in emergency departments in the United States, 2006–2012: sociodemographic characteristics. *J Head Trauma Rehabil.* 2017; 32 (4): E37–E46.
9. Kerr ZY, Yeargin S, Valovich McLeod TC, Nittoli VC, Mensch J, Dodge T, et al. Comprehensive coach education and practice contact restriction guidelines result in lower injury rates in youth American football. *Orthopaedic Journal of Sports Medicine.* 2015; 3 (7): 2325967115594578. DOI: 10.1177/2325967115594578. PMID: 26674011; PMCID: PMC4622331.
10. Bompadre V, Jinguji TM, Yanez ND, Satchell EK, Gilbert K, Burton M, et al. Washington State's Lystedt law in concussion documentation in Seattle public high schools. *Journal of Athletic Training.* 2014; 49 (4): 486–92.
11. Yang J, Comstock RD, Yi H, Harvey HH, Xun P. New and recurrent concussions in high-school athletes before and after traumatic brain injury laws, 2005–2016. *American Journal of Public Health.* 2017; e1–e7.
12. Coronado VG, Haileyesus T, Cheng TA, Bell JM, Haarbauer-Krupa J, Lionbarger MR, et al. Trends in sports- and recreation-related traumatic brain injuries treated in US emergency departments: the National Electronic Injury Surveillance System-All Injury Program (NEISS-AIP) 2001–2012. *J Head Trauma Rehabil.* 2015; 30 (3): 185–97.
13. Carroll LJ, Cassidy JD, Holm L, Kraus J, Coronado VG. Methodological issues and research recommendations for mild traumatic brain injury: the WHO collaborating centre task force on mild traumatic brain injury. *J Rehabil Med.* 2004; S (43): 113–25.
14. Babikian T, Satz P, Zaucha K, Light R, Lewis RS, Asarnow RF. The UCLA longitudinal study of neurocognitive outcomes following mild pediatric traumatic brain injury. *J Int Neuropsychol Soc.* 2011; 17 (5): 886–95.
15. Resch J, Driscoll A, McCaffrey N, Brown C, Ferrara MS, Macciocchi S, et al. ImPact test-retest reliability: reliably unreliable? *J Athl Train.* 2013; 48 (4): 506–11.
16. Bruce J, Echremendia R, Meeuwisse W, Comper P, Sisco A. 1 year test-retest reliability of ImPACT in professional ice hockey players. *Clin Neuropsychol.* 2014; 28 (1): 14–25.
17. Prasad MR, Swank PR, Ewing-Cobbs L. Long-term school outcomes of children and adolescents with traumatic brain injury. *J Head Trauma Rehabil.* 2017; 32: E24–E32.
18. Alexander DG, Shuttleworth-Edwards AB, Kidd M, Malcolm CM. Mild traumatic brain injuries in early adolescent rugby players: Long-term neurocognitive and academic outcomes. *Brain Injury.* 2015; 29: 1113–25.
19. Гусев Е. И., Скворцова В. И. Ишемия головного мозга. М.: Медицина, 2001; 328 с.
20. Ommaaya AK, Gennarelli TA. Cerebral concussion and traumatic unconsciousness. Correlation of experimental and clinical observations of blunt head injuries. *Brain.* 1974; 97 (4): 633–54.
21. Buzzini SR, Guskiewicz KM. Sport-related concussion in the young athlete. *Curr Opin Pediatr.* 2006; 18 (4): 376–82.
22. Румянцев А. Г., Древаль О. Н., Фениксов В. М. Синдром «Shaken Baby»: диагностика, лечение, профилактика. *Вопросы практической педиатрии.* 2007; 2 (2): 23–29.
23. Adam JO, Jai S, Kshitij M. Parenchymal brain injuries in abusive head trauma. *Pediatr Radiol.* 2021; Feb 27.
24. Emery C, Kang J, Shrier I, Goulet C, Hagel B, Benson B, et al. Risk of injury associated with bodychecking experience among youth hockey players. *Can Med Assoc J.* 2011; 183: 1249–56.
25. Hollis SJ, Stevenson MR, McIntosh AS. Incidence, Risk, and Protective Factors of Mild Traumatic Brain Injury in a Cohort of Australian Nonprofessional Male Rugby Players. *Am J Sports Med.* 2009; Dec; 37 (12): 2328–33.
26. Halstead ME, Walter KD, Moffatt K, Council on sports medicine and fitness. Sport-Related Concussion in Children and Adolescents. *Pediatrics* December. 2018; 142 (6): e20183074.
27. Virji-Babul N, Borich MR, Makan N, Moore T, Frew K, Emery CA, et al. Diffusion tensor imaging of sports-related concussion in adolescents. *Pediatr Neurol.* 2013; 48 (1): 24–29.
28. Feldman HM, Yeatman JD, Lee ES, Barde LH, Gaman-Bean S. Diffusion tensor imaging: a review for pediatric researchers and clinicians. *J Dev Behav Pediatr.* 2010; 31 (4): 346–56.
29. Van BL, Ghesquière P, Lagae L, De SB. Arithmetic difficulties in children with mild traumatic brain injury at the subacute stage of recovery. *Dev Med Child Neurol.* 2015; 57 (11): 1042–8.
30. Gasparovic C, Yeo R, Mannell M, Ling J, Elgie R, Phillips J, et al. Neurometabolite concentrations in gray and white matter in mild traumatic brain injury: an 1H-magnetic resonance spectroscopy study. *J Neurotrauma.* 2009; 26 (10): 1635–43.
31. Yeo RA, Phillips JP, Jung RE, Brown AJ, Campbell RC, Brooks WM. Magnetic resonance spectroscopy detects brain injury and predicts cognitive functioning in children with brain injuries. *J Neurotrauma.* 2006; 23 (10): 1427–35.
32. Vagnozzi R, Signoretti S, Floris R, Marziali S, Manara M, Amorini AM, et al. Decrease in N-acetylaspartate following concussion may be coupled to decrease in creatine. *J Head Trauma Rehabil.* 2013; 28 (4): 284–92.
33. Babikian T, Freier MC, Ashwal S, Riggs ML, Burley T, Holshouser BA. MR spectroscopy: predicting long-term neuropsychological outcome following pediatric TBI. *J Magn Reson Imaging.* 2006; 2 (4): 801–11.
34. McCrea M, Meier T, Huber D, Ptito A, Bigler E, Debert CT, et al. Role of advanced neuroimaging, fluid biomarkers and genetic testing in the assessment of sport-related concussion: a systematic review. *Br J Sports Med.* 2017; 51 (12): 919–29.
35. Halstead ME, Walter KD. Clinical report—sport-related concussion in children and adolescents. *Pediatrics.* 2010; 126 (3): 597–615.
36. Dambinova SA, Shikuev AV, Weissman JD, Mullins CD. AMPAR Peptide Values in Blood of Nonathletes and Club Sport Athletes With Concussions. *Military Medicine.* 2013; 178 (3): 285–90.
37. Дамбинова К. Т., Алиев Е. В., Бондаренко Г. В., Пономарев А. А., Скоромец А. П., Скоромец Т. А. и др. Биомаркеры ишемии головного мозга как новый метод доказательства эффективности нейротропных препаратов. *Журнал неврологии и психиатрии им. С. С. Корсакова.* 2017; 117 (5): 62–67.
38. Len TK, Neary JP, Asmundson GJG, Goodman DG, Bjornson B, Bhamhani YN. Cerebrovascular reactivity impairment after sport-induced concussion. *Med Sci Sports Exerc.* 2011; 43 (12): 2241–8.
39. Maugans TA, Farley C, Altave M, Leach J, Cecil KM. Pediatric sports-related concussion produces cerebral blood flow alterations. *Pediatrics.* 2012; 129 (1): 28–37.
40. Wang Y, West JD, Bailey JN, Westfall DR, Xiao H, Arnold TW, et al. Decreased cerebral blood flow in chronic pediatric mild TBI: an MRI perfusion study. *Dev Neuropsychol.* 2015; 40 (1): 40–44.
41. Moore DR, Pindus DM, Raine LB, Drollette ES, Scudder MR, Ellemberg D, et al. The persistent influence of concussion on attention, executive control, and neuroelectric function in preadolescent children. *Int J Psychophysiol.* 2016; 99: 85–95.
42. Moor RD, Jacob JK, Ellemberg D. The long-term outcomes of sport-related concussion in pediatric populations. *Int J Psychophysiol.* 2018; 132 (Pt A): 14–24.
43. Baillargeon A, Lassonde M, Leclerc S, Ellemberg D. Neuropsychological and neurophysiological assessment of sport concussion in children, adolescents and adults. *Brain Inj.* 2012; 26 (3): 211–20.
44. Nelson LD, Guskiewicz KM, Barr WB, Hammeke TA, Randolph C, Ahn KW, et al. Age differences in recovery after sport-related concussion: a comparison of high school and collegiate athletes. *J Athl Train.* 2016; 51 (2): 142–52.
45. Hessen E, Nestvold K, Anderson V. Neuropsychological function 23 years after mild traumatic brain injury: a comparison of outcome after pediatric and adult head injuries. *Brain Inj.* 2007; 21 (9): 963–79.
46. Babcock L, Byczkowski T, Wade SL, Ho M, Mookerjee S, Bazarian JJ. Predicting postconcussion syndrome after mild traumatic brain injury in children and adolescents who present to the emergency department. *JAMA Pediatr.* 2013; 167 (2): 156–61.
47. Baillargeon A, Lassonde M, Leclerc S, Ellemberg D. Neuropsychological and neurophysiological assessment of sport

- concussion in children, adolescents and adults. *Brain Inj.* 2012; 26 (3): 211–20.
48. Prins ML, Giza CC. Repeat traumatic brain injury in the developing brain. *Int J Dev Neurosci.* 2012; 30 (3): 185–90.
49. Moore RD, Pindus DM, Drolette ES, Scudder MR, Raine LB, Hillman CH. The persistent influence of pediatric concussion on attention and cognitive control during flanker performance. *Biol Psychol.* 2015; 109: 93–102.
50. Gessel LM, Fields SK, Collins CL, Dick RW, Comstock RD. Concussions among United States high school and collegiate athletes. *J Athl Train.* 2007; 42 (4): 495–503.
51. Covassin T, Moran R, Elbin RJ. Sex differences in reported concussion injury rates and time loss from participation: an update of the National Collegiate Athletic Association Injury Surveillance Program from 2004–2005 through 2008–2009. *J Athl Train.* Large study summarizing sex differences in concussion rates and recovery after SRC in collegiate athletes. 2016; 51: 189–94.
52. Ono KE, Burns TG, Bearden DJ, McManus SM, King H, Reisner A. Sex-based differences as a predictor of recovery trajectories in young athletes after a sports-related concussion. *Am J Sports Med.* 2016; 44 (3): 748–52.
53. Tanveer SR, Zecavati N, Delasobera EB, Oyegbile TO. Gender differences in concussion and post-injury cognitive findings in an older and younger pediatric population. *Pediatr Neurol.* 2017; 70: 40–49.
54. Caccese JB, Kaminski TW. Minimizing head acceleration in soccer: a review of the literature. *Sports Medicine.* 2016; 46 (11): 1591–604.
55. Wallace J, Covassin T, Beidler E. Sex differences in high school athletes' knowledge of sport-related concussion symptoms and reporting behaviors. *J Athl Train.* 2017; 52: 682–8.

CENTRAL VEIN SIGN FOR DIFFERENTIAL DIAGNOSIS OF DEMYELINATING DISEASES OF CNS

Belov SE^{1,2}, Gubsky IL², Lelyuk VG², Boyko AN^{1,2} ✉¹ Pirogov Russian National Research Medical University, Moscow, Russia² Federal Center of Brain Research and Neurotechnologies of FMBA, Moscow, Russia

The search for highly sensitive and highly specific biomarkers of MS, including neuroimaging biomarkers, continues. One of such biomarkers is the central vein sign detectable on SW and T2-weighted MR images. The sensitivity and specificity of methods used for central vein sign detection vary. This article describes two clinical cases of patients with similar neurological symptoms which required making differential diagnosis between multiple sclerosis and secondary demyelination in the presence of a systemic disorder (systemic lupus erythematosus). In addition to routine MR sequences, we used SWI generated by a 3T scanner. The lesions with the central vein sign were counted; the proportion of perivenular lesions was determined. In the multiple sclerosis case, all the lesions were perivenular; the proportion of lesions with the central vein sign in the patient with secondary demyelination in the presence of systemic lupus erythematosus was 16.7%. The use of SW images improved the informative value of the analysis.

Keywords: central vein sign, differential diagnosis, multiple sclerosis, demyelinating disease, CNS, secondary demyelination, MRI, SWI, SWAN

Author contribution: Belov SE — literature analysis, study design, recruitment of patients, clinical analysis, manuscript preparation; Gubsky IL — study design, MRI examinations, MRI data analysis, manuscript preparation; Lelyuk VG — study design, MRI data analysis, manuscript preparation; Boyko AN — study design, recruitment of patients, clinical analysis, manuscript preparation.

Compliance with ethical standards: informed consent was obtained from both patients.

✉ **Correspondence should be addressed:** Alexey N. Boyko
Ostrovityanova, 1, 117437, Москва; boykoan13@gmail.com

Received: 15.07.2021 **Accepted:** 04.08.2021 **Published online:** 18.08.2021

DOI: 10.47183/mes.2021.021

ИСПОЛЬЗОВАНИЕ СИМПТОМА ЦЕНТРАЛЬНОЙ ВЕНЫ ДЛЯ ДИФФЕРЕНЦИАЛЬНОЙ ДИАГНОСТИКИ ДЕМИЕЛИНИЗИРУЮЩИХ ЗАБОЛЕВАНИЙ ЦЕНТРАЛЬНОЙ НЕРВНОЙ СИСТЕМЫ

С. Е. Белов^{1,2}, И. Л. Губский², В. Г. Лелюк², А. Н. Бойко^{1,2} ✉¹ Российский национальный исследовательский медицинский университет имени Н. И. Пирогова, Москва, Россия² Федеральный центр мозга и нейротехнологий Федерального медико-биологического агентства, Москва, Россия

Продолжается поиск биомаркеров, в том числе выявляемых с помощью методов нейровизуализации, обладающих высокой чувствительностью и специфичностью в диагностике РС. В качестве одного из них можно рассматривать симптом центральной вены, выявляемый при МРТ с использованием импульсной последовательности SWI и T2⁺-взвешенных изображений. В то же время различаются данные по специфичности и чувствительности различных методов для выявления этого синдрома. Представлено два случая, близких по неврологическим нарушениям, требующих дифференциальной диагностики между РС и вторичной демиелинизацией на фоне системного заболевания (системной красной волчанки). Помимо рутинных МРТ-последовательностей, использовали SWI на томографе с индукцией магнитного поля 3 Тл. Подсчитывали очаги с симптомом центральной вены с определением доли перивенулярного поражения. В случае РС все рассматриваемые феномены локализовались перивенулярно, при вторичной демиелинизации на фоне системной красной волчанки доля очагов с симптомом центральной вены составила 16,7%. Последовательность SWI повышала информативность анализа.

Ключевые слова: симптом центральной вены, дифференциальная диагностика, рассеянный склероз, демиелинизирующее заболевание, ЦНС, вторичная демиелинизация, МРТ, SWI, SWAN

Вклад авторов: С. Е. Белов — анализ литературы, участие в разработке дизайна исследования, подбор пациентов, оценка клинических показателей, написание статьи; И. Л. Губский — участие в разработке дизайна исследования, получение и анализ данных МРТ, написание статьи; В. Г. Лелюк — участие в разработке дизайна исследования, анализ результатов МРТ, участие в написании статьи; А. Н. Бойко — участие в разработке дизайна исследования, подбор пациентов, оценка клинических показателей, написание статьи.

Соблюдение этических стандартов: все пациенты подписали добровольное информированное согласие на участие в исследовании.

✉ **Для корреспонденции:** Алексей Николаевич Бойко
ул. Островитянова, д. 1, 117437, г. Москва; boykoan13@gmail.com

Статья получена: 15.07.2021 **Статья принята к печати:** 04.08.2021 **Опубликована онлайн:** 18.08.2021

DOI: 10.47183/mes.2021.021

As new disease-modifying treatments (DMTs) for multiple sclerosis (MS) are being developed and introduced into clinical practice, and our knowledge about the pathogenesis and molecular underpinnings of this condition is expanding, adequate diagnostic criteria and procedures are becoming increasingly important. MS requires expensive long-term treatment; therefore, the diagnosis must be timely and accurate. The key 2017 McDonald criteria for MS [1] are: clinical and MRI evidence of dissemination of demyelinating lesions in time and space, exclusion of other disorders, and the presence of oligoclonal bands in the cerebrospinal fluid (CSF). However, despite the guidance provided by the McDonald

criteria, diagnostic errors are not uncommon, partly due to the absence of MS-specific MRI features and biochemical/immunological markers [2, 3]. This drives the search for specific MS biomarkers, one of which might be the central vein sign.

The central vein sign can be visualized on SWI (susceptibility-weighted imaging) and T2-weighted gradient-echo sequences. SWI is sensitive to paramagnetic, supermagnetic and ferromagnetic compounds like deoxyhemoglobin and iron and is capable of detecting local changes to the magnetic field [4]. The central vein sign shows on the SW-images of patients with progressive demyelination in the central nervous system (CNS) as a blood vessel inside a white matter lesion that appears as

a hypointensity due to the presence of deoxyhemoglobin in the vein. An area of autoimmune inflammation and demyelination (a plaque) forms around the vein [5, 6].

After a 2008 publication by Tallantyre et al., a series of reports demonstrated that the central vein sign was a sensitive diagnostic marker for MS and could be used to differentiate MS from other demyelinating diseases. Although those publications were scarce and the sample sizes were small, they showed the potential of the central vein sign as an MS biomarker [7–17]. In those studies, the proportion of lesions with the central vein sign was calculated and a threshold for reliable differentiation between MS and MS-resembling conditions was determined. The established threshold frequency of perivenular lesions that could be used to differentiate between MS and other demyelinating diseases of the CNS with high sensitivity and specificity was 40–50%. This article reports 2 clinical cases in which SWI, in addition to routine MRI sequences, was used to look for the central vein sign.

Description of clinical cases

Patients whose clinical cases are presented below underwent standard diagnostic tests for MS: physical examination, neurological assessment with EDSS (Expanded Disability Status Scale), lumbar puncture with CSF and serum analysis for the presence of oligoclonal bands, contrast-enhanced MRI with sequences routinely used in MS diagnosis, and SWI for central vein sign detection.

We used a 3T Discovery 750w scanner (General Electric; USA). In GE scanners, susceptibility-weighted imaging is called SWAN and has the following parameters: FOV (field of view) 22 cm; number of slices 178; TE (echo time) 28 ms; TR (repetition time) 47 ms; flip angle 8°; number of echoes 6; slice thickness 0.8 mm [18].

The clinical evaluation of the central vein sign was carried out using the criteria of the North American Imaging in Multiple Sclerosis Cooperative [19].

On MR images, the central vein sign has the following radiographic features:

- 1) it looks like a thin hypointense line or a small hypointense dot;
- 2) it can be visualized in at least 2 planes and appears as a thin line in at least one plane;
- 3) its diameter is under 2 mm;
- 4) it courses, partially or fully, through the lesion;
- 5) it is located in the center of the lesion at equal distances from its edges and passes through the edge at no more than 2 sites, regardless of the lesion's shape.

Exclusion criteria for lesions: diameter over 3 mm; confluent lesions; lesions with several different blood vessels inside; poorly visualized lesion.

Case 1

A 32-year-old female patient presented with complaints of numbness in her right arm, a burning sensation on the left side of the body and in her left extremities; the symptoms had started a month before the appointment. A contrast-enhanced brain MRI scan revealed multiple, possibly demyelinating MS lesions in the white brain matter, with contrast uptake in one of the lesions. The acquired MR images showed lesions of different age, with and without contrast uptake. A few days later, the patient developed tenderness to touch and a sensory disturbance (dysesthesia) on the left side of the body and in her left extremities. The patient was prescribed pulse therapy with 5 g

methylprednisolone, which slightly improved her condition. She was hospitalized to a neurology unit to undergo further tests and treatment. The patient had a history of chronic hypothyroidism and was on 50 µg L-thyroxine. Antibodies (IgG+IgA+IgM) to aquaporin-4 < 1:10 (which was within the reference range of < 1:10); oligoclonal IgG in CSF/serum as of April 14, 2021: type 2 synthesis typical for autoimmune processes in the CNS. The visual evoked potential test conducted on April 14, 2021 revealed no pathology of the visual system.

On examination the patient's condition was satisfactory. Her posture was active, and she was fully conscious. Height: 172 cm; weight: 58 kg; body type: normosthenic. Respiratory rate: 18 breaths per minute; heart rate: 68 beats per minute. Blood pressure: 110/70 mmHg. No pain on kidney percussion on both sides. The patient denied dysuria or fecal incontinence and reported regular bowel movements.

Neurological assessment. The patient was fully conscious and did not have any speech impairments. She was calm, cooperative, well-oriented in time and space, and knew her personal identity. No symptoms of non-focal brain or meningeal damage were detected. Cranial nerve (CN) I (*n. olfactorius*): sense of smell not impaired; CN II (*n. opticus*): acuity and visual fields not impaired; CN III (*n. oculomotorius*), IV (*n. trochlearis*), and VI (*n. abducens*): full range of eye movement preserved, palpebral fissures unremarkable, D = S. Pupils: OD = OS, round, pupil size was normal for the used lighting conditions, direct and consensual pupillary reflexes were intact. CN V (*n. trigeminus*): corneal reflexes preserved; no altered sensations in the face. The strength and function of mastication muscles were preserved. CN VII (*n. facialis*): the face was symmetrical; sense of taste preserved on the anterior two-thirds of the tongue. CN VIII (*n. vestibulocochlearis*): no hearing loss or nystagmus detected. CN IX (*n. glossopharyngeus*), X (*n. vagus*), and XI (*n. accessorius*): gag reflex preserved, D = S. No uvular deviation detected. No dysphonia, dysarthria or dysphagia. Head posture was unremarkable; the full range of motion was preserved for the head and the muscles of the upper chest and shoulders. CN XII (*n. hypoglossus*): no signs of tongue deviation. No changes in muscle tone. No paresis. Exaggerated deep tendon reflexes: S ≤ D. Abdominal reflexes were absent. The Babinski reflex was absent bilaterally. Abnormal superficial sensations were detected in the left extremities. Vibratory sense was normal. The Lasegue, Neri, Wasserman, and Matskevich tests were negative, indicating the absence of tension in the peripheral nerves. The patient had S-shaped thoracolumbar scoliosis, with a right arc. The right shoulder blade was prominent. The patient was a bit unsteady during the Romberg test; her performance during coordination tests was satisfactory. The patient denied any pelvic floor dysfunction. Her EDSS score was 2.0, suggesting moderate disability.

Brain, cervical and thoracic spine MRI conducted on April 23, 2021 was suggestive of possibly demyelinating supra- and infratentorial lesions in the white brain matter (MRI findings were consistent with dissemination in time and space). The total number of supratentorial lesions on SW and FLAIR images was 6. Of them, 4 were suitable for the analysis. The central vein sign was detected in all of those 4 lesions. Other 2 lesions could not be used for the analysis because of their size (< 3 mm); interestingly, the central vein sign was detected in one of those two lesions (Fig. 1)

Case 2

A 42-year-old female patient was hospitalized in March, 2021. Presenting complaints: malaise, easy fatigability, headaches,

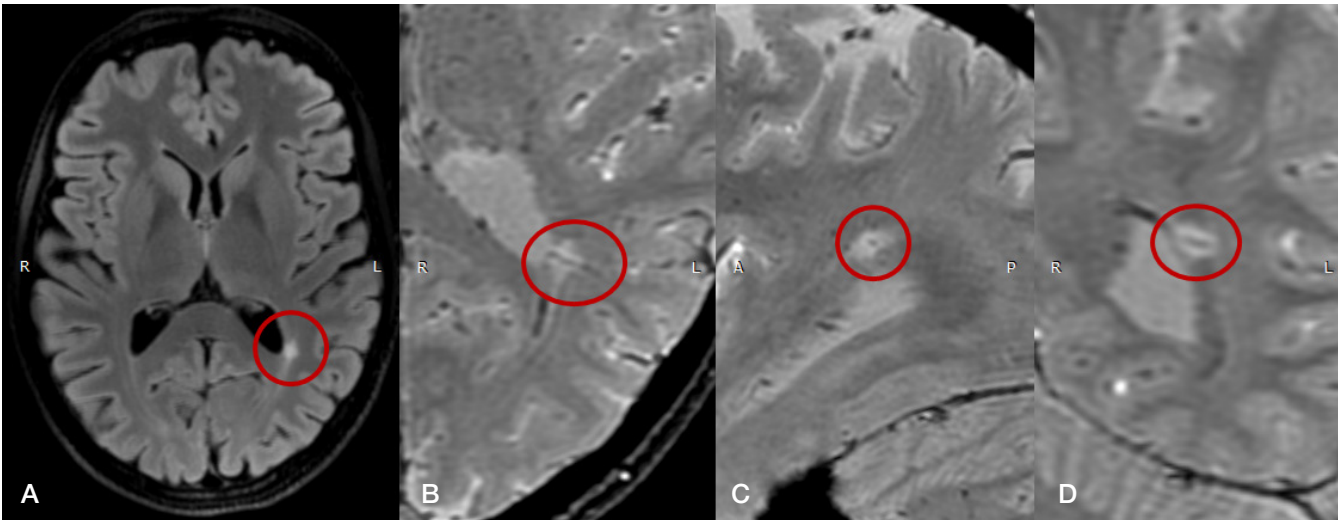


Fig. 1. Magnetic resonance images of patient 1. **A.** A T2-weighted fluid-attenuated inversion recovery (FLAIR) image, the axial plane. The image shows a periventricular lesion in the posterior horn of the left lateral ventricle (marked by the red oval). **B.** A susceptibility-weighted (SW) image, the axial plane. The image shows a central vein sign in the lesion near the posterior horn of the left ventricle (marked by the red oval). **C.** A susceptibility-weighted (SW) image; the sagittal plane, the central vein sign appears as a dot in the lesion (marked by the red oval). **D.** A susceptibility-weighted (SW) image, the coronal plane; the central vein sign appears as a thin line in the same lesion (marked by the red oval)

dizziness, limb numbness, migratory pain affecting the entire body, blurred vision, blind spots, weakness in the left leg during walking, episodes of urinary incontinence.

Past history: in August 2017, the patient had an attack of rotatory vertigo with nausea and vomiting, which lasted for 6–8 h. The patient was recommended to take betahistine. The second attack occurred in November and was also accompanied by nausea and vomiting. The patient was hospitalized but discharged home soon without a verified diagnosis. Her condition worsened in May 2018. Symptoms of non-focal brain damage (dizziness) were deteriorating, and vision loss was progressing. The patient developed numbness in the limbs, pain in the spine and joints, and overall was feeling weak. She developed painless mouth ulcers and was losing hair. A malar (butterfly-shaped) rash appeared on her cheeks and nose. The medical history reported increased photosensitivity of the skin. The patient underwent pulse therapy with methylprednisolone, which had a beneficial effect. Immunomodulatory drugs were not prescribed. In 2018, the patient underwent lumbar puncture; the analysis of CSF/serum

for oligoclonal IgG suggested type 3 synthesis. AT to aquaporin-4 were not detected. MOG antibody test (March 11, 2019): 10.5 pg/ml (the reference range: 0–15 pg/ml). The patient was hospitalized to undergo further tests and receive treatment.

On physical examination the patient's condition was satisfactory. Her posture was active. Height: 165 cm; weight: 55 kg; body temperature: 36.8 °C. A butterfly-shaped malar rash was visible on the patient's cheeks and nose. Heart rate: 16 beats per minute. Blood pressure: 120/70 mmHg. The patient denied any urinary or digestive disorders.

Neurological assessment: the patient was fully conscious, cooperative, well-oriented in time and space and knew her personal identity. She had complaints of vertigo. No symptoms of meningeal damage were detected. CN I (*n. olfactorius*): sense of smell not impaired. CN II (*n. opticus*): progressive loss of vision, blind spots; visual hallucinations not detected; no changes to color perception. CN III (*n. oculomotorius*), IV (*n. trochlearis*), and VI (*n. abducens*): full range of eye movement preserved. No signs of ptosis. Pupils: OD = OS; direct and consensual pupillary reflexes were intact;

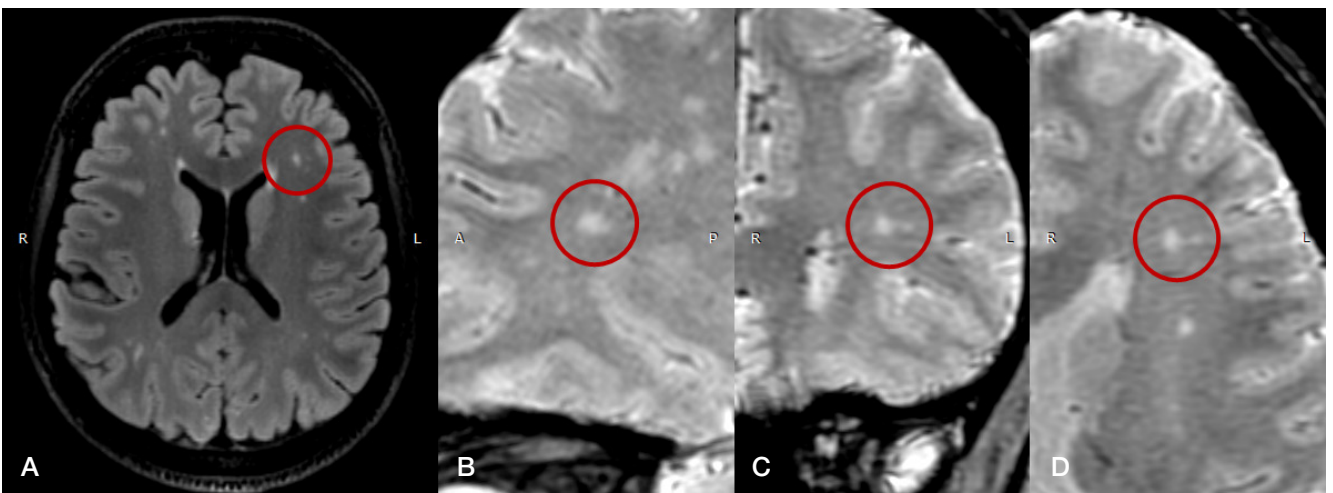


Fig. 2. Magnetic resonance images of patient 2. **A.** A T2-weighted fluid-attenuated inversion recovery (FLAIR) image, the axial plane. The image shows a round lesion in the deep white matter of the left frontal lobe (marked by the red oval). **B.** A susceptibility-weighted (SW) image, the axial plane. The image shows the same lesion, the central vein sign is not visualized (the red oval). **C.** A susceptibility-weighted (SW) image, the sagittal plane. The same lesion, the central vein sign is not visualized; a smaller lesion not suitable for the analysis is located in close proximity (the red oval). **D.** A susceptibility-weighted (SW) image, the coronal plane. The same lesion, the central vein sign is not visualized (the red oval)

accommodation and convergence were normal. CN V (*n. trigeminus*): corneal reflexes were intact; no altered sensations in the face. The strength and function of mastication muscles were preserved. CN VII (*n. facialis*): no facial asymmetry at rest or during tests; the range of facial movements was fully preserved. No tearing, dry eyes or sensory impairment on the anterior two-thirds of the tongue were detected. CN VIII (*n. vestibulocochlearis*): no signs of hearing loss, noise or ringing sensation in the ears. CN IX (*n. glossopharyngeus*): soft palate paresis not detected; the gag reflex was intact. No uvular deviation. CN X (*n. vagus*): the patient was able to swallow and showed no signs of dysphagia or dysphonia. CN XI (*n. accessorius*): head posture was unremarkable; the full range of motion was preserved for the head and the muscles of the upper chest and shoulders. CN XII (*n. hypoglossus*): the tongue was not deviated, without atrophy or fasciculations. Motor system assessment: muscle strength was not reduced, but muscle tone was decreased. Exaggerated tendon reflexes with extended reflexogenic zones; D = S. The Babinski reflex was absent bilaterally. No fasciculation or fibrillation was observed. No synkinesis, hyperkinesia or tremor were detected. Sensory system assessment: the patient had "conductive" hypoesthesia in her right limbs. The Lasague and Neri tests were negative, indicating the absence of tension in the peripheral nerves. Coordination: slight staggering during the Romberg test due to non-vestibular causes; slight bilateral intention tremor during coordination tests. No gait disturbances were detected.

Brain, cervical and thoracic spine MRI conducted on March 3, 2021 showed multiple nonspecific (possibly, autoimmune) supratentorial lesions in the white matter that did not meet the criteria of dissemination in time and space. No contrast enhancement of the lesions was observed immediately and 15 minutes after contrast agent administration. The total number of supratentorial lesions on SW and FLAIR images was about 40. Precise counting was impossible due to the small size of the lesions and their confluence. Of all the lesions, 6 were suitable for the analysis; the rest were too small (< 3 mm). Of those 6 lesions, the central vein sign was observed in only one (16.7%) (Fig. 2).

References

1. Thompson AJ, Banwell BL, Barkhof F, et al. Diagnosis of multiple sclerosis: 2017 revisions of the McDonald criteria. *Lancet Neurol.* 2018; 17 (2): 162–73. DOI: 10.1016/S1474-4422(17)30470-2.
2. Solomon AJ. Diagnosis, Differential Diagnosis, and Misdiagnosis of Multiple Sclerosis. *Continuum (Minneapolis, Minn).* 2019; 25 (3): 611–35. DOI: 10.1212/CON.0000000000000728.
3. Solomon AJ, Klein EP, Bourdette D. "Undiagnosing" multiple sclerosis: the challenge of misdiagnosis in MS. *Neurology.* 2012; 78 (24): 1986–91. DOI: 10.1212/WNL.0b013e318259e1b2.
4. Clarke MA, Pareto D, Pessini-Ferreira L, et al. Value of 3T Susceptibility-Weighted Imaging in the Diagnosis of Multiple Sclerosis. *Am J Neuroradiol.* 2020; 41 (6): 1001–8 DOI: 10.3174/ajnr.A6547.
5. Oh J, Sicotte NL. New imaging approaches for precision diagnosis and disease staging of MS? *Mult Scler.* 2020; 26 (5): 568–75. DOI: 10.1177/1352458519871817.
6. Tallantyre EC, Brookes MJ, Dixon JE, Morgan PS, Evangelou N, Morris PG. Demonstrating the perivascular distribution of MS lesions in vivo with 7-Tesla MRI. *Neurology.* 2008; 70: 2076–8. DOI: 10.1212/01.wnl.0000313377.49555.2e.
7. Tallantyre EC, Dixon JE, Donaldson I, Owens T, Morgan P S,

Discussion

Case 1

The proportion of lesions with the central vein sign was 100%. Considering that the patient had typical clinical signs of MS and that the 2017 McDonald criteria were fulfilled, the final diagnosis was relapsing-remitting multiple sclerosis [1].

Case 2

Given type 3 intrathecal IgG synthesis, the absence of AT to aquaporin-4 and the absence of MRI features of MS (the 2017 McDonald criteria [1]), there was no evidence of a primary demyelinating disease. The patient's condition was consistent with a systemic autoimmune disorder (4 criteria of 11): a facial rash, increased photosensitivity, elevated antinuclear antibodies (1:640), and a past history of painless mouth ulcers and arthritis. The final diagnosis was undifferentiated systemic connective tissue disorder, possibly systemic lupus erythematosus, complicated by a secondary demyelination disorder of the CNS.

CONCLUSION

The clinical cases described in the article demonstrate the feasibility of using the central vein sign for the differential diagnosis of MS. Although the presented cases are quite typical and did not pose real difficulty in making the accurate diagnosis, SWI may be helpful in differentiating between primary and secondary demyelination. The meta-analyses of yet scarce studies investigating the diagnostic significance of the central vein sign for the differential diagnosis of MS and MS-resembling conditions (cerebral small vessel disease, secondary demyelination in the presence of rheumatic diseases, neuromyelitis optica) show that the central vein sign has 97% sensitivity and 99% specificity as an MS marker if the proportion of lesions with the central vein sign is over 45% [15, 17–19]. However, the frequency of this sign and the approaches to its analysis in various diseases need to be studied further because the reported sample sizes were small and the analyzed range of diseases that need to be differentiated from MS is quite narrow [20].

- Morris PG, Evangelou N. Ultra-high-field imaging distinguishes MS lesions from asymptomatic white matter lesions. *Neurology.* 2011; 76: 534–9 DOI: 10.1212/WNL.0b013e31820b7630.
8. Mistry N, Dixon J, Tallantyre E, Tench C, Abdel-Fahim R, Jaspan T, Morgan PS, Morris P, Evangelou N. Central veins in brain lesions visualized with high-field magnetic resonance imaging: a pathologically specific diagnostic biomarker for inflammatory demyelination in the brain. *JAMA Neurol.* 2013; 70 (5): 623–8 DOI: 10.1001/jamaneurol.2013.1405.
9. Maggi P, Absinta M, Grammatico M, et al. Central vein sign differentiates Multiple Sclerosis from central nervous system inflammatory vasculopathies. *Ann Neurol.* 2018; 83 (2): 283–94 DOI: 10.1002/ana.25146.
10. Maggi P, Absinta M, Sati P, et al. The "central vein sign" in patients with diagnostic "red flags" for multiple sclerosis: A prospective multicenter 3T study. *Mult Scler.* 2020; 26 (4): 421–32 DOI: 10.1177/1352458519876031.
11. Champion T, Smith RJP, Altmann DR, et al. FLAIR* to visualize veins in white matter lesions: A new tool for the diagnosis of multiple sclerosis? *Eur Radiol.* 2017; 27 (10): 4257–63. DOI: 10.1007/s00330-017-4822-z.

12. Clarke MA, Samaraweera AP, Falah Y, et al. Single Test to ARrive at Multiple Sclerosis (STAR-MS) diagnosis: A prospective pilot study assessing the accuracy of the central vein sign in predicting multiple sclerosis in cases of diagnostic uncertainty. *Mult Scler.* 2020; 26 (4): 433–41. DOI: 10.1177/1352458519882282.
13. Cortese R, Magnollay L, Tur C, et al. Value of the central vein sign at 3T to differentiate MS from seropositive NMOSD. *Neurology.* 2018; 90 (14): e1183-e1190. DOI: 10.1212/WNL.0000000000005256.
14. Sparacia G, Agnello F, Gambino A, Sciortino M, Midiri M. Multiple sclerosis: High prevalence of the 'central vein' sign in white matter lesions on susceptibility-weighted images. *Neuroradiol J.* 2018; 31 (4): 356–61. DOI: 10.1177/1971400918763577.
15. Suh CH, Kim SJ, Jung SC, Choi CG, Kim HS. The "Central Vein Sign" on T2*-weighted Images as a Diagnostic Tool in Multiple Sclerosis: A Systematic Review and Meta-analysis using Individual Patient Data. *Sci Rep.* 2019; 9 (1): 18188. DOI: 10.1038/s41598-019-54583-3.
16. Sinnecker T, Clarke MA, Meier D, et al. Evaluation of the central vein sign as a diagnostic imaging biomarker in multiple sclerosis. *JAMA Neurol.* 2019; 76 (12): 1446–56. DOI: 10.1001/jamaneurol.2019.2478.
17. Bhandari A, Xiang H, Lechner-Scott J, Agzarian M. Central vein sign for multiple sclerosis: A systematic review and meta-analysis. *Clin Radiol.* 2020; 75 (6): 479.e9–479.e15. DOI: 10.1016/j.crad.2020.01.011.
18. Gaitán MI, Yañez P, Paday Formenti ME, Calandri I, Figueiredo E, Sati P, et al. SWAN-Venule: An Optimized MRI Technique to Detect the Central Vein Sign in MS Plaques. *Am J Neuroradiol.* 2020; 41 (3): 456–60. DOI: 10.3174/ajnr.A6437.
19. Sati P, Oh J, Constable RT, Evangelou N, Guttmann CR, Henry RG, et al. NAIMS Cooperative. The central vein sign and its clinical evaluation for the diagnosis of multiple sclerosis: a consensus statement from the North American Imaging in Multiple Sclerosis Cooperative. *Nat Rev Neurol.* 2016; 12 (12): 714–22. DOI: 10.1038/nrneurol.2016.166.
20. Belov SE, Boyko AN. The symptom of the central vein in the differential diagnosis of multiple sclerosis. *Neurology, Neuropsychiatry, Psychosomatics,* 2020, 12 (Suppl. 1): 29–32. Russian.

Литература

1. Thompson AJ, Banwell BL, Barkhof F, et al. Diagnosis of multiple sclerosis: 2017 revisions of the McDonald criteria. *Lancet Neurol.* 2018; 17 (2): 162–73. DOI: 10.1016/S1474-4422(17)30470-2.
2. Solomon AJ. Diagnosis, Differential Diagnosis, and Misdiagnosis of Multiple Sclerosis. *Continuum (Minneapolis, Minn).* 2019; 25 (3): 611–35. DOI: 10.1212/CON.0000000000000728.
3. Solomon AJ, Klein EP, Bourdette D. "Undiagnosing" multiple sclerosis: the challenge of misdiagnosis in MS. *Neurology.* 2012; 78 (24): 1986–91. DOI: 10.1212/WNL.0b013e318259e1b2.
4. Clarke MA, Pareto D, Pessini-Ferreira L, et al. Value of 3T Susceptibility-Weighted Imaging in the Diagnosis of Multiple Sclerosis. *Am J Neuroradiol.* 2020; 41 (6): 1001–8 DOI: 10.3174/ajnr.A6547.
5. Oh J, Sicotte NL. New imaging approaches for precision diagnosis and disease staging of MS? *Mult Scler.* 2020; 26 (5): 568–75. DOI: 10.1177/1352458519871817.
6. Tallantyre EC, Brookes MJ, Dixon JE, Morgan PS, Evangelou N, Morris PG. Demonstrating the perivascular distribution of MS lesions in vivo with 7-Tesla MRI. *Neurology.* 2008; 70: 2076–8. DOI: 10.1212/01.wnl.0000313377.49555.2e.
7. Tallantyre EC, Dixon JE, Donaldson I, Owens T, Morgan P S, Morris PG, Evangelou N. Ultra-high-field imaging distinguishes MS lesions from asymptomatic white matter lesions. *Neurology.* 2011; 76: 534–9 DOI: 10.1212/WNL.0b013e31820b7630.
8. Mistry N, Dixon J, Tallantyre E, Tench C, Abdel-Fahim R, Jaspan T, Morgan PS, Morris P, Evangelou N. Central veins in brain lesions visualized with high-field magnetic resonance imaging: a pathologically specific diagnostic biomarker for inflammatory demyelination in the brain. *JAMA Neurol.* 2013; 70 (5): 623–8 DOI: 10.1001/jamaneurol.2013.1405.
9. Maggi P, Absinta M, Grammatico M, et al. Central vein sign differentiates Multiple Sclerosis from central nervous system inflammatory vasculopathies. *Ann Neurol.* 2018; 83 (2): 283–94 DOI: 10.1002/ana.25146.
10. Maggi P, Absinta M, Sati P, et al. The "central vein sign" in patients with diagnostic "red flags" for multiple sclerosis: A prospective multicenter 3T study. *Mult Scler.* 2020; 26 (4): 421–32 DOI: 10.1177/1352458519876031.
11. Champion T, Smith RJP, Altmann DR, et al. FLAIR* to visualize veins in white matter lesions: A new tool for the diagnosis of multiple sclerosis? *Eur Radiol.* 2017; 27 (10): 4257–63. DOI: 10.1007/s00330-017-4822-z.
12. Clarke MA, Samaraweera AP, Falah Y, et al. Single Test to ARrive at Multiple Sclerosis (STAR-MS) diagnosis: A prospective pilot study assessing the accuracy of the central vein sign in predicting multiple sclerosis in cases of diagnostic uncertainty. *Mult Scler.* 2020; 26 (4): 433–41. DOI: 10.1177/1352458519882282.
13. Cortese R, Magnollay L, Tur C, et al. Value of the central vein sign at 3T to differentiate MS from seropositive NMOSD. *Neurology.* 2018; 90 (14): e1183-e1190. DOI: 10.1212/WNL.0000000000005256.
14. Sparacia G, Agnello F, Gambino A, Sciortino M, Midiri M. Multiple sclerosis: High prevalence of the 'central vein' sign in white matter lesions on susceptibility-weighted images. *Neuroradiol J.* 2018; 31 (4): 356–61. DOI: 10.1177/1971400918763577.
15. Suh CH, Kim SJ, Jung SC, Choi CG, Kim HS. The "Central Vein Sign" on T2*-weighted Images as a Diagnostic Tool in Multiple Sclerosis: A Systematic Review and Meta-analysis using Individual Patient Data. *Sci Rep.* 2019; 9 (1): 18188. DOI: 10.1038/s41598-019-54583-3.
16. Sinnecker T, Clarke MA, Meier D, et al. Evaluation of the central vein sign as a diagnostic imaging biomarker in multiple sclerosis. *JAMA Neurol.* 2019; 76 (12): 1446–56. DOI: 10.1001/jamaneurol.2019.2478.
17. Bhandari A, Xiang H, Lechner-Scott J, Agzarian M. Central vein sign for multiple sclerosis: A systematic review and meta-analysis. *Clin Radiol.* 2020; 75 (6): 479.e9–479.e15. DOI: 10.1016/j.crad.2020.01.011.
18. Gaitán MI, Yañez P, Paday Formenti ME, Calandri I, Figueiredo E, Sati P, et al. SWAN-Venule: An Optimized MRI Technique to Detect the Central Vein Sign in MS Plaques. *Am J Neuroradiol.* 2020; 41 (3): 456–60. DOI: 10.3174/ajnr.A6437.
19. Sati P, Oh J, Constable RT, Evangelou N, Guttmann CR, Henry RG, et al. NAIMS Cooperative. The central vein sign and its clinical evaluation for the diagnosis of multiple sclerosis: a consensus statement from the North American Imaging in Multiple Sclerosis Cooperative. *Nat Rev Neurol.* 2016; 12 (12): 714–22. DOI: 10.1038/nrneurol.2016.166.
20. Белов С. Е., Бойко А. Н. Симптом центральной вены в дифференциальной диагностике рассеянного склероза. *Неврология, нейропсихиатрия, психосоматика,* 2020, 12 (Прил. 1): 29–32.